

Electronic Thesis and Dissertation Repository

---

2-14-2020 2:30 PM

## microRNA156: A Short RNA with a Major Role in Abiotic Stress Tolerance in Alfalfa

Biruk Ayenew Feyissa, *The University of Western Ontario*

Supervisor: Hannoufa, Abdelali, *The University of Western Ontario*

Co-Supervisor: Kohalmi, Susanne, *The University of Western Ontario*

A thesis submitted in partial fulfillment of the requirements for the Doctor of Philosophy degree in Biology

© Biruk Ayenew Feyissa 2020

Follow this and additional works at: <https://ir.lib.uwo.ca/etd>



Part of the [Plant Biology Commons](#)

---

### Recommended Citation

Feyissa, Biruk Ayenew, "microRNA156: A Short RNA with a Major Role in Abiotic Stress Tolerance in Alfalfa" (2020). *Electronic Thesis and Dissertation Repository*. 6832.  
<https://ir.lib.uwo.ca/etd/6832>

This Dissertation/Thesis is brought to you for free and open access by Scholarship@Western. It has been accepted for inclusion in Electronic Thesis and Dissertation Repository by an authorized administrator of Scholarship@Western. For more information, please contact [wlsadmin@uwo.ca](mailto:wlsadmin@uwo.ca).

## Abstract

The highly conserved plant microRNA156, miR156, affects various aspects of plant development and stress response by silencing *SQUAMOSA-PROMOTER BINDING PROTEIN-LIKE* (SPL) transcription factors. Our understanding of the role of miR156 and its mode of action in alfalfa's (*Medicago sativa* L.) response to drought and flooding is still elusive, and thus this study was aimed at filling this gap in knowledge. Physiological parameters, metabolite and transcriptional analyses showed an interplay between miR156/SPL13 and WD40-1/DFR to mitigate drought stress. Low to moderate levels of *miR156* overexpression suppressed SPL13 and increased WD40-1 to fine-tune the *DIHYDROFLAVONOL-4-REDUCTASE* (DFR) level for enhanced anthocyanin biosynthesis. Moreover, RNAseq-derived weighted gene co-expression network analysis (WGCNA) of *SPL13RNAi* alfalfa plants showed tissue-and genotype-specific drought responses. Accordingly, transcripts mediating stress-mitigating metabolites, such as anthocyanin, were increased in stem tissues of drought-stressed plants, while those involved in photosynthesis were maintained in leaves. Moreover, drought-stressed roots showed elevated transcripts associated with metal ion transport, carbohydrate, and primary metabolism.

The role of miR156 in flooding tolerance was also investigated using flooding-tolerant (AAC-Trueman) and -sensitive (AC-Caribou) alfalfa cultivars, along with *miR156OE* and *SPL13RNAi* plants. Additionally, to examine the role of ABA and SnRK1 in regulating *miR156* expression, ABA insensitive (*abi1-2*, *abi5-8*) *Arabidopsis thaliana* mutants and transgenic lines with either overexpressed (*KIN10-OX1*, *KIN10-OX2*) or silenced (*KIN10RNAi-1*, *KIN10RNAi-2*) *SnRK1* were used. Investigation of physiological

parameters, hormone profiling, and global transcriptomics showed a positive role for miR156 in flooding tolerance, and a comparison of Arabidopsis mutants and transgenic lines showed that *miR156* expression was affected by SnRK1 to enhance anthocyanin and ABA metabolites. Transcriptomics analysis also revealed nine new alfalfa SPLs, three of which responded to flooding (SPL7a, SPL8, and SPL13a) along with the previously identified SPL4, SPL9, and SPL13.

Characterization of the newly identified SPLs, along with understanding the mode of action of miR156 in alfalfa's response to drought and flooding, will provide useful tools in marker-assisted breeding of alfalfa and resource to scientific knowledge.

## **Keywords**

ABA, Abiotic stress, alfalfa, *DFR*, drought, flooding, *Medicago sativa* L., microRNA, miR156, SPL, *SQUAMOSA-PROMOTER BINDING PROTEIN-LIKE*, *WD40-1*, *SnRK1*, *KIN10*, *KIN11*

## Summary for lay audience

Among the various abiotic stresses, drought and flooding are two extremes of water availability affecting the production and productivity of agricultural crops, including alfalfa (*Medicago sativa* L.). The frequency, distribution, and intensity of drought and flooding are increasing in conjunction with the current climate change phenomenon, highlighting the need for developing tolerant cultivars. The highly conserved plant microRNA156, miR156, affects various aspects of plant development and stress response by silencing *SQUAMOSA-PROMOTER BINDING PROTEIN-LIKE (SPL)* transcription factors. Our understanding of the role of miR156 and its mode of action in drought and flooding tolerance in alfalfa is limited, and thus this study is aimed to fill this gap.

In the current study, the role of miR156 and its mode of action in regulating drought and flooding tolerance was investigated. Hence, alfalfa plants with increased levels of *miR156* and altered miR156-regulated downstream genes (such as *SPL13*) were used to assess parameters linked to abiotic stress. The physiological and molecular responses revealed the positive role of miR156 in drought and flood stress tolerance. Upon drought stress, alfalfa plants with low to moderate level *miR156* maintained plant water status and physiological activity by increasing responsible genes and stress-reducing metabolites. On the other hand, plants containing *miR156* at higher levels coordinated genes to control membrane permeability, increase stress-reducing metabolites, keep physiological activity, and increase abscisic acid in response to flooding. The flooding experiment also identified nine new SPLs to be exploited in future studies. Knowledge gained on the role of miR156 and its target *SPL* genes in response to both drought and flooding will be utilized in developing tools for alfalfa breeding and as a resource for scientific knowledge.

## Co-Authorship statement

This thesis consists of materials from a published article, and manuscripts under revision, and in preparation. Co-authors who contributed to these articles are Biruk A Feyissa (BAF), Justin B Renaud (JR), Muhammad Arshad (MA), Vida Nasrollahi (VN), Lisa Amyot (LA), Margaret Y Gruber (MYG), Yousef Papadopoulos (YP), Susanne E Kohalmi (SEK), and Abdelali Hannoufa (AH).

### Chapter 2

This chapter contains i) data from one published article:

Feyissa BA, Arshad M, Gruber MY, Kohalmi SE and Hannoufa A 2019. The interplay between *miR156/SPL13* and *DFR/WD40-1* regulate drought tolerance in alfalfa, BMC Plant Biology 19:434.

BAF and MA developed materials; BAF performed the experiments; SEK and AH supervised the project; BAF and AH designed the research; BAF drafted the manuscript; BAF, MA, MYG, SEK and AH edited the manuscript.

and ii) from a manuscript under preparation:

Feyissa BA, Renaud JB, Nasrollahi V, Kohalmi SE and Hannoufa A. Spatially resolved transcriptomic and proteomic analysis reveal tissue-specific *miR156/SPL13* regulatory mechanism in alfalfa drought tolerance (under preparation).

BAF performed the experiments; JR helped with FASP proteomics; VN assisted in physiological data collection; SEK and AH supervised the project; BAF drafted the manuscript; BAF, JR, VN, SEK and AH edited the manuscript.

### **Chapter 3**

Findings reported in chapter three are under review for publication with the following authors' contributions:

Feyissa BA, Amyot L, Papadopoulos Y, Kohalmi SE, Hannoufa A, 2019. ABA-dependent SnRK1 expression mediate miR156/SPL module for flooding response in alfalfa (Under review).

BAF developed materials and performed the experiments at AAFC, London, Ontario; LA assisted in data collection; YP performed the experiments at AAFC, Kentville, Nova Scotia, Canada; YP, SEK and AH supervised the project; BAF, YP and AH designed the research; BAF drafted manuscript; BAF, LA, YP, SEK, and AH edited the manuscript.

# **Dedication**

Dedicated to my late father who planted seeds of education in me!!!

## Acknowledgments

First, I would like to thank my supervisor Dr. Abdelali Hannoufa for taking me as a Ph.D. student in his lab. Your unreserved support in exploring new research ideas and mentorship is phenomenal. Your door is always open to discuss my findings and layout of future research directions. Thanks, Ali.

Thank you Dr. Susanne Kohalmi, co-supervisor, for your support and editing manuscripts with details that I wouldn't find otherwise. Moreover, I would like to thank Dr. Danielle Way and Dr. Denis Maxwell, advisory committee members, for your insightful discussion, and guidance throughout my study. Furthermore, thank you Dr. Margaret Gruber and Dr. Yousef Papadopoulos, collaborators from Saskatoon and Nova Scotia AAFC research centers, respectively, for your contribution to manuscript editing and laying out experiments in your fields.

Previous and current members of Hannoufa's lab (Arshad, Susan, Scott, Craig, Lisa, Vida, Gigi, Lexi, Matei, and Roselyn): I thank you all for the valuable discussions we had during lab-meetings and the day-to-day positive vibe you created in the lab. Thank you Dr. Justin Renaud from AAFC, London, Ontario, Canada for your help with LCMS, GCMS and FASP-proteomics, and enthusiastic encouragements with my experiments.

It wouldn't feel right if I didn't appreciate the support and friendship I received from previous and current students at AAFC research center, London, ON. Thank you Raj, Jie, Gebb, Ebenezer, Coby, Jaya, Shrikar, Arina, Nishat, Marwan, Alex, and others. Similar appreciation goes to friends from the University of Western Ontario Biology department, especially to Eric and Badru. Special thanks go to the University of Western Ontario,



Department of Biology staff, Arzie Chant, Caroline Curtis, and Diane Gauley for your help.

Thank you all.

Last, but not least, I would like to thank my wife Tigist for giving me the most precious gift of fatherhood. Thank you, Mar for understanding my late nights in the lab and handling our newborn, Maya. The unreserved support from my siblings (Balem, Andinet, Tigist, and Betel), mom, and my late father are exceptional, and I thank you all for believing in me and endless support. Thank God, nothing would have been possible without you.

# Table of Contents

<b>Abstract</b> .....	ii
<b>Summary for lay audience</b> .....	iv
<b>Co-Authorship statement</b> .....	v
<b>Dedication</b> .....	vii
<b>Acknowledgments</b> .....	viii
<b>Table of Contents</b> .....	x
<b>List of Tables</b> .....	xvi
<b>List of Figures</b> .....	xvii
<b>List of Appendices</b> .....	xx
<b>List of Abbreviations</b> .....	xxiii
<b>1. General introduction</b> .....	1
<b>1.1 Background on <i>Medicago sativa</i> (alfalfa)</b> .....	1
<b>1.2 The impact of water availability on crop performance</b> .....	2
<b>1.3 Availability of water to plants and its impact on photosynthesis</b> .....	3
<b>1.4 Phytohormones and their role in stress tolerance</b> .....	5
<b>1.5 Reactive oxygen species (ROS) and ROS-scavenging metabolites under abiotic stress</b> .....	7
<b>1.6 Non-protein-coding microRNAs and their role in abiotic stress tolerance</b> .....	8
<b>1.7 miR156/SPL network and its impact on plant performance</b> .....	12

1.8 Hypothesis and objectives of the study.....	16
1.9. References.....	18
2. miR156/SPL13 module regulates drought tolerance in alfalfa.....	29
2.1 Background.....	29
2.2 Results .....	31
2.2.1 Enhanced <i>miR156</i> expression improves drought tolerance by altering root architecture and water holding capacity .....	31
2.2.2 <i>miR156</i> overexpression affects photosynthesis parameters .....	32
2.2.3 <i>miR156</i> OE plants accumulate anthocyanin and other stress-alleviating specialized metabolites under drought .....	33
2.2.4 Alfalfa plants expressing moderate levels of <i>miR156</i> accumulate stress-related primary metabolites under drought .....	42
2.2.5 miR156 regulates photosynthesis and flavonoid genes .....	46
2.2.7 Flavonoid- and photosynthesis-related genes are enhanced in <i>SPL13</i> -silenced plants.....	55
2.2.8 <i>SPL13</i> is a direct regulator of <i>DFR</i> .....	58
2.2.9 Global transcriptomic signature of <i>SPL13</i> in alfalfa drought tolerance ....	58
2.2.10 WD40-1 positively regulates <i>DFR</i> expression and drought tolerance .....	78
2.3 Discussion.....	86

2.3.1 Moderate levels of <i>miR156</i> overexpression, <i>WD40-1</i> overexpression or <i>SPL13</i> silencing are sufficient to induce phenotypic and physiological drought tolerance strategies in alfalfa .....	86
2.3.2 <i>miR156</i> overexpression enhances accumulation of stress-related metabolites .....	88
2.3.3 <i>miR156</i> , <i>WD40-1</i> and <i>SPL13</i> regulate phenylpropanoid and photosystem genes under drought.....	89
2.3.4 <i>SPL13</i> negatively regulates <i>DFR</i> expression and flavonoid biosynthesis...	91
2.3.5 Genotype-specific gene expression patterns in response to drought stress	92
2.3.6 Photosynthesis-related DEG are upregulated in leaves of <i>SPL13RNAi</i> plants during drought .....	93
2.3.7 Specialized metabolite-related DEG are upregulated in stems of <i>SPL13RNAi</i> plants during drought .....	94
2.3.8 The upregulated root-specific DEG are mainly attributed to ion transport in <i>SPL13RNAi</i> plants during drought stress .....	95
2.4 Conclusions .....	96
2.5 Methods .....	101
2.5.1 Genetic material.....	101
2.5.2 Imposing drought stress.....	102
2.5.3 Metabolite extraction for parallel LCMS and GCMS analysis.....	103
2.5.4 Total monomeric anthocyanin and polyphenol determination .....	105

2.5.5 Physiological and phenotypic data measurement.....	105
2.5.6 RNA extraction .....	106
2.5.7 qRT-PCR analysis .....	107
2.5.8 RNAseq and pathway analysis .....	108
2.5.9 ChIP-qPCR analysis of SPL13-DNA binding.....	108
2.5.10 Genome walking for WD40-1 promoter nucleotide sequence .....	110
2.5.11 Statistical data analysis .....	111
2.6 References .....	112
<b>3. ABA-dependent <i>SnRK1</i> expression mediates the miR156/SPL module for flooding response in alfalfa.....</b>	<b>122</b>
3.1 Background.....	122
3.2 Results .....	124
3.2.1 miR156/SPL module mediates physiological responses of alfalfa during flooding .....	125
3.2.2 miR156 increases ABA and ABA-catabolites for flooding tolerance.....	126
3.2.3 miR156 regulates specialized metabolite pathways to improve flooding tolerance .....	129
3.2.4 Phylogenic analysis reveals novel SPLs in alfalfa.....	138
3.2.5 Flooding enhances <i>SnRK1</i> expression in an ABA-dependent manner .....	146
3.2.6 Does <i>SnRK1</i> regulate miR156? .....	150

<b>3.2.7 miR156/SPL module enhances flooding adaptive mechanisms.....</b>	<b>151</b>
<b>3.3. Discussion.....</b>	<b>156</b>
<b>3.3.1 miR156 regulates physiological processes during flooding stress .....</b>	<b>156</b>
<b>3.3.2 Phaseic acid-dependent regulation of flooding tolerance in alfalfa .....</b>	<b>156</b>
<b>3.3.4 Identification of novel SPLs in alfalfa.....</b>	<b>159</b>
<b>3.3.5 miR156-regulated SPLs are involved in alfalfa flooding response .....</b>	<b>160</b>
<b>3.3.6 ABA-dependent regulation of SnRK1 enhances <i>miR156</i> expression for     flooding tolerance .....</b>	<b>161</b>
<b>3.4. Conclusions .....</b>	<b>163</b>
<b>3.5. Methods.....</b>	<b>168</b>
<b>3.5.1 Genetic material.....</b>	<b>168</b>
<b>3.5.2 Physiological data measurement .....</b>	<b>168</b>
<b>3.5.3 Hormone profiling .....</b>	<b>168</b>
<b>3.5.4 Total monomeric anthocyanin and polyphenol determination .....</b>	<b>170</b>
<b>3.5.5 RNA extraction for qRT-PCR and RNAseq analysis.....</b>	<b>170</b>
<b>3.5.6 RNAseq and pathway analysis .....</b>	<b>171</b>
<b>3.5.7 5'RACE-based miR156 cleavage site identification .....</b>	<b>171</b>
<b>3.5.8 Investigating Protein-Protein interaction between SnRK1 and miR156     biogenesis genes .....</b>	<b>172</b>
<b>3.5.9 Investigating SnRK1 regulation by low sugar and ABA in Arabidopsis .</b>	<b>173</b>

3.5.10 Investigating SnRK1 regulation by miR156 in alfalfa .....	174
3.5.11 Investigating <i>miR156</i> expression dependence on SnRK1 in Arabidopsis .....	174
3.5.12 Data analysis .....	174
3.6 References .....	176
4. General discussion and future research directions.....	182
4.1 microRNA156 and its role in alfalfa abiotic stress regulation .....	183
4.2 miR156-based stress tolerance in alfalfa involves <i>SQUAMOSA PROMOTER- BINDING PROTEIN-LIKE</i> transcription factors.....	185
4.3 References .....	187
Appendices.....	190
Curriculum vitae.....	247

## List of Tables

<b>Table 2.1</b> LCMS-based metabolite profiles of drought stressed alfalfa plants .....	42
<b>Table 2.3</b> GCMS-based relative metabolite abundance in drought stressed alfalfa plants .....	50
<b>Table 3.1</b> List of detected phytohormones and their abundance (ng/g dry weight) using UHPLC-MS analysis.....	132



## List of Figures

<b>Figure 1.1</b> miR156 biogenesis and post-transcriptional gene regulation module.....	10
<b>Figure 1.2</b> miR156/SPL module-based gene expression regulation .....	14
<b>Figure 2.1</b> Effects of <i>miR156</i> overexpression on drought tolerance and phenotypic responses in alfalfa.....	34
<b>Figure 2.2</b> Effects of <i>miR156</i> overexpression on drought tolerance and physiological responses in alfalfa .....	36
<b>Figure 2.3</b> LCMS-based metabolite profiling illustrates distinct profile in <i>miR156</i> OE genotypes during drought stress.....	38
<b>Figure 2.4</b> LCMS-based metabolite profiling illustrates enrichment of specialized metabolites in <i>miR156</i> OE genotypes during drought stress .....	40
<b>Figure 2.5</b> GCMS-based primary metabolite profiling demonstrates drought stress tolerance strategies by miR156.....	48
<b>Figure 2.6</b> Differential transcript levels of select genes in the phenylpropanoid pathway and photosystems during drought stress.....	53
<b>Figure 2.7</b> SPL13 silencing regulates drought response through coordinated metabolite, transcript and physiological adjustments .....	56
<b>Figure 2.8</b> SPL13 binds to <i>DFR</i> in a sequential and position-dependent manner .....	60
<b>Figure 2.9</b> Tissue and genotype-specific expression patterns of <i>SPL13</i> RNAi and EV genotypes of alfalfa plants in response to drought .....	64
<b>Figure 2.10</b> Weighted gene co-expression network analysis illustrates tissue and genotype-specific expression patterns of alfalfa plants in response to drought.....	66

<b>Figure 2.11</b> Summary of affected metabolites and pathways between drought stressed EV and <i>SPL13RNAi</i> leaf tissues .....	70
<b>Figure 2.12</b> Leaf-specific DEG attributed to photosynthesis are enhanced in <i>SPL13RNAi</i> plants .....	72
<b>Figure 2.13</b> Summary of affected metabolites and pathways between stems of drought stressed EV and <i>SPL13RNAi</i> plants .....	74
<b>Figure 2.14</b> Enhanced specialized metabolite pathway in stems of drought stressed <i>SPL13RNAi</i> plants .....	76
<b>Figure 2.15</b> Distribution of root-specific differentially expressed genes between EV and <i>SPL13RNAi</i> plants .....	80
<b>Figure 2.16</b> WD40-1 enhances drought tolerance in alfalfa .....	82
<b>Figure 2.17</b> WD40-1 regulates transcript levels of genes in the phenylpropanoid pathway and photosystem during drought stress .....	84
<b>Figure 2.18</b> Schematic representation of miR156-based alfalfa drought resilience model system .....	99
<b>Figure 3.1</b> Physiological responses of flood-stressed and control alfalfa plants .....	127
<b>Figure 3.2</b> UPLC/ESI-MS/MS based hormone profiling in flood stressed and control alfalfa genotypes .....	130
<b>Figure 3.3</b> Differentially expressed genes, DEG, and their associated function upon flood stress in alfalfa .....	135
<b>Figure 3.4</b> Functional distribution of differentially expressed genes upon flood stress in alfalfa .....	139
<b>Figure 3.5</b> Differentially expressed SPLs upon flood stress in alfalfa .....	141

<b>Figure 3.6</b> Phylogenetic analysis and identification of new SPLs in alfalfa.....	144
<b>Figure 3.7</b> ABA-dependent expression of SnRK1 regulates miR156 .....	148
<b>Figure 3.8</b> miR156-based regulation of SPL13 enhances photosynthesis and phenylpropanoid pathway in response to flooding .....	152
<b>Figure 3.9</b> miR156-based regulation of SPL13 enhances anthocyanin and ABA biosynthesis in response to flooding .....	154
<b>Figure 3.10</b> Proposed model for flooding tolerance in alfalfa .....	166

## List of Appendices

<b>Figure A1</b> Alignment of sequences amplified by qRT-PCR from <i>Medicago sativa</i> with those of their counterparts in <i>Medicago truncatula</i> .....	190
<b>Figure A2</b> Promoter sequence of the alfalfa <i>DIHYDROFLAVONOL-4-REDUCTASE</i> ( <i>DFR</i> ) gene with putative SBD binding elements. ....	191
<b>Figure A3</b> Nucleotide sequence of the alfalfa <i>WD40-1</i> promoter region .....	192
<b>Figure A4</b> Differentially affected biological processes tree map between <i>SPL13RNAi</i> and EV leaf tissues under drought stress .....	193
<b>Figure A5</b> Differentially affected molecular functions tree map and GO term clouds used for constructing tree maps between <i>SPL13RNAi</i> and EV leaf tissues under drought stress .....	194
<b>Figure A6</b> Differentially affected biological processes tree map between <i>SPL13RNAi</i> and EV stem tissues under drought stress.....	195
<b>Figure A7</b> Differentially affected molecular functions tree map and GO term clouds used for constructing tree maps between <i>SPL13RNAi</i> and EV stem tissues under drought stress .....	196
<b>Figure A8</b> Differentially affected biological processes tree map between <i>SPL13RNAi</i> and EV root tissues under drought stress.....	197
<b>Figure A9</b> Differentially affected molecular functions tree map and GO term clouds used for constructing tree maps between <i>SPL13RNAi</i> and EV root tissues under drought stress.....	198
<b>Figure A10</b> Performance of different alfalfa genotypes with altered expression of SPLs ( <i>SPLRNAi</i> ) and <i>miR156</i> overexpression in response to	

flooding stress. ....	199
<b>Figure A11</b> Investigating the expression of flooding responsive genes, SPLSs, and microRNA156 under flooding and well-drained control conditions. ...	200
<b>Figure A12</b> Transcript levels of flooding-responsive differentially expressed genes under flooding. ....	201
<b>Figure A13</b> Newly found MsSPLs and their nuclear localization signals. ....	202
<b>Table A1</b> List of primers used and their nucleotide sequences. ....	203
<b>Table A2</b> Buffers used in ChIP assay and their components. ....	208
<b>Table A3</b> Differentially increased genes and their functions common in all tissues of <i>SPL13RNAi</i> plants. ....	209
<b>Table A4</b> Top 50 out of 154 differentially decreased genes and their functions common to all <i>SPL13RNAi</i> tissues. ....	212
<b>Table A5</b> Top 50 out of 2824 differentially increased genes and their functions which are specific to <i>SPL13RNAi</i> leaf tissues. ....	214
<b>Table A6</b> Top 50 out of 572 differentially increased genes and their functions which are specific to <i>SPL13RNAi</i> stem tissues. ....	216
<b>Table A7</b> Top 50 out of 385 differentially increased genes and their functions which are specific to <i>SPL13RNAi</i> root tissues. ....	218
<b>Table A8</b> GO-term analysis represented molecular function, biological process and cellular components in leaf tissues. ....	220
<b>Table A9</b> GO-term analysis represented molecular function, biological process and cellular components in stem tissues. ....	223
<b>Table A10</b> GO-term analysis represented molecular function, biological process	

and cellular components in root tissues .....	226
<b>Table A11</b> List of significantly affected ABA-related genes fold-changes from well-drained control plants .....	228
<b>Table A12</b> DEG associated with phenylpropanoid pathway fold changes in <i>SPL13RNAi</i> plants.....	231
<b>Table A13</b> DEG associated with glycolysis and TCA fold changes in <i>SPL13RNAi</i> plants .....	241

## List of Abbreviations

7'OH-ABA	7'-Hydroxy-abscisic acid
AAFC	Agriculture and Agri-Food Canada
ABA	cis-abscisic acid
ABAGE	Abcisic acid glucose ester
<i>ABI1</i>	<i>ABA INSENSITIVE1</i>
<i>ABI5</i>	<i>ABA INSENSITIVE5</i>
<i>ACCI</i>	<i>ACETYL-CoA CARBOXYLASE1</i>
<i>AGO1</i>	<i>ARGONAUTE1</i>
ANOVA	Analysis of variance
<i>bHLH</i>	<i>basic HELIX-LOOP-HELIX</i>
CCI	Chlorophyll concentration index
CG	Cyanidin-3-o-glucoside (CG)
ChIP	Chromatin immunoprecipitation
CRISPR	Clustered Regularly Interspaced Short Palindromic Repeats
c-ZOG	(cis) Zeatin-O-glucoside
c-ZR	(cis) Zeatin riboside
DAG	Delphinidin 3-O-(6"-acetyl)-glucoside
<i>DCL1</i>	<i>DICER-LIKE1</i>
DEG	Differentially expressed genes
<i>DFR</i>	<i>DIHYDROFLAVONOL-4-REDUCTASE</i>
dhZR	Dihydrozeatin riboside
<i>DIN</i>	<i>DARK INDUCED</i>

DPA	Dihydrophaseic acid
<i>DRR</i>	<i>DEHYDRATION RESPONSIVE RD-22 LIKE</i>
EDTA	Ethylenediaminetetraacetic acid
ESI	Electrospray ionization
EV	Empty vector
<i>F3'5'H</i>	<i>FLAVANONE-3'5'HYDROXYLASE</i>
<i>F3H</i>	<i>FLAVANONE-3-HYDROXYLASE</i>
FAO	Food and Agriculture Organization
<i>FGT2</i>	<i>FLAVONOID GLUCOSE TRANSFERASE2</i>
GA1	Gibberellin 1
GA19	Gibberellin 19
GA29	Gibberellin 29
GA3	Gibberellin 3
GA53	Gibberellin 53
GA8	Gibberellin 8
GABA	Gamma-aminobutyric-acid
GAE	Gallic acid equivalent
GCMS	Gas chromatography mass spectrometry
GFP	GREEN FLUORESCENT PROTEIN
GSI	Gene-specific inner reverse primers
GSO	Gene-specific outer reverse primers
<i>HEN1</i>	<i>HUA ENHANCER1</i>
<i>HXK1</i>	<i>HEXOKINASE1</i>



<i>HYL1</i>	<i>HYPONASTIC LEAVES1</i>
IAA	Indole-3-acetic acid
IAA-Asp	N-(indole-3-yl-acetyl)-aspartic acid
IPCC	Intergovernmental Panel on Climate Change
iPR	Isopentenyladenosine
$J_{\max}$	Maximum photosynthetic electron transport
LCMS	Liquid chromatography mass spectrometry
<i>LOB1</i>	<i>LATERAL ORGAN BOUNDARIES-LIKE1</i>
MeOH	Methanol
<i>miR156</i>	<i>microRNA156</i>
miRNA	microRNA
MSTFA	<i>N</i> -methyl- <i>N</i> -[trimethylsilyl] trifluoroacetamide
MVA	Mevalonate pathway
NADP	Nicotinamide adenine dinucleotide phosphate
neo-PA	neo-Phaseic acid
PA	Proanthocyanidins
<i>PAL</i>	<i>PHENYLALANINE AMMONIA-LYASE</i>
<i>PAP1</i>	<i>PRODUCTION OF ANTHOCYANIN PIGMENT1</i>
PCA	Principal component analysis
PG	Peonidin 3-O-glucoside
Pol II	RNA POLYMERASE II
<i>PP2C</i>	<i>2C-TYPE PROTEIN PHOSPHATASES</i>
PPP	Pentose phosphate pathway

Pre-miRNA	Precursor-miRNAs
Pri-miRNA	Primary miRNA
PSI	Photosystem I
<i>PSI</i>	<i>PHOTOSYSTEM I p700 CHLOROPHYLL A APOPROTEIN APS I</i>
<i>PSII</i>	<i>PHOTOSYSTEM II Q(b)</i>
PSII	Photosystem II
<i>PYL9</i>	<i>PYRABACTIN RESISTANCE1-LIKE9</i>
<i>PYR1</i>	<i>PYRABACTIN RESISTANCE1</i>
QC	Quality control
<i>RalGDS</i>	<i>RAL GUANINE NUCLEOTIDE DISSOCIATION STIMULATOR</i>
<i>RCAR</i>	<i>REGULATORY COMPONENT OF ABA RECEPTOR</i>
RH	Relative humidity
<i>RISC</i>	<i>RNA-INDUCED SILENCING COMPLEXES</i>
RNAi	RNA interference
ROS	Reactive oxygen species
RRHD	Rapid resolution high definition
SBD	SPL binding domain
<i>SE</i>	<i>SERRATE</i>
siRNA	Small interfering RNA
<i>SK1</i>	<i>SNORKEL1</i>
<i>SK2</i>	<i>SNORKEL2</i>
<i>SnRK1</i>	<i>SUCROSE NON-FERMENTING-RELATED PROTEIN KINASE1</i>
<i>SnRK2</i>	<i>SUCROSE NON-FERMENTING-RELATED PROTEIN KINASE2</i>

SPEI	Standardized Precipitation and Evapotranspiration Index
<i>SPL</i>	<i>SQUAMOSA-PROMOTER BINDING PROTEIN-LIKE</i>
<i>SUBIA</i>	<i>SUBMERGENCE1A</i>
t-ABA	trans-Abscisic acid
TCA	Tricarboxylic acid
TE	Tris-EDTA
TMA	Total monomeric anthocyanin
TPP	Total polyphenol
<i>TPP</i>	<i>TREHALOSE-6-PHOSPHATE PHOSPHATASE</i>
<i>TPS</i>	<i>TREHALOSE-6-PHOSPHATE SYNTHASE</i>
tsRNA	Transfer RNA-derived small RNAs
t-ZOG	(trans) Zeatin-O-glucoside
UPLC	Ultra performance liquid chromatography
$V_{\text{cmax}}$	Maximum rubisco carboxylase activity
WGCNA	Weighted gene co-expression network
WT	Wild-type
<i>XPO5</i>	<i>EXPORTIN5</i>
Y2H	Yeast-two-hybrid system

# 1. General introduction

## 1.1 Background on *Medicago sativa* (alfalfa)

Alfalfa (*Medicago sativa* L.), one of the most important commercial crops, is well known for its high value as forage for animal feed (Humphries et al., 2018), for its potential as a bioenergy crop (Bhattarai et al., 2013), and as a human food supplement (Bora and Sharma, 2011). The crop is known as the ‘queen of forage’ due to its wide use in the forage industry, owing to its high nutritional benefits to animals (Russelle, 2001). Moreover, the well-established alfalfa root system that ranges between 1.5 to 2.1 m in length (Abdul-Jabbar et al., 1982) reduces soil erosion (Wu et al., 2011), fixes atmospheric nitrogen (Heichel et al., 1981), and helps the plant to establish in marginal lands. Although there are many benefits to growing alfalfa, little attention is given to resolving its production challenges.

The use of conventional breeding techniques in alfalfa is challenging due to its large (800-1000 Mb) autotetraploid ( $2n = 4x = 32$ ) genome (Blondon et al., 1994), and its allogamous (strict out-crossing) reproductive nature (Choi et al., 2004). Accordingly, developing improved cultivars that can withstand biotic and abiotic stresses is lagging. The lack of a publicly available alfalfa genome sequence has necessitated researchers to rely on the genome of the closely related species *Medicago truncatula* (<http://www.medicagogenome.org/>) as a reference genome for molecular genetic studies in alfalfa (Gao et al., 2016; Arshad et al., 2018). As a result, gene identification and functional characterization in alfalfa are difficult, and obtaining stable homozygous transgenic lines is hampered. Partly due to these challenges, the advanced genome editing technique of Clustered Regularly Interspaced Short Palindromic Repeats (CRISPR-Cas9)

known to have high precision in plants resulted in a very low (2.2%) genome editing efficiency in alfalfa (Gao et al., 2018).

Alfalfa production is affected by biotic and abiotic stresses declining acreage over time (Berhonger et al., 2019). For example, in the USA, alfalfa acreage declined between the 1960s and 2016 from 12 to 6.9 million hectares resulting in 33% production loss, while Canada lost 17% of the alfalfa acreage between 2011 and 2016 (Gardner and Putnam, 2018). Moreover, present-day frequent and extreme weather events correlated with climate change aggravate crop losses (Olesen et al., 2011; Ray et al., 2015). To cope with these weather events, plants respond by developing different resilience mechanisms at the phenotypic, physiological, and molecular levels (Theocharis et al., 2012; Hasanuzzaman et al., 2013).

## **1.2 The impact of water availability on crop performance**

According to the Standardized Precipitation and Evapotranspiration Index (SPEI) (<https://spei.csic.es/map/maps.html#months=1#month=5#year=2019>) which has been used to monitor drought since 1955, drought coverage and severity have increased significantly over the past 64 years. The Food and Agricultural Organization (FAO, 2018) reported that between 2005 and 2015 drought caused a loss of \$29 billion USD in developing countries, where rain-fed agriculture is predominant. With reduced water availability, various physiological activities of a plant are affected, mainly photosynthesis, nutrient uptake and transport, and temperature regulation through evaporative cooling (Kreuzwieser and Gessler, 2010; Osakabe et al., 2014). Besides water availability, photosynthesis, which assimilates atmospheric carbon dioxide into sugar, is affected by other climatic factors, such as ambient temperature, and carbon dioxide concentration (Xia

et al., 2014; Cai et al., 2016). Accordingly, investigating the impact of reduced and excess water availability on plant performance, and photosynthesis in particular, is important considering current trends in climate change.

### **1.3 Availability of water to plants and its impact on photosynthesis**

Photosynthesis involves two stages of reactions, a light-dependent one and a predominantly light-independent phase. In the light-dependent phase, water-derived electrons and protons are released as a result of captured light energy by the light harvesting complex (Ferreira et al., 2004; Umena et al., 2011). The light-dependent oxidation of a single water molecule in photosystem II (PSII) generates four electrons and four protons catalyzed by  $Mn_4Ca$  (Umena et al., 2011). Subsequently, the electron is transferred through the electron transport chain into photosystem I (PSI) and produces NADPH by ferredoxin. NADPH and ATP produced in the light-dependent reactions fuel the assimilation of atmospheric carbon dioxide in the dominantly light-independent Calvin-Benson cycle primarily by rubisco carboxylase activity (Kramer et al., 2004). Alternatively, the energy gained by the excited electron from the photosystem II is released in the form of heat or fluorescence (Wobbe et al., 2016). Accordingly, possessing an efficient electron transport chain ( $J_{max}$ ) and maximum rate of rubisco carboxylase activity ( $V_{cmax}$ ) greatly positively affects photosynthesis efficiency under a given environment (Walker et al., 2014).

Reduced plant water potential has both primary and secondary effects on photosynthesis. In the light-dependent reactions, electrons released in the oxygen-evolving complex are replenished by water molecules, producing oxygen in the process (Meyer, 2008). Therefore, as a primary effect, reduced availability of water may result in reduced photosynthesis assimilation. A reduced leaf water potential triggers reduction in stomatal

aperture for retaining moisture, which can have a secondary effect on photosynthesis by 1) reducing carbon dioxide and oxygen uptake and 2) raising leaf temperature affecting the activities of photosynthesis enzymes. Most importantly, water molecules have high thermo-conductance facilitating plant temperature regulation through evaporative cooling (Montero, 2006). Moreover, reduced water potential levels in a plant affects ion and nutrient transport and reduces enzymates efficiency (Figueiredo et al., 2001), including photosynthesis (Lawlor and Cornic, 2002).

Crop production and productivity are affected by climate change, the latter of which, according to the predicted climate models, is expected to be manifested as an increase in the global mean annual temperature and precipitation resulting in frequent flooding events (Alexander et al., 2006; Hirabayashi et al., 2013; Brown et al., 2018; Rogelj et al., 2018). Numerous reports in the literature document the devastating effects of flooding on plant production and productivity (e.g., Bailey-Serres et al., 2012; Brown et al., 2018; Yeung et al., 2018). Depending on the flood water level or duration of the flooding, accessibility of oxygen to the roots is reduced thus hampering root respiration and physiological rhythms. To compensate for the reduced oxygen levels in roots, some plants, such as *Carex* species, anatomically adapt by forming aerenchyma to facilitate oxygen movement from the leaves to the roots (Visser et al., 2000). Regardless of root adaptation to flooding, microorganisms change the oxidative status of some metal and non-metal elements under anaerobic conditions affecting the plant's nutrient uptake (McKee and McKevlin, 1993; Reuzwieser and Rennenberg, 2014). Furthermore, when plants are completely submerged, access to sunlight, oxygen, and carbon dioxide are significantly reduced, which negatively impacts photosynthesis and respiration, resulting in plant death.

## 1.4 Phytohormones and their role in stress tolerance

Phytohormones are vital in regulating various aspects of plant growth, development and interaction with the environment (Ciura and Kruk, 2018). For example, abscisic acid (ABA) functions as a cellular signaling element (Cutler et al., 2010), regulating seed dormancy and germination (Felemban et al., 2019) as well as stomatal aperture upon drought stress (Wan et al., 2009). Moreover, ABA catabolites, such as phaseic acid, contribute to adaptive plasticity of seed plants by activating sub-groups of the ABA receptors for signalling (Weng et al., 2016). Likewise, ethylene is involved in stress signalling (Guo and Ecker, 2004) such as flooding (Xu et al., 2006) and salinity stress (Cao et al., 2008), by inducing an ethylene signalling pathway involving constitutive triple response1 (CTR1), ethylene-insensitive2 (EIN2) (Alonso et al., 1999) and histidine kinase 1 (NTHK1) in tobacco (Cao et al., 2008). Apart from these, ethylene also induces fruit ripening (Gunaseelan et al., 2019).

Auxin plays a central role in the signalling pathways of growth, organogenesis and environmental response by regulating Aux/IAA family of proteins which consists of more than 29 members (Shani et al., 2017). The diverse members of the Aux/IAA proteins play unique and partially overlapping functions to finetune Arabidopsis responses. Similarly, Auxin regulates root development, which is important during drought stress to allow for access to water from deeper soil volumes (Vanneste and Friml, 2009). On the otherhand, cytokinin enhances vegetative growth through cell division and differentiation (Sakakibara, 2006; Perilli et al., 2010). Abiotic stress tolerance is also mediated by cytokinin, either positively in the case of drought through stomatal density by enhancing *Histidine Kinase1 (Ahk1)* (Kumar et al., 2013), or negatively in salt stress tolerance (Wang



et al., 2015a). Gibberellin affects internode elongation (Davière and Achard, 2013; Nagai et al., 2014), which is an important adaptation in flooded plants to overgrow and facilitate leaf aeration. Similarly, brassinosteroids (Bishop and Yokota, 2001) and strigolactones (Waldie et al., 2014; Jia et al., 2019) facilitate plant growth and development. In contrast to the above mentioned phytohormones, jasmonic acid (Farmer and Dubugnon, 2009) and salicylic acid (Chen et al., 1993; Ding et al., 2018) are mainly involved in the plants' response to herbivores and pathogens. Phytohormones can function at their point of synthesis or can be transported through the vascular system to function in other plant parts (Lacombe and Achard, 2016).

Some phytohormones function antagonistically or synergistically in response to environmental changes (Naseem and Dandekar, 2012). For example, with full submergence of plants, petioles tend to grow taller for aeration owing to a mutualistic effect between ethylene and gibberellin while the same environmental condition creates an antagonistic effect between gibberellin and ABA (Voisenek et al., 2003). In other instances, a mutualistic interaction among salicylic acid, jasmonic acid, and ethylene improved immunity to biotic stresses (Pieterse et al., 2012). Under a given environment, multiple stresses are encountered by plants inducing stress-specific mediating phytohormones (Nguyen et al., 2016; Zandalinas et al., 2018). The combined presence of stresses at a given time combined with the crosstalk among different phytohormones highlights the complex interconnections between phytohormones and unknown molecular regulatory factors, many of which remain uncharacterized (Weiss and Ori, 2007; Pieterse et al., 2012; Berens et al., 2019).

## **1.5 Reactive oxygen species (ROS) and ROS-scavenging metabolites under abiotic stress**

Reactive oxygen species (ROS) are by-products of cellular processes, with the main contributors being photosynthesis (in chloroplasts), aerobic metabolism (in mitochondria), and fatty acid beta-oxidation (in peroxisomes) (Asada, 2006). The most common ROS include free radicals such as the superoxide anion ( $O_2^-$ ), hydroxyl radical ( $OH^\cdot$ ), and non-free radicals such as hydrogen peroxide ( $H_2O_2$ ), and singlet oxygen ( $^1O_2$ ) (Tripathy and Oelmüller, 2012). Under normal plant growth conditions, ROS are used in photodamage protection, signal transduction, and in establishing cellular communication (Mittler, 2017; Waszczak et al., 2018). Under biotic and abiotic stresses, the level of ROS increases, affecting cellular integrity by damaging DNA, lipids, protein, and sugars (Van Breusegem and Dat, 2006).

Plants use different strategies to regulate cellular ROS levels, which include the use of primary (e.g., ascorbate) and specialized metabolites (e.g., flavonoids) (Kumari and Parida, 2018; Mishra et al., 2019). Ascorbate (Vitamin C) scavenges hydroxyl radicals, hydrogen peroxide, and superoxide anions (Mhamdi and Van Breusegem, 2018). Flavonoids also scavenge hydroxyl radicals and superoxide anions, but with higher efficiency owing to their higher electron and hydrogen atom donation capacity (Hernández et al., 2009; Mhamdi and Van Breusegem, 2018). So far, over 6000 flavonoids have been identified in plants with subclasses of anthocyanins, flavones, flavonols, flavonones, and dihydroflavonols synthesized via the phenylpropanoid pathway (Iwashina, 2000; Dixon and Pasinetti, 2010). In general, flavonoids have a C6-C3-C6 skeleton as a basic structure with the dihydroxy- $\beta$  ring involved in scavenging ROS (Agati et al., 2012). Plant genotypes

with high concentrations of these primary and specialized metabolites are naturally more tolerant to biotic and abiotic stresses (Zandalinas et al., 2018).

## **1.6 Non-protein-coding microRNAs and their role in abiotic stress tolerance**

The majority of the eukaryotic genome encodes untranslated RNAs with diverse roles in the organism's life cycle (Hou et al., 2019). While greater than 85-90% of the eukaryotic genome can potentially be transcribed (David et al., 2006; Wilhelm et al., 2008), only 1-2% of the RNA is translated into proteins (Tian et al., 2019). Based on sequence length, non-protein-coding RNAs are grouped into short (<200 bp) or long (> 200 bp) categories (Hombach and Kretz, 2016). According to their origins, processing modes, and effector protein associations, short non-protein-coding plant RNAs are classified into microRNAs (miRNA), small interfering RNAs (siRNA), and transfer RNA-derived small RNAs (tsRNA), which regulate target genes at the transcriptional and post-transcriptional levels (Ghildiyal and Zamore, 2009; Chitwood and Timmermans, 2010).

miRNAs are small molecules ranging from 16 to 26 nucleotides in length that regulate gene expression at the posttranscriptional level in a sequence-specific manner by either transcript cleavage or inhibition of mRNA translation (Sun, 2012a). miRNA genes are transcribed by RNA polymerase II (Pol II) and undergo a series of processes before they act on transcripts in the cytoplasm (Lee et al., 2004). The general microRNA biogenesis steps are conserved in the production of miR156 (Xu et al., 2016a) and a simplified illustration of miR156 biogenesis and subsequent mode of action is presented in **Figure 1.2**. First, the transcribed miRNA is trimmed producing a stem-loop (fold-back) transcript to form a pri-miRNA (Axtell and Meyers, 2018). Second, the pri-miRNA is

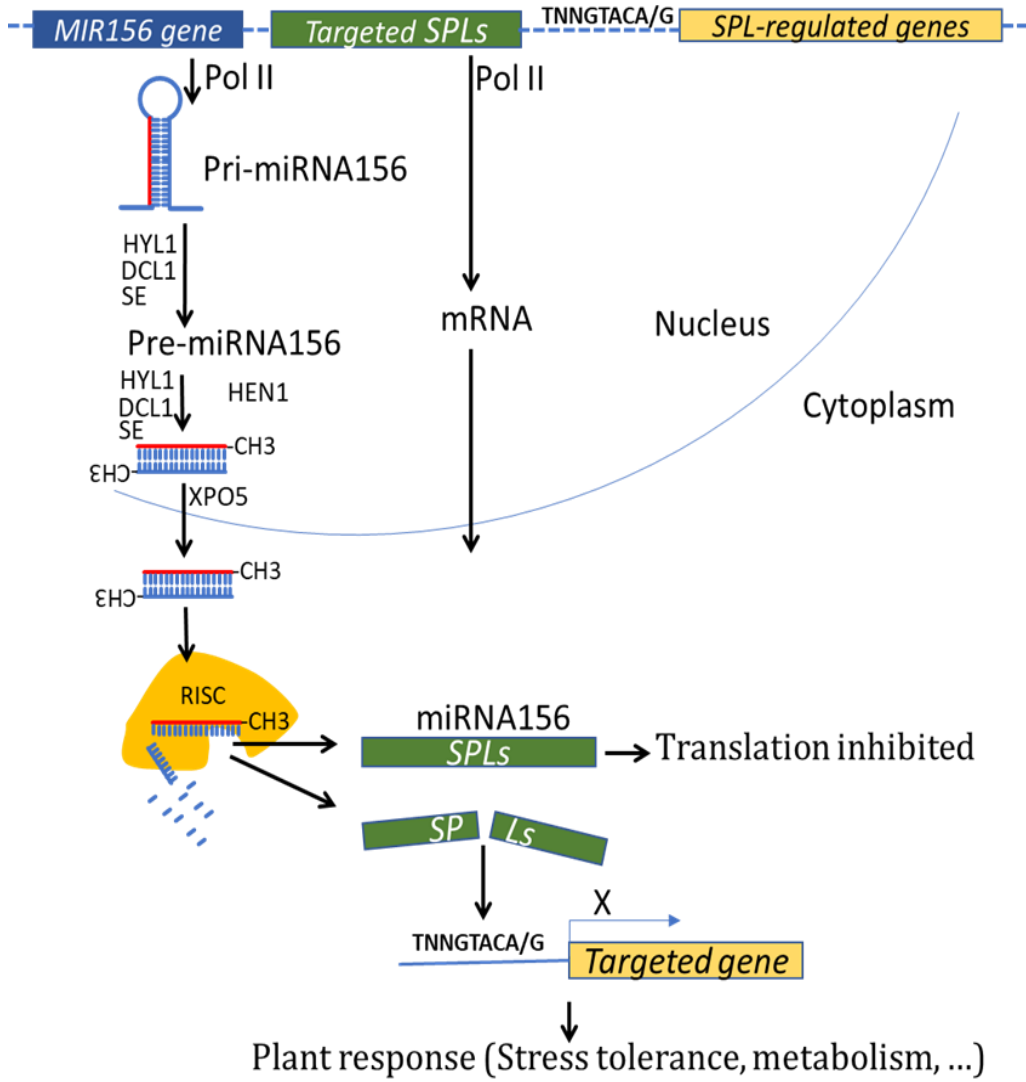
processed by the endonuclease DICER-LIKE1 (DCL1), the RNA binding zinc finger protein SERRTAE (SE), and the HYPONASTIC LEAVES1 (HYL1) to form a pre-miRNA (Rogers and Chen, 2012; Oliver et al., 2017). Subsequently, the pre-miRNA is processed into a miRNA/miRNA duplex, methylated by HUA ENHANCER1 (HEN1) methyltransferase at the 3' terminal, and exported into the cytoplasm by exportin 5 protein (XPO5) (Mateos et al., 2010; Muqbil et al., 2013; Yu et al., 2017). The miRNA duplex binds to the ARGONAUTE (AGO1) component of RNA-Induced Silencing Complexes (RISCs) in the cytoplasm. The duplex is then unwound and the leading strand is used as a guide to target genes in a sequence specific manner by transcript cleavage or by translation inhibition while the second strand is degraded in the cytoplasm (Schwarz et al., 2003; Yu et al., 2017; Armenta-Medina and Gillmor, 2019).

Since the discovery of the first miRNA, *lin-4*, in *Caenorhabditis elegans*, more than 2000 miRNAs (<http://www.mirbase.org>) have been discovered in at least 72 plant species, playing roles in various aspects of plant growth, development and adaptation to the environment (Hannoufa et al., 2018; Armenta-Medina and Gillmor, 2019). For example, overexpression of the highly conserved *miR397* in monocots and dicots (Jones-Rhoades and Bartel, 2004) increases yield in rice by 25% through enhanced panicle branching and grain size (Zhang et al., 2013) while increasing cold tolerance in Arabidopsis (Dong and Pei, 2014). In other findings, *miR397* increased tolerance to drought (Zhao et al., 2007) and oxidative stress (Li et al., 2011) in rice. Likewise, the highly conserved *miR156* (Zhang et al., 2005) enhances plant performance in various plant species.

### **Figure 1.1 miR156 biogenesis and post-transcriptional gene regulation module**

The schematic illustration includes concepts from Yu et al., (2017) and Armenta-Medina and Gillmor (2019). miRNA is transcribed by Pol II producing a stem-loop to form a pri-miRNA followed by further processing into pre-miRNA using the endonuclease DCL1, the RNA binding zinc finger protein SE, and the HYL1. Subsequently, the pre-miRNA is processed into a miRNA-duplex, methylated by HEN1 methyltransferase and exported to cytoplasm using exportin 5 protein. The miRNA-duplex binds to AGO1 component of RISCs (dark-orange colour in the illustration) in the cytoplasm, unwind and the leading strand is used as a guide to target genes in a sequence-specific manner by transcript cleavage or by translation inhibition while the second strand is degraded in the cytoplasm.

DCL1, DICER-LIKE1; HEN1, HUA ENHANCER1; HYL1, HYPOPLASTIC LEAVES1; Pol II, RNA polymerase II; pre-miRNA156, Precursor miRNA156; pri-miRNA156, Primary miRNA156; RISC, RNA-Induced Silencing Complexes; SE, SERRTAE; SPL, SQUAMOSA-PROMOTER BINDING PROTEIN-LIKE; XPO5, exportin5. microRNA coding regions of DNA are indicated with blue boxes while green boxes are for miR156-regulated SPLs. SPL-regulated genes are indicated with orange boxes containing SPL-binding target sequences of `TNNGTACA/G` where N is any nucleotide but identical sequentially.



For example, increased expression levels of *miR156* improved tolerance to salinity (Arshad et al., 2017b), drought (Arshad et al., 2017a), and heat (Matthews et al., 2019) stress in alfalfa. Moreover, miR156 improved abiotic stress tolerance in other species, such as salinity and drought tolerance in *Arabidopsis* (Liu et al., 2008; Cui et al., 2014) and drought tolerance in switchgrass (Sun et al., 2012b). On the other hand, overexpression of *miR156* decreased cold tolerance in maize (Cui et al., 2015).

### **1.7 miR156/SPL network and its impact on plant performance**

miR156 regulates the expression of *SQUAMOSA-PROMOTER BINDING PROTEIN-LIKE* (SPL) transcription factors to impact plant performance (Aung et al., 2015a; Gao et al., 2016). In addition, tissue and developmental stage-dependent expression of *miR156*, along with its coordinated expression with other microRNAs, shapes the plant (Yu et al., 2015). SPLs regulate the expression of a plethora of genes that regulate plant growth and development by binding to gene promoters at a consensus DNA sequence NNGTACR (where N= any nucleotide but identical sequentially, R=A or G) known as the SPL Binding Domain (SBD) (Yamaguchi et al., 2009; Wei et al., 2012; Aung et al., 2015b; Xu et al., 2016b).

SPLs regulate the expression of downstream genes positively or negatively (**Figure 1.2**). For example, in *Arabidopsis*, the expression of *DFR* is downregulated by SPL9 in which SPL9 destabilizes and prevents transcription factor complexes from assembling and transcribing *DFR* (Stief et al., 2014). Accordingly, with enhanced levels of miR156, mRNA of SPL9 is cleaved and prevented from translation process which represses the expression of *DFR*. On the otherhand, SPLs also positively regulate the expression of downstream genes. For example, in rice, it was observed that SPLs triggered inflorescence

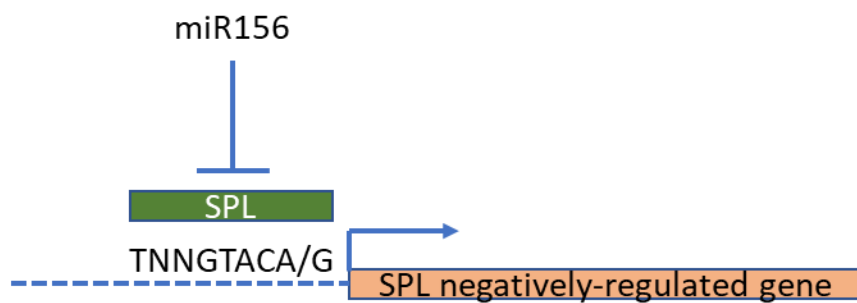
meristem and spikelet transition by regulating the *miR172/AP2* and *PANICLE PHYTOMER2 (PAP2)/Rice TFL1/CEN homolog 1 (RCN1)* pathways (Wang et al., 2015b). SPL-regulated transition of developmental stages (vegetative to reproductive) involves another microRNA, miR172, a negative regulator of miR156, where SPL positively regulates the expression of miR172. Moreover, the induction of flowering meristems is mediated by AP2 (Apetalla 2) and its expression is positively regulated by SPL. In addition, the expression of miR156, negative regulator of flowering in rice and other crops, is downregulated by miR172. Accordingly, the interplay among SPL, miR172 and AP2 combined with reduced level of miR156 trigger the transition of meristematic cells into inflorescence. The schematic representation in which the positive and negative roles of SPLs in gene expression governed by the interplay between SPL and miR156 is presented in **Figure 1.2**.



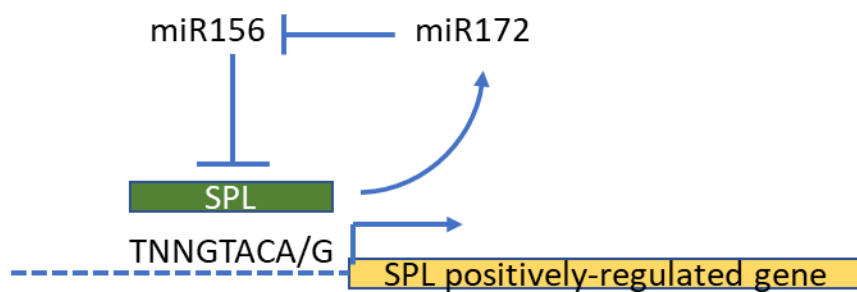
**Figure 1.2 miR156/SPL module-based gene expression regulation**

SPLs are involved in regulating gene expression either (A) negatively, or (B) positively. The negative role of SPLs in regulating gene expression involve miR156 which cleaves SPL mRNA and uplifts the repressive role of SPL. On the other hand, to increase the expression of genes which are positively regulated by SPL, other microRNAs, such as miR172, are involved to reduce the repressive role of miR156. SPL, SQUAMOSA-PROMOTER BINDING PROTEIN-LIKE transcription factors. SPL proteins are represented by green bars. Negatively and positively SPL-regulated genes are indicated with light red and yellow boxes, respectively.

(A)



(B)



Despite the conservation of miR156 among plant species, some of its regulation outputs are species-specific (Wang et al., 2015b; Aung et al., 2015b; 2015c). For example, some of the effects of the increased expression of *miR156* in potato tubers and during fruit development in tomato are absent in Arabidopsis. Moreover, overexpression of *miR156* reduced nodulation in *Lotus japonicus* (Wang et al., 2015b) while increasing it in *M. sativa* (Aung et al., 2015b). In Arabidopsis, miR156 regulates 11 out of 17 *SPLs*, affecting various aspects of plant growth and development (Wu et al., 2009; Yu et al., 2015). On the other hand, only seven of 17 *SPLs* found in barley have miR156 complementary sequence (Tripathi et al., 2018). Previously, it was determined in alfalfa that miR156 regulates at least seven *SPLs* (*SPL2*, *SPL3*, *SPL4*, *SPL6*, *SPL9*, *SPL12*, and *SPL13*) (Gao et al., 2016), necessitating further investigation to identify other *SPLs* and their potential role in alfalfa.

## **1.8 Hypothesis and objectives of the study**

**Hypothesis:** I hypothesize that miR156, through its effect on the expression of *SPL* genes and other downstream genes, alters specialized metabolite profiles under water stress in alfalfa.

**Objectives:** The main purpose of this research is to investigate the role of miR156 and its target *SPL* genes in improving drought and flooding resilience in alfalfa. The specific objectives are:

### **Specific objectives**

**1. Determine the effect of miR156 on primary and specialized metabolite profiles under abiotic stress.** The metabolite profile of alfalfa under abiotic stress using Gas and

Liquid Chromatography Mass Spectrometry (GCMS and LCMS) and spectrophotometric analysis will be investigated.

**2. Investigate the physiological, hormonal and phenotypic resilience mechanisms associated with *miR156* overexpression (*miR156OE*) and *SPL13* silencing during abiotic stress.** Photosynthetic and relative water potential parameters of physiological and phenotypic responses of alfalfa plants in *miR156* overexpression and *SPL13RNAi* plants will be determined. Moreover, with the use of LCMS analysis, the hormonal profiles of selected alfalfa genotypes in response to flooding stress will be determined.

**3. Characterize SPLs regulated by miR156 during drought and flooding stress and downstream genes regulated by these SPLs.** Through the use of transcriptomics, phenotypic analysis and hormone profiling, *SPL13* will be characterized for its role in drought and flooding stress tolerance in alfalfa. Moreover, new SPLs will be identified and investigated for their potential role in flooding tolerance.

**4. Determine the mode of action of the miR156/SPL network in regulating drought and flooding stress in alfalfa.** The *miR156* mode of action in regulating drought and flooding stress in alfalfa will be determined using transcriptomics, metabolomics, and phenomics and a working model will be formulated.

### **Significance of the project**

The long-term objective of this thesis is to generate knowledge that will shed light on the mechanism of action of *miR156* and SPLs in affecting drought and flooding stress resilience in alfalfa. Also, molecular tools for potential use by the breeding industry to improve alfalfa traits and resources for scientific knowledge will be generated.

## 1.9. References

**Abdul-Jabbar AS, Sammis TW, Lugg DG** (1982) Effect of moisture level on the root pattern of alfalfa. *Irrigation Science* 3: 197-207

**Agati G, Azzarello E, Pollastri S, Tattini M** (2012) Flavonoids as antioxidants in plants: Location and functional significance. *Plant Science* 196: 67-76

**Alexander LV, Zhang X, Peterson TC, Caesar J, Gleason B, Klein Tank AMG, Haylock M, Collins D, Trewin B, Rahimzadeh F, Tagipour A, Rupa Kumar K, Revadekar J, Griffiths G, Vincent L, Stephenson DB, Burn J, Aguilar E, Brunet M, Taylor M, New M, Zhai P, Rusticucci M, Vazquez-Aguirre JL** (2006) Global observed changes in daily climate extremes of temperature and precipitation. *Journal of Geophysical Research: Atmospheres* 111

**Alonso JM, Hirayama T, Roman G, Nourizadeh S, Ecker JR** (1999) EIN2, a bifunctional transducer of ethylene and stress responses in *Arabidopsis*. *Science* 284:2148–2152

**Armenta-Medina A, Gillmor CS** (2019) An introduction to methods for discovery and functional Analysis of microRNAs in plants. In S de Folter, ed, *Plant MicroRNAs: Methods and Protocols*, Springer, New York, 1932: 1-14

**Arshad M, Gruber MY, Hannoufa A** (2018) Transcriptome analysis of *microRNA156* overexpression alfalfa roots under drought stress. *Scientific Reports* 8: 9363

**Arshad M, Feyissa B, Amyot L, Aung B, Hannoufa A** (2017a) *microRNA156* improves drought stress tolerance in alfalfa (*Medicago sativa*) by silencing *SPL13*. *Plant Science* 258: 122-136

**Arshad M, Gruber MY, Wall K, Hannoufa A** (2017b) An insight into *microRNA156* role in salinity stress responses of alfalfa. *Frontiers in Plant Science* 8: 356

**Asada K** (2006) Production and scavenging of reactive oxygen species in chloroplasts and their functions. *Plant Physiology* 141: 391-396

**Aung B, Gruber MY, Amyot L, Omari K, Bertrand A, Hannoufa A** (2015a) Ectopic expression of *LjmiR156* delays flowering, enhances shoot branching, and improves forage quality in alfalfa. *Plant Biotechnology Reports* 9: 379-393

**Aung B, Gruber MY, Amyot L, Omari K, Bertrand A, Hannoufa A** (2015b) *microRNA156* as a promising tool for alfalfa improvement. *Plant Biotechnology Journal* 13: 779-790

**Aung B, Gruber MY, Hannoufa A** (2015c) The microRNA156 system: A tool in plant biotechnology. *Biocatalysis and Agricultural Biotechnology* 4: 432-442

**Axtell MJ, Meyers BC** (2018) Revisiting criteria for plant microRNA annotation in the era of big data. *The Plant Cell* 30: 272-284

**Bailey-Serres J, Lee SC, Brinton E** (2012) Water proofing crops: Effective flooding survival strategies. *Plant Physiology* 160: 1698-1709

**Berens ML, Wolinska KW, Spaepen S, Ziegler J, Nobori T, Nair A, Krüler V, Winkelmüller TM, Wang Y, Mine A, Becker D, Garrido-Oter R, Schulze-Lefert P, Tsuda K** (2019) Balancing trade-offs between biotic and abiotic stress responses through leaf age-dependent variation in stress hormone cross-talk. *Proceedings of the National Academy of Sciences of the United States of America* 116: 2364-2373

**Berhongaray G, Basanta M, Jauregui JM** (2019) Water table depth affects persistence and productivity of alfalfa in central Argentina. *Field Crops Research* 235: 54-58

**Bhattarai K, Brummer C, Monteros MJ** (2013) Alfalfa as a bioenergy crop. In MC Saha, HS Bhandari, JH Bouton, eds, *Bioenergy Feedstocks*: 207-231

**Bishop GJ, Yokota T** (2001) Plants steroid hormones, brassinosteroids: Current highlights of molecular aspects on their synthesis/metabolism, transport, perception and response. *Plant and Cell Physiology* 42: 114-120

**Blondon F, Marie D, Brown S, Kondorosi A** (1994) Genome size and base composition in *Medicago sativa* and *M. truncatula* species. *Genome* 37: 264-270

**Bora KS, Sharma A** (2011) Phytochemical and pharmacological potential of *Medicago sativa*: A review. *Pharmaceutical Biology* 49: 211-220

**Brown S, Nicholls RJ, Lázár AN, Hornby DD, Hill C, Hazra S, Appeaning Addo K, Haque A, Caesar J, Tompkins EL** (2018) What are the implications of sea-level rise for a 1.5, 2 and 3 °C rise in global mean temperatures in the Ganges-Brahmaputra-Meghna and other vulnerable deltas? *Regional Environmental Change* 18: 1829-1842

**Cai C, Yin X, He S, Jiang W, Si C, Struik PC, Luo W, Li G, Xie Y, Xiong Y, Pan G** (2016) Responses of wheat and rice to factorial combinations of ambient and elevated CO<sub>2</sub> and temperature in FACE experiments. *Global Change Biology* 22: 856-874

**Cao YR, Chen SY, Zhang J S** (2008) Ethylene signaling regulates salt stress response: An overview. *Plant Signaling and Behavior*, 3(10): 761-763.

**Chen Z, Silva H, Klessig D** (1993) Active oxygen species in the induction of plant systemic acquired resistance by salicylic acid. *Science* 262: 1883-1886

**Chitwood DH, Timmermans MCP** (2010) Small RNAs are on the move. *Nature* 467: 415

**Choi HK, Mun JH, Kim DJ, Zhu H, Baek JM, Mudge J, Roe B, Ellis N, Doyle J, Kiss GB, Young ND, Cook DR** (2004) Estimating genome conservation between crop and model legume species. *Proceedings of the National Academy of Sciences of the United States of America* 101: 15289-15294

**Ciura J, Kruk J** (2018) Phytohormones as targets for improving plant productivity and stress tolerance. *Journal of Plant Physiology* 229: 32-40

**Cui LG, Shan JX, Shi M, Gao JP, Lin HX** (2014) The miR156-SPL9-DFR pathway coordinates the relationship between development and abiotic stress tolerance in plants. *The Plant Journal* 80: 1108-1117

**Cui N, Sun X, Sun M, Jia B, Duanmu H, Lv D, Duan X, Zhu Y** (2015) Overexpression of *OsmiR156k* leads to reduced tolerance to cold stress in rice (*Oryza Sativa*). *Molecular Breeding* 35: 214

**Cutler SR, Rodriguez PL, Finkelstein RR, Abrams SR** (2010) Abscisic acid: Emergence of a core signaling network. *Annual Review of Plant Biology* 61: 651-679

**David L, Huber W, Granovskaia M, Toedling J, Palm CJ, Bofkin L, Jones T, Davis RW, Steinmetz LM** (2006) A high-resolution map of transcription in the yeast genome. *Proceedings of the National Academy of Sciences of the United States of America* 103: 5320-5325

**Davière J-M, Achard P** (2013) Gibberellin signaling in plants. *Development* 140: 1147-1151

**Ding Y, Sun T, Ao K, Peng Y, Zhang Y, Li X, Zhang Y** (2018) Opposite roles of salicylic acid receptors NPR1 and NPR3/NPR4 in transcriptional regulation of plant immunity. *Cell* 173: 1454-1467

**Dixon RA, Pasinetti GM** (2010) Flavonoids and isoflavonoids: From plant biology to agriculture and neuroscience. *Plant Physiology* 154: 453-457

**Dong C-H, Pei H** (2014) Over-expression of miR397 improves plant tolerance to cold stress in *Arabidopsis thaliana*. *Journal of Plant Biology* 57: 209-217

**FAO** (2018) The impact of disasters and crises on agriculture and food security. In *Impact of natural disasters on crop and livestock production in developing countries*. Food and Agriculture Organization of the United Nation, Rome: 23-37

- Farmer EE, Dubugnon L** (2009) Detritivorous crustaceans become herbivores on jasmonate-deficient plants. *Proceedings of the National Academy of Sciences of the United States of America* 106: 935-940
- Felemban A, Braguy J, Zurbriggen MD, Al-Babili S** (2019) Apocarotenoids involved in plant development and stress response. *Frontiers in Plant Science* 10:1168
- Ferreira KN, Iverson TM, Maghlaoui K, Barber J, Iwata S** (2004) Architecture of the photosynthetic oxygen-evolving center. *Science* 303: 1831
- Figueiredo MdVB, Bezerra-Neto E, Burity HA** (2001) Water stress response on the enzymatic activity in cowpea nodules. *Brazilian Journal of Microbiology*. 32: 195-200
- Gao R, Austin RS, Amyot L, Hannoufa A** (2016) Comparative transcriptome investigation of global gene expression changes caused by *miR156* overexpression in *Medicago sativa*. *BMC Genomics* 17: 658
- Gao R, Feyissa BA, Croft M, Hannoufa A** (2018) Gene editing by CRISPR/Cas9 in the obligatory outcrossing *Medicago sativa*. *Planta* 247: 1043-1050
- Gardner D, Putnam D** (2018) Alfalfa situation in the USA and Canada. In Daniel Basigalup, María del Carmen Spada, Ariel Odorizzi, V Arolfo, eds, *Second World Alfalfa Congress: Global interaction for alfalfa innovation*, CORDOBA, ARGENTINA: 30-33
- Ghildiyal M, Zamore PD** (2009) Small silencing RNAs: an expanding universe. *Nature Reviews Genetics* 10: 94
- Gunaseelan K, McAtee PA, Nardozza S, Pidakala P, Wang R, David K, Burdon J, Schaffer RJ** (2019) Copy number variants in kiwifruit ETHYLENE RESPONSE FACTOR/APETALA2 (ERF/AP2)-like genes show divergence in fruit ripening associated cold and ethylene responses in C-REPEAT/DRE BINDING FACTOR-like genes. *PLOS ONE* 14: e0216120
- Guo H, Ecker JR** (2004) The ethylene signaling pathway: New insights. *Current Opinion in Plant Biology* 7: 40-49
- Hannoufa A, Matthews C, Feyissa BA, Gruber MY, Arshad M** (2018) Progress toward deep sequencing-based discovery of stress-related MicroRNA in plants and available bioinformatics tools. In: *Progress in Botany*. Springer, Berlin, Heidelberg 1:36
- Hasanuzzaman M, Nahar K, Alam MM, Roychowdhury R, Fujita M** (2013) Physiological, biochemical, and molecular mechanisms of heat stress tolerance in plants. *International Journal of Molecular Sciences* 14: 9643-9684



**Heichel GH, Barnes DK, Vance CP** (1981) Nitrogen fixation of alfalfa in the seeding Year. *Crop Science* 21: 330-335

**Hernández I, Alegre L, Van Breusegem F, Munné-Bosch S** (2009) How relevant are flavonoids as antioxidants in plants? *Trends in Plant Science* 14: 125-132

**Hirabayashi Y, Mahendran R, Koirala S, Konoshima L, Yamazaki D, Watanabe S, Kim H, Kanae S** (2013) Global flood risk under climate change. *Nature Climate Change* 3: 816

**Hombach S, Kretz M** (2016) Non-coding RNAs: Classification, biology and functioning. In Slaby O., C G., eds, *Advances in Experimental Medicine and Biology* 937: 3-17

**Hou J, Lu D, Mason AS, Li B, Xiao M, An S, Fu D** (2019) Non-coding RNAs and transposable elements in plant genomes: Emergence, regulatory mechanisms and roles in plant development and stress responses. *Planta* 250: 23-40

**Humphries A, Ovalle C, del Pozo A, Inostroza L, Barahona V, Ivelic-Saez J, Yu L, Yerzhanova S, Meirman G, Abayev S, Brummer E, Hughes S, Bingham E, Kilian B** (2018) Introgression of alfalfa crop wild relatives for climate change adaptation. In Daniel Basigalup, María del Carmen Spada, Ariel Odorizzi, V Arolfo, eds, *Second World Alfalfa Congress: Global interaction for alfalfa innovation, CORDOBA, ARGENTINA*: 72-76

**Iwashina T** (2000) The structure and distribution of the flavonoids in plants. *Journal of Plant Research* 113: 287-299

**Jia K-P, Li C, Bouwmeester HJ, Al-Babili S** (2019) Strigolactone biosynthesis and signal transduction. In H Koltai, C Prandi, eds, *Strigolactones - biology and applications*. Springer International Publishing, Cham: 1-45

**Jones-Rhoades MW, Bartel DP** (2004) Computational identification of plant microRNAs and their targets, including a stress-induced miRNA. *Molecular Cell* 14: 787-799

**Kramer DM, Avenson TJ, Edwards GE** (2004) Dynamic flexibility in the light reactions of photosynthesis governed by both electron and proton transfer reactions. *Trends in Plant Science* 9: 349-357

**Kreuzwieser J, Gessler A** (2010) Global climate change and tree nutrition: Influence of water availability. *Tree Physiology* 30: 1221-1234

**Kumar MN, Jane WN, Verslues PE** (2013) Role of the putative osmosensor Arabidopsis *Histidine Kinase1* in dehydration avoidance and low-water-potential response. *Plant Physiology* 161 (2): 942-953

- Kumari A, Parida AK** (2018) Metabolomics and network analysis reveal the potential metabolites and biological pathways involved in salinity tolerance of the halophyte *Salvadora persica*. *Environmental and Experimental Botany* 148: 85-99
- Lacombe B, Achard P** (2016) Long-distance transport of phytohormones through the plant vascular system. *Current Opinion in Plant Biology* 34: 1-8
- Lawlor DW, Cornic G** (2002) Photosynthetic carbon assimilation and associated metabolism in relation to water deficits in higher plants. *Plant, Cell and Environment* 25: 275-294
- Lee Y, Kim M, Han J, Yeom K-H, Lee S, Baek SH, Kim VN** (2004) microRNA genes are transcribed by RNA polymerase II. *The EMBO Journal* 23: 4051-4060
- Li T, Li H, Zhang Y-X, Liu J-Y** (2011) Identification and analysis of seven H<sub>2</sub>O<sub>2</sub>-responsive miRNAs and 32 new miRNAs in the seedlings of rice (*Oryza sativa* L. ssp. indica). *Nucleic Acids Research* 39: 2821-2833
- Liu H-H, Tian X, Li Y-J, Wu C-A, Zheng C-C** (2008) Microarray-based analysis of stress-regulated microRNAs in *Arabidopsis thaliana*. *RNA* 14: 836-843
- Mateos JL, Bologna NG, Chorostecki U, Palatnik JF** (2010) Identification of MicroRNA processing determinants by random mutagenesis of *Arabidopsis* miR172a Precursor. *Current Biology* 20: 49-54
- Matthews C, Arshad M, Hannoufa A** (2019) Alfalfa response to heat stress is modulated by microRNA156. *Physiologia Plantarum* 165: 830-842
- McKee Jr. WH, McKevelin MR** (1993) Geochemical processes and nutrient uptake by plants in hydric soils. *Environmental Toxicology and Chemistry* 12: 2197-2207
- Meyer TJ** (2008) The art of splitting water. *Nature* 451: 778-779
- Mhamdi A, Van Breusegem F** (2018) Reactive oxygen species in plant development. *Development* 145: dev164376
- Mishra B, Chand S, Singh Sangwan N** (2019) ROS management is mediated by ascorbate-glutathione- $\alpha$ -tocopherol triad in co-ordination with secondary metabolic pathway under cadmium stress in *Withania somnifera*. *Plant Physiology and Biochemistry* 139: 620-629
- Mittler R** (2017) ROS are good. *Trends in Plant Science* 22: 11-19

**Montero JI** (2006) Evaporative cooling in greenhouse: Effect on microclimate, water use efficiency and plant respons. In, Ed 719. International Society for Horticultural Science (ISHS), Leuven, Belgium: 373-384

**Muqbil I, Bao B, Abou-Samra AB, Mohammad RM, Azmi AS** (2013) Nuclear export mediated regulation of microRNAs: Potential target for drug intervention. *Current Drug Targets* 14: 1094-1100

**Nagai K, Kondo Y, Kitaoka T, Noda T, Kuroha T, Angeles-Shim RB, Yasui H, Yoshimura A, Ashikari M** (2014) QTL analysis of internode elongation in response to gibberellin in deepwater rice. *AoB PLANTS* 6: plu028

**Naseem M, Dandekar T** (2012) The role of auxin-cytokinin antagonism in plant-pathogen interactions. *PLOS PATHOGENS* 8: e1003026

**Nguyen D, Rieu I, Mariani C, van Dam NM** (2016) How plants handle multiple stresses: Hormonal interactions underlying responses to abiotic stress and insect herbivory. *Plant Molecular Biology* 91: 727-740

**Olesen JE, Trnka M, Kersebaum KC, Skjelvåg AO, Seguin B, Peltonen-Sainio P, Rossi F, Kozyra J, Micale F** (2011) Impacts and adaptation of european crop production systems to climate change. *European Journal of Agronomy* 34: 96-112

**Oliver C, Pradillo M, Jover-Gil S, Cuñado N, Ponce MR, Santos JL** (2017) Loss of function of Arabidopsis microRNA-machinery genes impairs fertility, and has effects on homologous recombination and meiotic chromatin dynamics. *Scientific Reports* 7: 9280

**Osakabe Y, Osakabe K, Shinozaki K, Tran L-SP** (2014) Response of plants to water stress. *Frontiers in Plant Science* 5: 86-86

**Perilli S, Moubayidin L, Sabatini S** (2010) The molecular basis of cytokinin function. *Current Opinion in Plant Biology* 13: 21-26

**Pieterse CMJ, Van der Does D, Zamioudis C, Leon-Reyes A, Van Wees SCM** (2012) Hormonal modulation of plant immunity. *Annual Review of Cell and Developmental Biology* 28: 489-521

**Ray DK, Gerber JS, MacDonald GK, West PC** (2015) Climate variation explains a third of global crop yield variability. *Nature Communications* 6: 5989

**Reuzwieser J, Rennenberg H** (2014) Molecular and physiological responses of trees to waterlogging stress. *Plant, Cell and Environment* 37: 2245-2259

**Rogelj J, Popp A, Calvin KV, Luderer G, Emmerling J, Gernaat D, Fujimori S, Strefler J, Hasegawa T, Marangoni G, Krey V, Kriegler E, Riahi K, van Vuuren DP,**

**Rogers K, Chen X** (2012) microRNA biogenesis and turnover in plants. *Cold Spring Harbor Symposia on Quantitative Biology* 77: 183-194

**Russelle MP** (2001) Alfalfa: After an 8,000-year journey, the "Queen of Forages" stands poised to enjoy renewed popularity. *American Scientist* 89: 252-261

**Sakakibara H** (2006) Cytokinins: Activity, biosynthesis, and translocation. *Annual Review of Plant Biology* 57: 431-449

**Schwarz DS, Hutvagner G, Du T, Xu Z, Aronin N, Zamore PD** (2003) Asymmetry in the assembly of the RNAi enzyme complex. *Cell* 115: 199-208

**Shani E, Salehin M, Zhang Y, Sanchez S, Doherty C, Wang R, Mangado C, Song L, Tal I, Pisanty O, Ecker J, Kay S, Pruneda-Paz J, Estelle M** (2017) Plant Stress Tolerance Requires Auxin-Sensitive Aux/IAA Transcriptional Repressors, *Current Biology* 27 (3):437-444

**Stief A, Altmann S, Hoffmann K, Pant BD, Scheible WR, Baurle I** (2014) Arabidopsis miR156 regulates tolerance to recurring environmental stress through SPL transcription factors. *The Plant Cell* 26: 1792-1807

**Sun G** (2012a) microRNAs and their diverse functions in plants. *Plant Molecular Biology* 80: 17-36

**Sun G, Stewart CN, Jr., Xiao P, Zhang B** (2012b) microRNA expression analysis in the cellulosic biofuel crop switchgrass (*Panicum virgatum*) under abiotic stress. *PLOS ONE* 7: e32017

**Theocharis A, Clément C, Barka EA** (2012) Physiological and molecular changes in plants grown at low temperatures. *Planta* 235: 1091-1105

**Tian Y, Bai S, Dang Z, Hao J, Zhang J, Hasi A** (2019) Genome-wide identification and characterization of long non-coding RNAs involved in fruit ripening and the climacteric in *Cucumis melo*. *BMC Plant Biology* 19: 369

**Tripathi RK, Bregitzer P, Singh J** (2018) Genome-wide analysis of the SPL/miR156 module and its interaction with the AP2/miR172 unit in barley. *Scientific Reports* 8: 7085

**Tripathy BC, Oelmüller R** (2012) Reactive oxygen species generation and signaling in plants. *Plant Signaling and Behavior* 7: 1621-1633

**Umena Y, Kawakami K, Shen J-R, Kamiya N** (2011) Crystal structure of oxygen-evolving photosystem II at a resolution of 1.9 Å. *Nature* 473: 55-60

- Van Breusegem F, Dat JF** (2006) Reactive oxygen species in plant cell death. *Plant Physiology* 141: 384-390
- Vanneste S, Friml J** (2009) Auxin: A trigger for change in plant development. *Cell* 136: 1005-1016
- Visser EJW, BÖGemann GM, Van De Steeg HM, Pierik R, Blom CWPM** (2000) Flooding tolerance of *Carex* species in relation to field distribution and aerenchyma formation. *New Phytologist* 148: 93-103
- Voesenek LACJ, Benschop JJ, Bou J, Cox MCH, Groeneveld HW, Millenaar FF, Vreeburg RAM, Peeters AJM** (2003) Interactions between plant hormones regulate submergence-induced shoot elongation in the flooding-tolerant dicot *Rumex palustris*. *Annals of Botany* 91: 205-211
- Waldie T, McCulloch H, Leyser O** (2014) Strigolactones and the control of plant development: Lessons from shoot branching. *The Plant Journal* 79: 607-622
- Walker AP, Beckerman AP, Gu L, Kattge J, Cernusak LA, Domingues TF, Scales JC, Wohlfahrt G, Wullschlegel SD, Woodward FI** (2014) The relationship of leaf photosynthetic traits -  $V_{cmax}$  and  $J_{max}$  - to leaf nitrogen, leaf phosphorus, and specific leaf area: A meta-analysis and modeling study. *Ecology and Evolution* 4: 3218-3235
- Wan J, Griffiths R, Ying J, McCourt P, Huang Y** (2009) Development of drought-tolerant canola (*Brassica napus* L.) through genetic modulation of ABA-mediated stomatal responses. *Crop Science* 49: 1539-1554
- Wang Y, Shen W, Chan Z, Wu Y** (2015a) Endogenous cytokinin overproduction modulates ROS homeostasis and decreases salt stress resistance in *Arabidopsis thaliana*. *Frontier in Plant Sciences* 6:1004
- Wang L, Sun S, Jin J, Fu D, Yang X, Weng X, Xu C, Li X, Xiao J, Zhang Q** (2015b) Coordinated regulation of vegetative and reproductive branching in rice. *Proceedings of the National Academy of Sciences of the United States of America* 112: 15504-15509
- Waszczak C, Carmody M, Kangasjärvi J** (2018) Reactive oxygen species in plant signaling. *Annual Review of Plant Biology* 69: 209-236
- Wei S, Gruber MY, Yu B, Gao M-J, Khachatourians GG, Hegedus DD, Parkin IA, Hannoufa A** (2012) *Arabidopsis* mutant sk156 reveals complex regulation of SPL15 in a miR156-controlled gene network. *BMC Plant Biology* 12: 169
- Weiss D, Ori N** (2007) Mechanisms of cross talk between gibberellin and other hormones. *Plant Physiology* 144: 1240-1246

- Weng JK, Ye M, Li B, Noel JP** (2016) Co-evolution of hormone metabolism and signaling networks expands plant adaptive plasticity. *Cell* 166: 881-893
- Wilhelm BT, Marguerat S, Watt S, Schubert F, Wood V, Goodhead I, Penkett CJ, Rogers J, Bähler J** (2008) Dynamic repertoire of a eukaryotic transcriptome surveyed at single-nucleotide resolution. *Nature* 453: 1239-1243
- Wobbe L, Bassi R, Kruse O** (2016) Multi-level light capture control in plants and green algae. *Trends in Plant Science* 21: 55-68
- Wu G, Park MY, Conway SR, Wang J-W, Weigel D, Poethig RS** (2009) The sequential action of miR156 and miR172 regulates developmental timing in *Arabidopsis*. *Cell* 138: 750-759
- Wu S, Wu P, Feng H, Merkley GP** (2011) Effects of alfalfa coverage on runoff, erosion and hydraulic characteristics of overland flow on loess slope plots. *Frontiers of Environmental Science and Engineering in China* 5: 76-83
- Xia JB, Zhang GC, Wang RR, Zhang SYJP** (2014) Effect of soil water availability on photosynthesis in *Ziziphus jujuba* var. *spinus* in a sand habitat formed from seashells: Comparison of four models. *Photosynthetica* 52: 253-261
- Xu K, Xu X, Fukao T, Canlas P, Maghirang-Rodriguez R, Heuer S, Ismail AM, Bailey-Serres J, Ronald PC, Mackill DJ** (2006) Sub1A is an ethylene-response-factor-like gene that confers submergence tolerance to rice. *Nature* 442: 705-708
- Xu M, Hu T, Smith MR, Poethig RS** (2016a) Epigenetic regulation of vegetative phase change in *Arabidopsis*. *The Plant Cell* 28: 28-41
- Xu M, Hu T, Zhao J, Park M-Y, Earley KW, Wu G, Yang L, Poethig RS** (2016b) Developmental functions of miR156-regulated SQUAMOSA PROMOTER BINDING PROTEIN-LIKE (SPL) genes in *Arabidopsis thaliana*. *PLOS Genetics* 12: e1006263
- Yamaguchi A, Wu M-F, Yang L, Wu G, Poethig RS, Wagner D** (2009) The microRNA-regulated SBP-Box transcription factor SPL3 is a direct upstream activator of LEAFY, FRUITFULL, and APETALA1. *Developmental Cell* 17: 268-278
- Yeung E, van Veen H, Vashisht D, Sobral Paiva AL, Hummel M, Rankenberg T, Steffens B, Steffen-Heins A, Sauter M, de Vries M, Schuurink RC, Bazin J, Bailey-Serres J, Voisenek LACJ, Sasidharan R** (2018) A stress recovery signaling network for enhanced flooding tolerance in *Arabidopsis thaliana*. *Proceedings of the National Academy of Sciences of the United States of America* 115: E6085-E6094
- Yu N, Niu Q-W, Ng K-H, Chua N-H** (2015) The role of miR156/SPLs modules in *Arabidopsis* lateral root development. *Plant Journal* 83: 673-685

**Yu Y, Jia T, Chen X** (2017) The ‘how’ and ‘where’ of plant microRNAs. *New Phytologist* 216: 1002-1017

**Zandalinas SI, Mittler R, Balfagón D, Arbona V, Gómez-Cadenas A** (2018) Plant adaptations to the combination of drought and high temperatures. *Physiologia Plantarum* 162: 2-12

**Zhang BH, Pan XP, Cannon CH, Cobb GP, Anderson TA** (2005) Identification and characterization of new plant microRNAs using EST analysis. *Cell Research* 15: 336–360

**Zhang YC, Yu Y, Wang CY, Li ZY, Liu Q, Xu J, Liao JY, Wang XJ, Qu LH, Chen F, Xin P, Yan C, Chu J, Li HQ, Chen YQ** (2013) Overexpression of microRNA *OsmiR397* improves rice yield by increasing grain size and promoting panicle branching. *Nature Biotechnology* 31: 848

**Zhao B, Liang R, Ge L, Li W, Xiao H, Lin H, Ruan K, Jin Y** (2007) Identification of drought-induced microRNAs in rice. *Biochemical and Biophysical Research Communications* 354: 585-590

## 2. miR156/SPL13 module regulates drought tolerance in alfalfa

### 2.1 Background

Climate change is expected to result in frequent and extreme weather events causing major damage to crop production (Olesen et al., 2011; Ray et al., 2015). Plants may respond to these changes (abiotic stress) by developing different resilience mechanisms that can be manifested at the phenotypic, physiological and molecular levels (Mba et al., 2012). To improve plant response to abiotic stress, microRNAs play a pivotal role in adjusting plant traits (Zhou and Luo, 2013) through mechanisms such as altering leaf and root architecture (Couzigou and Combier, 2016; Yang et al., 2018), and increasing levels of stress mitigating metabolites (Cui et al., 2014).

microRNAs are small RNAs of approximately 16-26 nucleotides in length that regulate gene expression at the posttranscriptional level in a sequence-specific manner (Sun, 2012). Of the hundreds of microRNAs (Zhang et al., 2005), microRNA156 (miR156) is highly conserved in plants, where it functions by down-regulating a group of *SQUAMOSA-PROMOTER BINDING PROTEIN-LIKE (SPL)* transcription factors (Aung et al., 2015a; 2015c; Gao et al., 2016). There are at least eight members (a to h) of miR156 in *Arabidopsis*, with g and h being unique to the species. A smaller number of miR156 members (a to f) have been discovered in other plant species, including *Medicago truncatula* (Xie et al., 2005). SPLs regulate positively or negatively a network of downstream genes affecting plant development and physiology by binding to gene promoters at a consensus DNA sequence known as the SPL Binding Domain (SBD) (Yamaguchi et al., 2009; Wei et al., 2012; Aung et al., 2015b; Wang et al., 2015; Xu et al., 2016). It was previously shown that overexpression of *miR156* in alfalfa delays flowering,



enhances root nodulation, and improves vegetative and root growth (Aung et al., 2015a, 2015b). Many of these traits are associated with abiotic stress tolerance (Malik et al., 2002; Serraj, 2003). Moreover, overexpression of *miR156d* was shown to improve alfalfa's tolerance to heat (Matthews et al., 2019), salinity (Arshad et al., 2017b) and drought stress (Arshad et al., 2017a). miR156-mediated silencing of *SPL2*, *SPL9* and *SPL11* improved heat, salt and drought stress resilience in *Arabidopsis* (Stief et al., 2014) and rice (Cui et al., 2014). *Arabidopsis* mutants overexpressing *miR156* had reduced levels of *SPL9*, and enhanced expression of *DIHYDROFLAVONOL-4-REDUCTASE* (*DFR*) and *PRODUCTION OF ANTHOCYANIN PIGMENT1* (*PAP1*), which resulted in increased anthocyanin accumulation and improved stress tolerance in *Arabidopsis* (Stief et al., 2014). The enhancement of anthocyanins and proanthocanidins are regulated by transcription factors such as WD40, MYB and BASIC HELIX-LOOP-HELIX (bHLH) (Pang et al., 2009; Verdier et al., 2012). These specialized metabolites scavenge free radicals in plants exposed to abiotic stress (Nakabayashi et al., 2014; Ayenew et al., 2015; Degu et al., 2016) and function in a coordinated manner with transient stress-related primary metabolites such as proline, galactinol, raffinose and gamma-aminobutyric-acid (GABA) to alleviate stress symptoms (Fait et al., 2008; Nakabayashi et al., 2014).

Drought stress was recently reported to enhance *miR156* expression in alfalfa, resulting in improved resilience to this stress by increasing leaf gas exchange and abscisic acid (ABA), while reducing water loss (Arshad et al., 2017a). Despite these findings, our understanding of how the miR156/SPL network regulates downstream genes such as *DFR* and *WD40-1* to affect stress tolerance in alfalfa is still lacking, especially as it relates to drought stress and specialized metabolites. In this study, the mechanism of how miR156

regulates drought stress response in alfalfa was investigated by analyzing genotypes with altered expression levels of *miR156*, *SPL13*, and *WD40-1* at the metabolomic, transcriptomic and physiological levels. To understand tissue- and genotype-specific transcriptional regulation, the global transcriptomic profiles of leaf, stem and root tissues of *SPL13*RNAi plants in response to drought stress were evaluated. Moreover, binding of *SPL13* to the *DFR* promoter to regulate flavonoid biosynthesis was investigated. The findings from this report provide insight into the mechanisms deployed by *miR156* in regulating drought stress and could be used as a tool in marker-assisted breeding to improve alfalfa and potentially other crops.

## 2.2 Results

### 2.2.1 Enhanced *miR156* expression improves drought tolerance by altering root architecture and water holding capacity

To determine drought stress regulation by *miR156*, one-month-old *miR156*OE alfalfa plants with low (low-*miR156A8a*= 0.5), moderate (moderate-*miR156A8*= 1.5) and higher (higher-*miR156A11*= 2.5) relative *miR156* expression levels than the empty vector (EV) (Aung et al., 2015b) were grown under drought and well-watered conditions. Root weight, root length, stem basal width and fresh root-to-shoot weight ratios were affected by drought stress depending on the genotype (**Figure 2.1**). Relative to EV, low-*miR156A8a* had an 1.8-fold increased root length (**Figure 2.1A,B**) and a 1.7-fold increase in root weight (**Figure 2.1C**). The increment of root biomass in low-*miR156A8a* was the result of longer roots rather than shorter and thicker roots (**Figure 2.1B,C**). To understand if the improved root architecture affected plant water potential, leaf water potential (Argyrokastritis et al., 2015) and changes in the lower stem diameter before and after drought were measured

(Cohen et al., 2001; Goldhamer and Fereres, 2001; Intrigliolo and Castel, 2004). *miR156OE* genotypes, low-*miR156A8a* and A8, maintained a higher leaf water potential and also either maintained or increased basal stem diameter (**Figure 2.1D**) while EV plants showed a reduction over the two weeks of stress. The unchanged basal stem diameter was accompanied by an increase in root/shoot biomass ratio in low-*miR156A8a* and moderate-*miR156A8* under drought (**Figure 2.1E**).

### **2.2.2 *miR156* overexpression affects photosynthesis parameters**

Since drought stress negatively affects photosynthetic parameters (Pinheiro and Chaves, 2011), this effect was investigated in *miR156OE* and EV plants. Accordingly, photosystem II (PS II) chlorophyll fluorescence, as the Fv/Fm ratio, was measured. The maximum rate of rubisco carboxylase activity  $V_{\text{cmax}}$  was maintained at a relatively high level in low-*miR156A8a* and moderate-*miR156A8* plants while a 64% - 75% reduction was observed in EV and higher-*miR156A11* plants during drought stress (**Figure 2.2B**). Consistent with these findings, the maximum photosynthetic electron transport rate,  $J_{\text{max}}$ , was also maintained at higher levels in low-*miR156A8a* and moderate-*miR156A8* during drought stress while it was reduced (64%) in EV and higher-*miR156A11* (**Figure 2.2C**). Fv/Fm was significantly affected by genotype, drought exposure time and a combination of both. *miR156OE* plants maintained higher levels of Fv/Fm ratio ( $\geq 0.75$ ) at later stages of drought (day 11 and 14) comparable to unstressed plants, while EV plants showed a gradual reduction to 0.69 after 14 days of drought (**Figure 2.2D**). Furthermore, photosynthesis assimilation rate was significantly affected by genotype and the duration of drought exposure. During drought stress the photosynthetic assimilation rate was two-fold higher in moderate-*miR156A8* than EV, gradually decreased (1.8-fold) in low-*miR156A8a*, and

further decreased (1.5-fold) in higher-miR156A11 on day 14 when it was greater than in EV (**Figure 2.2E**).

### **2.2.3 *miR156OE* plants accumulate anthocyanin and other stress-aleviating specialized metabolites under drought**

Since plants deploy stress-mitigating primary and specialized metabolites to cope with stress (Ayenew et al., 2015); the metabolite responses of alfalfa to drought stress were investigated. Using more than 4000 metabolite features, a Principal Component Analysis (PCA) plot of LCMS-based metabolite profiles revealed a distinct difference between drought-treated EV and *miR156OE* stem tissues (**Figure 2.3A**). These metabolite features are spectral data generated from metabolites with fragmentation (Alonso et al., 2015; Matsuda, 2016). Principal component-1 (PC-1) contributed 32.7% of the variance and clearly separated EV from *miR156OE* genotypes stem samples while principal component-2 (PC-2) accounted for 13% of the variance.

Leaves of low-miR156A8a and EV were metabolically closer (**Figure 2.3B**), whereas the higher *miR156* overexpressor, higher-miR156A11, possessed a distinct metabolic profile, with PC-1 and PC-2 variance of 18.85% and 12.96%, respectively. Unlike stem and leaf tissues (**Figure 2.3A,B**), roots had a differential metabolite features profile for all genotypes with PC-1 and PC-2 variance of 19.21% and 11.05%, respectively (**Figure 2.3C**). Also, stems of *miR156OE* plants showed stem basal internode pigmentation (**Figure 2.3D**). Based on their significance level and fold change relative to EV, the numbers of metabolite features common or different in stem, leaf and root tissues of *miR156OE* genotypes under drought stress are presented in **Figure 2.4A, 2.4B** and **2.4C**, respectively.

**Figure 2.1 Effects of *miR156* overexpression on drought tolerance and phenotypic responses in alfalfa**

(A) Roots; (B) root length; (C) root weight; (D) stem basal diameter change after two weeks of drought stress; (E) root/shoot biomass ratio of EV and *miR156*OE plants under drought stress. Values are sample means  $\pm$  SE, n = 4 individual plants except in 'D', 'E', where n=5. ANOVA was followed by *Post hoc* Tukey multiple comparisons test when a statistically significant value at  $p < 0.05$  was observed and indicated with different letters. Values assigned with same letters are statistically not significant from each other.

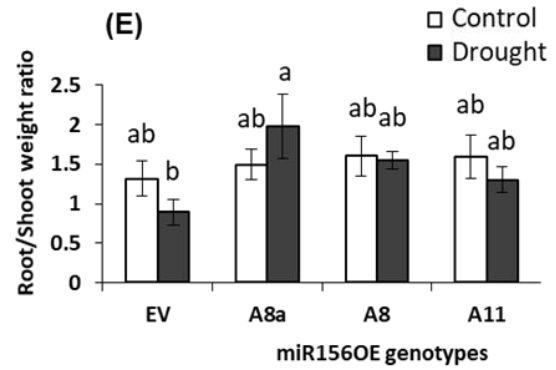
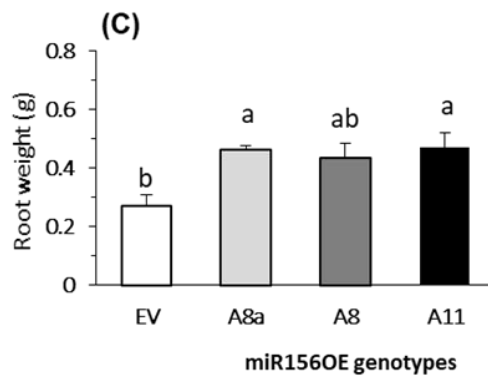
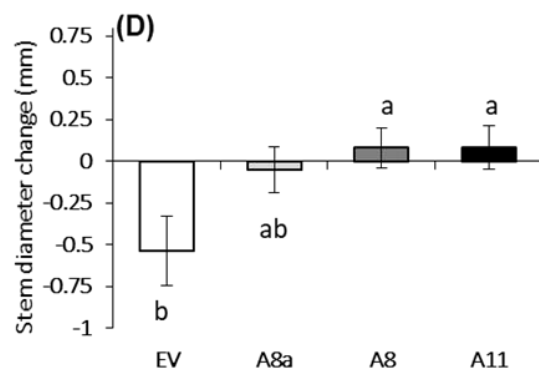
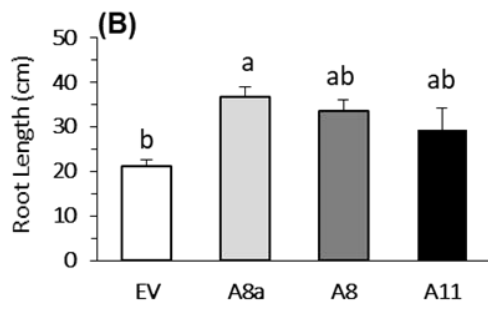


**Figure 2. 2 Effects of *miR156* overexpression on drought tolerance and physiological responses in alfalfa**

(A) leaf water potential; (B)  $V_{\text{cmax}}$ , maximum rate of rubisco carboxylase activity; (C)  $J_{\text{max}}$ , maximum rate of photosynthetic electron transport; (D) dark-adapted chlorophyll fluorescence, Fv/Fm, and (E) photosynthesis (P.) assimilation rate in well-watered (control) and drought stressed plants. Values are sample means  $\pm$  SE, n = 4 individual plants except in 'A', where n=5. ANOVA was followed by *Post hoc* Tukey multiple comparisons test when a statistically significant value at  $p < 0.05$  was observed. Values assigned the same letters are not statistically significant from each other at each time point. Multiple time point data of 'D' and 'E' were analyzed separately for each time points. The abbreviations '-Con' and '-Dry' in 'D' and 'E' stands for control and drought treatments, respectively.

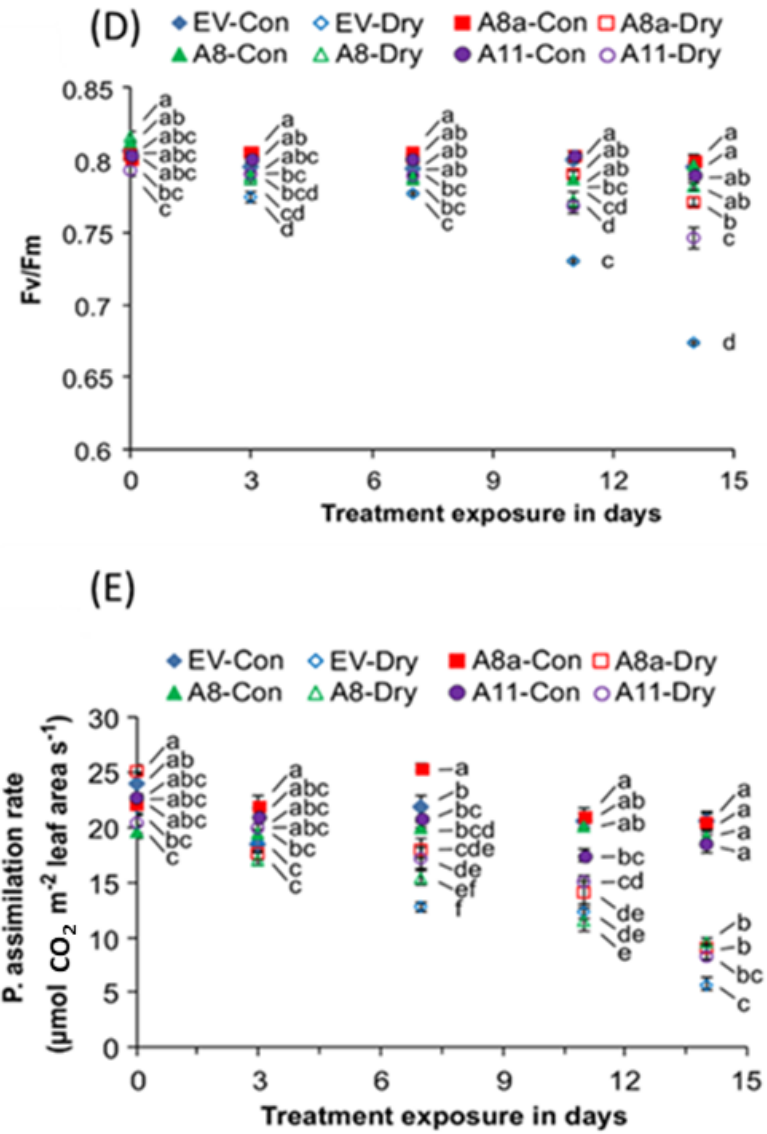
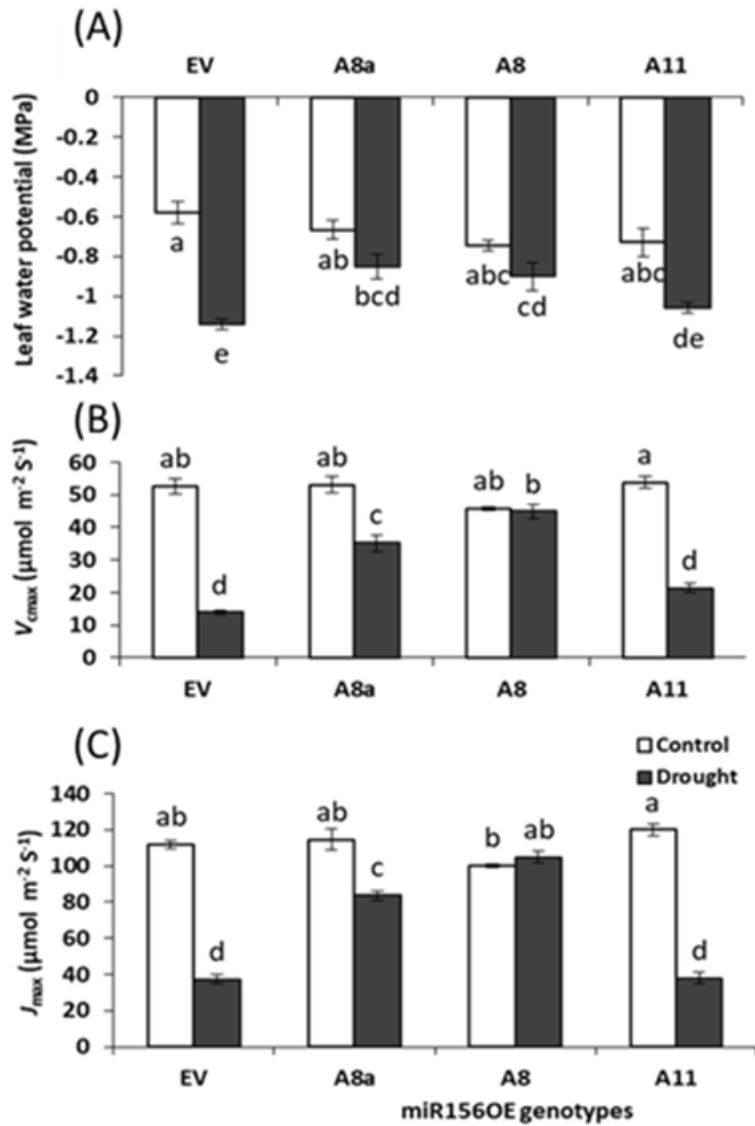
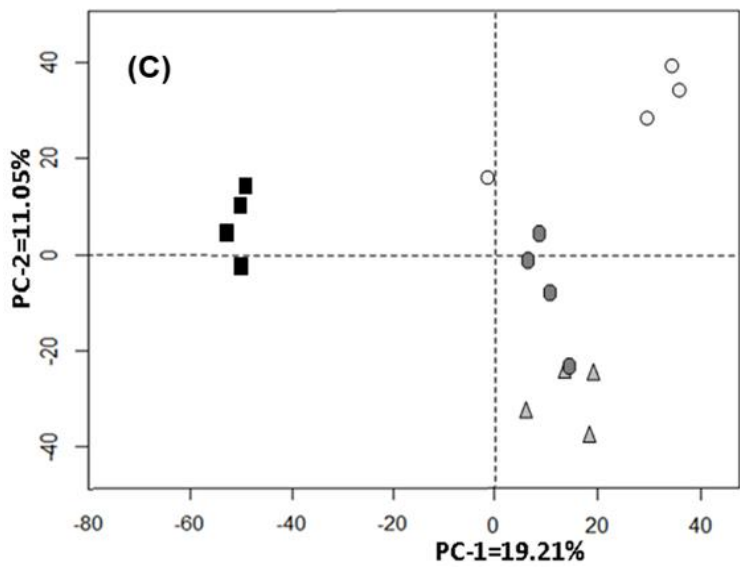
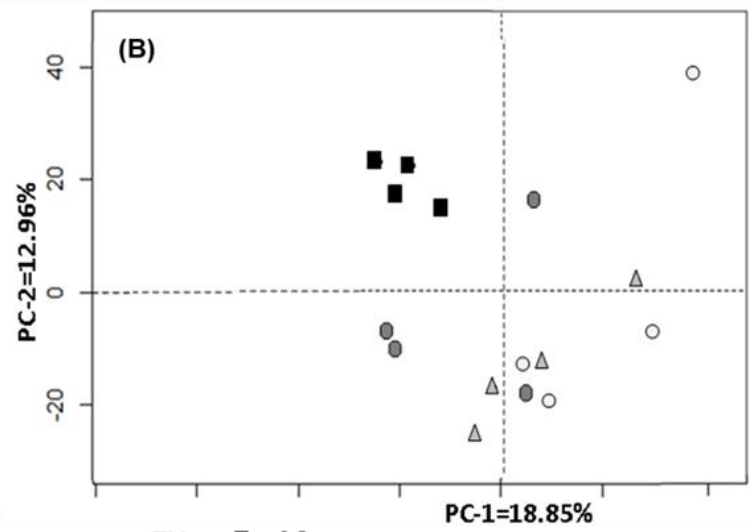
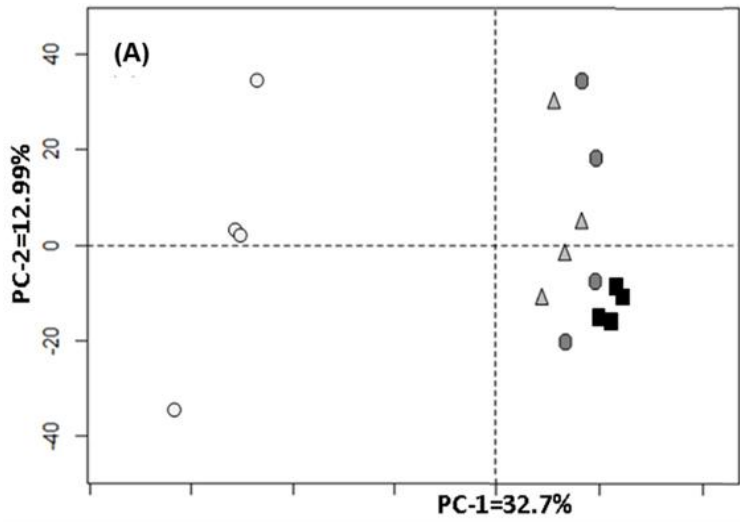




**Figure 2.3 LCMS-based metabolite profiling illustrates distinct profile in *miR156OE* genotypes during drought stress**

Principal component analysis (PCA) of metabolite profile in (A) stem, (B) leaf, and (C) root tissues under drought stress; (D) stem colour development in drought-stressed *miR156OE* plants compared to EV plants. Metabolite profile data were subjected to pareto scaling before principal component analysis (PCA), in which metabolites abundances were mean-centered followed by dividing with square root of the standard deviation using R-software environment 3.2.5.

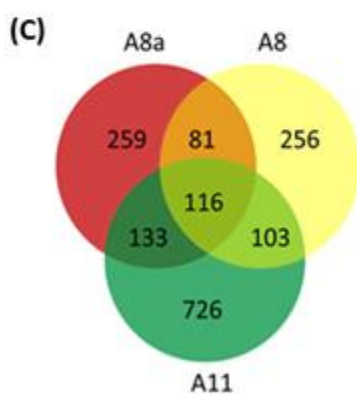
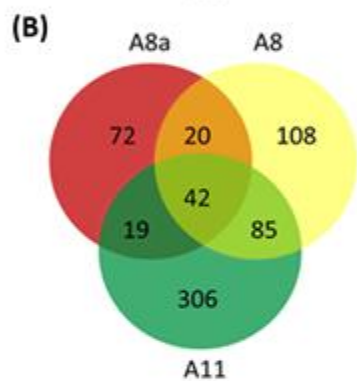
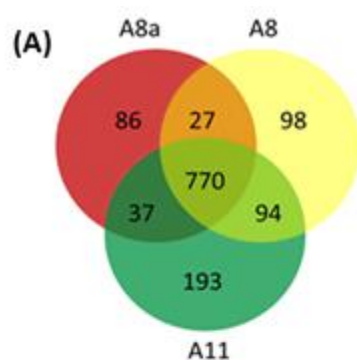


○ EV    ● A8  
 ▲ A8a    ■ A11



**Figure 2.4 LCMS-based metabolite profiling illustrates enrichment of specialized metabolites in *miR156OE* genotypes during drought stress**

Metabolite features that are significantly different at between *miR156OE* and EV plants at  $p < 0.01$  in tissues of (A) stem, (B) leaf, and (C) root tissues; (D) percentage of metabolite features that are significantly increased ( $\geq 1.5 \log_2$  fold change) or decreased ( $\leq -1.5 \log_2$  fold change) relative to EV under drought stress; relative concentrations of anthocyanin metabolites of (E) peonidin 3-O-glucoside, PG, and (F) delphinidin 3-O-(6"-acetyl)-glucoside, DAG. The relative abundance of metabolites is normalized to an internal standard (ampicillin and corticosterone). Values are sample means  $\pm$  SE,  $n=4$  individual plants. ANOVA was followed by *Post hoc* Tukey multiple comparisons test when a statistically significant value at  $p < 0.05$  was observed. Values assigned with same letters are statistically not significant from each other.



(D)

Genotype	Relative abundance	Stem	Leaf	Root
A8a	Increased	85.1	51.8	27.8
	Decreased	14.9	48.2	72.2
A8	Increased	81.1	40.4	27.9
	Decreased	18.9	59.6	72.1
A11	Increased	73.4	32.5	37.8
	Decreased	26.6	67.5	62.2

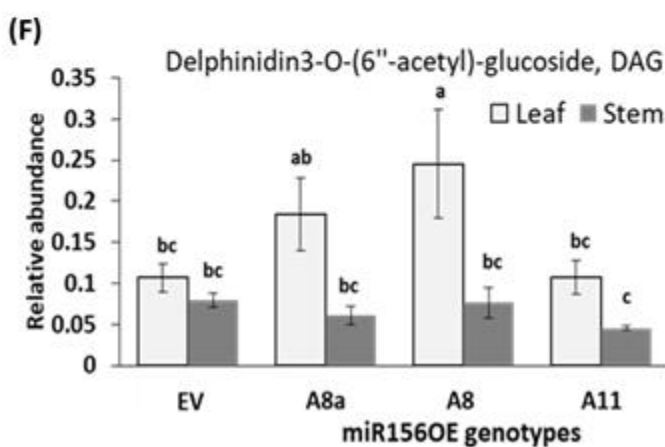
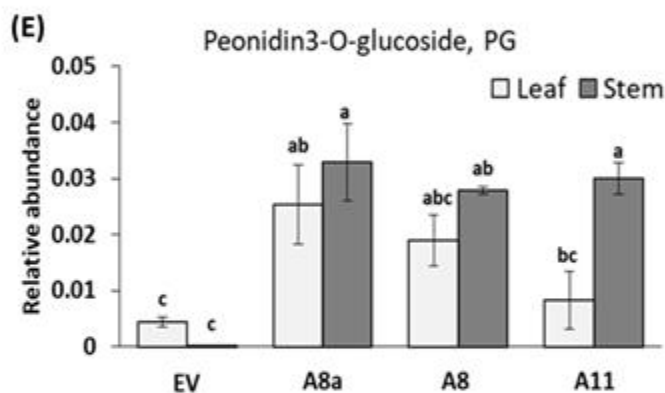


**Figure 2.4A** reveals a high number of differentially abundant metabolite features (770) in stems of *miR156OE* in common compared to EV plants. Majority (85.1%, 81.1%, and 73.4% for low-*miR156A8a*, moderate-*miR156A8*, and higher-*miR156A11*, respectively) of the differentially abundant stem metabolites were increased than in EV stems (**Figure 2.4D**). Here, levels of anthocyanins such as peonidin 3-O-glucoside (PG) and delphinidin 3-O-(6"-acetyl)-glucoside (DAG) were affected by genotype and tissue in response to drought stress. LCMS-based metabolite profiling showed anthocyanins and other ROS scavenging phenolic metabolites were increased mainly in stems of low-*miR156A8a* and moderate-*miR156A8*, although PG was also increased in higher-*miR156A11* (**Figure 2.4E,F** and **Table 2.1**). It remains to be determined whether such acylation is a factor in the improved drought tolerance observed for moderate-*miR156A8*, given that leaves of moderate-*miR156A8* had higher levels of DAG relative to higher-*miR156A11* and EV (**Figure 2.4F**).

#### **2.2.4 Alfalfa plants expressing moderate levels of *miR156* accumulate stress-related primary metabolites under drought**

GCMS was used for analysis of primary metabolites to determine their levels during drought stress. Concentration levels of metabolites were governed by tissue and genotype. In general, the relative abundance of proteinogenic amino acids was higher in leaf tissues of moderate *miR156OE* plants, but reduced in highly overexpressing higher-*miR156A11* plants (**Figure 2.5A** and **Table 2.2**). With the exception of valine, which showed no significant differences in stem, root and leaf tissues, levels of proteinogenic amino acids were significantly affected by tissue type and a combination of genotype and tissue.

Alanine, asparagine, glycine and tryptophan showed a relatively higher abundance in leaves of moderate-miR156A8 (**Figure 2.5A**).

Interestingly, proline, which functions as an osmolyte to maintain plant water potential (Nakabayashi et al., 2014), was significantly increased in root tissues of low-miR156A8a, comparable in moderate-miR156A8, but was reduced in leaf, stem and root tissues of higher-miR156A11 relative to EV plants (**Figure 2.5B**). Levels of  $\gamma$ -aminobutyric acid, GABA, a stress-responsive metabolite that mediates carbon to nitrogen balance between glutamate and succinate in the TCA cycle (Fait et al., 2008), were enhanced in root tissues of moderate-miR156A8 and low-miR156A8a (**Figure 2.5C**). The higher *miR156* overexpressor, higher-miR156A11, on the other hand, had reduced GABA levels in all tissues as compared to EV (**Figure 2.5C**).

The level of fructose, one of the main sugar sources for the carbon skeleton of downstream metabolites and a source of energy, was increased in leaf tissues of moderate-miR156A8 but unchanged in stems and roots relative to EV and low-miR156A8a (**Figure 2.5D**). On the other hand, fructose was reduced in stems of higher-miR156A11 compared to EV and the other genotypes (**Figure 2.5D**). Arabinose, which is metabolized in the pentose phosphate pathway (PPP), is an important component of cell wall polysaccharides, glycoproteins, and arabinogalactan proteins (Stincone et al., 2015). Here, arabinose levels were increased in low-miR156A8a and moderate-miR156A8 stems while they were reduced in roots of higher-miR156A11 compared to EV (**Figure 2.5E**). A complete list of annotated metabolites using GCMS analysis is presented in **Table 2.2**.

**Table 2.1 LCMS-based metabolite profiles of drought stressed alfalfa plants**

Relative metabolite abundance values using peak area were normalized to internal standards corticosterone and ampicillin. N=4 biological replicates from different plants obtained from drought exposed plants. The samples were analyzed with both positive and negative ion mode, independently, using electron spray ionization (ESI) to resolve the metabolites better.

Name of compound	Formula	m/z	RT	EV			A8a			A8			A11		
				Leaf	Stem	Root	Leaf	Stem	Root	Leaf	Stem	Root	Leaf	Stem	Root
p-coumaric acid	C <sub>9</sub> H <sub>8</sub> O <sub>3</sub>	163.02	1.95	0.001	0.002	0.006	0.001	0.003	0.007	0.001	0.003	0.006	0.001	0.001	0.008
Phenylalanine	C <sub>9</sub> H <sub>11</sub> NO <sub>2</sub>	164.07	2.67	0.031	0.010	0.010	0.075	0.036	0.008	0.091	0.012	0.054	0.032	0.008	0.038
Ferulate	C <sub>10</sub> H <sub>10</sub> O <sub>4</sub>	193.05	2.61	0.001	0.002	0.007	0.003	0.002	0.006	0.004	0.003	0.005	0.001	0.002	0.006
Astilbin	C <sub>21</sub> H <sub>22</sub> O <sub>11</sub>	449.10	2.55	0.003	0.003	0.069	0.008	0.003	0.039	0.010	0.006	0.036	0.006	0.004	0.087
Quercetin	C <sub>15</sub> H <sub>10</sub> O <sub>7</sub>	301.03	2.75	0.003	0.006	0.001	0.007	0.004	0.001	0.009	0.005	0.001	0.003	0.005	0.001
Tryptophan	C <sub>11</sub> H <sub>12</sub> N <sub>2</sub> O <sub>2</sub>	203.08	2.76	0.020	0.011	0.009	0.045	0.011	0.014	0.055	0.017	0.015	0.011	0.017	0.015
Kaempferol 3-O-rutinoside	C <sub>27</sub> H <sub>31</sub> O <sub>15</sub>	595.17	2.44	0.002	0.001	0.001	0.003	0.002	0.001	0.003	0.002	0.001	0.001	0.001	0.001
trans-Cinnamate	C <sub>9</sub> H <sub>8</sub> O <sub>2</sub>	148.05	2.37	0.001	0.002	0.001	0.001	0.002	0.001	0.001	0.002	0.001	0.001	0.002	0.001
Citric acid	C <sub>6</sub> H <sub>8</sub> O <sub>7</sub>	191.02	0.52	0.013	0.024	0.017	0.029	0.016	0.006	0.025	0.013	0.007	0.011	0.015	0.022
Sucrose	C <sub>12</sub> H <sub>22</sub> O <sub>11</sub>	341.12	0.52	0.008	0.019	0.017	0.046	0.022	0.020	0.031	0.036	0.017	0.049	0.016	0.025
4-hydroxybenzoic acid	C <sub>7</sub> H <sub>6</sub> O <sub>3</sub>	139.04	2.19	0.004	0.010	0.009	0.014	0.008	0.008	0.017	0.009	0.010	0.005	0.006	0.009
Caffeic acid	C <sub>9</sub> H <sub>8</sub> O <sub>4</sub>	181.05	3.25	0.003	0.004	0.006	0.013	0.004	0.008	0.013	0.003	0.006	0.004	0.002	0.006
Catechin	C <sub>15</sub> H <sub>14</sub> O <sub>6</sub>	291.10	2.33	0.004	0.008	0.001	0.010	0.007	0.001	0.012	0.006	0.001	0.003	0.004	0.001
Epicatechin	C <sub>15</sub> H <sub>14</sub> O <sub>6</sub>	291.09	2.86	0.009	0.015	0.014	0.038	0.009	0.008	0.045	0.008	0.010	0.028	0.011	0.008
Corticosterone	C <sub>19</sub> H <sub>25</sub> NO <sub>5</sub>	347.22	3.76												
Ampicillin	C <sub>16</sub> H <sub>19</sub> N <sub>3</sub> O <sub>4</sub> S	350.12	2.43												



### 2.2.5 miR156 regulates photosynthesis and flavonoid genes

Physiological and metabolite profiling analyses showed alfalfa plants overexpressing *miR156* at low-to-moderate levels (low-miR156A8a and A8) had higher anthocyanin levels (**Figure 2.4E,F**) and maintained higher photosynthetic efficiency during drought stress (**Figure 2.2B-E**). I, therefore, investigated if photosynthesis and anthocyanins are regulated at the molecular level by determining relative transcript abundance for genes involved in these pathways, such as *PHOTOSYSTEM I p700 CHLOROPHYLL A APOPROTEIN APS I (PSI)* and *PHOTOSYSTEM II Q(b) (II)*. Genotype, tissue and their interaction had a significant impact on the transcript abundance of flavonoid biosynthesis genes *DFR* (**Figure 2.6A**) and *MYB112* (**Figure 2.6B**), although *MYB112* showed little difference between tissues. Accordingly, higher transcript levels of *DFR* and *MYB112* were observed in stem and leaf tissues of some *miR156OE* plants.

*DFR* had two- to 15-fold higher transcription in *miR156OE* leaf tissues compared to EV (**Figure 2.6A**). *DFR* transcription was also 25- to 35-fold higher in *miR156OE* root samples. *MYB112* transcript abundance was five- to 19-times higher in leaf tissues of *miR156OE* compared to EV while a four-fold higher expression abundance was observed in *miR156OE* stem tissues regardless of genotype (**Figure 2.6B**). A slight increment in the expression abundance of *WD40-1* (1.9-fold), a transcription factor in the phenylpropanoid pathway, was observed in moderate-miR156A8 root tissues, whereas expression decreased in stem and leaf tissues (**Figure 2.6C**). Moreover, *FLAVONOID GLUCOSYLTRANSFERASE2, (FGT2)*, was significantly increased up to six-fold in leaves of low-miR156A8a while a 19-fold increment was observed in roots (**Figure 2.6D**). The photosynthesis efficiency-related *PHOTOSYSTEM I p700 CHLOROPHYLL A*

*APOPROTEIN APS I (PSI)* and *PHOTOSYSTEM II Q(b) (PSII)* transcript levels were influenced by genotype and tissue type in alfalfa's response to drought stress. *PSI* and *PSII* transcripts abundance were five- and four-fold higher in low-miR156A8a leaves and roots, respectively (**Figure 2.6E,F**). On the other hand, these two genes were significantly decreased in stems of *miR156OE* plants (**Figure 2.6E,F**).

### **2.2.6 SPL13 regulates physiological responses and anthocyanin accumulation during drought stress in alfalfa**

Since miR156 functions in alfalfa by downregulating *SPL* genes, including *SPL13* (Aung et al., 2015b; Gao et al., 2016), I investigated the effect of drought on some physiological and phenotypic parameters of alfalfa plants having RNAi-silenced *SPL13*. Leaf water potential was significantly influenced by genotype in alfalfa's response to drought stress. Accordingly, *SPL13RNAi-5* and *SPL13RNAi-6* plants maintained higher midday leaf water potential during drought stress (**Figure 2.7A**).

Moreover, measurement of photosynthesis efficiency parameter showed that *SPL13RNAi-5* and *SPL13RNAi-6* with moderate *SPL13* silencing (Arshad et al., 2017a), maintained a higher Fv/Fm ratio of 0.74 (**Figure 2.7B**) after eight days of drought stress. The level of Fv/Fm was significantly influenced by genotype, length of drought exposure, and a combination of both in alfalfa's response to drought stress. *SPL13RNAi-6* plants had a significantly higher basal monomeric anthocyanin level under a well-watered conditions (**Figure 2.7C**). Interestingly, all *SPL13RNAi* genotypes accumulated a higher level of total monomeric anthocyanin during drought stress while levels in EV did not change (**Figure 2.7C**). A comparable total polyphenol content was maintained by all genotypes regardless of whether the plants were under well-watered or drought conditions (**Figure 2.7D**).

**Figure 2.5 GCMS-based primary metabolite profiling demonstrates drought stress tolerance strategies by miR156**

Relative abundance of proteinogenic amino acids in leaf tissues during drought stress: alanine, asparagine, aspartate, glycine, isoleucine, serine, threonine, tryptophan and valine (**A**); relative levels of metabolites from the  $\gamma$ -aminobutyric acid (GABA) shunt in leaf, stem and root tissues of (**B**) proline, and (**C**) GABA; relative levels of fructose (**D**) and arabinose (**E**) of leaf, stem and root under drought stress. Values are sample means  $\pm$  SE, n= 4 individual plants. ANOVA was followed by *Post hoc* Tukey multiple comparisons test when a statistically significant value at  $p < 0.05$  was observed. Values assigned with same letters are statistically not significant from each other.

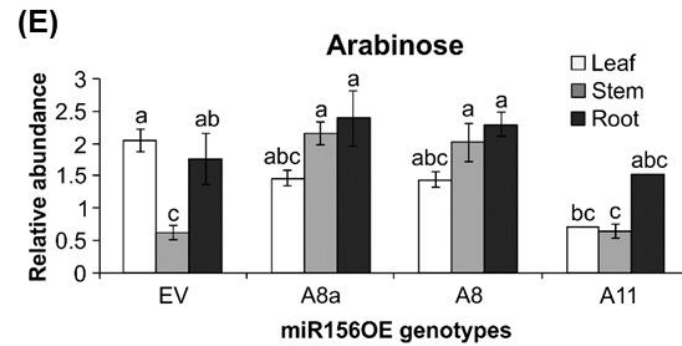
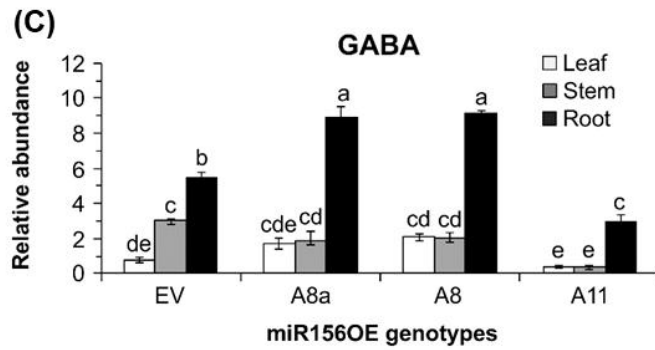
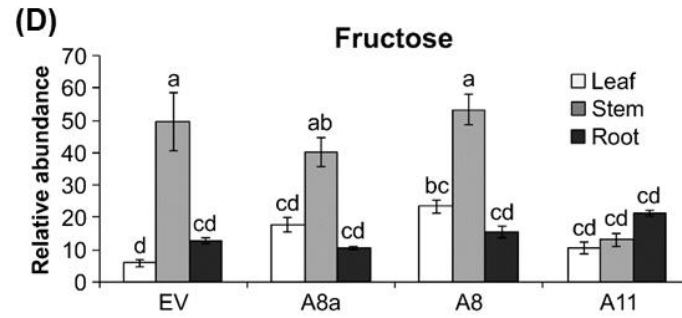
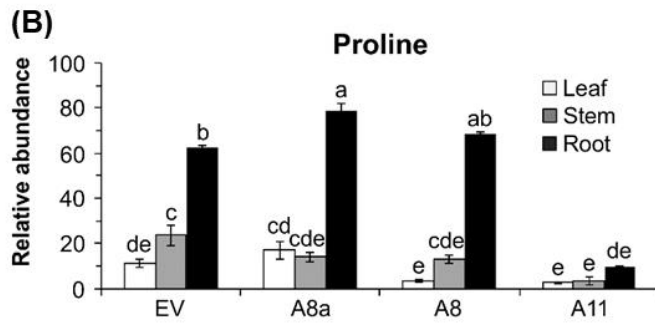
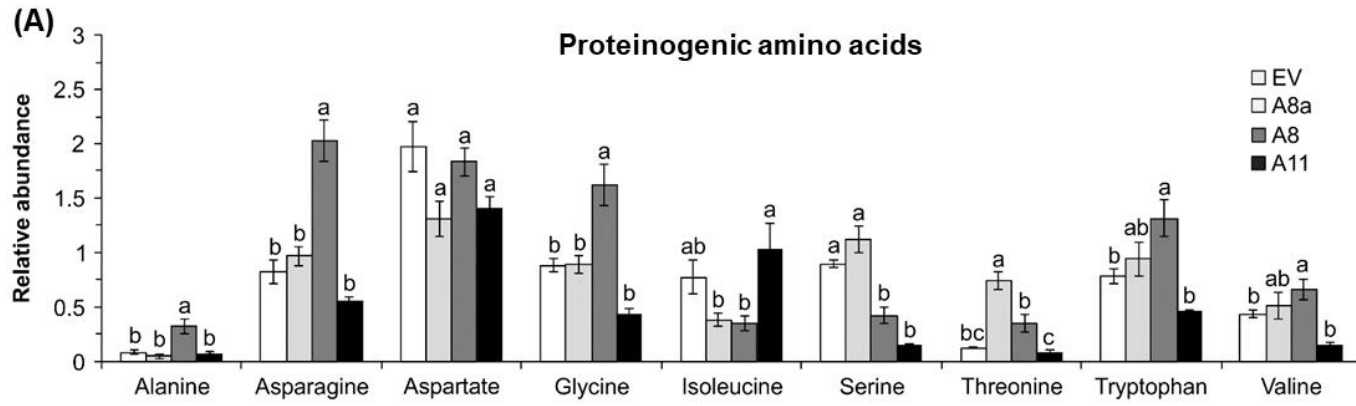


**Table 2.2 GCMS-based relative metabolite abundance in drought stressed alfalfa plants**

Relative metabolite abundance values using peak area were normalized to internal standard ribitol. Aliquots from the LCMS extraction were used for GCMS after derivatization using *O*-methylhydroxylamine hydrochloride in pyridine followed by *N*-methyl-*N*-[trimethylsilyl] trifluoroacetamide (MSTFA) for silylation. Standards of alkane mix (0.029% v/v C10-C20) were used to determine the metabolites retention index in combination with NIST 2011 mass spectral library and in-house metabolite library. N = 4 biological replicates from different plants obtained from drought exposed plants of EV, low-miR156A8a, moderate-miR156A8, and All leaf, stem, and root tissues. The abbreviation GABA stands for  $\gamma$ -aminobutyric acid while 1279NA is an unidentified metabolite based on in-house metabolite database with a retention index of 12.79.

Metabolite	EV			low-miR156A8a			Moderate-miR156A8			higher-miR156A11		
	Leaf	Stem	Root	Leaf	Stem	Root	Leaf	Stem	Root	Leaf	Stem	Root
Hydroxylamine	0.79	1.65	1.48	0.56	1.31	1.92	1.06	1.83	2.05	1.35	1.97	1.67
Citrate	6.07	8.88	23.26	9.26	10.19	12.31	12.92	12.98	22.17	12.56	22.51	22.83
Fumarate	1.82	1.76	1.20	1.64	1.52	1.36	1.96	2.48	1.26	1.29	2.00	1.99
Malate	81.77	126.63	62.02	101.67	76.36	58.52	100.98	149.79	62.50	35.15	80.79	63.33
Succinate	1.94	2.47	2.64	1.78	2.89	2.73	5.60	5.20	2.80	1.40	1.61	3.33
Lactate	0.27	0.49	0.75	0.64	0.49	1.41	0.73	1.06	1.37	0.55	0.67	1.19
Xylitol	1.82	0.69	1.04	0.55	0.33	1.67	2.57	2.25	1.36	0.99	0.53	0.35
Xylulose	38.14	6.30	11.84	49.87	3.30	12.40	38.74	6.56	13.58	14.54	3.27	0.42
Sucrose	436.64	626.02	675.26	350.48	439.24	940.36	436.28	571.35	683.04	256.67	431.57	858.28
Ribose	1.25	0.99	1.20	1.56	0.66	1.69	1.37	1.08	1.98	0.71	0.64	1.36
Allose	67.68	259.53	48.54	57.02	224.51	104.09	131.58	294.98	152.09	44.07	200.93	214.20
Aconitate	1.83	1.58	0.51	1.05	0.77	0.37	1.74	1.10	0.66	1.75	1.36	0.38
Azelaiate	0.17	0.11	0.07	0.46	0.25	0.12	0.09	0.27	0.14	0.07	0.11	0.06
Benzoate	1.54	0.49	0.40	0.80	1.10	0.67	0.89	0.94	0.78	0.56	0.72	0.57
Butan	0.39	0.63	0.21	0.37	0.07	0.95	1.29	1.92	0.84	0.10	0.21	0.11
Callobiose	5.71	0.43	0.29	0.47	0.19	0.41	6.69	0.29	1.26	2.12	0.16	0.18
Erythrose	1.50	0.68	0.77	1.88	0.73	0.79	1.68	0.72	1.02	0.66	0.37	0.36
Glucarate	0.28	0.13	0.06	0.24	0.26	0.07	0.21	0.14	0.08	0.15	0.10	0.14
Gluconate	2.87	3.05	0.86	2.80	1.98	1.48	2.96	3.26	1.66	1.49	2.10	1.09
Glutarate	0.11	0.12	0.14	0.08	0.08	0.21	0.08	0.14	0.17	0.09	0.12	0.23
Glycerate	0.18	0.16	0.20	0.53	0.31	0.32	0.31	0.27	0.34	0.09	0.11	0.22
Inositol	66.88	10.45	8.40	120.06	13.06	9.75	70.45	11.87	9.34	28.04	13.13	7.11
Itaconate	0.07	0.29	0.27	0.24	0.27	0.36	0.14	0.36	0.29	0.31	0.40	0.30
Maleate	1.36	1.39	0.95	1.28	2.98	1.27	1.85	1.44	1.06	1.78	1.49	1.73
Malonate	12.56	37.82	14.41	6.03	11.63	17.04	16.33	28.08	14.77	5.72	14.76	9.27
Maltose	0.11	1.52	0.52	0.21	1.35	1.20	0.75	0.89	1.21	1.22	1.15	1.38
Mannitol	1.65	13.33	5.49	2.14	8.17	10.92	2.48	15.17	13.96	1.81	6.34	21.12
Phosphor. acid	1.42	39.58	53.00	1.77	27.39	63.53	1.55	48.25	88.46	0.90	52.35	38.28

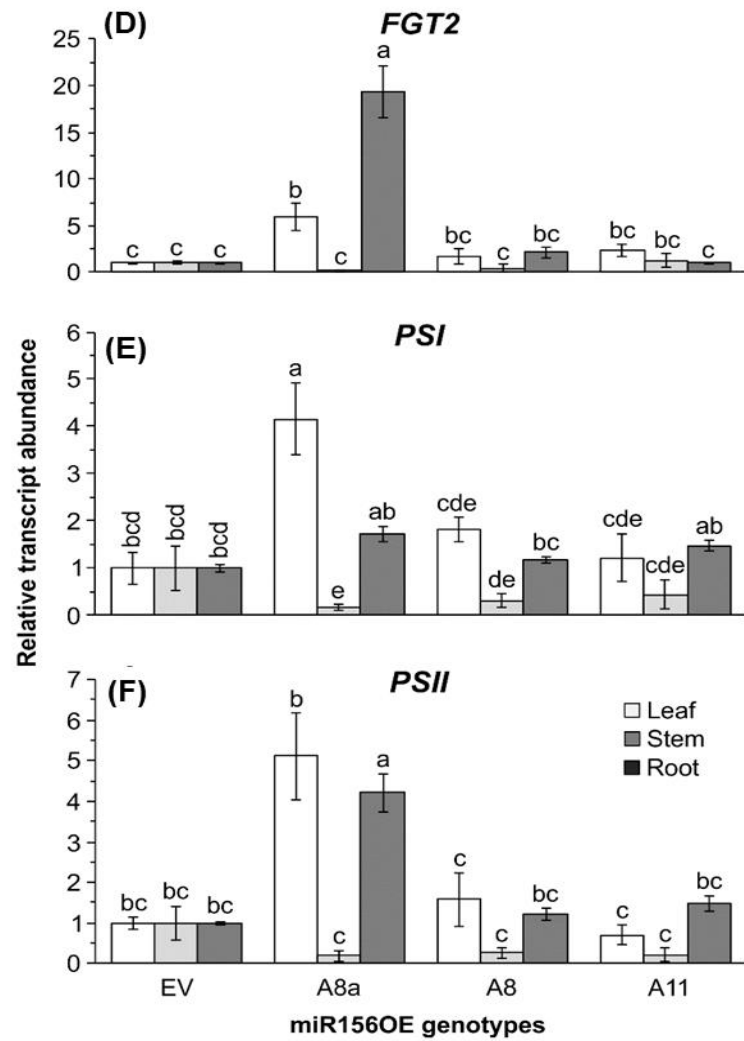
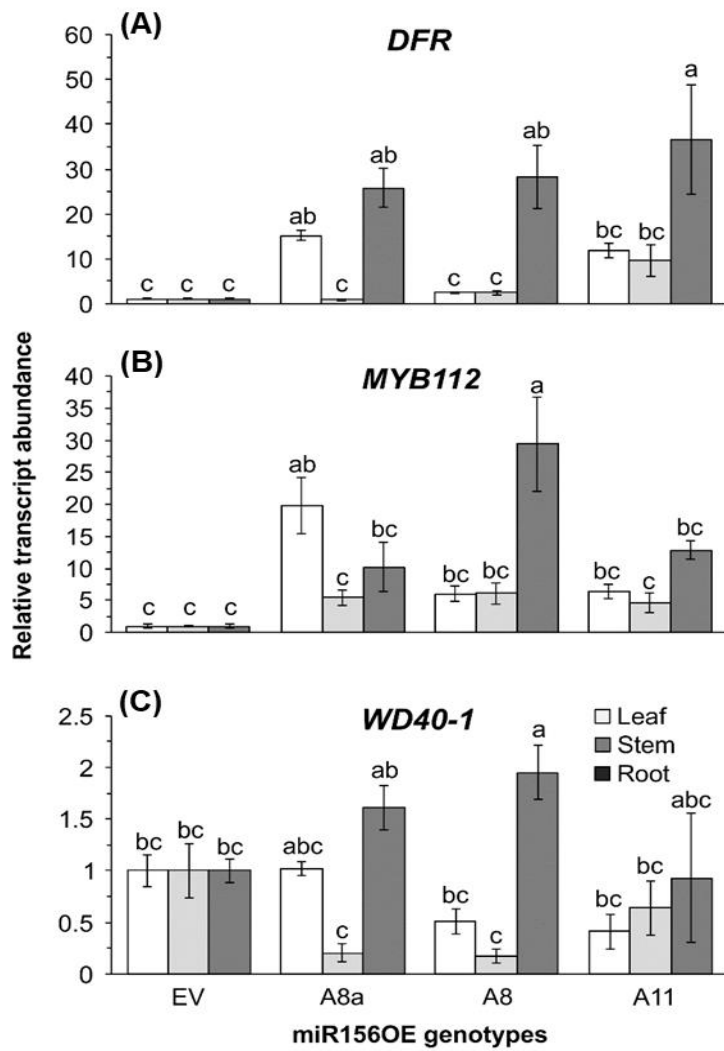
**Table 2.2 Continued ...**

Metabolite	EV			low-miR156A8a			moderate-miR156A8			higher-miR156A11		
	Leaf	Stem	Root	Leaf	Stem	Root	Leaf	Stem	Root	Leaf	Stem	Root
PineridineC	0.29	0.39	0.62	0.29	0.36	0.82	0.67	0.24	0.68	0.21	0.35	0.09
Pinitol	548.49	558.43	485.53	611.33	511.23	567.52	591.56	678.14	594.62	249.64	369.53	395.88
Pinitol-2	63.03	21.86	21.26	55.04	18.52	19.30	64.81	23.92	19.36	19.59	18.37	14.80
Tartarate	0.78	1.18	1.14	0.39	0.43	1.61	0.50	0.82	1.29	0.27	0.79	0.50
Threonate	2.52	2.55	0.43	2.60	1.59	0.54	4.08	2.61	0.47	1.57	2.17	0.43
Turanose	4.61	5.64	0.07	1.98	3.35	0.11	4.23	4.29	0.12	0.81	2.02	0.17
1279NA	0.19	0.15	0.18	0.31	0.14	0.10	0.16	0.41	0.19	0.07	0.17	0.16

**Figure 2.6 Differential transcript levels of select genes in the phenylpropanoid pathway and photosystems during drought stress**

qRT-PCR-based transcript levels in leaf, stem and root tissues of (A) *DIHYDROFLAVONOL-4-REDUCTASE*, *DFR*; (B) *MYB112*; (C) *WD40-1*; (D) *FLAVONOID GLUCOSYLTRANSFERASE2*, *FGT2*; (E) *PHOTOSYSTEM I p700 CHLOROPHYLL A APOPROTEIN APS I*, *PSI*; and (F) *PHOTOSYSTEM II Q(b)*, *PSII*. Values are sample means  $\pm$  SE, n=4 individual plants. Transcript abundance is relative to empty vector control after being normalized to *acetyl-CoA carboxylase*, *ACCI*, and *ACTIN* housekeeping genes. ANOVA was followed by *Post hoc* Tukey multiple comparisons test when a statistically significant value at  $p < 0.05$  was observed. Values assigned with same letters are statistically not significant from each other.





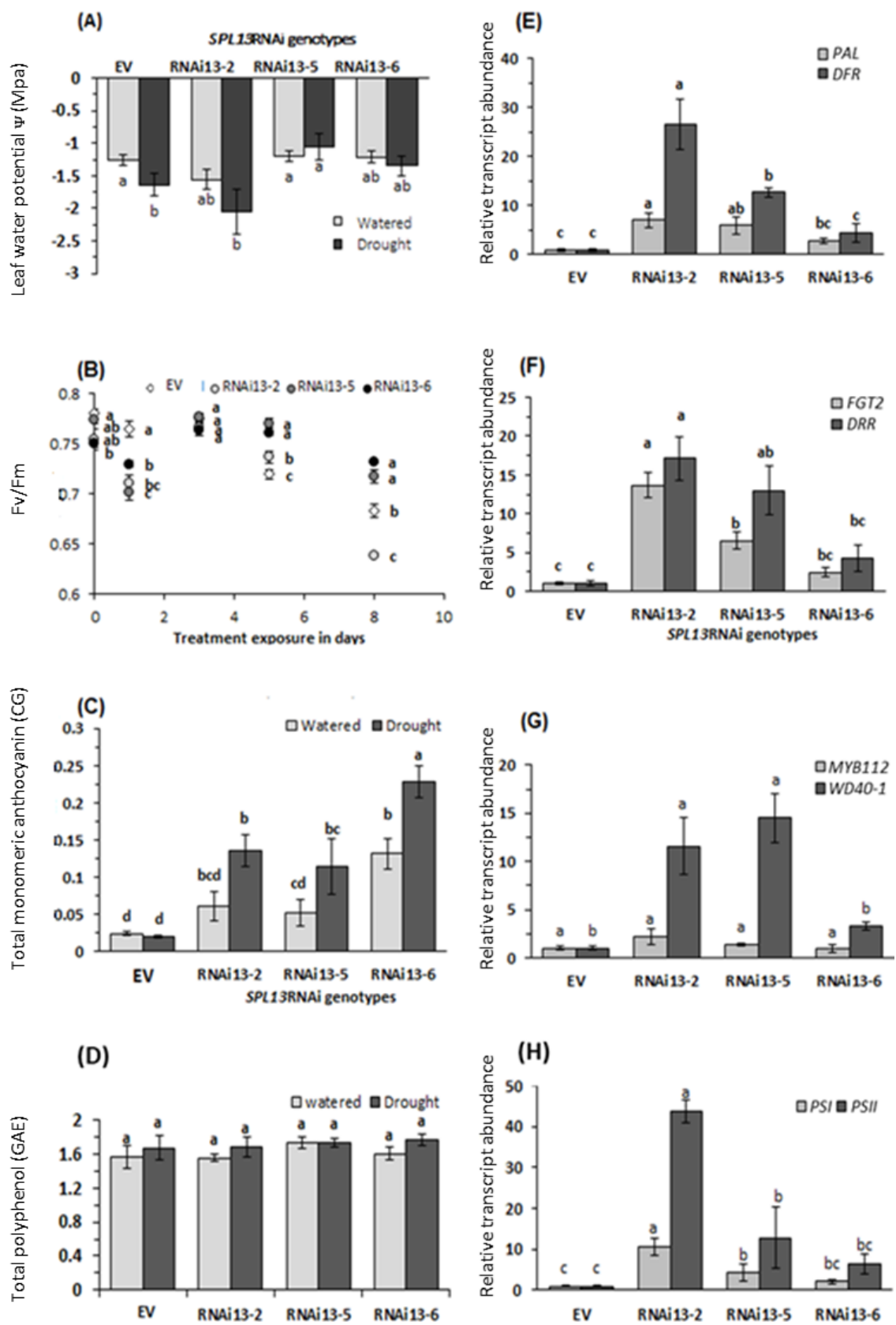
### **2.2.7 Flavonoid- and photosynthesis-related genes are enhanced in *SPL13*-silenced plants**

To determine whether the observed increases in total monomeric anthocyanin levels and maintenance of photosynthesis efficiency under drought stress were regulated at the transcriptional level, the expressions of anthocyanin-related and dehydration responsive genes were analyzed. There were significant differences among genotypes in relative transcript abundance under drought and control conditions (**Figure 2.7E-H**). As expected, the transcript level of *PHENYLALANINE AMMONIA-LYASE (PAL)* the first committed step in the phenylpropanoid pathway, was significantly higher in two out of three *SPL13RNAi* plants (**Figure 2.7E**). Similarly, *DFR* and *FGT2* were also significantly higher in two out of three *SPL13RNAi* plants (**Figure 2.7E,F**).

The *DEHYDRATION RESPONSIVE RD-22-LIKE (DRR)* gene, which is regulated by MYB and MYC transcription factors and induced by drought and ABA (Abe et al., 2003; Tuteja, 2007), was expressed four- to 17-fold higher in *SPL13RNAi* plants (**Figure 2.7F**). Likewise, the transcription factor *WD40-1* was increased three- to 14-fold in *SPL13RNAi* plants during drought stress (**Figure 2.7G**). For photosynthesis-related genes, transcript analysis of *PSI* and *PSII* revealed a two- to 10-fold and six to 43-fold increase in expression levels, respectively, in *SPL13RNAi* plants relative to EV (**Figure 2.7H**).

**Figure 2.7 *SPL13* silencing regulates drought response through coordinated metabolite, transcript and physiological adjustments**

(A) Leaf water potential in *SPL13*RNAi and EV plants; (B) dark adapted chlorophyll fluorescence, Fv/Fm, during drought stress; (C) total monomeric anthocyanin expressed as cyanidin-o-glucoside equivalent (CG); and (D) total polyphenol content expressed as gallic acid equivalent (GAE); (E) transcript levels of *PHENYLALANINE AMMONIA-LYASE* (*PAL*), and *DIHYDROFLAVONOL-4-REDUCTASE* (*DFR*); (F) *FLAVONOID GLUCOSYLTRANSFERASE2* (*FGT2*), and *DEHYDRATION RESPONSIVE RD-22-LIKE*, (*DRR*); (G) *MYB112* and *WD40-1* transcription factor genes from the phenylpropanoid pathway in stems of *SPL13*RNAi and EV genotypes; (H) transcript levels of *PHOTOSYSTEM I p700 CHLOROPHYLL A APOPROTEIN APS I* (*PSI*), and *PHOTOSYSTEM II Q(b)* (*PSII*) under drought stress; Values are means  $\pm$  SE, Light gray bars in ‘A’, ‘C’ and ‘D’ represent values under well-watered condition while dark gray bars represent under drought stressed. Relative transcript levels in ‘E’, ‘F’, ‘G’ and ‘H’ are shown relative to EV after being normalized to *acetyl-CoA carboxylase*, *ACC1*, and *ACTIN* housekeeping genes. ANOVA was followed by *Post hoc* Tukey multiple comparisons test when a statistically significant value at  $p < 0.05$  was observed. Values assigned with same letters are statistically not significant from each other. Letters in multiple time point data of ‘B’ were analyzed separately. Abbreviations of EV, RNAi13-2, RNAi13-5 and RNAi13-6 corresponds to empty vector, *SPL13*RNAi-2, *SPL13*RNAi-5, and *SPL13*RNAi-6, respectively.



### 2.2.8 SPL13 is a direct regulator of *DFR*

miR156 represses the expression of *SPLs*, including *SPL13* in alfalfa, to affect various aspects of plant growth and development (Gao et al., 2016). Analysis of the the *DFR* promoter revealed the presence of at least four putative SBD binding motifs with the core GTAC sequence (**Figure 2.8A** and **Figure S2**), the occupancy with SPL13 in the promoter region of *DFR* was studied using ChIP-qPCR in p35S:SPL13-GFP plants. Three regions (I, II & III) were selected with the conserved SBD core sequences located at 750, 544 and 260 bp, respectively, upstream of the translation start codon of *DFR* as potential SPL13 binding sites, and tested for SPL13 occupancy. Compared to WT, SPL13 binding to the *DFR* promoter region was significantly higher in p35S:SPL13-GFP plants (**Figure 2.8B**). There is a preferential binding of SPL13 towards the two most downstream putative SBD regions (II & III) in the *DFR* promoter while region I did not show strong binding (**Figure 2.8** and **Figure S2**). Of the three regions, region III showed the strongest binding to SPL13 (**Figure 2.8**) indicating that SPL13 could bind directly to *DFR* to negatively regulate its expression.

### 2.2.9 Global transcriptomic signature of SPL13 in alfalfa drought tolerance

To identify SPL13-regulated genes that contribute to drought tolerance, high throughput transcriptomic analysis was conducted on alfalfa plants with reduced expression of *SPL13* (*SPL13*RNAi-5) and empty vector (EV) plants. To determine tissue-specific gene expression patterns, total mRNA was extracted from leaf, stem, and root tissues exposed to drought stress and control conditions for transcriptomic analysis.

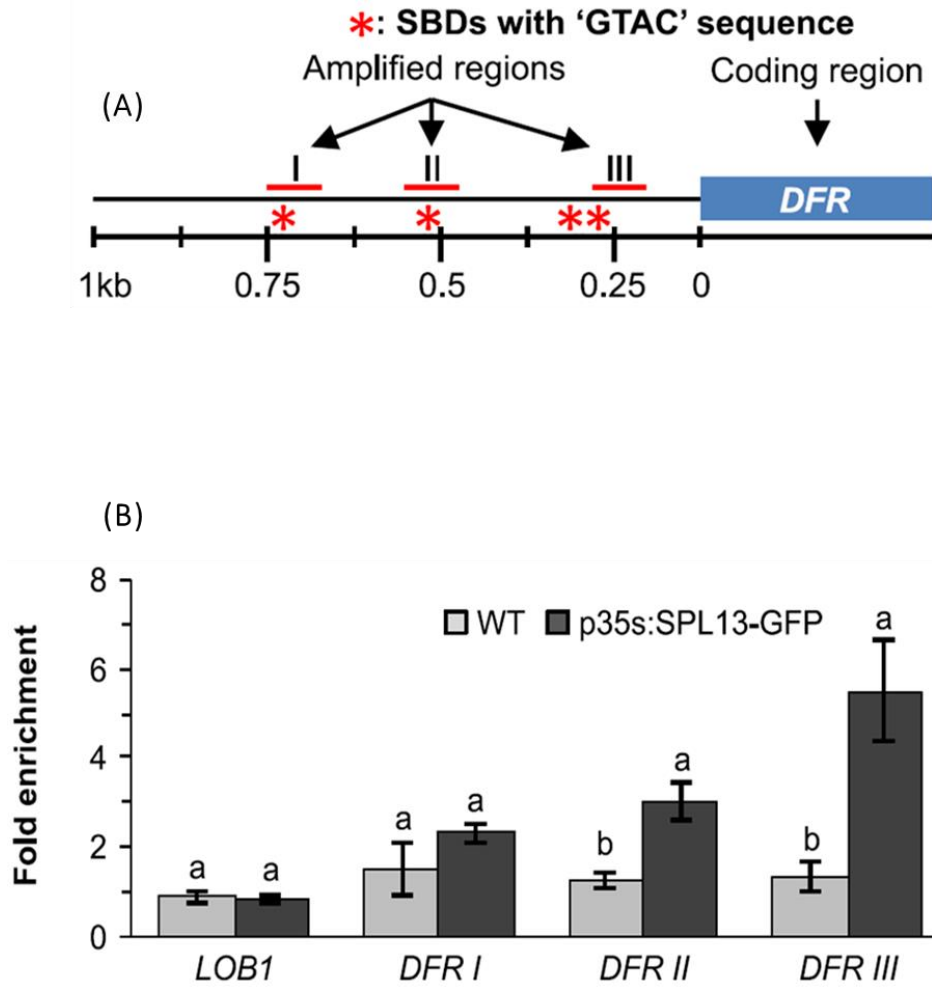
### 2.2.9.1 Genotype-specific transcript profile of alfalfa in response to drought stress

Plants deploy metabolic, physiological, and phenotypic adjustments to cope with different abiotic and biotic stress conditions (Fenollosa and Munné-Bosch, 2019; Mishra et al., 2019). Determining the molecular signature of these adjustments is necessary for exploiting this knowledge in marker-assisted breeding to screen genotype collections for the regulated genes. In earlier sections (2.2.1 - 2.2.8), I investigated the role of the miR156/SPL13 module in alfalfa drought tolerance. Here, I compared the global transcriptomic profile of leaf, stem, and root tissues of RNAi-silenced *SPL13* and EV plants under drought condition. The observed physiological and phenotypic adjustments in *SPL13*RNAi plants in response to drought were investigated to determine if they were attributed to differential gene expression. More than 5900, 2100, and 1500 differentially expressed genes (DEG) were found between leaf, stem, and root tissues, respectively, of drought-stressed *SPL13*RNAi and EV plants (**Figure 2.9A**). Among the DEG, 74 were commonly increased in all tissues of *SPL13*RNAi plants, while 154 transcripts were commonly decreased (**Figure 2.9A**).

Among the commonly increased genes, the highest fold change was observed from a vacuolar ion transporter-like (Medtr2g008110) followed by genes encoding a gibberellin-regulated family protein (Medtr6g007897), a fasciclin-like arabinogalactan protein (Medtr5g098420), a proline dehydrogenase (Medtr7g020820), Pmr5/Cas1p GDSL/SGNH-like acyl-esterase family protein (Medtr4g079700), LRR receptor-like kinase (Medtr5g090100) and an abscisic acid receptor (Medtr7g070050), respectively (**Table S3**).

**Figure 2.8 SPL13 binds to *DFR* in a sequential and position-dependent manner**

(A) Schematic representation of potential SPL13 binding sites in the promoter region of *DFR*, (B) Chromatin Immunoprecipitation-qPCR (ChIP-qPCR) based fold enrichment analysis of SPL13 in p35S:SPL13-GFP and WT plants from means of  $n = 3$  individual plants with  $\pm$  SE where *LATERAL ORGAN BOUNDARES-1 (LOB1)* was used as a negative control. Comparisons between WT and p35S:SPL13-GFP plants in each potential SPL13 binding regions (I, II, and III) were performed separately and indicated with different letters when significant at  $p < 0.05$ . In 'A' "\*" represents SBD with 'GTAC' sequence for potential SPL13 binding. In 'B' *DFRI*, *DFRII*, and *DFRIII* represents ChIP-qPCR amplification of regions I, II, III located at 750, 544 and 260 bp, respectively, upstream of the translation start codon of *DFR* as potential SPL13 binding sites.





Of the commonly reduced genes in *SPL13RNAi* plants under drought stress, transcripts encoding an ABC transporter family protein (Medtr2g095440), a plasma membrane H<sup>+</sup>-ATPase (Medtr3g108800), and a PLAT-plant-stress protein (Medtr3g087490) showed the highest fold-changes, respectively (**Table S4**). Moreover, transcript analysis between drought-stressed and unstressed tissues of *SPL13RNAi* plants showed 998, 1195 and 587 DEG whereas a significantly higher number were of DEG (an average of 4.5 fold) observed in EV plants with 5521, 4426 and 2607 DEG in leaf, stem and root tissues, respectively (**Figure 2.7B,C**). Gene ontology (GO) term annotation of the DEG between drought-stressed *SPL13RNAi* and EV plants leaf, stem and root tissues mainly correspond to molecular function (average of 83%) followed by biological process (11%) and cellular components (5%) roles (**Figure 2.9D-F**).

### **2.2.9.2 Leaf-specific transcript profile of alfalfa plants under drought stress**

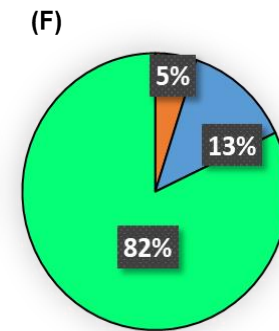
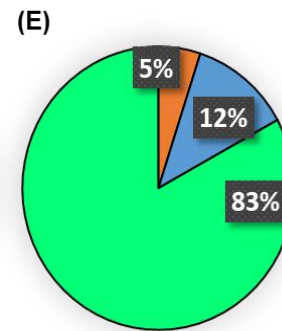
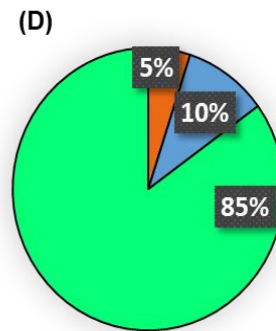
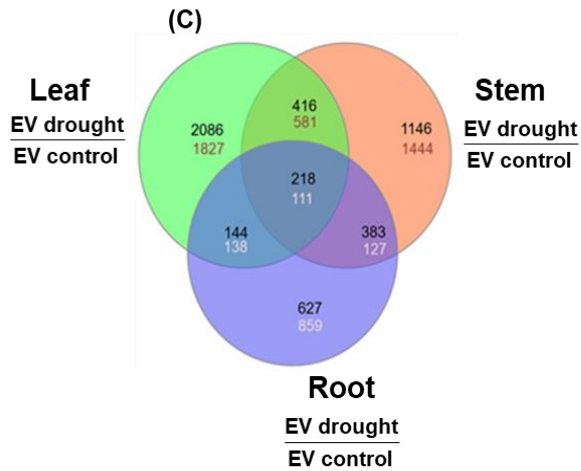
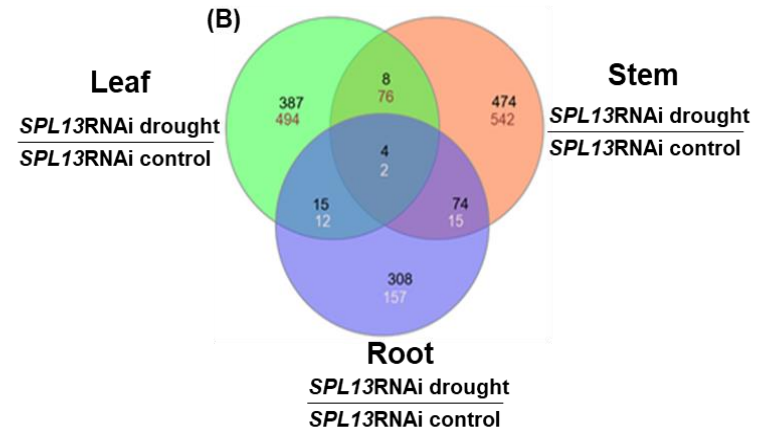
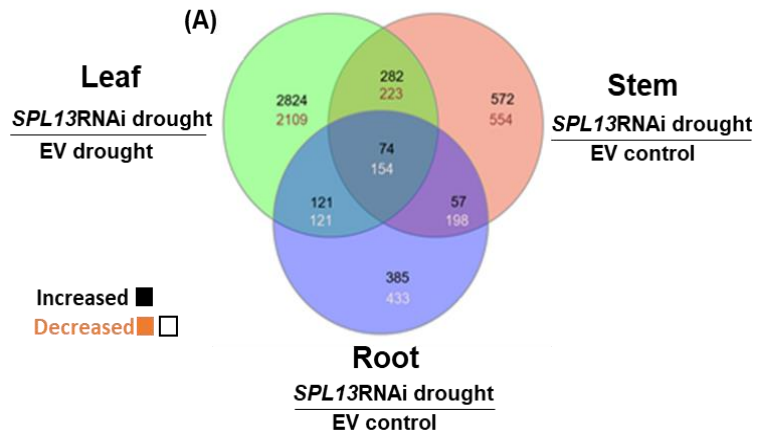
Different plant tissues would be expected to have different roles to play in drought response owing to their gene expression profiles. Total transcript counts were subjected to weighted gene co-expression network analysis (WGCNA) (Langfelder and Horvath, 2008) to understand the gene co-expression pattern upon drought stress across tissues and genotypes. Transcript profiles from leaf, stem, and root tissues of *SPL13RNAi* and EV changed in response to drought in a tissue-specific manner; presenting different clusters based on tissue type (**Figure 2.10**). Of the 5900 DEG present between leaf tissues of drought-stressed *SPL13RNAi* and EV, 55.8% of the genes were significantly increased in *SPL13RNAi* plants (**Figure 2.9A**), of this 2824 were leaf-specific (**Table S5**). On the other hand, considering tissue plasticity between well-watered and drought-stressed leaf tissues, 41.5 % of the 998 DEG were increased in *SPL13RNAi* leaves while 51.9 % of 5521 DEG

were increased in EV leaves (**Figure 2.9B,C**). Moreover, 24.9 % (387 of 998) and 31.8 % (494 of 998) of leaf-specific DEG in *SPL13RNAi* plants were increased and decreased, respectively (**Figure 2.9B**). Likewise, 37.8 % (2086 of 5521) and 33.1 % (1827 of 5521) of DEG in EV plants were increased and decreased, respectively, only in leaves (**Figure 2.9C**). Gene ontology (GO) -terms were analyzed and categorized into molecular function, biological process, and cellular components to understand the role of differentially regulated genes in leaves of drought-stressed *SPL13RNAi* and EV plants. The analysis from leaf tissues showed 85% of GO-terms corresponds to molecular function followed by 10% and 5% to biological process and cellular components, respectively (**Figure 2.9D**).

The top three DEG associated with molecular function correspond to transcription activity (phosphorelay response regulator activity, sequence-specific DNA binding transcription factor activity, and transcription cofactor activity) (**Figure S5, Table S8**). Likewise, the top biological processes associated DEG between *SPL13RNAi* and EV plants correspond to telomere maintenance, translation and alcohol metabolic process in addition to glutamine catabolic process and porphyrin-containing compound biosynthetic process (comprises chlorophyll biosynthesis) (**Figure A4, Table S8**). The DEG were mapped to the *M. truncatula* genome to understand their functional associations. Accordingly, leaf-specific DEG between drought-stressed *SPL13RNAi* and EV were mapped using MapMan-based pathway analysis. Various metabolic pathways were affected, including carbohydrate metabolism, photosynthesis, and primary metabolism (**Figure 2.11**). Most importantly, photosynthesis-associated transcripts were highly increased in *SPL13RNAi* plants (**Figure 2.11**).

**Figure 2.9 Tissue and genotype-specific expression patterns of *SPL13RNAi* and EV genotypes of alfalfa plants in response to drought**

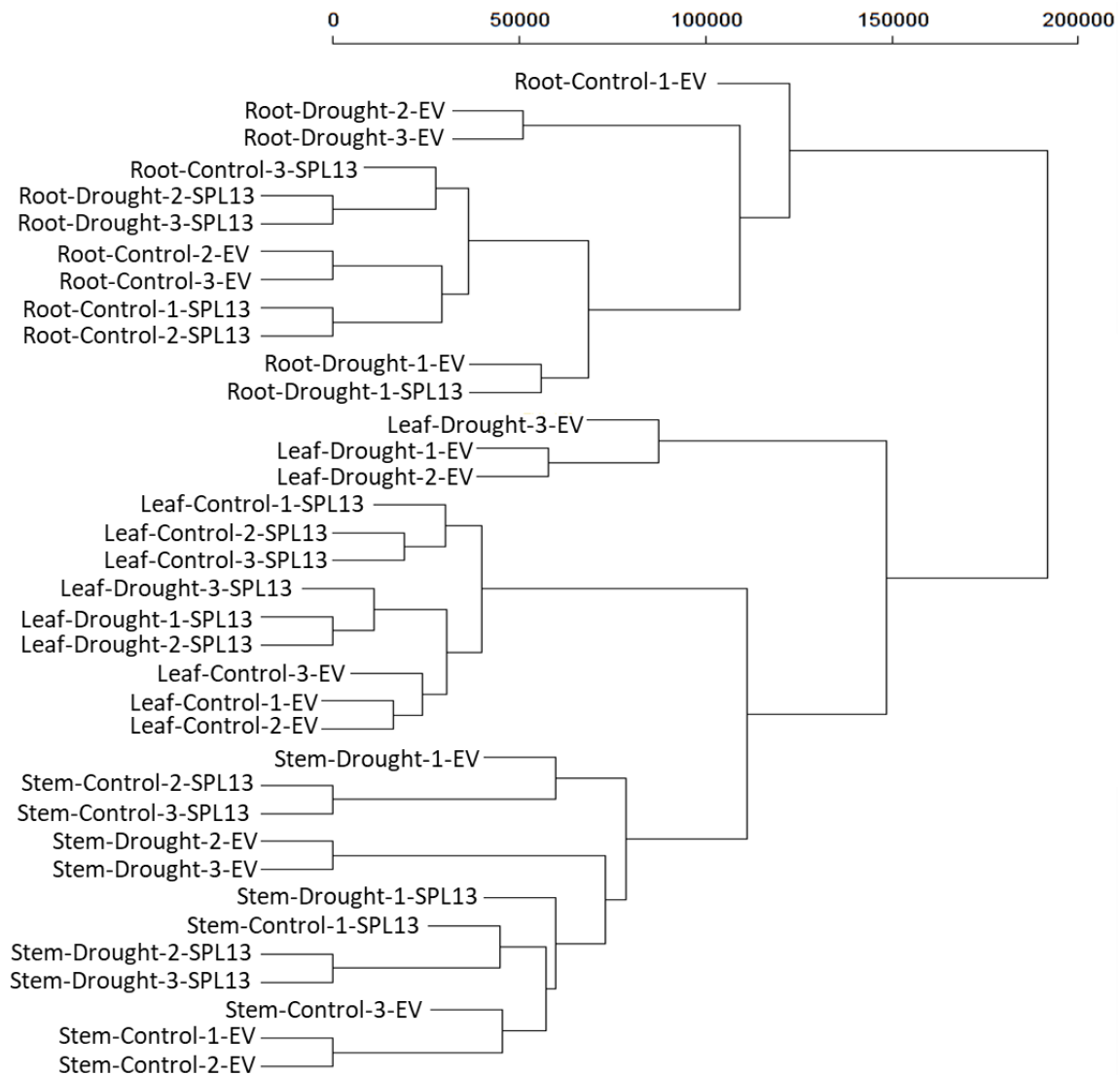
(A) Differentially expressed genes between drought stressed *SPL13RNAi* and EV plants; (B) *SPL13RNAi*-specific gene expression plasticity in response to drought stress; (C) EV-specific gene expression plasticity in response to drought stress; percent representation of DEG into cellular components, biological process, and molecular functions between *SPL13RNAi* and EV (D) leaf (E) stem, and (F) root tissues.



■ Cellular component   ■ Biological process   ■ Molecular function

**Figure 2.10 Weighted gene co-expression network analysis (WGCNA) illustrates tissue and genotype-specific expression patterns of alfalfa plants in response to drought**

Tissue and treatment-specific expression patterns of total transcripts. Tissue-specific expression patterns are indicated with blue line boxes indicating transcript from leaf, stem, and root tissues are distinct. WGCNA were analysed using R-software environment 3.2.5. 'BiocManager' package considering all transcripts detected in each sample. S13, *SPL13RNAi*; EV, empty vector plants.



Further investigation of transcripts associated with photosynthesis revealed that light-dependent reaction centers, mainly of photosystem I and photosystem II, were higher in *SPL13RNAi* (**Figure 2.12A**). Unlike the light-dependent reaction centers, the Calvin cycle (**Figure 2.12B**) and photorespiration-associated transcripts (**Figure 2.12C**) were either slightly increased or not altered. Similarly, the photorespiration-associated transcript, rubisco (Ribulose-1,5-bisphosphate carboxylase/oxygenase), was slightly higher in *SPL13RNAi* plants under drought stress (**Figure 2.12C**).

### 2.2.9.3 Stem-specific transcript changes of alfalfa plants upon drought stress

Expression levels of 46.5% of the 2114 DEG between drought-stressed stem tissues of *SPL13RNAi* and EV plants indicated an increased level in *SPL13RNAi* plants (**Figure 2.9A**), of which 572 were stem-specific (**Table S6**). On the other hand, genotype-specific and stem-derived drought stress responsive transcripts revealed 46.9% of the 1195 DEG in *SPL13RNAi* plants were increased while EV plants showed a 48.9% increase out of 4426 DEG (**Figure 2.9B,C**). To understand the function of stem-derived DEG, the genes were annotated (GO-term analysis) and grouped their roles into molecular function, biological process, and cellular components. Like leaf tissues, the majority (83%) of the DEG correspond to molecular function followed by biological process (12%) and cellular components (5%), despite differences in DEG between leaves and stems (**Figure 2.9E**). The most enriched DEG molecular functions between *SPL13RNAi* and EV stem tissues were acyl-CoA dehydrogenase activity, ubiquinol-cytochrome-c reductase activity, and hydroxymethylglutaryl-CoA reductase (NADPH) activity (**Figure S7, Table S9**). On the other hand, the highly enriched categories of the affected biological processes include

ATP catabolic process, response to stress, defense response, intercellular signal transduction and response to desiccation (**Figure S6, Table S9**).

Furthermore, to understand the association of DEG of stem tissues with metabolic pathways, I subjected DEG to MapMan-based pathway analysis (**Figure 2.13**). DEG of stem tissues were increased in *SPL13RNAi* plants that correspond mainly to flavonoid biosynthesis, carbohydrate metabolism and response to desiccation-related genes (**Figure 2.13, Table S5**). On the other hand, genes associated with photosynthesis were decreased significantly in *SPL13RNAi* plants compared to EV (**Figure 2.13**). Transcriptomic analysis of DEG obtained from stem tissues combined with MapMan-based pathway analysis revealed an activation of the phenylpropanoid pathway in *SPL13RNAi* plants under drought stress (**Figure 2.14**).

#### **2.2.9.4 Root-specific transcript profile of alfalfa plants in response to drought stress**

A total of 1543 DEG were detected between roots of drought-stressed *SPL13RNAi* and EV plants, with 41.2 % of them increased in the former (**Figure 2.9A**), of which 385 were root-specific (**Table S7**). Further analysis on the plasticity between well-watered and drought stressed root samples showed 68.3% of 587 DEG in *SPL13RNAi* roots were upregulated while 52.6% of 2607 DEG were increased in EV (**Figure 2.9B,C**). To shed light on the role of root-specific DEG in alfalfa during drought, I subjected DEG to GO-term analysis and categorized them into biological process, molecular function and cellular components.



**Figure 2.11 Summary of differentially expressed genes-related metabolite pathways between drought stressed EV and *SPL13RNAi* leaf tissues**

Transcript fold changes are provided in log 2 with red and blue colours representing increased and decreased transcript levels, respectively, relative to EV. Minor CHO corresponds to minor carbohydrate; TCA, Tricarboxylic acid cycle; OPP, oxidative pentose phosphate pathway. N = 3 biological replicates for each genotype and treatment conditions.

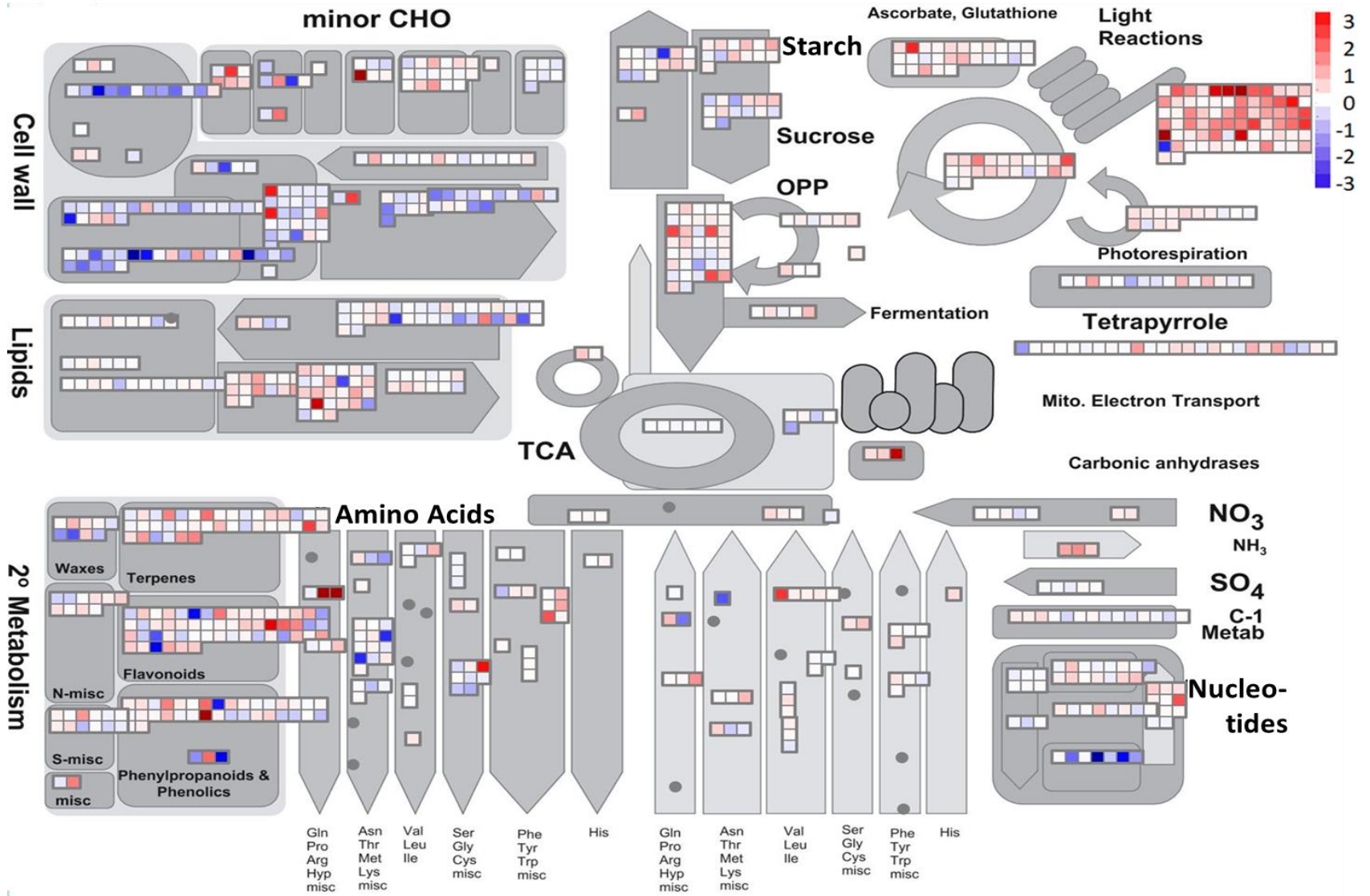


**Figure 2.12 Leaf-specific DEG attributed to photosynthesis are enhanced in *SPL13RNAi* plants**

(A) Summary of DEG-related metabolites pathways in light-dependent photosynthetic reaction of the chloroplast thylakoids, (B) carbon dioxide fixation in Calvin cycle in chloroplast stroma region, (C) photorespiration-associated transcripts involving chloroplast, mitochondria and peroxisome differentially regulated between drought-stressed *SPL13RNAi* and EV plants. Transcript fold changes are provided in log 2 with red and blue colours representing increased and decreased transcript levels, respectively, relative to EV. N = 3 biological replicates for each genotype and treatment conditions.

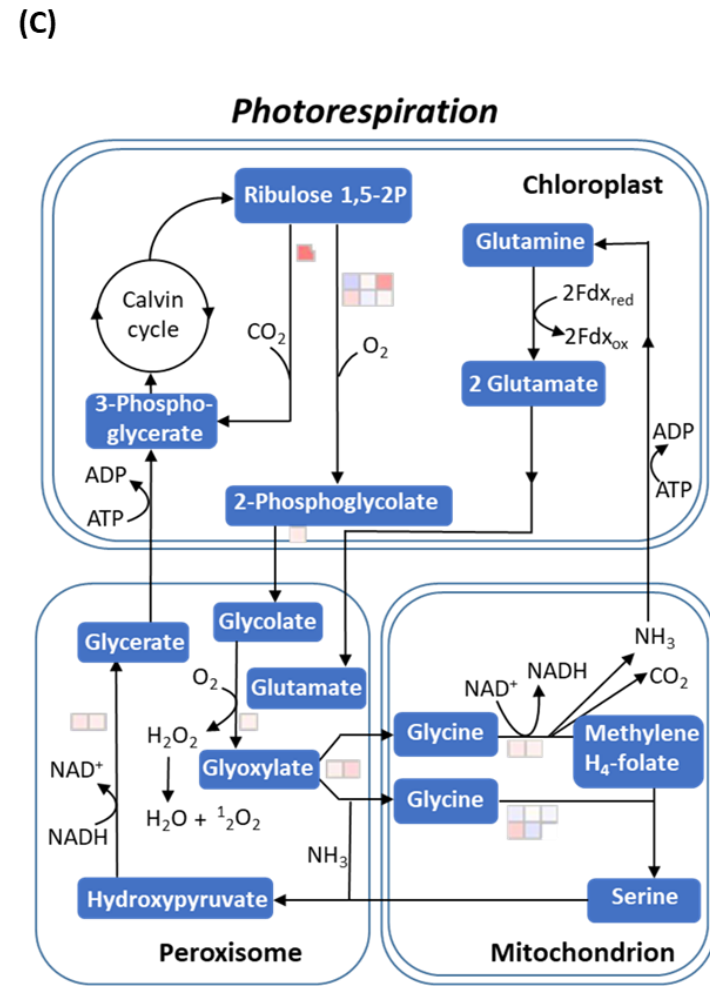
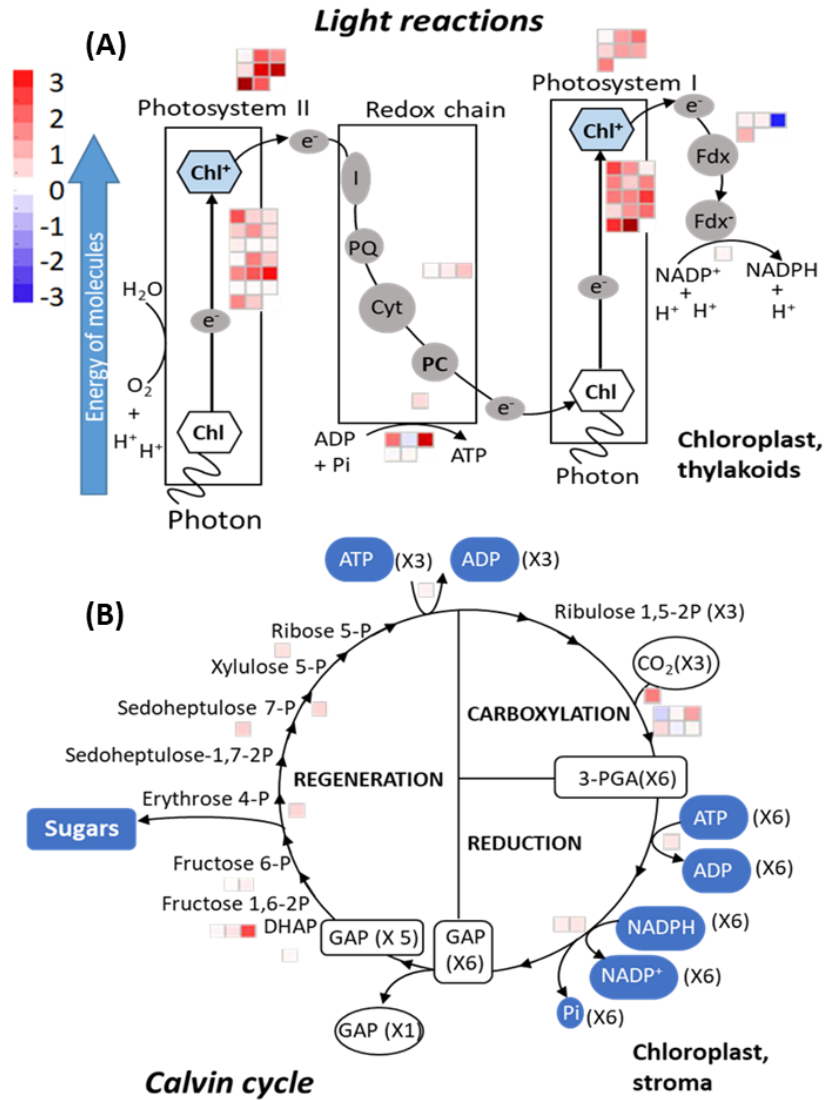


**Figure 2.13 Summary of affected metabolites and pathways between stems of drought stressed EV and *SPL13RNAi* plants**

Distribution of the DEG associated with specialized metabolism. Pathway analysis was performed using MapMan V3.6 (<https://mapman.gabipd.org/>). Transcript fold changes are provided in log 2 with red and blue colours representing increased and decreased transcript levels, respectively, relative to EV. Minor CHO corresponds to minor carbohydrate; TCA, Tricarboxylic acid cycle; OPP, oxidative pentose phosphate pathway. N = 3 biological replicates for each genotype and treatment conditions.

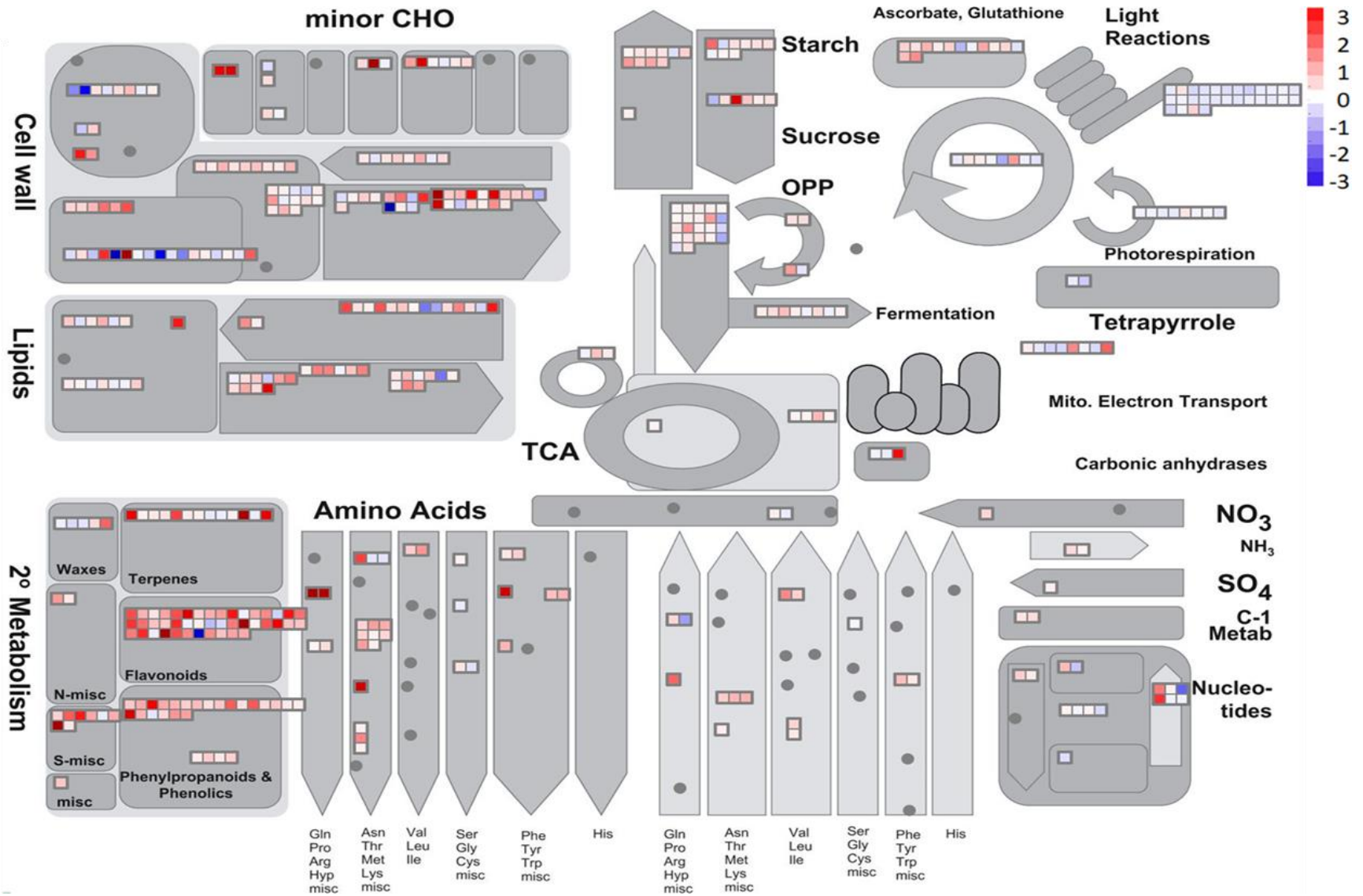
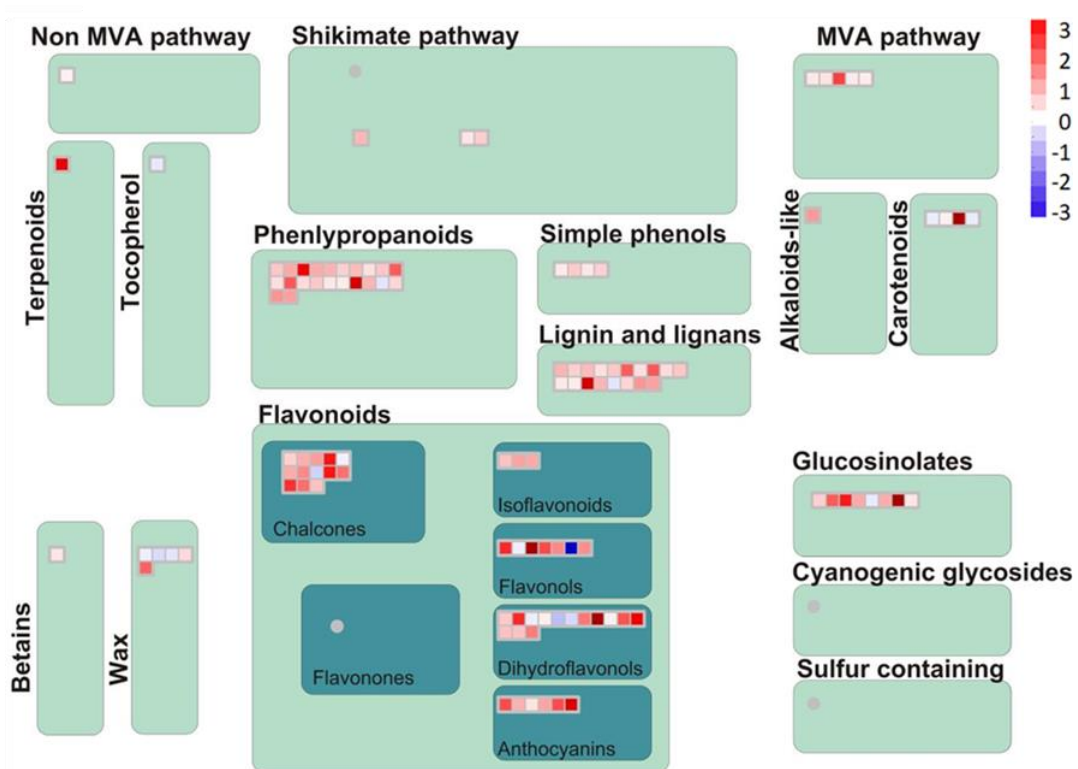


**Figure 2.14 Enhanced specialized metabolite pathway in stems of drought stressed *SPL13RNAi* plants**

Pathway analysis was performed using MapMan V3.6 (<https://mapman.gabipd.org/>). Transcript fold changes are provided in log 2 with red and blue colours representing increased and decreased transcript levels, respectively, relative to EV. N = 3 biological replicates for each genotype and treatment conditions. MVA pathway corresponds to mevalonate pathway.





A similar proportion of components to that of stem and leaf tissues were found where the majority (82%) of transcripts belong to molecular function followed by biological process (13 %) and cellular components (5 %), but the transcript profile varied (**Figure 2.9F**). The top contributing DEG from biological process encompass ATP catabolic process, response to stress, defense response, intercellular signal transduction, phosphorelay signal transduction system, metabolic process, metal ion transport and transmembrane transport (**Figure S8, Table S10**). On the other hand, the major proportion containing molecular function-associated DEG were attributed to phosphorelay response regulator activity, sequence-specific DNA binding transcription factor activity, catalytic activity, GTPase activity, secondary active sulfate transmembrane transporter activity (**Figure S9, Table S10**). Moreover, to further understand the DEG association, I subjected DEG to MapMan-based pathway analysis. Accordingly, metal ion transport, carbohydrate and primary metabolism were significantly and differentially affected between *SPL13RNAi* and EV plants in response to drought (**Figure 2.15; Table S10**). Moreover, cell wall and lipid biosynthesis were increased in roots of *SPL13RNAi* plants as compared to EV plants.

#### **2.2.10 WD40-1 positively regulates *DFR* expression and drought tolerance**

The observed higher *WD40-1* expression and flavonoid accumulation in *miR156OE* genotypes during drought stress (**Figure 2.6C**) and findings from the literature regarding the involvement of WD40-1 in the phenylpropanoid pathway (Gao et al., 2018c), prompted the investigation of whether miR156 or SPL13 directly regulate the expression of *WD40-1*. Hence, I searched for the conserved SPL binding domain (SBD) in the promoter region of *WD40-1*. Genome walking was used to obtain 1.5 kb of the *WD40-1* promoter sequence

(**Figure S3**). However, neither a miR156 target sequence nor a SBD motif could be found in the *WD40-1* promoter, which suggested indirect regulation of *WD40-1* by miR156.

To further understand the potential role of *WD40-1* in alfalfa drought tolerance, alfalfa plants with overexpressed or silenced (RNAi) *WD40-1* were generated and exposed to drought stress. Four different event-derived plants of *WD40-IOE* (OE04, OE09, OE14 and OE15) and *WD40-IRNAi* (RNAi03, RNAi04, RNAi10 and RNAi11) in comparison to WT plants were used (**Figure 2.16A,B**). *WD40-IOE* genotypes were drought tolerant while the RNAi silenced *WD40-1* genotypes were susceptible to drought stress when compared to WT (**Figure 2.16A**). *WD40-IOE* genotypes maintained a relatively higher leaf water potential during drought stress (**Figure 2.16C**).

*WD40-IOE* genotypes developed longer roots resulting in higher root biomass (**Figure 2.16D,E**) and maintained higher leaf chlorophyll concentration during drought stress (**Figure 2.16F**). To understand whether *WD40-1* improves drought tolerance involving *DFR* and other genes in the phenylpropanoid pathway (Pang et al., 2009), transcript abundances of phenylpropanoid-associated genes were determined under drought and well-watered conditions in *WD40-IOE* and *WD40-IRNAi* genotypes. *WD40-IOE* had enhanced expression of *DFR*, *PAL* and *FGT2* during drought stress while levels similar to that of WT were observed when plants were kept under well-watered condition (**Figure 2.17A,B,C**). Moreover, the ABA-related dehydration responsive gene, *DRR*, and photosynthesis related genes, *PSI* and *PSII*, were increased in some *WD40-IOE* genotypes compared to *WD40-IRNAi* and WT plants (**Figure 2.17D,E,F**).

**Figure 2.15 Distribution of root-specific differentially expressed genes between EV and *SPL13*RNAi plants**

Transcript fold changes are provided in log 2 with red and blue colours representing an increased and decreased transcript levels, respectively, relative to EV. Minor CHO corresponds to minor carbohydrate; TCA, Tricarboxylic acid cycle; OPP, oxidative pentose phosphate pathway. N = 3 biological replicates for each genotype and treatment conditions.

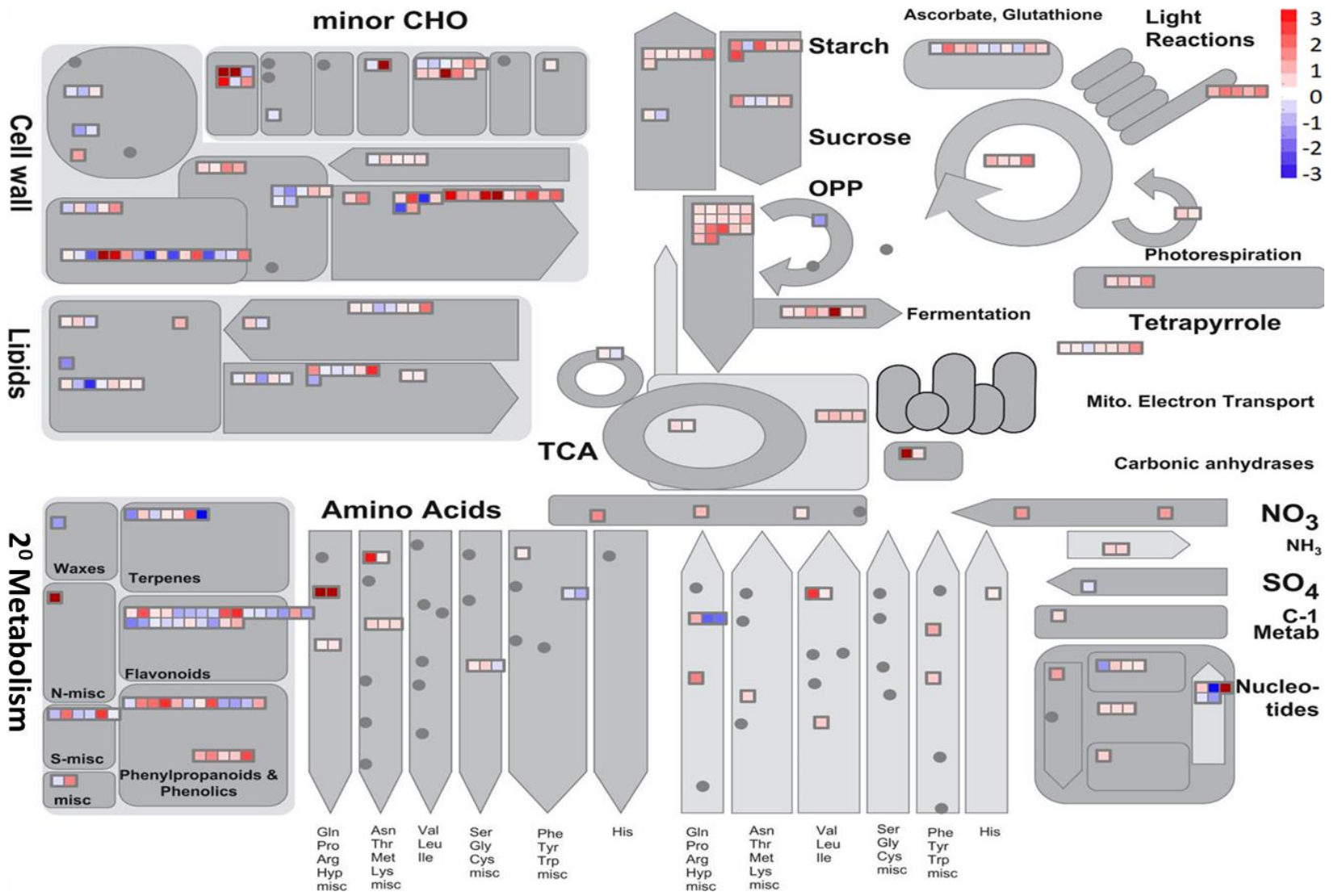


**Figure 2.16 WD40-1 enhances drought tolerance in alfalfa**

(A) Phenotypes of WT, *WD40-1*RNAi and *WD40-1*OE genotypes under drought stress; (B) transcript levels of *WD40-1* in WT, *WD40-1*RNAi, and *WD40-1*OE genotypes; (C) leaf water potential; (D) root fresh weight; (E) root length; and (F) chlorophyll concentration. Values are means  $\pm$  SE; n=4 individual plants for 'B' to 'E' and n=20 in 'F'. In 'B' Transcript levels are shown relative to WT after being normalized to acetyl-CoA carboxylase, *ACCI*, and *ACTIN* housekeeping genes. ANOVA was followed by *Post hoc* Tukey multiple comparisons test when a statistically significant value at  $p < 0.05$  was observed. Values assigned with same letters are not statistically significant from each other. Pair-wise comparison was done between WT and *WD40-1* -OE or with -RNAi genotypes and indicated with '\*' when significant at  $p < 0.05$  and '\*\*' at  $p < 0.01$ , respectively.

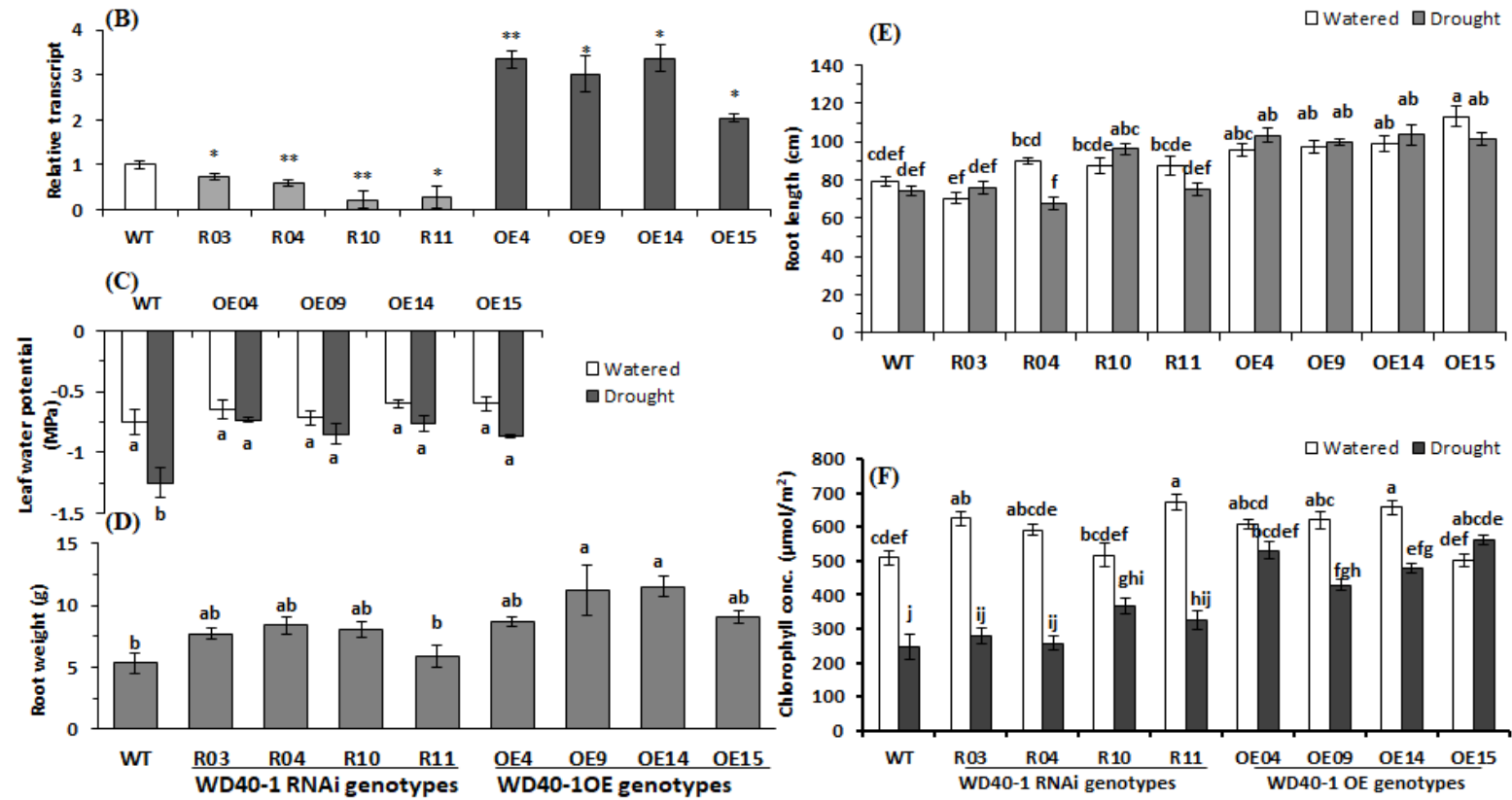
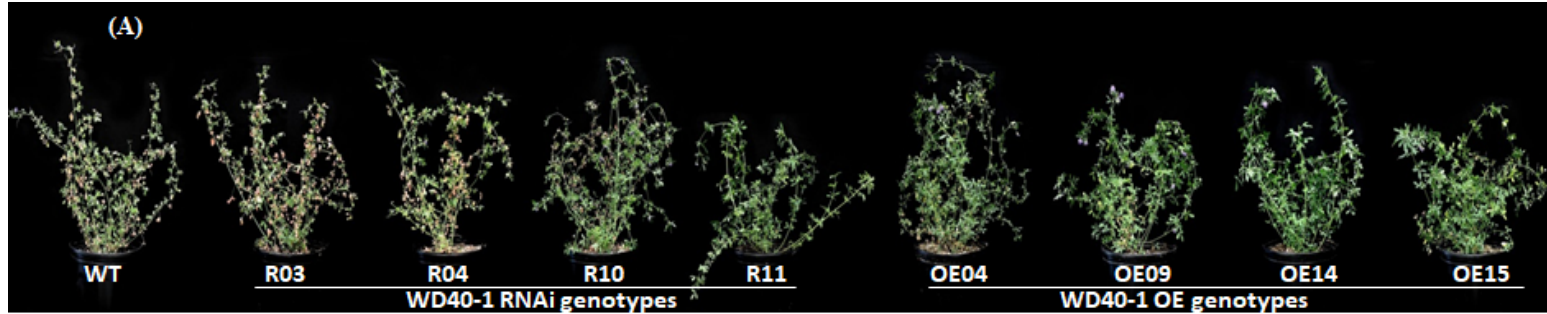
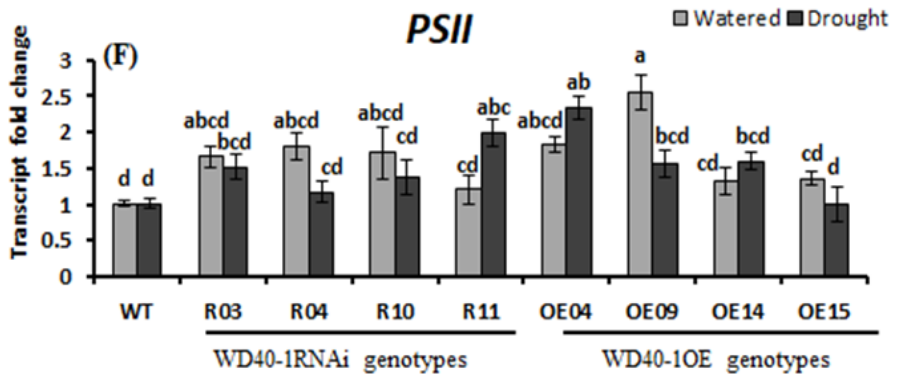
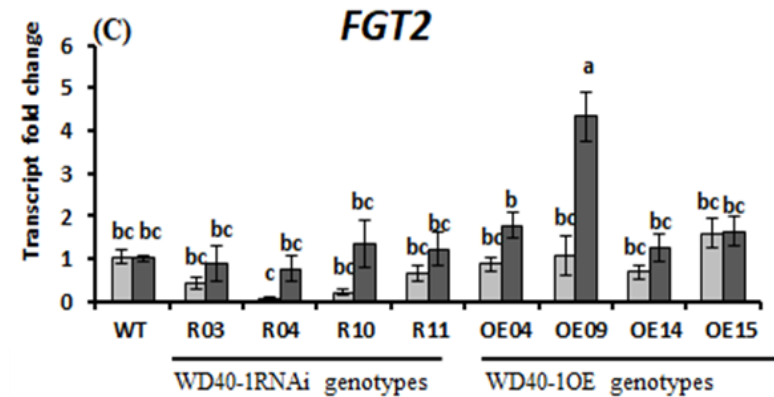
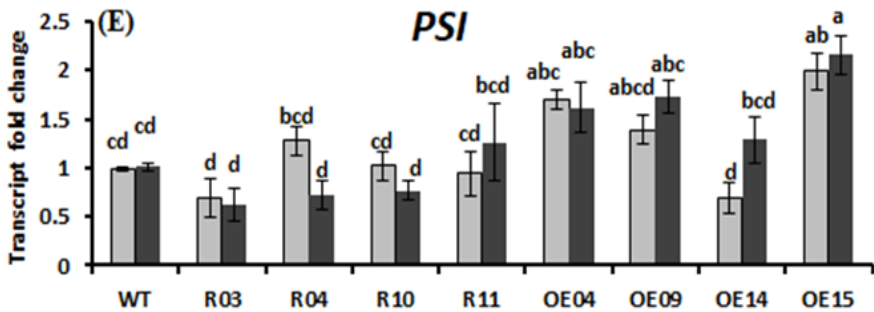
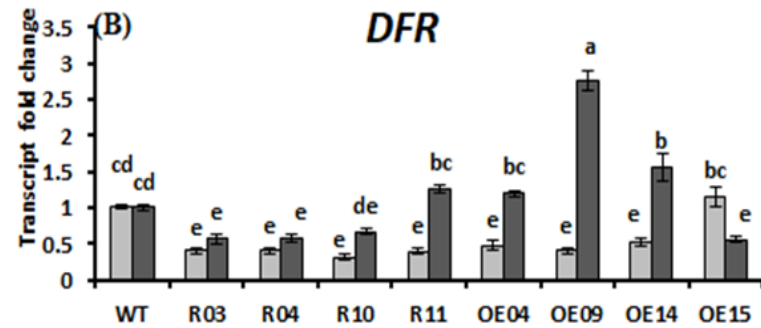
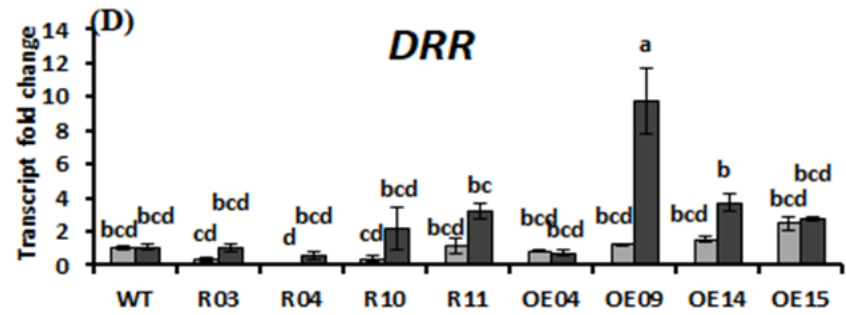
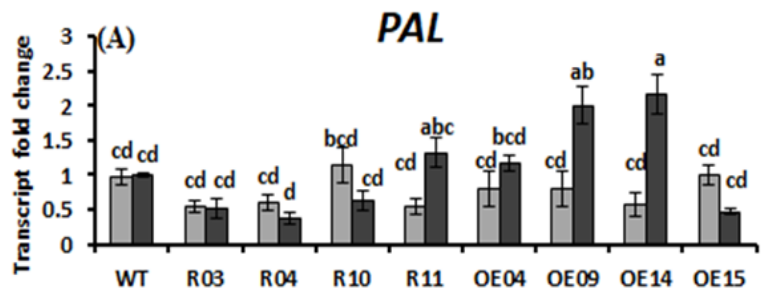


**Figure 2.17 WD40-1 regulates transcript levels of genes in the phenylpropanoid pathway and photosystem during drought stress**

(A) Transcript levels of *PHENYLALANINE AMMONIA-LYASE*, *PAL*; (B) *DIHYDROFLAVONOL-4-REDUCTASE*, *DFR*; (C) *FLAVONOID GLUCOSYLTRANSFERASE2*, *FGT2*; (D) *DEHYDRATION RESPONSIVE RD-22-LIKE*, *DRR*; (E) *PHOTOSYSTEM I p700 CHLOROPHYLL A APOPROTEIN APS I*, *PSI*; (F) *PHOTOSYSTEM II Q(b)*, *PSII*. Transcript levels are shown relative to EV after being normalized to acetyl-CoA carboxylase, *ACCI*, and *ACTIN* housekeeping genes. Values are means  $\pm$  SE, n= 4 individual plants. ANOVA was followed by *Post hoc* Tukey multiple comparisons test when a statistically significant value at  $p < 0.05$  was observed. Values assigned with same letters are not statistically significant from each other.





## 2.3 Discussion

Drought is one of the main factors that impairs plant growth and development (Mpelasoka et al., 2008). Plants respond to drought by showing deleterious effects, or by engaging in adaptive responses involving various molecular, biochemical and physiological strategies (Obidiegwu et al., 2015; Kayum et al., 2016; Pandey and Shukla, 2016). In this study, I used *miR156*OE, *WD40-IOE*, *WD40-IRNAi*, *SPL13RNAi* and GFP-tagged *SPL13* genotypes to investigate the molecular and physiological strategies by *miR156* to regulate drought stress in alfalfa.

### 2.3.1 Moderate levels of *miR156* overexpression, *WD40-1* overexpression or *SPL13* silencing are sufficient to induce phenotypic and physiological drought tolerance strategies in alfalfa

Of the different plant organs that respond to soil water deficit, roots are first to encounter changes in the rhizosphere. Findings in model plants showed initiation and elongation of lateral roots in drought tolerant genotypes to improve water uptake (Xiong et al., 2006; Chen et al., 2012). In this study, an increase in root length accompanied by higher root biomass was observed in alfalfa plants moderately overexpressing *miR156* (low-*miR156A8a* and *A8*) and *WD40-1*. This is associated with a reportedly enhanced level of ABA (Arshad et al., 2017a) in *miR156* overexpressing genotypes under drought stress. ABA enhances primary and lateral root development by regulating the expression of *LATERAL ROOT ORGAN DEFECTIVE (LATD)* gene (Liang et al., 2007). Moreover, *miR156* contributes to root development by silencing *SPL10* to decrease the expression of *AGAMOUS-LIKE MADS box protein 79 (AGL79)* in *Arabidopsis* (Gao et al., 2018b; Yu et al., 2015). Accordingly, the enhanced root development under drought stress helps alfalfa

plants to better access water from deeper soil surface. This finding is consistent with a previous report that showed increased root length in *miR156OE* and *SPL13RNAi* genotypes under drought conditions (Arshad et al., 2017a). Moreover, moderate *miR156OE*, *SPL13RNAi* and *WD40-IOE* genotypes had higher relative water content despite their exposure to drought condition. The observed drought tolerance in *miR156OE* (low-*miR156A8a* and *A8*), *WD40-IOE* and *SPL13RNAi* genotypes suggests this trait is at least partially negatively regulated by *SPL13* and positively by *miR156* and *WD40-1*.

Photosynthesis is negatively impacted by drought stress in alfalfa and other plant species (Aranjuelo et al., 2011; Pinheiro and Chaves, 2011). Of the many photosynthesis efficiency parameters,  $F_v/F_m$  reflects the maximum efficiency of PSII photochemistry possible in a dark-adapted state, and is considered a good indicator of stress in plants (Flagella et al., 1995; Murchie and Lawson, 2013; Gautam et al., 2014; Sharma et al., 2015; Su et al., 2015). Therefore, maintenance of a higher  $F_v/F_m$  was observed in abiotic stress tolerant cultivars of tomato and wheat (Mishra et al., 2012; Sharma et al., 2015; Merchuk-Ovnat et al., 2016) and rice (Nounjan et al., 2018). The observed higher level of  $F_v/F_m$  in low-*miR156A8a* and moderate-*miR156A8* genotypes in the current study suggests their leaves may have a functional photosynthetic unit, in agreement with the observed maintained photosynthesis assimilation rate under drought. The observed higher  $V_{cmax}$  (rubisco carboxylase activity) and  $J_{max}$  (photosynthesis-related electron transport rate) in low-*miR156A8a* and moderate-*miR156A8* under drought further illustrate the maintenance of their photosystems despite drought stress. Such physiology were low to absent in higher-*miR156A11* plants which showed susceptibility to drought stress. A higher  $F_v/F_m$  ratio in *SPL13RNAi-05* and *SPL13RNAi-06* was observed, which is

consistent with previously reported findings of increased photosynthesis assimilation rate in drought-treated *SPL13*RNAi genotypes (Arshad et al., 2017a). This suggests that the maintenance of a higher photosynthesis assimilation rate,  $V_{\text{cmax}}$ ,  $J_{\text{max}}$  and high Fv/Fm ratio during drought stress in *miR156*OE and *WD40-IOE* genotypes may be regulated at least in part by a reduced transcript level of *SPL13* and increased transcript level of *WD40-1*.

### **2.3.2 *miR156* overexpression enhances accumulation of stress-related metabolites**

The impact of environmental perturbations on plant metabolism varies among plant species, cultivars, and tissues (Cramer et al., 2011). Accumulation of specific specialized and transient primary metabolites (primary metabolites that are direct precursors of specialized metabolites) in various tissues is used in part to mitigate drought (Ayenew et al., 2015; Batushansky et al., 2015; Hochberg et al., 2015; Degu et al., 2016) and biotic stress (Zhang et al., 2013). Naya et al. (2007) indicated the role of carbon metabolism and oxidative damage on nitrogenase activity reduction during moderate and higher drought stress levels in alfalfa. Other studies in *M. truncatula*, have shown a decrease in symbiotic nitrogen fixation under drought stress resulting in low levels of nitrogen-based metabolites (Larrainzar et al., 2009).

In the current study, alfalfa with a moderately enhanced expression of *miR156* showed anthocyanin, flavonols, and proteinogenic amino acids in leaf and stem tissues. The accumulation of these metabolites may help the plant to scavenge ROS produced during drought stress (Zhang et al., 2015; Xu et al., 2017). Moreover, these metabolites could help the plants to reduce water loss, and further absorb any remaining tightly bound water from the soil by lowering the osmotic balance in the root tissues. The high level of

GABA in leaf, stem and root tissues of low-miR156A8a and moderate-miR156A8 should help maintain a carbon-to-nitrogen balance through a GABA shunt bypassing the decarboxylation part of the TCA cycle (Fait et al., 2008). The importance of GABA in mediating abiotic stress has been well documented in various plant species, including *Arabidopsis* (Renault et al., 2010), black pepper (Vijayakumari and Puthur, 2016) and bentgrass (Li et al., 2016). Proline was also increased in low-miR156A8a and moderate-miR156A8 but not in higher-miR156A11 roots to regulate osmotic homeostasis as reported in other studies (Nakabayashi et al., 2014; Arshad et al., 2017a). The relatively lower concentration of proline abundance in roots of the highest *miR156* overexpressor, higher-miR156A11, might have prevented these plants from maintaining high water levels in their system. The higher level of fructose and arabinose in leaf and stem tissues, respectively, of drought-treated moderate *miR156* overexpressors could provide an energy source and/or an osmolyte. The higher sugar concentration suggests an actively functioning photosynthetic assimilation with the potential to supplement a carbon source for downstream metabolites. This is consistent with a previous finding that drought-stressed alfalfa plants accumulate sugars (Aranjuelo et al., 2013). Moreover, the increased total monomeric anthocyanin and comparable total polyphenol levels in *SPL13RNAi* genotypes illustrated a targeted enhancement of flavonoids, at least partially governed by silencing *SPL13*, in alfalfa to scavenge ROS during drought stress.

### **2.3.3 miR156, WD40-1 and SPL13 regulate phenylpropanoid and photosystem genes under drought**

Due to the various roles that polyphenols play in stress response, efforts have been made to increase their levels in many plants, including alfalfa (Ray et al., 2003). Enhanced

accumulation of flavonoids and PA in alfalfa has important quality implications for animal feed, as moderate amounts of PA tend to reduce bloating in ruminant animals (Aerts et al., 1999; McMahon et al., 2000; Dixon and Sumner, 2003). In the current study, phenylpropanoid pathway-related genes transcript level were enhanced in moderately overexpressing *miR156* alfalfa plants, which is consistent with the increase in anthocyanin and flavonol levels in these plants. *DFR*, *WD40-1* and *MYB112* were higher in low-*miR156A8a* and moderate-*miR156A8* during drought, contributing to anthocyanin accumulation, like in *Arabidopsis* (Lotkowska et al., 2010). Similarly, *SPL13RNAi* genotypes had enhanced *DFR*, *FGT2* and *PAL* transcripts abundance associated with enhanced concentrations of total monomeric anthocyanin, indicating enhancement of the phenylpropanoid/flavonoid pathway. In another study, *Arabidopsis* plants overexpressing *miR156* accumulated anthocyanin in response to salt and mannitol (mimicking drought) treatments by increasing *DFR* expression (Cui et al., 2014). The enhanced *DFR* expression level in *Arabidopsis* was regulated by silencing *SPL9* (Cui et al., 2014). The current findings suggest that accumulation of anthocyanin and other polyphenols may be regulated via *SPL13* in alfalfa. Moreover, the enhanced level of *DFR* in *WD40-IOE* plants and reduced in *WD40-IRNAi* plants suggests that *DFR* is positively regulated by *WD40-1* to promote flavonoid biosynthesis, but the mechanism of this regulation remains to be investigated.

To investigate whether the higher photosynthesis assimilation rate during drought stress in *SPL13RNAi* (Arshad et al., 2017a) and *WD40-IOE*, *WD40-IRNAi* and *miR156OE* genotypes (current study) are regulated at the transcription level, the expression of genes mediating photosynthesis was investigated. *PSI* and *PSII* transcript abundance

increased in moderately overexpressing *miR156*OE genotypes and *SPL13*RNAi genotypes upon drought. Previously, it was reported that an increased abundance of ABA, which regulates stomatal aperture by active hydrolysis during drought stress, in *miR156*OE moderate-*miR156A8* plants (Arshad et al., 2017a). In the current study, I examined expression of the ABA-induced dehydration responsive gene (*RD22*) and found it to be increased in *SPL13*RNAi plants during drought stress. The consistent observation of higher polyphenols and photosynthetic assimilation rate with associated transcripts during drought stress in moderate *miR156*OE and *SPL13*RNAi genotypes suggests a drought resilience functions for *miR156*.

#### **2.3.4 SPL13 negatively regulates *DFR* expression and flavonoid biosynthesis**

To investigate whether the increased flavonoid accumulation and expression of phenylpropanoid-associated genes, especially *DFR*, are directly regulated by the *miR156/SPL13* module, a ChIP-qPCR analysis was conducted to determine binding of *SPL13* to *DFR*. *DFR* catalyses flavonoid biosynthesis by reducing dihydroflavonols to leucoanthocyanidins playing a critical role in anthocyanin biosynthesis (Li et al., 2012). A previous report showed *SPL9* directly negatively regulates the expression level of *DFR* to enhance accumulation of anthocyanin in response to NaCl and mannitol treatment in *Arabidopsis* (Cui et al., 2014). In the current study, *DFR* expression increased during drought stress in moderately overexpressing *miR156* and *SPL13*RNAi plants. Accordingly, I selected *DFR* to test for *SPL13* binding, given the presence of multiple potential SBD core GTAC sequences in the *DFR* promoter. The fold enrichment from ChIP-qPCR showed the strongest *SPL13* binding was observed closest to coding sequence of *DFR* at region III of the promoter. This is in line with reports that showed conserved core SBD

element is not by itself sufficient for SPL binding, but rather binding is also determined by the position of SBD and the flanking DNA sequences (Yamaguchi et al., 2009; Yu et al., 2010; Wang et al., 2016). SPL13 acts as a transcriptional suppressor of *DFR* during drought stress as confirmed by higher expression of *DFR* in *SPL13RNAi* and the *miR156OE* plants which reduces the expression of the repressor SPL13.

### **2.3.5 Genotype-specific gene expression patterns in response to drought stress**

Alfalfa plants with reduced expression of *SPL13*, a target of miR156, affected a plethora of genes leading to improved drought stress tolerance. To understand how SPL13-modulated genes contribute to drought stress tolerance, I compared the transcript profiles of drought stressed *SPL13RNAi* and EV leaf, stem, and root tissues. Differentially expressed genes were distributed in leaf, stem and root tissues. A total of 228 transcripts (74 increased and 154 decreased) were differentially expressed and present across all tissues. One of the commonly increased transcripts, fasciclin-like arabinogalactan protein (FLAP), which is primarily reported to have cell adhesion function in Arabidopsis and also involved in abiotic stress tolerance (Johnson et al., 2003; Zang et al., 2015) was increased in *SPL13RNAi* plants. In addition to *FLAP* genes, proline dehydrogenase (*PDH*) was commonly increased in all tissues of *SPL13RNAi* plants. The role of proline metabolism is well established in drought tolerance by either scavenging ROS, balancing the carbon to nitrogen ratio through the GABA shunt (Ghafoor et al., 2019), or serving as an osmolytes (Hare and Cress, 1997). Proline and its catabolic products are more important to drought tolerance than high accumulation of proline itself (Bhaskara et al., 2015). In line with this, I noticed an increase in the transcript level of *PDH*, which is involved in proline catabolism (Bhaskara et al., 2015). The other commonly increased transcripts with higher fold-changes

were those of Pmr5/Cas1p GDSL/SGNH-like acyl-esterase family proteins, whose functions are still not well characterized, and ABA receptors with known roles in abiotic stress tolerance (Li et al., 2018; Liu et al., 2019). Accordingly, the increased transcript abundance of *FLAP*, *PDH*, *GDSL*, and ABA receptor along with other transcripts across the three tissue types in *SPLI3RNAi* alfalfa relative to EV suggests that these protein coding genes may play a major role in the response of *SPLI3RNAi* plants to drought stress.

### **2.3.6 Photosynthesis-related DEG are upregulated in leaves of *SPLI3RNAi* plants during drought**

Physiological investigation of *SPLI3RNAi* plants under drought stress showed maintenance of vital physiological processes, such as photosynthesis. This was accompanied by an upregulation of photosynthesis-related genes (*PSI* and *PSII*) in *SPLI3RNAi* plants. Comparison of transcript profiles of leaves of both genotypes under control and drought conditions revealed that various metabolic pathways were affected with photosynthesis being predominantly enhanced in *SPLI3RNAi* plants. The observed upregulation of photosynthesis-associated DEG were mainly in the light-dependent reaction, consistent with the physiological data that showed *SPLI3RNAi* plants maintained the photosynthesis process during drought stress, while photosynthesis was reduced in EV. Other studies have shown that the light-dependent reaction centers were significantly affected by drought in maize (Zhang et al., 2018; Zenda; et al., 2019). The maintained or slightly increased photorespiration-associated transcripts in *SPLI3RNAi* plants may serve as energy sink to prevent over-reduction of photosynthetic electron chain and photo-inhibition in *SPLI3RNAi* plants. Moreover, an increased level of photo-inhibition, unreduced NADPH with lower photosynthetic assimilation rate, was reported previously



in drought stressed plants (Wingler et al., 1999). The observed higher photosynthetic assimilation rate in *SPL13RNAi* plants potentially lowers the reductive power of NADPH that affects photosynthesis otherwise.

### **2.3.7 Specialized metabolite-related DEG are upregulated in stems of *SPL13RNAi* plants during drought**

Specialized metabolites are important in plant growth and development, and the association of high levels of specialized metabolites with reduced ROS levels were reported in *in vivo* (Agati et al., 2012) and *in vitro* assays (Ramya et al., 2015). Accordingly, increasing the abundances of specialized and associated primary metabolites, such as ascorbates and proline, are considered as a marker for enhanced biotic and abiotic stress tolerance. In the current study, I observed enhanced stress tolerance associated with primary and specialized metabolites in *miR156* overexpressing genotypes. I also observed an increase in anthocyanin accumulation in *SPL13RNAi* plants. This suggests anthocyanin and possibly other ROS scavenging metabolites are regulated by SPL13 in a miR156-dependent manner involving *DFR*. To further investigate the involvement of SPL13 in regulating levels of secondary metabolites, especially phenylpropanoids, the global transcript levels of *SPL13RNAi* plants from leaf, stem and root tissues was investigated relative to EV. Importantly, stem-derived samples had an enhanced abundance of transcripts mainly associated with the phenylpropanoid pathway, unlike leaf and root tissues that had an increase in photosynthesis- and ion transport-associated transcripts, respectively. The enhanced abundance of transcripts associated with the phenylpropanoid pathway is consistent with the observed pigmentation in *miR156* overexpressing stem tissues. An earlier study showed the accumulation of anthocyanin to be positively correlated with level

of *DFR* expression in potato in a non-tissue specific manner (Wang et al., 2013). The ChIP-qPCR analysis revealed that while SPL13 indeed binds to *DFR* promoter presumably to regulate its expression, enhanced anthocyanin accumulation was observed only in the stem, like in *Cornus stolonifera* (Gould et al., 2010). RNAseq analysis also indicated upregulation of transcripts involved in the biosynthesis of anthocyanin and other polyphenols from the phenylpropanoid pathway mainly in stem tissues during drought stress. Whether SPL13 also regulates the phenylpropanoid pathway in tissues other than the stems remains to be further investigated.

### **2.3.8 The upregulated root-specific DEG are mainly attributed to ion transport in *SPL13RNAi* plants during drought stress**

Roots are the first plant tissues to encounter low moisture availability in soil, but maintenance of plant water potential is not completely dependent on roots but rather on a continuum that involves soil, root, leaf, and the atmosphere through the transpiration stream (Elfving et al., 1972; Meinzer et al., 2001). To maintain water potential, drought-tolerant plants use different strategies to affect the osmotic balance and/or hydrostatic force governed through the transpiration stream. To adjust and maintain the osmotic balance, the use of osmolytes, such as sugars and proline, was observed in different plants (Hayat et al., 2012; Slama et al., 2015). In the current study, drought-tolerant genotypes of *miR156OE* had higher concentrations of the osmolytes proline and sugars. Furthermore, to understand the involvement of SPL13 in maintaining water potential under drought, transcripts from *SPL13RNAi* and EV root tissues were profiled under control and drought conditions. The differentially expressed genes had increased levels of transcripts associated with the GABA shunt and membrane integrity, such as *GDSL*, in *SPL13RNAi*

plants. Primary metabolites, such as ascorbate and glutathione, and phenylpropanoid-specialized metabolites known to scavenge ROS were increased. To verify the transcript-based metabolite pathway analysis and identify non-enzymatic metabolite conversions (Keller et al., 2015), primary and specialized metabolite analysis using *SPL13*RNAi plants is important. The eventual release of the alfalfa genome sequence should allow for pathway analysis to potentially identify novel metabolite pathways unmapped to the *M. truncatula* genome in the current study, but which may contribute to the drought stress response in alfalfa.

## 2.4 Conclusions

Following to the report of Arshad et al. (2017a), which stated that miR156 regulates drought tolerance in alfalfa by silencing *SPL13*, I investigated the mechanisms deployed by miR156 and *SPL13* in this response with the aim of developing tools for molecular marker-assisted breeding of alfalfa. Metabolomic, physiological and molecular mechanisms were investigated to show how low- to moderate levels of *miR156* overexpression are sufficient to induce drought-tolerance in alfalfa. Moderate level *miR156*OE genotypes low-miR156A8a and moderate-miR156A8 induced accumulation of stress mitigating metabolites. These metabolites could help the plants to scavenge ROS, reduce water loss and further absorb any remaining tightly bound water from the soil by lowering the osmotic pressure in the root tissues. In addition, the plants had physiological adjustments such as improved photosynthesis assimilation rate, maintenance of high Fv/Fm ratios, and enhanced root growth and development. The relatively low levels of stress-mitigating metabolites and reduced physiological adjustments may have resulted in drought susceptibility in the highest *miR156* overexpressor (higher-miR156A11). I also

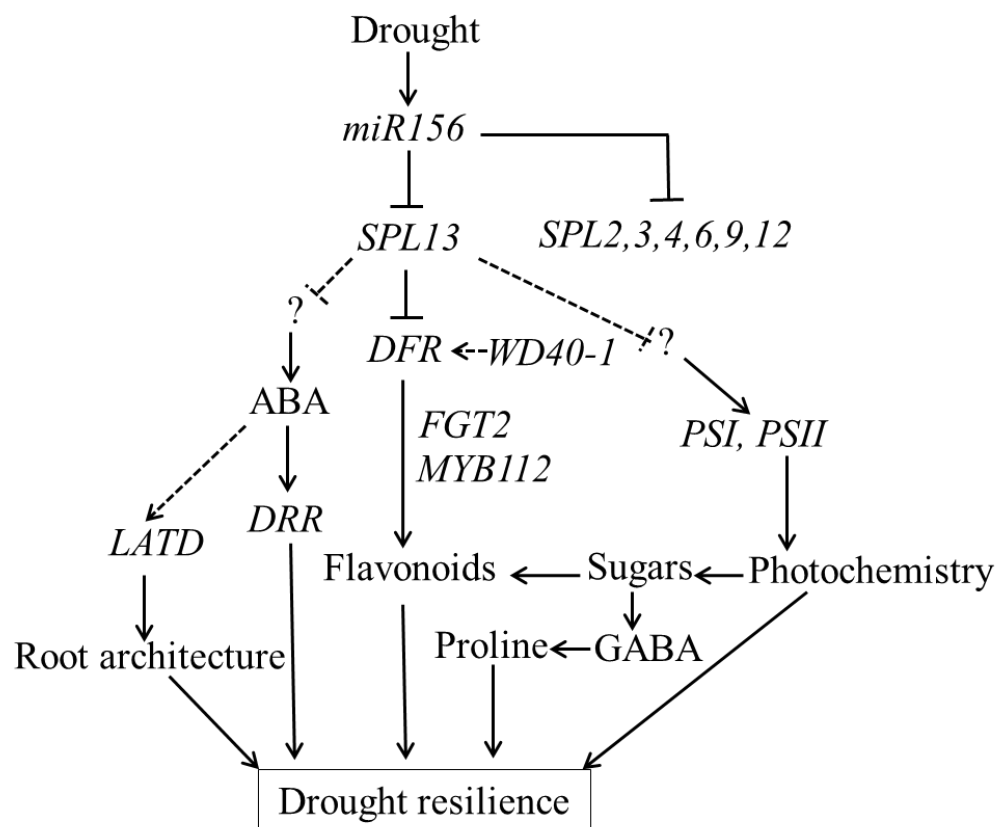
demonstrated direct binding of *SPL13* to the *DFR* promoter. *SPL13* acts as a transcriptional suppressor of *DFR* during drought stress as confirmed by higher expression of *DFR* in *SPL13RNAi* and *miR156OE* plants. A similar observation of SPLs suppressing the expression of *DFR* has been reported in *Arabidopsis* (Gou et al., 2011) in which *SPL9* silences *DFR* in response to salt and mannitol treatment (Cui et al., 2014). Moreover, I detected an increase in expression of genes involved in the phenylpropanoid and photosynthesis pathways in *miR156OE* plants under drought stress. Similar group of genes were also increased in *SPL13RNAi* plants under drought stress. Moreover, the global transcriptomic profile of *SPL13RNAi* plants showed tissue-specific regulation of transcripts and associated pathways. In leaf tissues, the transcript levels of mainly photosynthesis- and photo-respiration-associated genes were increased while increasing phenylpropanoid pathway-associated transcripts in stem tissues of *SPL13RNAi* plants under drought stress. Furthermore, the root-based transcriptomic analysis in *SPL13RNAi* plants illustrated increased transcript abundances in ion transporters, primary and specialized metabolites to transport osmolytes and scavenge ROS while maintaining membrane integrity through GDSL.

I propose a model for a drought tolerance mechanism regulated by moderate levels of *miR156* overexpression (**Figure 2.18**). The schematic representation shows the central role of *miR156* in regulating drought stress in alfalfa. *MiR156* is induced by drought stress, which in turn silences *SPL13* (Arshad et al., 2017a). Reduced expression of *SPL13* driven by *miR156* and enhanced level of *WD40-1* enhances *DFR* resulting in accumulation of anthocyanin in stem tissues. In moderate *miR156OE* plants, primary metabolites such as GABA, proline and sugars also accumulate for carbon-to-nitrogen balance and osmotic

homeostasis. Induction of *miR156* during drought stress also enhances phenotypic plasticity, such as longer roots and higher biomass to access more water from the rhizosphere. With reduced *SPL13* expression, *miR156OE* and *WD40-1OE*, higher photosynthetic efficiency is also achieved during drought stress. I conclude that moderate levels of *miR156* expression silence *SPL13* and increase *WD40-1* expression to fine-tune *DFR* and other phenylpropanoid-associated transcripts for anthocyanin biosynthesis and regulate various developmental, physiological and biochemical processes in alfalfa leading to improved drought resilience.

**Figure 2.18 Schematic representation of miR156-based alfalfa drought resilience model system**

With drought prevalence, *miR156* expression level is increased regulating the expression levels of SPLs, specifically SPL13 in alfalfa. The reduced level of SPL13, which is a negative regulator of *DFR* expression, elevates the expression of *DFR* and other phenylpropanoid pathway genes enhancing flavonoid biosynthesis mainly in stem tissues. On the other hand, the reduction of SPL13 transcript level in alfalfa leaves maintained photochemistry of the plants sustaining photosynthetic process under drought stress. Maintenance of photosynthesis activity provides carbon skeleton for the biosynthesis of phenylpropanoid-associated metabolites by converting acetyl-CoA into malonyl-CoA which can be facilitated by vascular sugar movement from leaves to stem. Furthermore, the reduced level of SPL13 in root tissues results in accumulated primary metabolites biosynthesis-associated transcripts to scavenge reactive oxygen species under drought stress. Solid line represents an experimentally confirmed mechanism while broken lines are hypothesized functions. Arrow heads indicate positive regulation while line heads indicate negative regulation. miR156, microRNA156; SPL13, Squamosa promoter binding protein like transcription factor 13; DFR, Dihydroflavonol-4-reductase; FGT2, Flavonoid glucose transferease2; GABA, Gamaminobutyric acid; ABA, abiscisic acid; DRR, dehydration responsive gene; LATD, lateral development; PSI, *PHOTOSYSTEM I p700 CHLOROPHYL A APOPROTEIN APS I*; PSII, *PHOTOSYSTEM IIQ(b) (II)*.



## 2.5 Methods

### 2.5.1 Genetic material

#### *miR156* overexpressing and *SPL13*RNAi plants

*Medicago sativa* L. N4.4.2 (Badhan et al., 2014) were obtained from Dr. Daniel Brown (Agriculture and Agri-Food Canada) and used as wild-type (WT) genotypes. Plants overexpressing *miR156* (*miR156*OE) at different levels (low-*miR156*A8a, moderate-*miR156*A8 and higher-*miR156*A11) and an empty vector control (EV) were generated previously in the Hannoufa laboratory and used in this experiment (Aung et al., 2015b). *miR156* is slightly (0.5) elevated in low-*miR156*A8a, but is moderate (1.5) to higher (2.5) relative transcript level in moderate-*miR156*A8 and higher-*miR156*A11, respectively (Aung et al., 2015b). The plants were grown in a fully automated greenhouse with 16-hour light (380–450 W/m<sup>2</sup>), relative humidity (RH) of 70% and temperature of 25±2<sup>0</sup>C at the Agriculture and Agri-Food Canada London Research and Development Center, London, Ontario, Canada. Given that alfalfa is an obligatory outcross, vegetative cuttings were used for propagation according to Aung et al. (2015b) to maintain genotypes throughout the study. Since *miR156* down-regulates seven *SPL* genes (including *SPL13*) to regulate a network of downstream genes, I used *SPL13*RNAi genotypes (*SPL13*RNAi-2, *SPL13*RNAi-5 and *SPL13*RNAi-6) (Arshad et al., 2017a) selected for their low *SPL13* expression levels relative to WT alfalfa and other *SPL13*RNAi transgenic alfalfa plants.

#### Generation of *WD40-1* overexpressing and *WD40-1*RNAi alfalfa plants

Four *WD40-1*OE (OE04, OE09, OE14 and OE15) and four *WD40-1*RNAi (R03, R04, R10 and R11) genotypes were generated to investigate the role of *WD40-1* in drought tolerance.



*WD40-1* overexpression and downregulated genotypes were generated using constructs made from alfalfa homolog *WD40-1* (Medtr3g074070) using the Gateway cloning system (Thermo Fisher Scientific, Mississauga ON). For overexpression studies, full-length of *WD40-1* was amplified from alfalfa cDNA using primers with *AttB* sites attached, forward (B1-WD40-1) and reverse (B2-WD40-1) (**Table S1**) and cloned into the pDONR/Zeo entry vector. For downregulation studies, a 253 bp putative *WD40-1* fragment was amplified from alfalfa cDNA using *AttB* sites attached forward (B1-WD40-1-RNAi) and reverse (B2-WD40-1-RNAi) (**Table S1**) primers and cloned into pDONR/Zeo entry vector.

After PCR screening and confirmation by sequencing, LR reactions were performed for the overexpression and RNAi constructs to recombine the fragments into the pMDC83 (overexpression) and pHELLSGATE12 (RNAi) vectors (Gao et al., 2018a). Subsequently, overexpression and RNAi constructs were used to transform *Agrobacterium tumefaciens* strain EHA105 and subsequently into alfalfa (Aung et al., 2015b). qRT-PCR was then used to analyze the *WD40-1* gene in *WD40-1* overexpressing and downregulation in corresponding genotypes using primers WD1-qPCR-F and WD1-qPCR-R (**Table S1**).

### **2.5.2 Imposing drought stress**

Drought stress was imposed on alfalfa plants by withholding water for two weeks at 30 days post vegetative propagation (juvenile vegetative) stage. Plants were kept in a completely randomized design with equal growing soil moisture levels maintained before starting the experiment using a SM 100 soil moisture sensor (Spectrum Technologies Inc., Jakarta, Indonesia). At least four biological replicates were used per genotype per treatment for transcript and metabolite analysis, while 4 to 10 plants were used for physiological analyses (each replicate being an individual plant). The entire experiment was repeated

under the same growth and drought stress conditions to test the repeatability of results. Leaves (newly developed upper leaves), stems (lower 5 cm internode close to soil) and roots (7.5 cm of main and auxiliary root tips) were harvested from *miR156OE*, *SPL13RNAi*, *WD40-IOE*, *WD40-IRNAi*, EV and WT plants depending on the experiment. Samples were flash frozen with liquid nitrogen and kept at  $-80^{\circ}\text{C}$  for later metabolomic and transcriptomic analyses.

### **2.5.3 Metabolite extraction for parallel LCMS and GCMS analysis**

To explore miR156-related regulation of specialized metabolites and transient primary metabolites, extracts of stem, leaf and root tissues of drought-stressed *miR156OE* and EV plants were subjected to LCMS and GCMS analysis. Extraction of samples was performed according to Ayenew et al. (2015) for parallel LCMS and GCMS analysis. Unless stated otherwise, chemicals used for the analysis were obtained from Sigma-Aldrich, Canada. Briefly, frozen 50 mg tissues were crushed with a RETCH-mill (Retsch GmbH, 42787 Haan, Germany) and stainless-steel beads. One ml prechilled extraction solution, methanol/chloroform/water (2.5/1/1 v/v/v), was added containing an internal standard ribitol/adonitol 0.225 mg/mL for GCMS analysis while ampicillin (Sigma, and Saint Luis, Missouri, USA) and corticosterone were used at 1 mg/mL for LCMS to normalize extraction variability. The mixture was vortexed and ultra-sonicated for 10 min. Following centrifugation at 20,800 G for 10 min (at  $4^{\circ}\text{C}$ ), supernatant was collected and mixed with equal volumes of 300  $\mu\text{L}$  water and chloroform. The mixtures were vortexed briefly and centrifuged at 20,800 G for 5 min to collect the upper aqueous phase for parallel LCMS and GCMS analyses.

LCMS analysis was performed using an Agilent 1290 Infinity LC system coupled with a Thermo Q-Exactive Quadrupole-Orbitrap mass spectrometer. Analytes were separated with an Agilent Eclipse Plus C18 ZORBAX Rapid Resolution High Definition (RRHD) 1.8  $\mu\text{m}$  particle 2.1 i.d.  $\times$  50 mm column. The instrument was equipped with electrospray ionization (ESI) interface operating in a negative and positive ion mode for better metabolite identification. Metabolites were identified based on mass to charge ratio ( $m/z$ ), retention time, and fragmentation pattern in comparison to commercial standards, ChemSpider and ReSpect phytochemical databases (Ayenew et al., 2015; Hochberg et al., 2015). MZmine2 software (Pluskal et al., 2010) was also used for LCMS metabolite mass detection, chromatogram building, and the separation of overlapping peaks. In parallel, transient primary metabolites were explored using 75  $\mu\text{L}$  aliquots of the extracted samples for LCMS after processing the aliquots. An Agilent 5975C Triple-Axis Detector MSD and 7890A GC system in splitless mode with 30-m VF-5 ms column with 0.25 mm i.d. were used. GCMS temperature and running conditions are as described in Hochberg et al. (2013). First, the aliquots were dried using an Eppendorf Vacufuge<sup>TM</sup> concentrator (Hamburg, Germany), derivatized with 40  $\mu\text{L}$  *O*-methylhydroxylamine hydrochloride in pyridine with 7  $\mu\text{L}$  standard alkane mixture (0.029% v/v C10-C20 of each 50 mg/L) for two hrs at 37<sup>0</sup>C followed by 70  $\mu\text{L}$  *N*-methyl-*N*-[trimethylsilyl] trifluoroacetamide (MSTFA) for silylation. Metabolites from GCMS were identified using the retention time of the standard alkane mixture with their mass spectra and a NIST 2011 mass spectral library (Ayenew et al., 2015; Batushansky et al., 2015; Degu et al., 2016).

#### **2.5.4 Total monomeric anthocyanin and polyphenol determination**

Total monomeric anthocyanin, TMA, and total polyphenol, TPP, were determined using a pH differential extraction method (Lee et al., 2005; Cheok et al., 2013). Briefly, flash-frozen in liquid nitrogen samples were crushed with mortar and pestle under liquid nitrogen and 500 mg tissue were used for the combined analysis of TMA and TPP. Samples were treated with two ml acidified methanol (MeOH with 1% HCL), vortexed and sonicated at 20 KHz for 15 min. Homogenate was stirred at 3000 rpm for one hour and centrifuged (at 4°C) for 10 minutes at full speed (20,800 G). The supernatant was collected, added two ml chloroform, vortexed and centrifuged at full speed for 10 minutes. The upper aqueous phase was collected, filtered with Whatman 0.2 µm filters, and divided into three equal aliquots for TMA (pH 1.0 and 4.5) and TPP analysis. The first aliquot was mixed with an equal volume of 0.025 M KCl at pH 1.0 while the second was mixed with equal volumes of 0.4 M sodium acetate at pH 4.5 and measured absorbance at 520 nm and 700 nm with water as a blank. TPP was analysed by mixing an equal volume of the third aliquot with Folin-chiocalteu reagent (diluted 1:10 with water) and vortexed for 3 min. Four ml of sodium carbonate (7.5% w/v) was added to the mixture, which was then vortexed and incubated for 30 min in the dark. TPP was determined as gallic acid equivalent (GAE) after measuring absorbance of the aliquot at 765 nm with acidified methanol as blank. TMA level was expressed as mg cyanidin-3-o-glucoside (CG) equivalent.

#### **2.5.5 Physiological and phenotypic data measurement**

To determine drought-mitigating strategies, phenotypic and physiological parameters were investigated. Midday photosynthesis assimilation rates and dark-adapted chlorophyll fluorescence (Fv/Fm) were measured in newly growing upper unshaded leaves using a LI-

6400XT portable photosynthesis meter coupled with Fluorescence System (LI-COR Biosciences, Lincoln, Nebraska, USA). Photosynthesis assimilation rate responses across a gradient of CO<sub>2</sub> level ( $A/C_i$ ) (0 - 2000 ppm) in the mesophyll cells to determine the maximum rate of rubisco carboxylase activity ( $V_{cmax}$ ) and maximum photosynthetic electron transport rate ( $J_{max}$ ) were calculated to determine photosynthesis efficiency using the R statistical software *plantecophys* package (Duursma, 2015). Chlorophyll concentration indexes (CCI) of newly growing upper leaves were also determined using an Apogee MC100 instrument (Apogee instruments, Logan, Utah, USA) (Sawada et al., 2012). To determine plant water status, the midday leaf water potential was measured using a SAPS II Portable Plant Water Status Console (Soilmoisture Equipment Corp., Santa Barbara, CA, USA) in dark-adapted leaves by covering leaves with a polyethylene bag and aluminium foil for 20 min. In addition, above and below ground phenotypic parameters were measured, such as stem number and shoot weight, root length and weight according to Aung et al. (2015b), and stem basal diameter at 1 cm above stem-soil interface.

### **2.5.6 RNA extraction**

Lower basal stem internode, young top leaves and root tip samples were collected and flash frozen in liquid nitrogen and kept in a -80°C freezer until used for qRT-PCR analysis and RNA sequencing. Approximately 50 mg fresh weight was used for total RNA extraction using a QIAGEN RNeasy® Plant mini kit for leaf, stem and root tissues (Cat # 74904), and a PowerLyzer®24 bench top bead-based homogenizer (Cat # 13155) following manufacturer protocols. Total RNA quality was checked using BioRad Bioanalyzer for integrity and Nanodrop for concentration before RNAseq analysis.

### 2.5.7 qRT-PCR analysis

The extracted RNA was treated with Ambion®TURBO DNA-free<sup>TM</sup> DNase (Cat # AM1907) followed by iScript<sup>TM</sup> cDNA synthesis (Cat # 1708891). Transcript levels of selected genes involved in specialized metabolite biosynthesis and photosynthesis were investigated in this study. Using publicly available transcriptomics data of two *miR156OE* alfalfa genotypes under control (unstressed) conditions (Gao et al., 2016) and *M. truncatula* genome sequence Mt4.0V2 (<http://www.medicagogenome.org/downloads>), transcripts of differentially expressed genes with the SBD core GTAC sequence within 2.5 kb of their promoter regions were identified. Among those, genes shown by Gene Ontology analysis to be involved in flavonoid biosynthesis, photosynthetic efficiency and stress tolerance were chosen for expression analysis by qRT-PCR. Primers specific to the above genes (**Table S1**) were designed using *M. truncatula* genome sequence and amplified product was sequenced for an identity check (**Figure S1**). Publicly available Primer3 software (<http://primer3.ut.ee/>) was used to design primers, and their efficiency was verified at different concentrations with gradient annealing temperature PCR before using for qRT-PCR analysis.

qRT-PCR was performed using the CFX96<sup>TM</sup> Real-Time PCR detection system and SsoFast<sup>TM</sup> EvaGreen® Supermixes (Bio-Rad Cat # 1725204). Specifically, 2 µL cDNA (equivalent to 200 ng cDNA), 1 µL forward and reverse gene-specific primers (10 µM each), 5 µL SsoFast<sup>TM</sup> EvaGreen® Supermixes, and 2 µL of nuclease-free water was used to make the final reaction volume of 10 µL. PCR amplification was performed at: cDNA denaturation at 95<sup>0</sup>C for 30 sec followed by 40 cycles of 95<sup>0</sup>C for 10 sec, 58<sup>0</sup>C for 30 sec and 72<sup>0</sup>C for 30 sec (denaturation, annealing and extension, respectively) followed by a

melting curve that ran from 65<sup>0</sup>C to 95<sup>0</sup>C with a gradual increment of 0.5 per 5 sec. All reactions were performed with three technical and four biological replicates. Transcript levels were analysed relative to *acetyl-CoA carboxylase (ACCI)* and *ACTIN* housekeeping genes designed based on alfalfa sequences (Aung et al., 2015b; Arshad et al., 2017a).

### **2.5.8 RNAseq and pathway analysis**

NEBNext<sup>®</sup>Ultra<sup>™</sup> kit (New England Biolabs Inc., Canada) was used for stranded mRNA library preparation followed by Illumina HiSeq 2500 sequencing with 126 pair end nucleotide bases were performed at the Center for Applied Genomics, The Hospital for Sick Children, Toronto, ON, Canada pay for service. RNAseq data was analyzed according to Trapnell et al., (2012) on biocluster with Linux interface. To identify the expression pattern of genes and module identification, R-software environment-based network analysis with weighted gene co-expression network, WGCNA, in ‘BiocManager’ package was performed according to Langfelder and Horvath (2008). Moreover, differential gene expression-based pathway analysis was done using MapMan free software V3.6 (<https://mapman.gabipd.org/>) with a *M. truncatula* reference sequence, Mt4.0 V2 (<http://www.medicagogenome.org/downloads>).

### **2.5.9 ChIP-qPCR analysis of SPL13-DNA binding**

Shoot tips of alfalfa plants overexpressing *SPL13* tagged with GFP driven by the CaMV35S promoter (p35S:SPL13-GFP) (Gao et al., 2018a) were used to understand the occupancy of SPL13 on promoters of downstream genes contributing to drought tolerance. One-month-old SPL13-GFP overexpressing genotypes and WT control plants were used for ChIP-qPCR analysis based on a previously published protocol (Gendrel et al., 2005) with some modifications. Briefly, 500 mg of shoot tips from WT and p35S:SPL13-GFP

plants were collected, washed, proteins bound to DNA were cross-linked using 1% formaldehyde and mixtures were ground with liquid nitrogen. Extraction reagents and buffers are listed in **Table S2**. Powdered tissues were homogenized with 15 mL of prechilled Extraction Buffer 1 and filtered with two layers of Miracloth (Millipore, Canada). Subsequently, the filtered mixture was centrifuged at 3000 G for 20 min and the supernatant was discarded while the pellets were resuspended in 1 ml of prechilled Extraction Buffer 2 and centrifuged at 12000 G for 10 min. Afterwards, pellets were resuspended in 300  $\mu$ L prechilled Extraction Buffer 3 and centrifuged at 16000 G for 1 hr. The supernatant was removed, and chromatin pellets were resuspended in 300  $\mu$ L of Nuclei Lysis Buffer by gentle pipetting and sheared twice at power 3 for 15 sec on ice using a Sonic Dismembrator (Fisher Scientific, USA). Supernatant aliquots of 20  $\mu$ L were kept aside for later use as an input DNA control while using the remaining solution for immunoprecipitation. Chromatin solution was brought to 1.5 mL using a ChIP dilution buffer and divided into two equal parts for chromatin immunoprecipitation and a negative control. To each tube, 30  $\mu$ L of protein A-agarose beads (Millipore, Canada) were added and the mixture was gently agitated, centrifuged (3500 G) for 1 min, and supernatant was transferred for immunoprecipitation while discarding the beads. Five  $\mu$ L (5 mg/ml) of Ab290 GFP antibody was added to one of the chromatin solutions (keeping the second one as a no-antibody negative control) for an overnight gentle agitation at 4  $^{\circ}$ C. After 12 hr, 40  $\mu$ L of protein A-agarose beads were added and immune complexes were recovered by centrifugation and washed with cycle of low normality salt, high salt, LiCl, and TE buffer. Immunocomplexes were eluted from beads using 250  $\mu$ L of Elution Buffer and cross linking was reversed with 20  $\mu$ L of 5 M NaCl incubated at 65  $^{\circ}$ C for 5 hours. To each



sample, 10  $\mu$ L 0.5 M EDTA, 20  $\mu$ L 1 M Tris-HCl (pH 6.5) and 2  $\mu$ L of 10 mg/mL proteinase K (Sigma-Aldrich, Canada) were added. DNA was extracted using phenol:chloroform (1:1, v:v), recovered by precipitation with ethanol and 0.3 M sodium acetate (pH=5.2) and 2  $\mu$ L glycogen carrier 10 mg/mL (Sigma-Aldrich, Canada) after overnight incubation at -20  $^{\circ}$ C. After 12 hrs, the solution was centrifuged at 20800 G for 20 min to pellet the DNA and pellet was then washed with 70% ethanol, resuspended with 16  $\mu$ L of distilled water, and DNA was used for ChIP-qPCR analysis. To obtain the *DFR* promoter region sequence from *M. sativa*, proDFR1-MTR primers (**Table S1**) were designed using a close relative *M. truncatula* sequence and amplified region was cloned into TOP10 competent *E. coli* cells using CloneJET (Thermo Scientific) and sequenced. Subsequently, proDFR ChIP-qPCR primers (**Table S1**) were designed based on alfalfa sequences. qRT-PCR was performed using ChIP-precipitated DNA as described in section 2.5.7 while fold enrichment was calculated by dividing Ct values of p35S:SPL13-GFP to WT and comparing with the *LOB1* reference gene (Gao et al., 2018a).

#### **2.5.10 Genome walking for WD40-1 promoter nucleotide sequence**

Due to the lack of alfalfa genome sequence, Clontech GenomeWalker<sup>TM</sup> (California, USA Cat No. 638904) was used to obtain nucleotide sequence of the *WD40-1* promoter region. In brief, genomic DNA were extracted from wild-type alfalfa plants using a Nucleospin<sup>®</sup>Tissue DNA extraction kit (MACHEREY-NAGEL GmbH & Co. KG Germany, Cat. No. 740952). GenomeWalker “libraries” were prepared by digesting the DNA with four different restriction enzymes (*DraI*, *EcoRV*, *PvuII* and *StuI*) at 37 $^{\circ}$ C for two hrs to generate blunt ends. Subsequently, two nested PCR amplifications were performed sequentially for each library using gene-specific primers (GSP1 and GSP2) and

adapter primers (AP1 and AP2) from the kit (**Table S1**). PCR products were analyzed on a 1.5% agarose gel followed by cloning into a pJET1.2 cloning vector to facilitate sequencing. Subsequently, sequences obtained from the four libraries were aligned together to generate the consensus promoter region sequence of *WD40-1* in alfalfa.

### **2.5.11 Statistical data analysis**

Shapiro-Wilk test were used for checking the normal distribution of data before proceeding to analysis of variance (ANOVA). Subsequently, Tukey *post hoc* multiple comparison tests were done on molecular (qRT-PCR and ChIP-qPCR), metabolomic (LCMS and GCMS), physiological and phenotypic data. A pair-wise t-test comparison was implemented between *WD40-IOE* and WT plants and with *WD40-IRNAi* plants for *WD40-1* transcript abundance. Metabolite profile data were subjected to pareto scaling before principal component analysis (PCA) in which metabolites were mean-centered followed by dividing with the square root of the standard deviation. All statistical data analyses were undertaken using R-software environment 3.2.5.

## 2.6 References

- Abe H, Urao T, Ito T, Seki M, Shinozaki K, Yamaguchi-Shinozaki K (2003)** *Arabidopsis* AtMYC2 (bHLH) and AtMYB2 (MYB) function as transcriptional activators in abscisic acid signaling. *The Plant Cell* 15: 63-78
- Aerts RJ, Barry TN, McNabb WC (1999)** Polyphenols and agriculture: Beneficial effects of proanthocyanidins in forages. *Agriculture, Ecosystems and Environment* 75: 1-12
- Agati G, Azzarello E, Pollastri S, Tattini M (2012)** Flavonoids as antioxidants in plants: Location and functional significance. *Plant Science* 196: 67-76
- Alonso A, Marsal S, Julià A (2015)** Analytical methods in untargeted metabolomics: State of the art in 2015. *Frontiers in Bioengineering and Biotechnology* 3
- Aranjuelo I, Molero G, Erice G, Avice JC, Nogués S (2011)** Plant physiology and proteomics reveals the leaf response to drought in alfalfa (*Medicago sativa* L.). *Journal of Experimental Botany* 62: 111-123
- Aranjuelo I, Tcherkez G, Molero G, Gilard F, Avice JC, Nogués S (2013)** Concerted changes in N and C primary metabolism in alfalfa (*Medicago sativa*) under water restriction. *Journal of Experimental Botany* 64: 885-897
- Argyrokastritis IG, Papastylianou PT, Alexandris S (2015)** Leaf water potential and crop water stress index variation for full and deficit irrigated cotton in mediterranean conditions. *Agriculture and Agricultural Science Procedia* 4: 463-470
- Arshad M, Feyissa B, Amyot L, Aung B, Hannoufa A (2017a)** MicroRNA156 improves drought stress tolerance in alfalfa (*Medicago sativa*) by silencing SPL13. *Plant Science* 258: 122-136
- Arshad M, Gruber MY, Wall K, Hannoufa A (2017b)** An Insight into microRNA156 role in salinity stress responses of alfalfa. *Frontiers in Plant Science* 8:356
- Aung B, Gruber MY, Amyot L, Omari K, Bertrand A, Hannoufa A (2015a)** Ectopic expression of LjmiR156 delays flowering, enhances shoot branching, and improves forage quality in alfalfa. *Plant Biotechnology Reports* 9: 379-393
- Aung B, Gruber MY, Amyot L, Omari K, Bertrand A, Hannoufa A (2015b)** MicroRNA156 as a promising tool for alfalfa improvement. *Plant Biotechnology Journal* 13: 779-790
- Aung B, Gruber MY, Hannoufa A (2015c)** The microRNA156 system: A tool in plant biotechnology. *Biocatalysis and Agricultural Biotechnology* 4: 432-442

**Ayeneu B, Degu A, Manela N, Perl A, Shamir MO, Fait A** (2015) Metabolite profiling and transcript analysis reveal specificities in the response of a berry derived cell culture to abiotic stresses. *Frontiers in Plant Science* 6: 728

**Badhan A, Jin L, Wang Y, Han S, Kowalczyk K, Brown DC, Ayala CJ, Latoszek-Green M, Miki B, Tsang A, McAllister T** (2014) Expression of a fungal ferulic acid esterase in alfalfa modifies cell wall digestibility. *Biotechnology for Biofuels* 7: 39

**Batushansky A, Kirma M, Grillich N, Pham PA, Rentsch D, Galili G, Fernie AR, Fait A** (2015) The transporter GAT1 plays an important role in GABA-mediated carbon-nitrogen interactions in Arabidopsis. *Frontiers in Plant Science* 6: 785

**Bhaskara GB, Yang TH, Verslues PE** (2015) Dynamic proline metabolism: Importance and regulation in water limited environments. *Frontiers in plant science* 6: 484-484

**Chen H, Li Z, Xiong L** (2012) A plant microRNA regulates the adaptation of roots to drought stress. *FEBS Letters* 586: 1742-1747

**Cheok CY, Chin NL, Yusof YA, Talib RA, Law CL** (2013) Optimization of total monomeric anthocyanin (TMA) and total phenolic content (TPC) extractions from mangosteen (*Garcinia mangostana* Linn.) hull using ultrasonic treatments. *Industrial Crops and Products* 50: 1-7

**Cohen M, Goldhamer DA, Fereres E, Girona J, Mata M** (2001) Assessment of peach tree responses to irrigation water deficits by continuous monitoring of trunk diameter changes. *The Journal of Horticultural Science and Biotechnology* 76: 55-60

**Couzigou JM, Combier JP** (2016) Plant microRNAs: Key regulators of root architecture and biotic interactions. *New Phytologist* 212: 22-35

**Cramer GR, Urano K, Delrot S, Pezzotti M, Shinozaki K** (2011) Effects of abiotic stress on plants: A systems biology perspective. *BMC Plant Biology* 11: 163

**Cruz de Carvalho MH** (2008) Drought stress and reactive oxygen species: Production, scavenging and signaling. *Plant Signaling and Behavior* 3: 156-165

**Cui LG, Shan JX, Shi M, Gao JP, Lin HX** (2014) The miR156-SPL9-DFR pathway coordinates the relationship between development and abiotic stress tolerance in plants. *The Plant Journal* 80: 1108-1117

**Degu A, Ayeneu B, Cramer GR, Fait A** (2016) Polyphenolic responses of grapevine berries to light, temperature, oxidative stress, abscisic acid and jasmonic acid show specific developmental-dependent degrees of metabolic resilience to perturbation. *Food Chemistry* 212: 828-836

**Dixon RA, Sumner LW** (2003) Legume natural products: Understanding and manipulating complex pathways for human and animal health. *Plant Physiology* 131: 878-885

**Duursma RA** (2015) Plantecophys - An R package for analysing and modelling leaf gas exchange data. *PLOS ONE* 10: e0143346

**Elfving DC, Kaufmann MR, Hall AE** (1972) Interpreting leaf water potential measurements with a model of the soil-plant-atmosphere continuum. *Physiologia Plantarum* 27: 161-168

**Fait A, Fromm H, Walter D, Galili G, Fernie AR** (2008) Highway or byway: The metabolic role of the GABA shunt in plants. *Trends in Plant Science* 13: 14-19

**Fenollosa E, Munné-Bosch S** (2019) Physiological Plasticity of Plants Facing Climate Change. In *Annual Plant Reviews online* 2:837-866

**Flagella Z, Pastore D, Campanile RG, Fonzo ND** (1995) The quantum yield of photosynthetic electron transport evaluated by chlorophyll fluorescence as an indicator of drought tolerance in durum wheat. *The Journal of Agricultural Science* 125: 325-329

**Gao R, Austin RS, Amyot L, Hannoufa A** (2016) Comparative transcriptome investigation of global gene expression changes caused by miR156 overexpression in *Medicago sativa*. *BMC Genomics* 17: 658

**Gao R, Gruber MY, Amyot L, Hannoufa A** (2018a) SPL13 regulates shoot branching and flowering time in *Medicago sativa*. *Plant Molecular Biology* 96:119-133

**Gao R, Wang Y, Gruber MY, Hannoufa A** (2018b) miR156/SPL10 modulates lateral root development, branching and leaf morphology in *Arabidopsis* by silencing AGAMOUS-LIKE 79. *Frontiers in Plant Science* 8: 2226-2226

**Gao Y, Liu J, Chen Y, Tang H, Wang Y, He Y, Ou Y, Sun X, Wang S, Yao Y** (2018c) Tomato SlAN11 regulates flavonoid biosynthesis and seed dormancy by interaction with bHLH proteins but not with MYB proteins. *Horticulture Research* 5: 27

**Gautam A, Agrawal D, SaiPrasad SV, Jajoo A** (2014) A quick method to screen high and low yielding wheat cultivars exposed to high temperature. *Physiology and Molecular Biology of Plants* 20: 533-537

**Gendrel AV, Lippman Z, Martienssen R, Colot V** (2005) Profiling histone modification patterns in plants using genomic tiling microarrays. *Nature Methods* 2: 213-218

**Ghafoor R, Akram NA, Rashid M, Ashraf M, Iqbal M, Lixin Z** (2019) Exogenously applied proline induced changes in key anatomical features and physio-biochemical

attributes in water stressed oat (*Avena sativa* L.) plants. *Physiology and Molecular Biology of Plants* 25:1121-1135

**Goldhamer DA, Fereres E** (2001) Irrigation scheduling protocols using continuously recorded trunk diameter measurements. *Irrigation Science* 20: 115-125

**Gou JY, Felippes FF, Liu CJ, Weigel D, Wang JW** (2011) Negative regulation of anthocyanin biosynthesis in *Arabidopsis* by a miR156-targeted SPL transcription factor. *The Plant Cell* 23: 1512-1522

**Gould KS, Dudle DA, Neufeld HS** (2010) Why some stems are red: Cauline anthocyanins shield photosystem II against high light stress. *Journal of Experimental Botany* 61: 2707-2717

**Hare PD, Cress WA** (1997) Metabolic implications of stress-induced proline accumulation in plants. *Plant Growth Regulation* 21: 79-102

**Hayat S, Hayat Q, Alyemeni MN, Wani AS, Pichtel J, Ahmad A** (2012) Role of proline under changing environments: A review. *Plant Signaling and Behavior* 7: 1456-1466

**He F, Mu L, Yan GL, Liang NN, Pan QH, Wang J, Reeves MJ, Duan C-Q** (2010) Biosynthesis of anthocyanins and their regulation in colored grapes. *Molecules* 15: 9057

**Hochberg U, Degu A, Cramer GR, Rachmilevitch S, Fait A** (2015) Cultivar specific metabolic changes in grapevines berry skins in relation to deficit irrigation and hydraulic behavior. *Plant Physiology and Biochemistry* 88: 42-52

**Hochberg U, Degu A, Toubiana D, Gendler T, Nikoloski Z, Rachmilevitch S, Fait A** (2013) Metabolite profiling and network analysis reveal coordinated changes in grapevine water stress response. *BMC Plant Biology* 13: 184

**Intrigliolo DS, Castel JR** (2004) Continuous measurement of plant and soil water status for irrigation scheduling in plum. *Irrigation Science* 23: 93-102

**Johnson KL, Jones BJ, Bacic A, Schultz CJ** (2003) The fasciclin-like arabinogalactan proteins of *Arabidopsis*. A multigene family of putative cell adhesion molecules. *Plant Physiology* 133: 1911-1925

**Kayum MA, Kim HT, Nath UK, Park JI, Kho KH, Cho YG, Nou IS** (2016) Research on biotic and abiotic stress related genes exploration and prediction in *Brassica rapa* and *B. oleracea*: A review. *Plant Breeding and Biotechnology* 4: 135-144

**Keller MA, Piedrafita G, Ralser M** (2015) The widespread role of non-enzymatic reactions in cellular metabolism. *Current Opinion in Biotechnology* 34: 153-161

**Langfelder P, Horvath S** (2008) WGCNA: An R package for weighted correlation network analysis. *BMC Bioinformatics* 9: 559

**Larrainzar E, Wienkoop S, Scherling C, Kempa S, Ladrera R, Arrese-Igor C, Weckwerth W, González EM** (2009) Carbon metabolism and bacteroid functioning are involved in the regulation of nitrogen fixation in *Medicago truncatula* under drought and recovery. *Molecular Plant-Microbe Interactions* 22: 1565-1576

**Lee J, Durst R, Wrolstad R** (2005) Determination of total monomeric anthocyanin pigment content of fruit juices, beverages, natural colorants, and wines by the pH differential method: Collaborative study. *Journal of AOAC International* 88: 1269-1278

**Li H, Qiu J, Chen F, Lv X, Fu C, Zhao D, Hua X, Zhao Q** (2012) Molecular characterization and expression analysis of DIHYDROFLAVONOL 4-REDUCTASE (DFR) gene in *Saussurea medusa*. *Molecular Biology Reports* 39: 2991-2999

**Li X, Li G, Li Y, Kong X, Zhang L, Wang J, Li X, Yang Y** (2018) ABA receptor subfamily III enhances abscisic acid sensitivity and improves the drought tolerance of arabidopsis. *International Journal of Molecular Sciences* 19: 1938

**Li Z, Yu J, Peng Y, Huang B** (2016) Metabolic pathways regulated by  $\gamma$ -aminobutyric acid (GABA) contributing to heat tolerance in creeping bentgrass (*Agrostis stolonifera*). *Scientific Reports* 6: 30338

**Liang Y, Mitchell DM, Harris JM** (2007) Abscisic acid rescues the root meristem defects of the *Medicago truncatula latd* mutant. *Developmental Biology* 304: 297-307

**Liu J, Zhao FL, Guo Y, Fan XC, Wang YJ, Wen YQ** (2019) The ABA receptor-like gene VvPYL9 from drought-resistance wild grapevine confers drought tolerance and ABA hypersensitivity in Arabidopsis. *Plant Cell, Tissue and Organ Culture* 138: 543-558

**Lotkowska ME, Tohge T, Fernie AR, Xue G-P, Balazadeh S, Mueller-Roeber B** (2015) The Arabidopsis transcription factor MYB112 promotes anthocyanin formation during salinity and under high light stress. *Plant Physiology* 169: 1862-1880

**Malik AI, Colmer TD, Lambers H, Setter TL, Schortemeyer M** (2002) Short-term waterlogging has long-term effects on the growth and physiology of wheat. *New Phytologist* 153: 225-236

**Matsuda F** (2016) Regular expressions of MS/MS spectra for partial annotation of metabolite features. *Metabolomics* 12: 113

**Matthews C, Arshad M, Hannoufa A** (2019) Alfalfa response to heat stress is modulated by microRNA156. *Physiologia Plantarum* 165: 830-842

**Mba C, Guimaraes EP, Ghosh K** (2012) Re-orienting crop improvement for the changing climatic conditions of the 21st century. *Agriculture and Food Security* 1: 1-17

**McMahon LR, McAllister TA, Berg BP, Majak W, Acharya SN, Popp JD, Coulman BE, Wang Y, Cheng KJ** (2000) A review of the effects of forage condensed tannins on ruminal fermentation and bloat in grazing cattle. *Canadian Journal of Plant Science* 80: 469-485

**Meinzer FC, Clearwater MJ, Goldstein G** (2001) Water transport in trees: Current perspectives, new insights and some controversies. *Environmental and Experimental Botany* 45: 239-262

**Merchuk-Ovnat L, Fahima T, Krugman T, Saranga Y** (2016) Ancestral QTL alleles from wild emmer wheat improve grain yield, biomass and photosynthesis across environments in modern wheat. *Plant Science* 251: 23-34

**Mishra KB, Iannaccone R, Petrozza A, Mishra A, Armentano N, La Vecchia G, Trtílek M, Cellini F, Nedbal L** (2012) Engineered drought tolerance in tomato plants is reflected in chlorophyll fluorescence emission. *Plant Science* 182: 79-86

**Mishra B, Chand S, Singh Sangwan N** (2019) ROS management is mediated by ascorbate-glutathione- $\alpha$ -tocopherol triad in co-ordination with secondary metabolic pathway under cadmium stress in *Withania somnifera*. *Plant Physiology and Biochemistry* 139: 620-629

**Mpelasoka F, Hennessy K, Jones R, Bates B** (2008) Comparison of suitable drought indices for climate change impacts assessment over Australia towards resource management. *International Journal of Climatology* 28: 1283-1292

**Murchie EH, Lawson T** (2013) Chlorophyll fluorescence analysis: A guide to good practice and understanding some new applications. *Journal of Experimental Botany* 64: 3983-3998

**Nakabayashi R, Yonekura-Sakakibara K, Urano K, Suzuki M, Yamada Y, Nishizawa T, Matsuda F, Kojima M, Sakakibara H, Shinozaki K, Michael AJ, Tohge T, Yamazaki M, Saito K** (2014) Enhancement of oxidative and drought tolerance in *Arabidopsis* by overaccumulation of antioxidant flavonoids. *The Plant Journal* 77: 367-379

**Naya L, Ladrera R, Ramos J, González EM, Arrese-Igor C, Minchin FR, Becana M** (2007) The response of carbon metabolism and antioxidant defenses of alfalfa nodules to drought stress and to the subsequent recovery of plants. *Plant Physiology* 144: 1104-1114

**Nounjan N, Chansongkrow P, Charoensawan V, Siangliw JL, Toojinda T, Chadchawan S, Theerakulpisut P** (2018) High performance of photosynthesis and



osmotic adjustment are associated with salt tolerance ability in rice carrying drought tolerance QTL: Physiological and co-expression network analysis. *Frontiers in Plant Science* 9: 1135-1135

**Obidiegwu JE, Bryan GJ, Jones HG, Prashar A** (2015) Coping with drought: Stress and adaptive responses in potato and perspectives for improvement. *Frontiers in Plant Science* 6: 542

**Olesen JE, Trnka M, Kersebaum KC, Skjelvåg AO, Seguin B, Peltonen-Sainio P, Rossi F, Kozyra J, Micale F** (2011) Impacts and adaptation of European crop production systems to climate change. *European Journal of Agronomy* 34: 96-112

**Pandey V, Shukla A** (2016) Improving crop yield under drought stress through physiological breeding. In MA Hossain, SH Wani, S Bhattacharjee, DJ Burritt, L-SP Tran, eds, *Drought stress tolerance in plants, Physiology and Biochemistry*. Springer International Publishing, 1: 331-348

**Pang Y, Wenger JP, Saathoff K, Peel GJ, Wen J, Huhman D, Allen SN, Tang Y, Cheng X, Tadege M, Ratet P, Mysore KS, Sumner LW, Marks MD, Dixon RA** (2009) A WD40 repeat protein from *Medicago truncatula* is necessary for tissue-specific anthocyanin and proanthocyanidin biosynthesis but not for trichome development. *Plant Physiology* 151: 1114-1129

**Pinheiro C, Chaves MM** (2011) Photosynthesis and drought: Can we make metabolic connections from available data? *Journal of Experimental Botany* 62: 869-882

**Pluskal T, Castillo S, Villar-Briones A, Orešič M** (2010) MZmine 2: Modular framework for processing, visualizing, and analyzing mass spectrometry-based molecular profile data. *BMC Bioinformatics* 11: 395

**Ramya R, Kalaiselvi M, Narmadha R, Gomathi D, Bhuvaneshwari V, Amsaveni R, Devaki K** (2015) Secondary metabolite credentials and in vitro free radical scavenging activity of *Alpinia calcarata*. *Journal of Acute Medicine* 5: 33-37

**Ray DK, Gerber JS, MacDonald GK, West PC** (2015) Climate variation explains a third of global crop yield variability. *Nature Communications* 6: 5989

**Ray H, Yu M, Auser P, Blahut-Beatty L, McKersie B, Bowley S, Westcott N, Coulman B, Lloyd A, Gruber MY** (2003) Expression of anthocyanins and proanthocyanidins after transformation of alfalfa with maize Lc. *Plant Physiology* 132: 1448-1463

**Renault H, Roussel V, El Amrani A, Arzel M, Renault D, Bouchereau A, Deleu C** (2010) The Arabidopsis pop2-1 mutant reveals the involvement of GABA transaminase in salt stress tolerance. *BMC Plant Biology* 10: 20

**Sawada Y, Nakabayashi R, Yamada Y, Suzuki M, Sato M, Sakata A, Akiyama K, Sakurai T, Matsuda F, Aoki T, Hirai MY, Saito K** (2012) RIKEN tandem mass spectral database (ReSpect) for phytochemicals: A plant-specific MS/MS-based data resource and database. *Phytochemistry* 82: 38-45

**Serraj R** (2003) Effects of drought stress on legume symbiotic nitrogen fixation: Physiological mechanisms. *Indian Journal of Experimental Biology* 41: 1136-1141

**Sharma DK, Andersen SB, Ottosen CO, Rosenqvist E** (2015) Wheat cultivars selected for high Fv/Fm under heat stress maintain high photosynthesis, total chlorophyll, stomatal conductance, transpiration and dry matter. *Physiologia Plantarum* 153: 284-298

**Slama I, Abdelly C, Bouchereau A, Flowers T, Savouré A** (2015) Diversity, distribution and roles of osmoprotective compounds accumulated in halophytes under abiotic stress. *Annals of Botany* 115: 433-447

**Stief A, Altmann S, Hoffmann K, Pant BD, Scheible WR, Baurle I** (2014) Arabidopsis miR156 regulates tolerance to recurring environmental stress through SPL transcription factors. *The Plant Cell* 26: 1792-1807

**Stincone A, Prigione A, Cramer T, Wamelink MMC, Campbell K, Cheung E, Olin-Sandoval V, Grüning NM, Krüger A, Alam MT, Keller MA, Breitenbach M, Brindle KM, Rabinowitz JD, Ralser M** (2015) The return of metabolism: Biochemistry and physiology of the pentose phosphate pathway. *Biological Reviews of the Cambridge Philosophical Society* 90: 927-963

**Su L, Dai Z, Li S, Xin H** (2015) A novel system for evaluating drought-cold tolerance of grapevines using chlorophyll fluorescence. *BMC Plant Biology* 15: 82

**Sun G** (2012) MicroRNAs and their diverse functions in plants. *Plant Molecular Biology* 80: 17-36

**Trapnell C, Roberts A, Goff L, Pertea G, Kim D, Kelley DR, Pimentel H, Salzberg SL, Rinn JL, Pachter L** (2012) Differential gene and transcript expression analysis of RNA-seq experiments with TopHat and Cufflinks. *Nature Protocols* 7: 562

**Tuteja N** (2007) Abscisic acid and abiotic stress signaling. *Plant Signaling and Behavior* 2: 135-138

**Verdier J, Zhao J, Torres-Jerez I, Ge S, Liu C, He X, Mysore KS, Dixon RA, Udvardi MK** (2012) MtPAR MYB transcription factor acts as an on switch for proanthocyanidin biosynthesis in *Medicago truncatula*. *Proceedings of the National Academy of Sciences of the United States of America* 109: 1766-1771

**Vijayakumari K, Puthur JT** (2016)  $\gamma$ -Aminobutyric acid (GABA) priming enhances the osmotic stress tolerance in *Piper nigrum* Linn. plants subjected to PEG-induced stress. *Plant Growth Regulation* 78: 57-67

**Wang H, Fan W, Li H, Yang J, Huang J, Zhang P** (2013) Functional characterization of dihydroflavonol-4-reductase in anthocyanin biosynthesis of purple sweet potato underlies the direct evidence of anthocyanins function against abiotic stresses. *PLOS ONE* 8: e78484

**Wang L, Sun S, Jin J, Fu D, Yang X, Weng X, Xu C, Li X, Xiao J, Zhang Q** (2015) Coordinated regulation of vegetative and reproductive branching in rice. *Proceedings of the National Academy of Sciences of the United States of America* 112: 15504-15509

**Wang Z, Wang Y, Kohalmi SE, Amyot L, Hannoufa A** (2016) SQUAMOSA PROMOTER BINDING PROTEIN-LIKE 2 controls floral organ development and plant fertility by activating ASYMMETRIC LEAVES 2 in *Arabidopsis thaliana*. *Plant Molecular Biology* 92: 661-674

**Wei S, Gruber MY, Yu B, Gao MJ, Khachatourians GG, Hegedus DD, Parkin IA, Hannoufa A** (2012) Arabidopsis mutant sk156 reveals complex regulation of SPL15 in a miR156-controlled gene network. *BMC Plant Biology* 12: 169

**Wingler A, Quick WP, Bungard RA, Bailey KJ, Lea PJ, Leegood RC** (1999) The role of photorespiration during drought stress: An analysis utilizing barley mutants with reduced activities of photorespiratory enzymes. *22*: 361-373

**Xie Z, Allen E, Fahlgren N, Calamar A, Givan SA, Carrington JC** (2005) Expression of Arabidopsis MIRNA genes. *Plant Physiology* 138: 2145-2154

**Xiong L, Wang R-G, Mao G, Koczan JM** (2006) Identification of drought tolerance determinants by genetic analysis of root response to drought stress and abscisic acid. *Plant Physiology* 142: 1065-1074

**Xu M, Hu T, Zhao J, Park MY, Earley KW, Wu G, Yang L, Poethig RS** (2016) Developmental functions of miR156-regulated SQUAMOSA PROMOTER BINDING PROTEIN-LIKE (SPL) genes in *Arabidopsis thaliana*. *PLOS Genetics* 12: e1006263

**Xu Z, Mahmood K, Rothstein S** (2017) ROS induces anthocyanin production via late biosynthetic genes and anthocyanin deficiency confers the hypersensitivity to ROS-generating stresses in Arabidopsis. *Plant and Cell Physiology* 58: 1364-1377

**Yamaguchi A, Wu M-F, Yang L, Wu G, Poethig RS, Wagner D** (2009) The microRNA-regulated SBP-Box transcription factor SPL3 is a direct upstream activator of LEAFY, FRUITFULL, and APETALA1. *Developmental Cell* 17: 268-278

**Yang T, Wang Y, Teotia S, Zhang Z, Tang G** (2018) The making of leaves: How small RNA networks modulate leaf development. *Frontiers in Plant Science* 9:824

**Yu N, Niu Q-W, Ng K-H, Chua N-H** (2015) The role of miR156/SPLs modules in *Arabidopsis* lateral root development. *The Plant Journal* 83: 673-685

**Yu N, Cai WJ, Wang S, Shan CM, Wang LJ, Chen XY** (2010) Temporal control of trichome distribution by microRNA156-targeted SPL genes in *Arabidopsis thaliana*. *The Plant Cell* 22: 2322-2335

**Zang L, Zheng T, Chu Y, Ding C, Zhang W, Huang Q, Su X** (2015) Genome-wide analysis of the fasciclin-like arabinogalactan protein gene family reveals differential expression patterns, localization, and salt stress response in populus. *Frontiers in Plant Science* 6:1140

**Zenda T, ; Songato L, Wang X, Liu G, ; Jin H, Dong A, Yang Y, Duan H** (2019) Key maize drought-responsive genes and pathways revealed by comparative transcriptome and physiological analyses of contrasting inbred lines. *International Journal of Molecular Science* 20: 1268

**Zhang BH, Pan XP, Cannon CH, Cobb GP, Anderson TA** (2005) Identification and characterization of new plant microRNAs using EST analysis. *Cell Research* 15: 336–360

**Zhang X, Lei L, Lai J, Zhao H, Song W** (2018) Effects of drought stress and water recovery on physiological responses and gene expression in maize seedlings. *BMC Plant Biology* 18: 68

**Zhang Y, Butelli E, De Stefano R, Schoonbeek HJ, Magusin A, Pagliarani C, Wellner N, Hill L, Orzaez D, Granell A, Jones Jonathan D, Martin C** (2013) Anthocyanins double the shelf life of tomatoes by delaying overripening and reducing susceptibility to gray mold. *Current Biology* 23: 1094-1100

**Zhang Y, De Stefano R, Robine M, Butelli E, Bulling K, Hill L, Rejzek M, Martin C, Schoonbeek H-j** (2015) Different reactive oxygen species scavenging properties of flavonoids determine their abilities to extend the shelf life of tomato. *Plant Physiology* 169: 1568-1583

**Zhou M, Luo H** (2013) MicroRNA-mediated gene regulation: Potential applications for plant genetic engineering. *Plant Molecular Biology* 83: 59-75

### **3. ABA-dependent *SnRK1* expression mediates the miR156/SPL module for flooding response in alfalfa**

#### **3.1 Background**

Climate change is expected to increase the mean annual temperature and precipitation, which are both correlated with frequent flooding events (Alexander et al., 2006; Brown et al., 2018; Rogelj et al., 2018) that affect crop quality and yield (Bailey-Serres et al., 2012; Brown et al., 2018; Yeung et al., 2018). Plants deploy two main strategies in response to flooding stress: 1) an escape mechanism by elongating stems to emerge above the water surface, or 2) an adaptive mechanism by reducing growth and development to conserve energy. For example, flood-escaping rice genotypes elongate their stems by increasing stem cell size (a strategy regulated by gibberellin) (Dubois et al., 2011). In line with these strategies *SUBMERGENCE1A* (*SUB1A*), *SNORKEL1* (*SK1*) and *SK2* were identified in *Arabidopsis* through their sequence similarity to the rice homologs and were found to play a major role in flooding response (Xu et al., 2006; Hattori et al., 2009). Unlike plants that mainly employ the energy-demanding flood-escape strategy, flood adapting plants, such as wheat, lower their energy metabolism, remaining submerged, and subsequently revive after the stress has ceased to exist (Herzog et al., 2018).

Regulating energy metabolism is important, especially under environmental stress during which a reduced carbon assimilation rate results in reduced cellular glucose concentrations despite the increased demand for carbon skeletons needed for the biosynthesis of specialized metabolites to scavenge ROS. Reduced energy metabolism associated with decreased oxygen availability and reduced photosynthetic carbon

assimilation rate during flood stress has been reported in different studies (Branco-Price et al., 2008; Gupta et al., 2009; Mustroph et al., 2009). This lower energy metabolism is perceived by a sucrose non-fermenting-related protein kinase, SnRK1 (Baena-González et al., 2007; Ramon et al., 2019), which is associated with a HEXOKINASE1 (HXK1) (Moore et al., 2003). The heterotrimeric protein kinase SnRK1 is activated by the  $\alpha$  subunits KIN10 and KIN11 (Fragoso et al., 2009) and regulated by the  $\beta$  and  $\gamma$  subunits in *Arabidopsis* (Wurzinger et al., 2018). *SnRK1* expression is also reported to be triggered in *Arabidopsis* by the stress-related hormone ABA (Jossier et al., 2009). Accordingly, the activation of SnRK1 regulates metabolic stress response and development in *Arabidopsis* (Ramon et al., 2019).

Previous reports showed that overexpression of *miR156* in *M. sativa* increased shoot branching, delayed flowering, reduced stem length (Aung et al., 2015a, 2015b, 2015c), and also played a positive role in abiotic stress tolerance (Arshad et al., 2017a; 2017b; Feyissa et al., 2019; Matthews et al., 2019). Considering the function that miR156 plays in metabolic, physiological and stress response processes in alfalfa I hypothesize that miR156 plays a role in flooding tolerance and that its expression is regulated by SnRK1. Deep sequencing analysis of non-coding RNAs revealed multiple differentially expressed microRNAs by comparing flooding stress vs well-drained poplar and maize plants (Lu et al., 2008; Zhang et al., 2008). In the maize study, Zhang and his colleagues (2008) identified more than 100 differentially expressed microRNAs in response to flooding, of which, miR159, miR395, miR474 were increased while others (miR166, miR167, miR171, miR396, and miR399) were decreased. These microRNAs, along with their proposed mechanisms of action, were reviewed in a recent article indicating the potential role of

microRNAs in flooding response (Fukao et al., 2019). Apart from screening for differentially expressed microRNAs and associated downstream genes, it is important to validate the identified microRNAs and downstream genes by modulating their expression levels and investigating the plant's response under flooding stress. miR156 functions by regulating *SQUAMOSA-PROMOTER BINDING PROTEIN-LIKE (SPL)* genes (Wang et al., 2008; Gao et al., 2016). So far, at least seven *SPLs* (*SPL2*, *SPL3*, *SPL4*, *SPL6*, *SPL9*, *SPL12* and *SPL13*) have been identified as direct targets of miR156 in alfalfa (Gao et al., 2016). The role of the miR156/SPL module in flooding tolerance was investigated in this study using hormone profiling, global transcriptomic profiling and physiological responses of *miR156OE* and miR156-regulated SPL RNAi alfalfa plants. The cross-talk between miR156/SPL and ABA-dependent SnRK1 was also investigated in this study using ABA insensitive (*abi1-2* and *abi5-8*) Arabidopsis mutants along with *KIN10* over-expressing and RNAi silenced Arabidopsis plants under ABA and low sugar treatments. To determine how SnRK1 affects the biosynthesis of miR156, I investigated the protein-protein interaction between SnRK1 and two of the miR156 biogenesis proteins, DICER-LIKE 1 (DCL1) and SERRATE (SE), using a yeast-two-hybrid assay.

### **3.2 Results**

To investigate the role of miR156 in flooding tolerance in alfalfa, I compared *miR156* overexpression (*miR156OE*), *SPL6*RNAi, *SPL13*RNAi, WT, and empty vector plants. Alfalfa cultivars previously identified as flood sensitive (AC-Caribou) and flooding tolerant (AAC-Trueman) served as negative and positive controls, respectively. The plants were initially characterized, under field conditions, for their flooding response using physiological parameters and expression of select flooding-responsive genes at Agriculture

and Agri-Food Canada (AAFC) Research Centre in Kentville, Nova Scotia, Canada (**Figure S10**). Based on these results, I narrowed my focus to *miR156*OE (A8), *SPL13RNAi-5*, *SPL13RNAi-6*, AC-Caribou, AAC-Trueman and WT genotypes, which showed tolerance and susceptible responses and repeated the experiment twice at the AAFC research center in London, Ontario, Canada.

### **3.2.1 miR156/SPL module mediates physiological responses of alfalfa during flooding**

Flooding negatively affects photosynthesis and respiration in plants (Caudle and Maricle, 2012), so I investigated whether the miR156/SPL module regulates this response. One-month old post propagation stage alfalfa plants were subjected to flooding stress and well-drained conditions for two weeks (**Figure 3.1A,B; Figure S10**). Leaf yellowing was observed in all genotypes under flooding stress, but it was more severe in AC-Caribou and wild-type plants (**Figure 3.1B**), which also had reduced photosynthesis rates relative to the other genotypes (**Figure 3.1D**). The flooding tolerant cultivar, AAC-Trueman, showed increased red colouration in the stems of plants under flooding stress (**Figure 3.1C**). Under well-drained, there were no differences between genotypes in the photosynthesis assimilation rate (**Figure 3.1D**). Moreover, dark-adapted chlorophyll fluorescence (Fv/Fm), often used as a stress tolerance indicator (Sharma et al., 2015; Su et al., 2015), was maintained at a higher level in AAC-Trueman, A8, and *SPL13RNAi* plants relative to WT plants under flooding stress (**Figure 3.1E**). To further understand the photosynthesis efficiency, photosynthetic carbon assimilation rate was measured across a gradient of intercellular CO<sub>2</sub> and the maximum rubisco carboxylase activity,  $V_{\text{cmax}}$ , and maximum photosynthesis electron transport,  $J_{\text{max}}$ , were determined (**Figure 3.1F,G**). The data



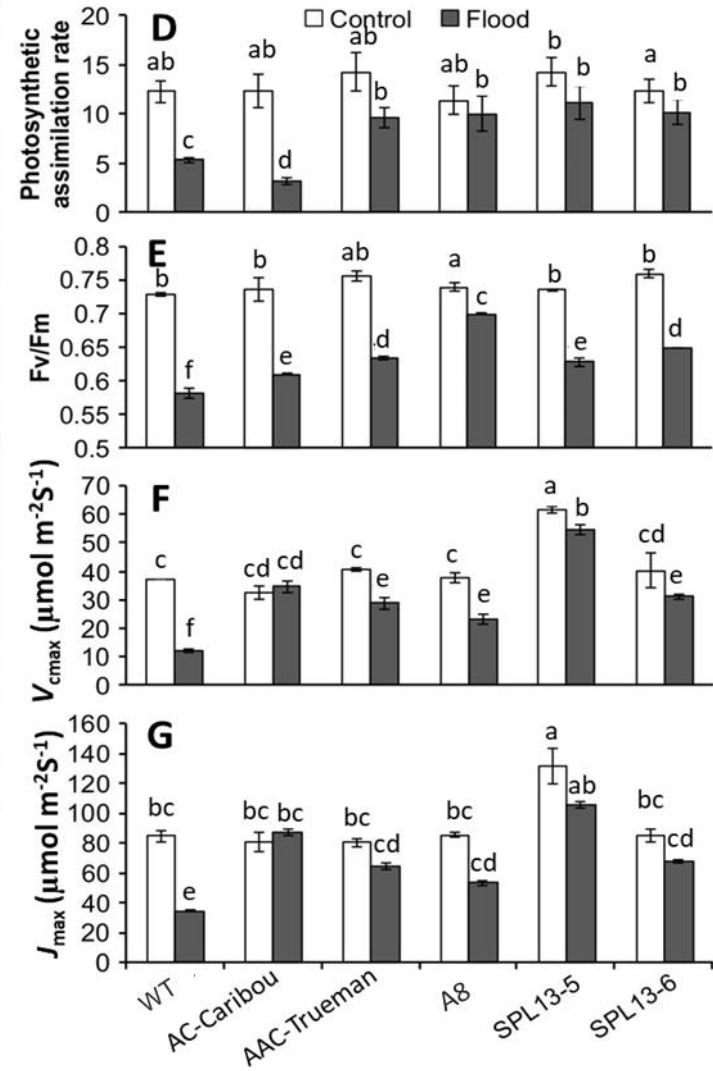
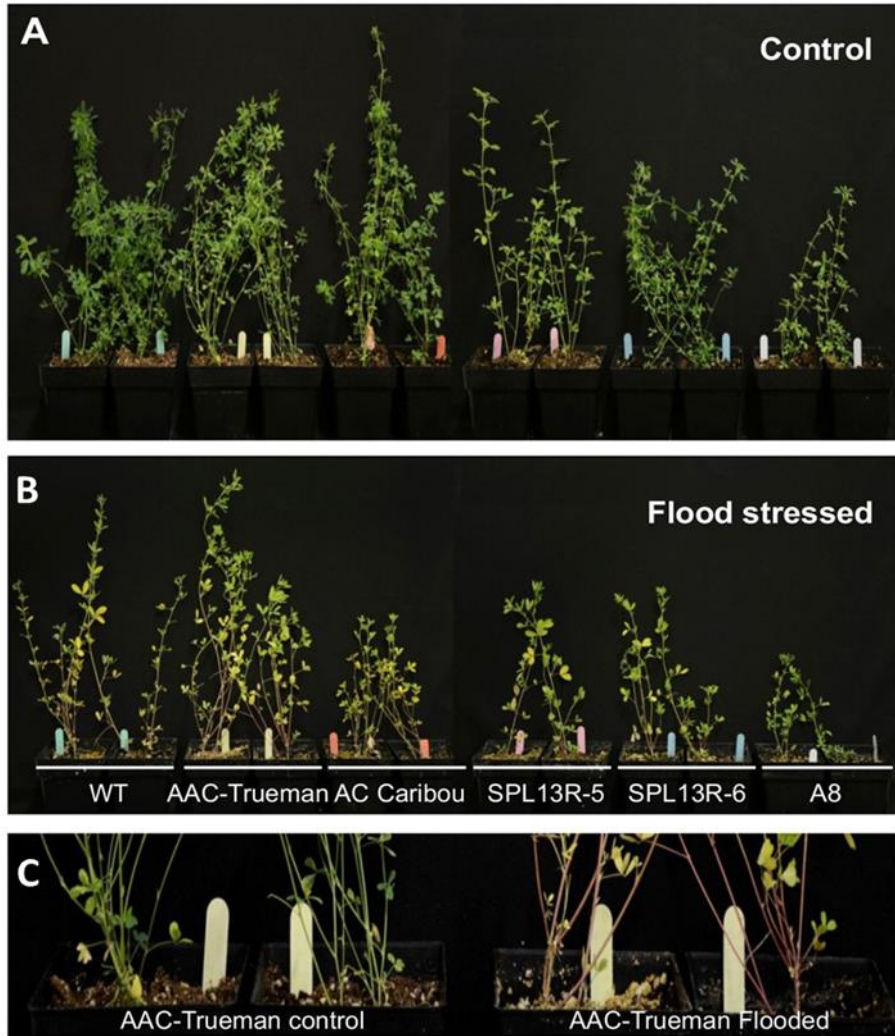
showed a similar pattern to the measurements of photosynthesis assimilation rate (**Figure 3.1D**) and Fv/Fm ratio (**Figure 3.1E**). As a result, *SPL13RNAi*, A8, and AAC-Trueman maintained a higher level of  $V_{max}$  and  $J_{max}$  except for AC-Caribou which showed comparable levels irrespective of flooding stress (**Figure 3.1F,G**).

### 3.2.2 miR156 increases ABA and ABA-catabolites for flooding tolerance

The hormone profiles of flood-stressed and well-drained alfalfa genotypes were investigated to understand hormonal changes in response to flooding. Total ABA metabolites comprising ABA, phaseic acid, ABA-glucose ester (ABAGE), and another four ABA derivatives were all increased in flood-treated plants relative to their well-drained controls by 1.5- (AAC-Trueman) to 2.5-fold (A8) in flood-tolerant genotypes, while a 30% reduction was observed in WT plants (**Figure 3.2A**). Specifically, ABA-catabolites from glucosyl esterification and oxidation reactions, ABAGE and phaseic acid, respectively, contributed a significant portion of the total ABA metabolite abundance under flooding in tolerant genotypes, second only to ABA (**Figure 3.2B,C,D**). For instance, while phaseic acid concentration was not changed between flood stress and well-drained wild-type plants, an average fold increase of 2.95- (AAC-Trueman) to 3.75- (*SPL13RNAi*-6) was observed in the tolerant genotypes (**Figure 3.2C**).

**Figure 3.1 Selected physiological responses of flood-stressed and control alfalfa plants**

One-month alfalfa plants growing under (A) control, and (B) flood-stressed conditions; (C) stem colour development in AAC-Trueman plants upon flood stress, (D) photosynthesis assimilation rate, (E) chlorophyll fluorescence response,  $F_v/F_m$ , (F)  $V_{\max}$ , the maximum rate of rubisco carboxylase activity, (G)  $J_{\max}$ , maximum photosynthesis electron transport rate. Values are sample means  $\pm$  SE, n=8 individual plants. ANOVA was followed by *Post hoc* Tukey multiple comparisons test when a statistically significant value at  $p < 0.05$  was observed. Values assigned with same letters are not statistically significant from each other.



In the current study, there was a trend toward decreased levels of total auxin comprising indole-3-acetic acid (IAA) and N-(indole-3-yl-acetyl)-aspartic acid (IAA-Asp) in response to flooding stress in all genotypes. Total gibberellin (GA) comprising GA8, GA19, GA29 and GA53 were increased slightly in susceptible WT plants (**Figure 3.2E-H**). Variable reductions in vegetative growth (**Figure 3.1A**) were correlated with reduced cytokinin concentrations in all alfalfa genotypes (**Figure 3.2I**). The detailed phytohormone profile is provided in **Table 3.1**.

### **3.2.3 miR156 regulates specialized metabolite pathways to improve flooding tolerance**

To investigate whether the miR156 gene regulatory network is involved in flooding tolerance, qRT-PCR was used to determine RNA expression levels of the flooding responsive *SNORKEL1* gene (Hattori et al., 2009), as well as *miR156* and miR156-regulated *SPL4* and *SPL13* genes (Aung et al., 2015b; Gao et al., 2016). *MiR156OE* and *SPL13RNAi* plants were used along with WT, AC-Caribou and AAC-Trueman grown at AAFC Kentville Research and Development Centre field condition. Transcript levels of *SNORKEL1* and *miR156* were increased in *miR156OE* plants, whereas those of *SPL4* and *SPL13* were decreased upon flood stress (**Figure S11**). Based on these results the role of miR156 and miR156-regulated SPLs in flooding response were investigated at the global transcriptomic levels using *miR156OE* (A8), *SPL13RNAi-6*, AC-Caribou, AAC-Trueman and WT alfalfa genotypes grown at AAFC research center in London, Ontario, Canada.

**Figure 3.2 UPLC/ESI-MS/MS-based hormone profiling in flood stressed and control alfalfa genotypes**

(A) Total ABA metabolites; (B) ABA glucose ester (ABAGE); (C) phaseic acid; (D) ABA; (E) IAA-aspartic acid (IAA-Asp); (F) total auxin; (G) gibberellic acid GA19; (H) total GA; (I) total cytokinin. Values are sample means  $\pm$  SE, n=3 individual plants. ANOVA was followed by *Post hoc* Tukey multiple comparisons test when a statistically significant value at  $p < 0.05$  was observed. Values assigned with same letters are not statistically significant from each other.

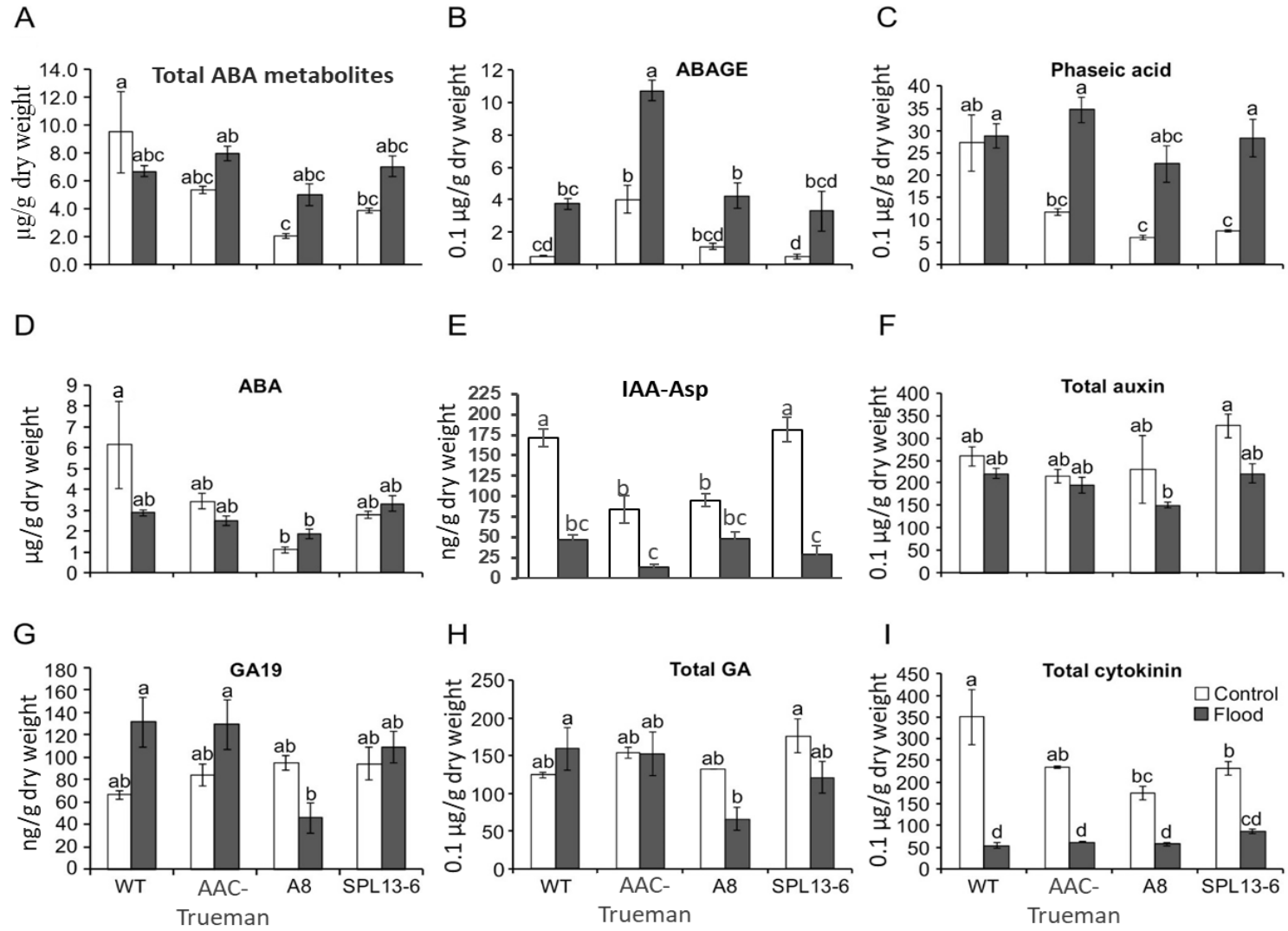


**Table 3.1 List of detected phytohormones and their abundance (ng/g dry weight) using UHPLC-MS analysis**

Phytohormone profiling was performed in lyophilized (freeze dried) triplicate (three biological replicates) samples of wild-type, AAC-Trueman, moderate-miR156A8 (*miR156OE*), and *SPL13RNAi-6* plants under well-drained control and flood-stressed conditions. Metabolite abundance are presented in average. ABA, *cis*-Abscisic acid; ABAGE, Abscisic acid glucose ester; DPA, Dihydrophaseic acid; PA, Phaseic acid; 7'OH-ABA, 7'-Hydroxy-abscisic acid; neo-PA, *neo*-Phaseic acid; *t*-ABA, *trans*-Abscisic acid; *t*-ZOG, (*trans*) Zeatin-O-glucoside; *c*-ZOG, (*cis*) Zeatin-O-glucoside; *c*-ZR, (*cis*) Zeatin riboside; dhZR, Dihydrozeatin riboside; iPR, Isopentenyladenosine; IAA, Indole-3-acetic acid; IAA-Asp, N-(Indole-3-yl-acetyl)-aspartic acid; GA1, Gibberellin 1; GA3, Gibberellin 3; GA7, Gibberellin 7; GA8, Gibberellin 8; GA19, Gibberellin 19; GA29, Gibberellin 29; GA34, Gibberellin 34; GA53, Gibberellin 53. Phytohormones labeled '**ND**' were not detected from the specific samples.

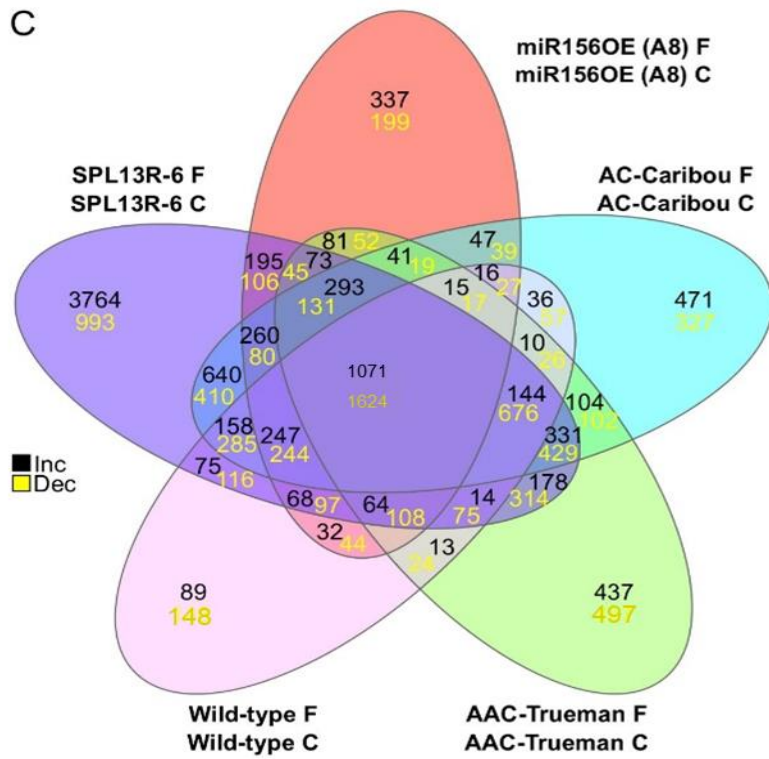
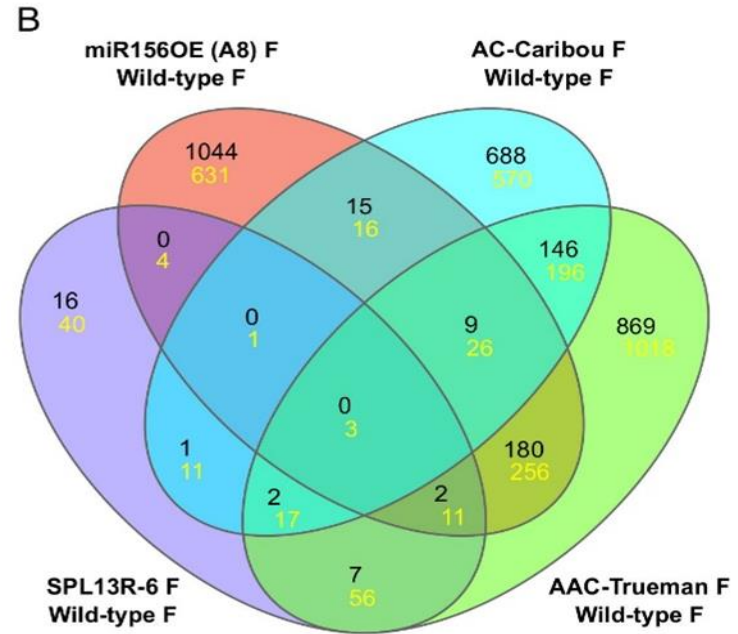
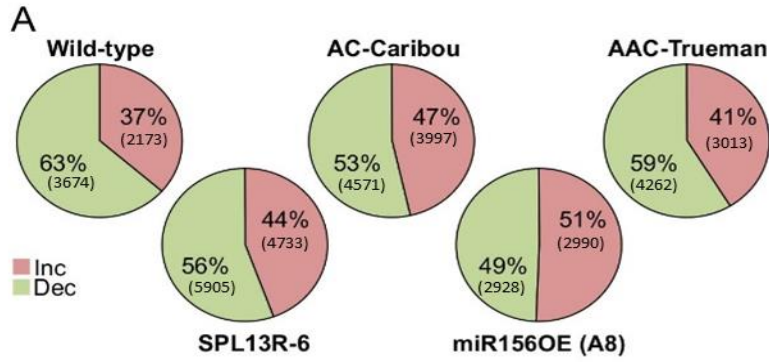
Phytohormones	Abbreviations	Wild-type		AAC-Trueman		A8 (miR156OE)		<i>SPL13</i> RNAi	
		Control	Flood	Control	Flood	Control	Flood	Control	Flood
ABA metabolites	ABA	6129.42	2879.37	3436.01	2494.99	1118.73	1871.10	2795.64	3319.30
	DPA	308.11	334.79	223.85	730.86	105.05	324.19	133.04	368.09
	ABAGE	50.40	373.88	401.74	1073.29	110.15	423.27	47.52	329.98
	PA	2724.02	2883.30	1173.19	3470.77	607.34	2252.90	758.16	2835.76
	7'OH-ABA	183.18	158.16	64.38	116.98	66.46	91.75	76.90	80.92
	neo-PA	8.74	ND	4.45	ND	ND	ND	3.90	4.00
	t-ABA	82.56	43.31	73.83	67.06	35.73	62.06	40.39	79.38
	t-ZOG	ND	ND	1.76	ND	2.64	2.23	2.89	1.62
	c-ZOG	18.75	17.43	6.69	9.59	13.49	14.02	16.47	14.97
Cytokinins	t-ZR	1.00	ND	0.95	0.90	2.40	1.50	1.00	ND
	c-ZR	109.14	13.91	74.15	18.77	60.00	14.70	69.54	21.36
	dhZR	2.45	1.23	3.13	ND	2.14	1.40	3.99	1.30
	iP	1.13	1.10	1.35	1.00	ND	1.35	1.70	ND
	iPR	220.17	22.62	149.02	32.71	105.67	26.38	133.81	50.74
Auxins	IAA	87.56	174.55	130.75	181.39	134.61	102.40	145.66	191.95
	IAA-Asp	171.57	46.59	84.02	13.33	95.34	47.98	181.67	29.20
Gibberellins	GA1	ND	ND	ND	ND	ND	ND	9.65	ND
	GA3	3.90	4.00	8.45	ND	ND	ND	ND	ND
	GA7	ND	ND	3.90	ND	7.40	5.90	3.95	ND
	GA8	29.04	6.05	40.81	4.76	13.29	5.95	55.02	4.90
	GA19	66.54	131.06	83.96	129.10	94.89	45.97	94.30	108.96
	GA29	29.10	23.64	24.96	16.15	26.20	18.37	22.18	13.67
	GA34	ND	ND	ND	3.70	ND	ND	ND	4.00
GA53	3.90	8.28	4.28	9.45	7.40	5.60	4.27	6.33	



Transcript profile analysis comparing well-drained and flood stress conditions revealed that more than 60% of the DEG were decreased in flood-stressed WT plants, whereas the difference between upregulated vs downregulated genes was minimal (51% increased and 49% decreased) in flood-stressed-exposed moderate-miR156A8 plants (**Figure 3.3A**). On the other hand, AC-Caribou, SPL13R-6, and AAC-Trueman had 53, 56 and 59% of the a reduced DEG, respectively, under flooding stress. To further identify genes contributing to alfalfa flooding tolerance, I compared DEG from flood-stressed WT plants to those from AC-Caribou, AAC-Trueman, *SPL13RNAi*, and flood-stressed moderate-miR156A8 plants. Results of this analysis are summarized in a Venn-diagram (**Figure 3.3B**). Genotype-specific and commonly shared DEG were observed. Among the DEG, 16, 1044, 688, and 869 were increased and found unique to genotypes of SPL13R-6, A8, AC-Caribou, and AAC-Trueman, respectively, whereas 40, 631, 570 and 1018 were decreased, respectively (**Figure 3.3B**). Moreover, two upregulated and 11 downregulated genes were commonly shared by the flood tolerant AAC-Trueman, moderate-miR156A8 and *SPL13RNAi*-6 genotypes under flooding stress. The two upregulated transcripts encode for Gly-Asp-Ser-Leu (GDSDL)-like lipase/ acyl hydrolase (Medtr8g087870) and a reticuline oxidase-like protein (Medtr2g031560). On the other hand, five of the commonly down-regulated 11 transcripts under flood stress code for carbonic anhydrase (Medtr0219s0070), galactinol-raffinose galactosyltransferase (Medtr7g091880), AP2 domain class transcription factor (Medtr3g098580), PAR1 protein (Medtr1g101120), and sieve element occlusion protein (Medtr1g074990).

**Figure 3.3 Differentially expressed genes, DEG, and their associated function upon flood stress in alfalfa**

(A) DEG plasticity in each genotype during flood stress, (B) Venn diagram illustrating communalities and differences of DEG in AC-Caribou, AAC-Trueman, *SPL13RNAi-6* and moderate-miR156A8 genotypes compared to WT in response to flood stress, (C) Venn diagram illustrating communalities of DEG across genotypes in plants exposed to flood stress compared to their respective well-drained counter parts, Upper (black) and lower panel (yellow) numbers in 'B' and 'C' indicate increased and decreased DEG, respectively, compared to flood-stressed WT or the same genotype under well-drained conditions, respectively. N = 3 biological replicates for each genotype and treatment conditions. Novaseq 6000-based RNAseq analysis was performed with three biological replicates for each treatment condition. The venn diagram was constructed using an online tool <http://www.interactivenn.net/>.



A comparison of WT plants with the other genotypes under flood stress, identified DEG from two other major GDSL-related genes, including GDSL-like lipase/acyl hydrolase and Pmr5/Cas1p GDSL/SGNH-like acyl-esterase (**Figure S12A**). Of these genes, one of three in *SPLI3RNAi-6*, 29 of 33 in A8, two of six in AC-Caribou and nine of 14 in AAC-Trueman were increased under flooding stress compared to flood-stressed WT plants (**Figure S12A**). The second commonly increased transcript among A8, *SPLI3RNAi-6* and AAC-Trueman encodes the reticuline oxidase-like protein that binds to flavin adenine dinucleotide (FAD) as an acceptor of hydrogen in a bi-covalent manner, and possesses an oxidoreductase activity in (S)-scoulerine biosynthesis (Sato et al., 2001). Transcripts of this gene were increased 1.7-fold in flood-stressed AAC-Trueman relative to its well-drained while other genotypes (WT, AC-Caribou, A8, and *SPLI3R-6*) showed 0.22 to 0.53-fold reduction compared to their respective well-drained (**Figure S12B**). Despite this reduction, reticuline oxidase-like protein transcripts were increased 1.6 to 6-fold higher in flood tolerant genotypes relative to wild-type plants under flooding stress (**Figure S12B**).

To understand transcript plasticity of genotypes in response to flood stress, the transcript profiles of well-drained and flood-stressed plants of each genotype were compared across all genotypes. 1071 upregulated and 1624 downregulated DEG were shared by all genotypes (**Figure 3.3C**). In addition, 89, 3764, 337, 471, and 437 upregulated and 148, 993, 199, 327, and 497 downregulated genotype-specific DEG were detected in WT, *SPLI3RNAi-6*, A8, AC-Caribou, and AAC-Trueman genotypes, respectively (**Figure 3.3C**). Among the transcripts differentially expressed in all genotypes upon flood stress, ABA biosynthesis, SnRK1, and phenylpropanoid pathway genes were

upregulated (**Figure S12C,D**). Moreover, the number and distribution of different molecular function-associated differentially expressed transcripts between flood-stressed WT and all the other genotypes code primarily for protein post-translational modification, miscellaneous UDP glucosyl and glucuronyl transferases, RNA regulation of transcription, signalling receptor kinase, biotic and abiotic stress, transport, specialized metabolite, plant hormone metabolism, development and cell wall cellulose synthase (**Figure 3.4**).

### 3.2.4 Phylogenic analysis reveals novel SPLs in alfalfa

The observation of enhanced levels of *miR156* expression under flooding stress (**Figure S11**) prompted me to investigate whether miR156-regulated SPLs contribute to alfalfa's response to flooding stress. RNAseq analysis followed by transcript annotation of five alfalfa genotypes exposed to flooding stress showed that 15 *SPLs* were differentially expressed relative to their well-drained counterparts (**Figure 3.5A**). In addition to the previously known seven *SPLs* (Aung et al., 2015b; Gao et al., 2016), nine new *SPLs* (*SPL1*, *SPL1a*, *SPL2a*, *SPL7*, *SPL7a*, *SPL8*, *SPL13a*, *SPL14* and *SPL16*) were identified in this study (**Figure 3.5A,B**). The naming of the new *SPLs* is based on the closely related known *SPLs* from the phylogenetic tree in the clade (**Figure 3.6A**).

**Figure 3.4 Functional distribution of differentially expressed genes upon flood stress in alfalfa**

Functional distribution of DEG obtained by comparing SPL13R-6 (*SPL13RNAi-6*), moderate-miR156A8 (*miR156OE*), AC-Caribou and AAC-Trueman vs well-drained under flooding stress. Novaseq 6000-based RNAseq analysis was performed with three biological replicates for each treatment condition. N = 3 biological replicates for each genotype and treatment conditions. TCA, Tricarboxylic acid; UDP, Uridine diphosphate.

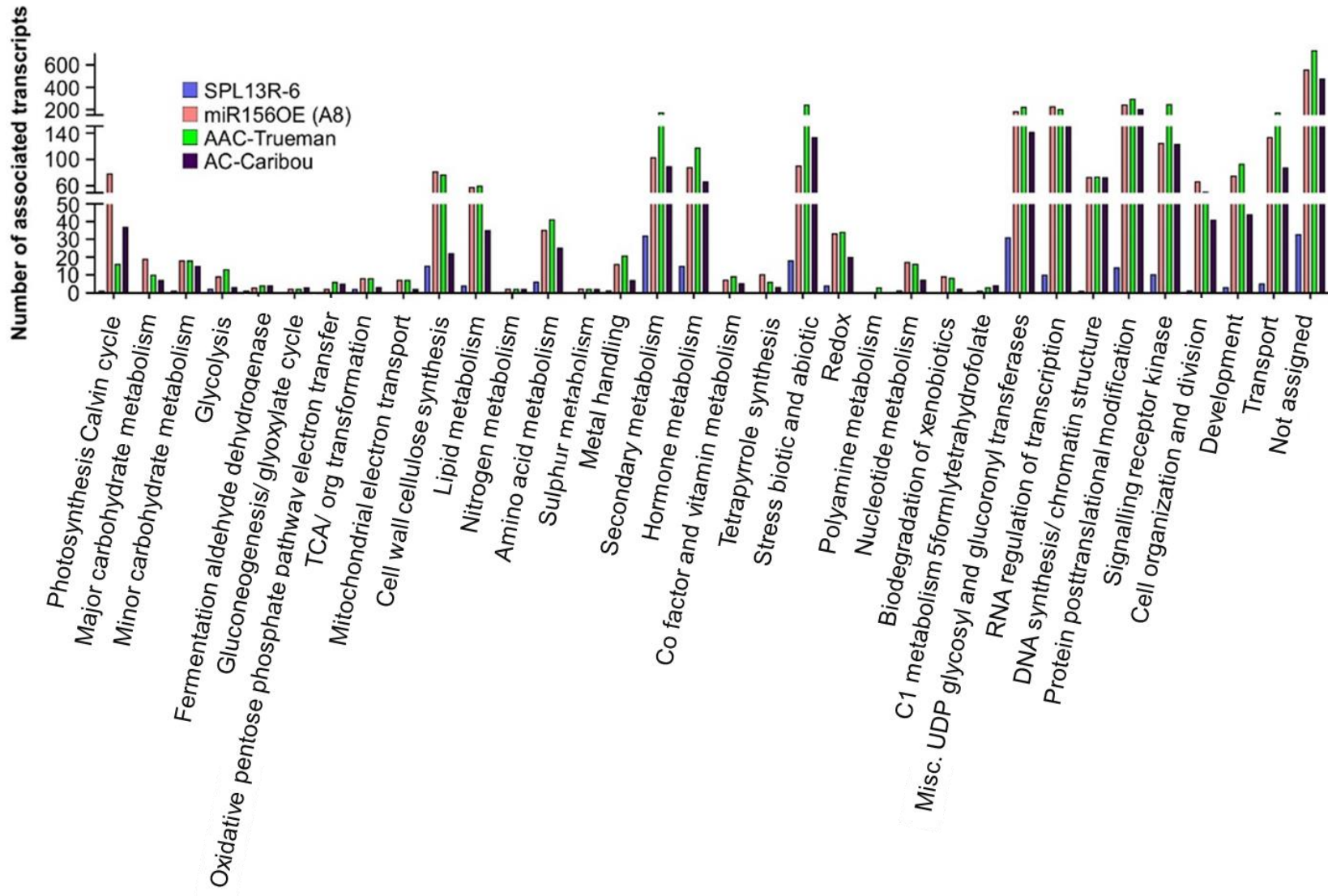
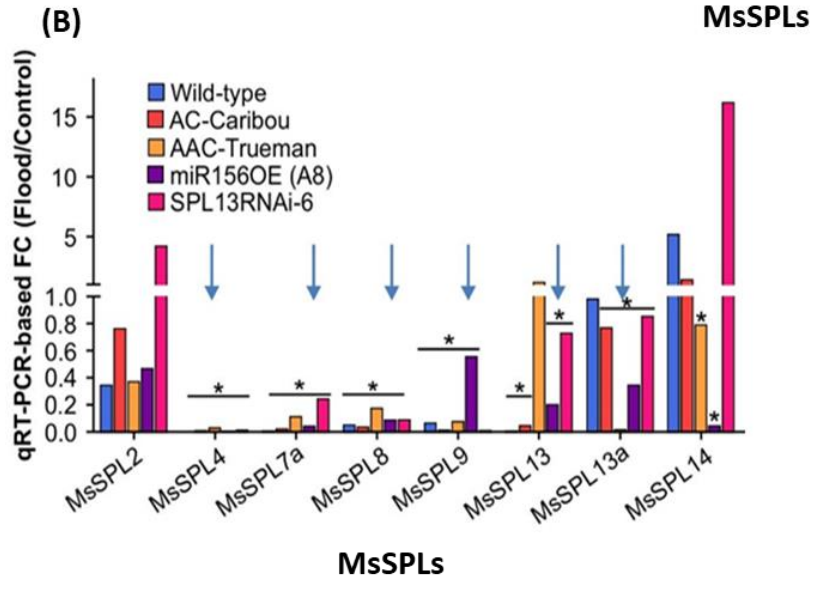
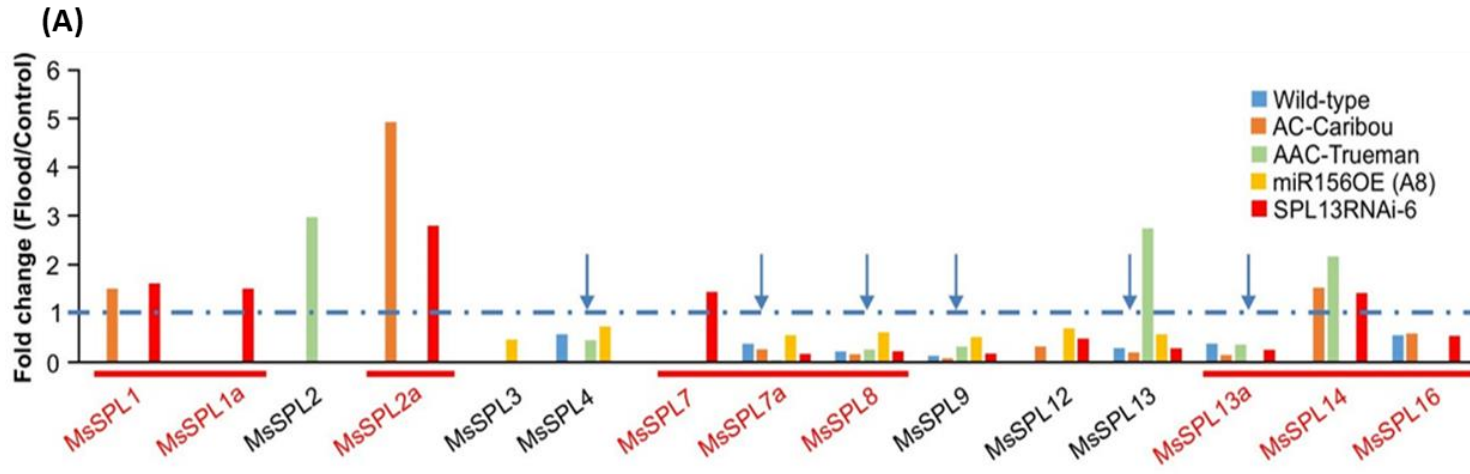


**Figure 3.5 Differentially expressed SPLs upon flood stress in alfalfa**

(A) Differentially expressed SPLs between well-drained and flood stressed alfalfa plants, (B) validation of the consistently regulated SPLs from RNAseq using qRT-PCR. SPLs underlined with red line in 'A' are newly identified SPLs while the others were previously identified (Aung et al., 2015b; Gao et al., 2016). Arrows in 'A' and 'B' indicate commonly reduced SPLs during flooding stress. The '\*' in 'B' indicates significance difference between biological samples at  $p < 0.05$  when compared between well-drained and flooding stress transcript abundances.

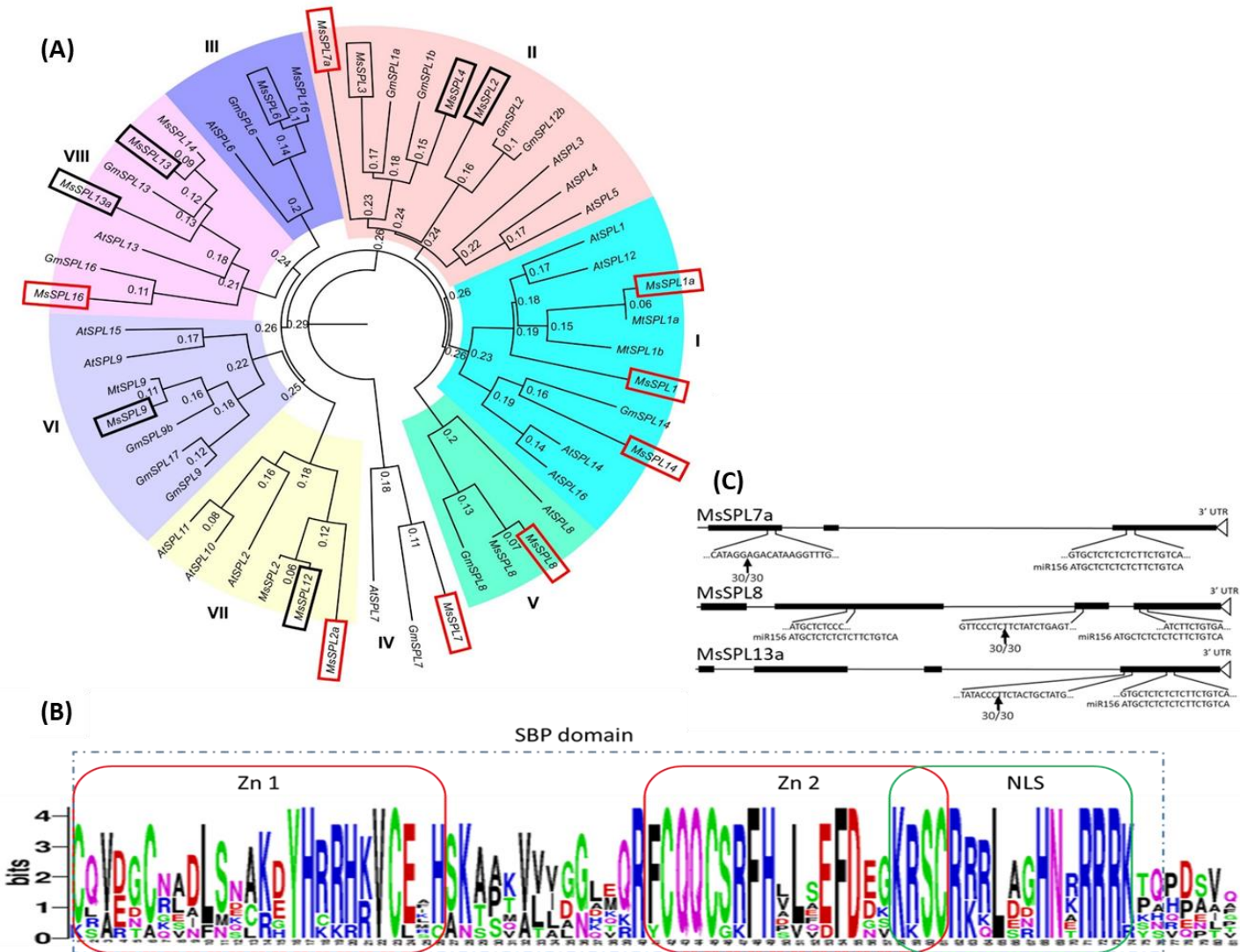




Phylogenetic analysis grouped the SPLs into eight clades that have more than 75% coding sequence similarity. Clade I (SPL1, SPL1a, SPL14), clade II (SPL2, SPL3, SPL4, SPL7a), clade III (SPL6), clade IV (SPL7), clade V (SPL8), clade VI (SPL9), clade VII (SPL2a, SPL12), and clade VIII (SPL13, SPL13a, SPL16) (**Figure 3.6A**). Of these *SPLs*, *SPL4*, *SPL7a*, *SPL8*, *SPL9*, *SPL13*, and *SPL13a* were downregulated under flooding stress compared to well-drained in all genotypes, *SPL3* was downregulated only in A8, while *SPL12* and *SPL16* were not consistently downregulated in all the genotypes (**Figure 3.5A**). The results of transcriptomic data were validated by qRT-PCR (**Figure 3.5B**) using primers specifically designed to amplify each *SPLs* (**Table S1**). The newly identified *SPLs* were further analyzed for their conserved SBP domain, nuclear localization signal, and the presence of miR156 binding nucleotide sequences. *In silico* amino acid sequence analysis (<http://weblogo.berkeley.edu/logo.cgi>) of the newly identified *SPLs* revealed they all contained the conserved SBP domain containing two zinc fingers (Zn1 and Zn2) and nuclear localization signal (NLS) (**Figure 3.6B**) similar to the previously identified ones (Gao et al., 2016). Using an amino acid sequence-based ([http://nls-mapper.iab.keio.ac.jp/cgi-bin/NLS\\_Mapper\\_form.cgi](http://nls-mapper.iab.keio.ac.jp/cgi-bin/NLS_Mapper_form.cgi)) analysis, putative nuclear localization signals were also detected in the newly identified *SPLs* (**Figure S13**).

### Figure 3.6 Phylogenetic analysis and identification of new SPLs in alfalfa

(A) Amino acid coding sequences-based phylogenetic analysis of SPLs, (B) the conserved SQUAMOSA PROMOTER-BINDING PROTEIN, SBP, domain in the newly identified SPLs containing two zinc-finger binding domains (Zn 1 and 2) and nuclear localization signal (NLS), (C) complementarity of SPL7a, 8 and 13a to that of matured miR156 sequence along with 5' RLM RACE determined cleavage sites. SPLs boxed with red line in 'A' are newly identified SPLs while boxed with black lines were previously identified (Aung et al., 2015b; Gao et al., 2016). Different shades of colour in 'A' represents different clades having more than 70% protein coding sequence similarity within a clade. Phylogenetic analysis is done using clustal omega online tool (<https://www.ebi.ac.uk/Tools/msa/clustalo/>) followed by FigTree v.1.4.2 free software. *In silico* amino acid sequence in 'B' is analysed using <http://weblogo.berkeley.edu/logo.cgi>. In 'B' zinc-finger binding domains (Zn 1 and 2) and nuclear localization signals (NLS) are indicated with red and green boxes, respectively. Arrows in 'C' indicate cleavage sites by *miR156*. Values in 'A' are dissimilarity index between the protein coding sequences of the SPLs.



To understand whether the newly identified SPLs are regulated by miR156, the complementarity of the mature miR156 sequence ‘ATGCTCTCTCTTCTGTCA’ was checked in a 5’ to 3’ orientation and found variable amount of miR156 matching sequence in SPLs ranging from 13/20 in *SPL1* and *SPL7* to 19/20 in *SPL2a*, *SPL7a* and *SPL13a*. Of these different numbers of miR156 matching nucleotide sequence to SPLs, *SPL7a*, *SPL8* and *SPL13a* possessed 19/20, 18/20 (in two fragments) and 19/20 nucleotide matches to miR156, respectively, indicating a potential cleavage target by miR156 (**Figure 3.6C**). 5’-RACE was performed to confirm the miR156 cleavage site in transcripts of the newly identified SPLs that consistently responded to flooding in all the genotypes (*SPL7a*, *SPL8*, and *SPL13a*) (**Figure 3.6C**). The ligated 5’RACE adapter-mRNA site was amplified with two sequential PCRs using gene-specific and manufacturer-provided primers (**Table S1**). Subsequently, the PCR products were cloned into *E. coli* and 30 independent events for each gene were sequenced and scored to identify the miR156 cleavage sites. The sequencing result revealed *SPL7a*, *SPL8* and *SPL13a* were cleaved by miR156 upstream of the complementary target sequence (**Figure 3.6C**). These results revealed that miR156 downregulates *SPL4*, *SPL7a*, *SPL8*, *SPL9*, *SPL13* and *SPL13a* in alfalfa in response to flooding stress.

### 3.2.5 Flooding enhances *SnRK1* expression in an ABA-dependent manner

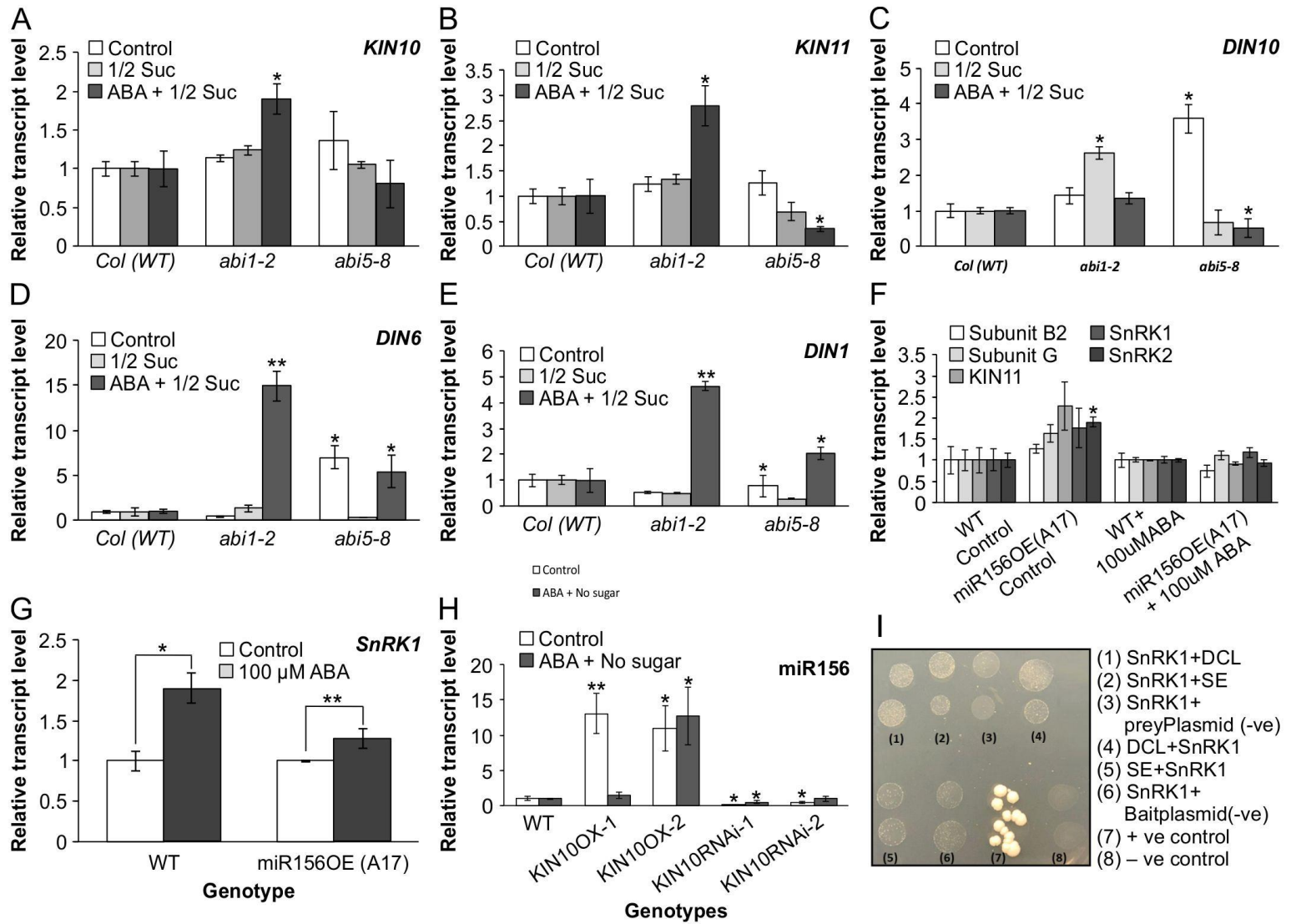
An upregulation of *SnRK1* (Medtr1g034030) and its regulatory  $\beta$  subunit (Medtr5g098510 and Medtr2g095290) were observed in alfalfa under flooding stress (**Figure S12C**). The catalytic  $\alpha$  subunit *KIN11* (Medtr6g048250 and Medtr6g012990) was also increased consistent with *SnRK1* expression in two of the genotypes (AC-Caribou and *SPL13RNAi-6*) (**Figure S12C**). Considering the elevated level of ABA-catabolites in AAC-Trueman,

moderate-miR156A8 and *SPL13RNAi-6* genotypes (**Figure 3.2**) upon flooding stress, the ABA signaling pathway and ABA-responsive elements in these plants were investigated. The ABA signaling *PYL9/PYR1* receptors as well as *ABI2* and the ABA-responsive element *ABRE* were upregulated, whereas *ABII* was downregulated under flooding stress (**Figure 3.2, Figure S12D**). Given an enhanced level of *SnRK1* and ABA, and findings from the literature showing that SnRK1 has a central role in sugar and ABA signalling (Jossier et al., 2009; Rodrigues et al., 2013), I decided to investigate whether the expression of *SnRK1* is ABA-dependent.

The finding that *SnRK1*, ABA-signaling elements (**Figure S12**) and ABA-catabolites (**Figure 3.2**) were upregulated in alfalfa under flooding stress prompted me to determine the transcript levels of *KIN10*, *KIN11* and *DARK INDUCED* genes (*DIN*). This was done in ABA insensitive *Arabidopsis* mutants (*abi1-2*, and *abi5-8*) (Rubio et al., 2009; Zou et al., 2013), due to the lack of similar mutants in alfalfa. Expression levels of one of the catalytic  $\alpha$  subunits, *KIN11*, was reduced in *abi5-8* while both *KIN10* (**Figure 3.7A**) and *KIN11* (**Figure 3.7B**) were increased in *abi1-2* plants during ABA treatment where only one of the calcium and protein binding elements is silenced (**Figure 3.7A,B**). Moreover, the expression of dark-induced and multiple stress responsive *DIN* genes (*DIN1*, *DIN6* and *DIN10*) (Baena-González et al., 2007) was investigated to determine whether it was affected by ABA treatment. The expression of *DIN10* was increased with reduced sugar level in *abi1-2* mutants while reduced in *abi5-8* mutants with ABA application (**Figure 3.7C**).

**Figure 3.7 ABA-dependent expression of SnRK1 regulates miR156**

(A) SnRK1 catalytic subunit *KIN10*, and (B) *KIN11*, (C) relative transcript levels of *DARK INDUCED*, *DIN*, *DIN10*, (D) *DIN6*, and (E) *DIN1* genes in Arabidopsis, (F) relative transcript levels of *SnRK1* and *SnRK2* along with *SnRK1* regulatory and catalytic subunits in response to 100  $\mu$ M ABA treatment, (G) transcript levels of *SnRK1* upon 100  $\mu$ M ABA treatment relative to their counter part control alfalfa plants, (H) relative transcript levels of *miR156* in *KIN10* overexpressing and RNAi silenced Arabidopsis plants, (I) Yeast-two-hybrid (Y2H) assay for protein-protein interaction between *SnRK1* and *DCL1* or *SE*. n=50 of Arabidopsis seedlings in 'A' to 'E' and 'H' were used while three alfalfa plants were used as replicates in 'F' and 'G'. Arabidopsis-specific three house keeping genes (elongation factor alpha, tubulin and actin) were used for relative transcript analysis relative to wild-type in 'A' to 'E' and 'H' while alfalfa specific elongation factor, actin and ubiquitin10 were used in 'F' and 'G'. Values are means with  $\pm$  SE. The interaction between the pEXP32/Krev1 (rat Krev1) with pEXP22/RalGDS-wt (ras association domain of RalGDS) is used as a positive control while for the negative control pEXP32/Krev1 with the mutated ras association domain of RalGDS, pEXP22/RalGDS-m2, were used according to the user's manual. Pair-wise comparison tests ('\*' at  $p < 0.05$  while '\*\*' at  $p < 0.01$ ) were performed between wild-type (WT) and other genotypes for similar growth conditions except 'G' that compared ABA treated alfalfa plants of WT and *miR156*OE (A17) to their counter part control conditions.





This result shows *DIN10* expression is ABA-dependent and regulated by ABI5 (**Figure 3.7C**). On the other hand, Transcript levels of *DIN1* and *DIN6* were increased in the presence of ABA despite a reduced level of ABI1 and ABI5 (**Figure 3.7D,E**).

To understand whether the transcript level of *SnRK1* in alfalfa is miR156-dependent, one-month old rooted cuttings of alfalfa plants (*miR156OE* and WT plants) were exposed to flooding for one week followed by treatment with of 100  $\mu$ M ABA for 4 hrs. Subsequently, the RNA transcript levels of *SnRK2*, *SnRK1* and its catalytic  $\alpha$  (*KIN10* and *KIN11*) and regulatory ( $\beta$  and  $\gamma$ ) subunits were determined. Under control conditions, only *SnRK2* was increased in *miR156OE* plants whereas the other regulatory and catalytic subunits were not different from WT (**Figure 3.7F**). Interestingly, under 100  $\mu$ M ABA treatment, the expression of all the catalytic (*KIN11*  $\alpha$  subunit), regulatory subunits ( $\beta$  and  $\gamma$  subunits), SnRK1 and SnRK2 were similar in their expression levels to that of WT (**Figure 3.7F**). Moreover, both WT and *miR156OE* (A17) genotypes had higher SnRK1 expression under 100  $\mu$ M ABA treatment compared to their counter part controls (**Figure 3.7G**).

### 3.2.6 Does SnRK1 regulate miR156?

To understand whether SnRK1 regulates miR156 to mediate the miR156/SPLs module in flooding response, I used Arabidopsis plants with altered expression of *KIN10* (*KIN10-OX-1*, *KIN10-OX-2*, *KIN10RNAi-1*, *KIN10RNAi-2*) (Baena-González et al., 2007) and treated with 3  $\mu$ M ABA, and determined *miR156* transcript levels. *MiR156* expression was higher in *KIN10* overexpressing genotypes while *KIN10RNAi* genotypes showed comparable (*KIN10RNAi-2*) or lower (*KIN10RNAi-1*) levels relative to WT control plants (**Figure 3.7H**). Under ABA treatment, *miR156* expression level remained significantly

higher at least in one of the two overexpression genotypes (*KIN10-OX-2*) but lower in *KIN10RNAi* plants when compared to wild-type plants (**Figure 3.7H**).

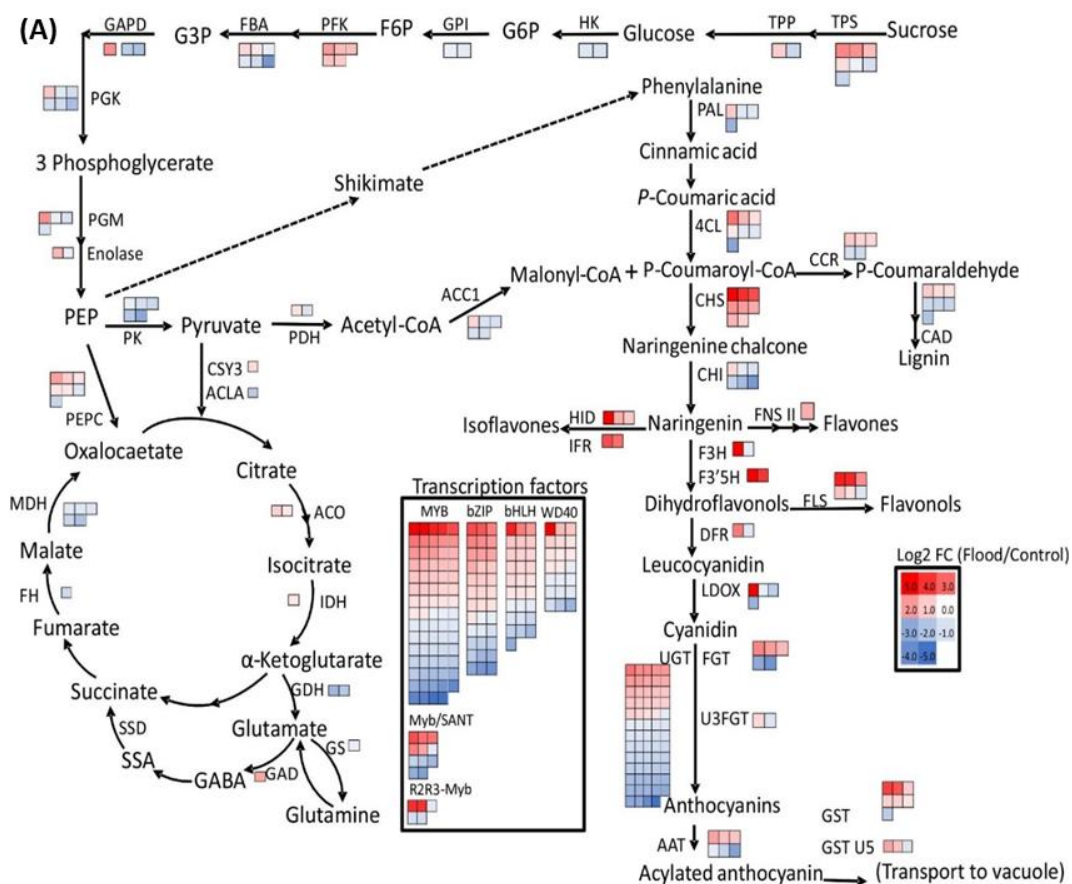
*DICER-LIKE 1 (DCL1)*, *SERRATE (SE)* and *HYPONASTIC LEAVES (HYL1)* are critical for the biogenesis of microRNAs (Yu et al., 2017). There was an increase in *KIN10* expression coupled with upregulation of *miR156* (**Figure 3.7H**), but overexpression of *miR156* did not affect *KIN10* (**Figure 3.7F**). This led me to investigate whether SnRK1 is involved in regulating miR156 biogenesis. Accordingly, using a yeast-two-hybrid assay the *in vivo* pairwise protein-protein interactions between SnRK1 with DCL1 and SE were investigated. Under my experimental conditions no interaction could be detected between SnRK1 and neither DCL1 nor SE (**Figure 3.7I**)

### 3.2.7 miR156/SPL module enhances flooding adaptive mechanisms

The transcriptomic profile of *SPL13RNAi* plants showed an increase in genes coding for *TREHALOSE-6-PHOSPHATE SYNTHASE (TPS)* and *TREHALOSE-6-PHOSPHATE PHOSPHATASE (TPP)* under flooding stress (**Figure 3.8A**). The reduction in photosynthesis assimilation rate after two weeks of flooding (**Figure 3.1C**) but greater than WT (**Figure 3.8B**) may result in lower levels of fructose and glucose, which in flooding tolerant plants are compensated for by increased levels of TPS and TPP to enhance sucrose hydrolysis (**Table S13**). Likewise, an enhanced level of *SnRK1* along with its catalytic and regulatory subunits was observed in alfalfa during flooding stress (**Figure 3.7G**). Moreover, induction of the phenylpropanoid pathway-related metabolites was observed in flood-tolerant *SPL13RNAi* plants to scavenge ROS (**Figure 3.8A, Table S12**). Consistent with these findings, an increased level of total anthocyanin monomers was detected under flooding stress (**Figure 3.9A**).

**Figure 3.8 miR156-based regulation of SPL13 enhances photosynthesis and phenylpropanoid pathway in response to flooding**

(A) Reduced glycolysis and TCA cycle and enhanced phenylpropanoid pathway in flood stress *SPL13*RNAi plants; (B) MapMan-based pathway analysis illustrating photosystem I and II associated increased transcript abundance along with electron transport chain in moderate-miR156A8 plants compared to WT plants during flood stress. Red and blue colours in phenylpropanoid pathway represent an increase and decrease in fold-change levels of transcripts in *SPL13*RNAi flood stressed plants relative to wild-type flood stressed plants, respectively. N = 3 biological replicates for each genotype and treatment conditions.



**(B)**

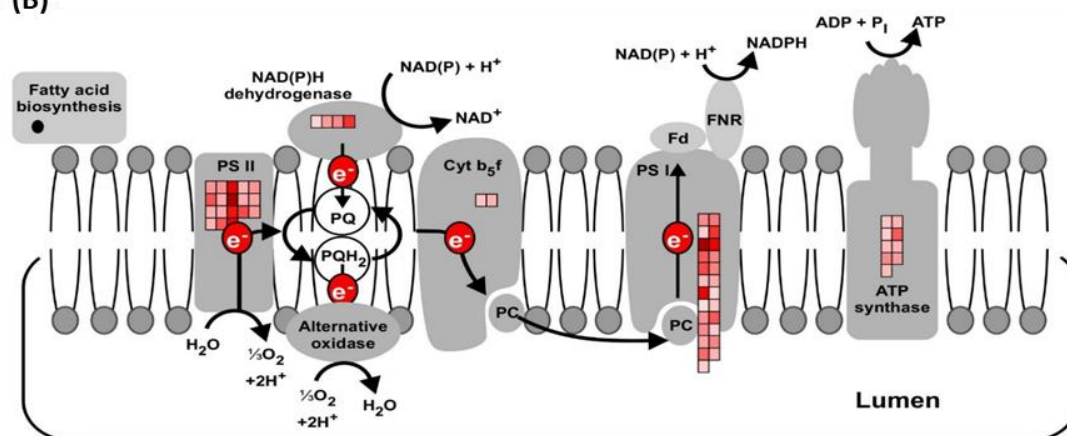
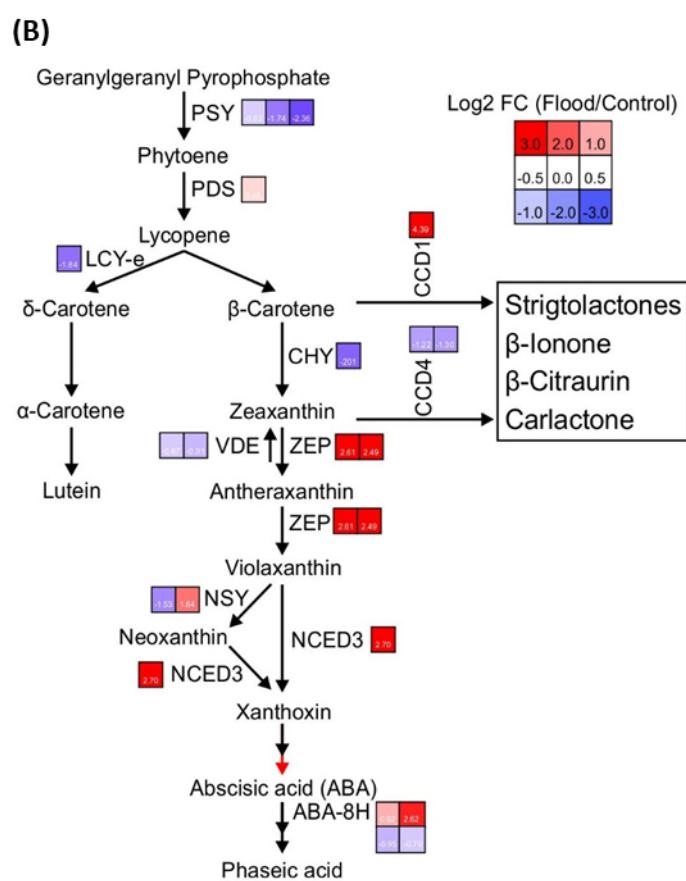
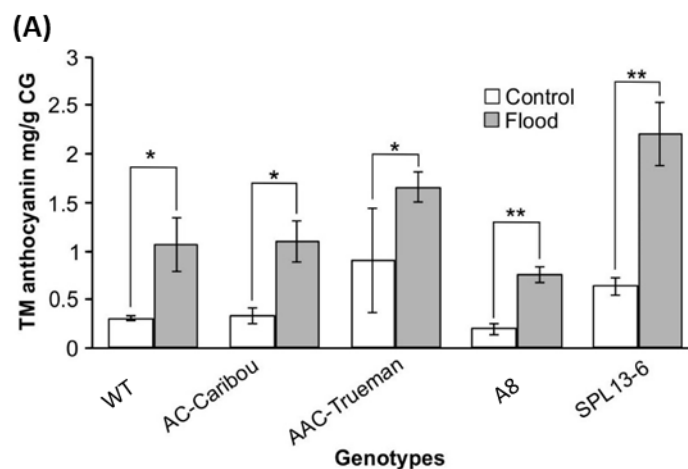


**Figure 3.9 miR156-based regulation of SPL13 enhances anthocyanin and ABA biosynthesis in response to flooding**

(A) Total monomeric anthocyanin in gallic acid equivalents; (B) enrichment of ABA biosynthesis in *SPL13*RNAi plants under flood stress. Values in ‘A’ are mean with  $\pm$  SE with N = 3 biological replicates for each genotype and treatment conditions. Red and blue colours in ABA biosynthesis pathway represent an increase and decrease in fold-change levels of transcripts in *SPL13*RNAi flood stressed plants relative to wild-type flood stressed plants, respectively.



The increase in accumulation of ABA metabolites under flooding stress was regulated at the transcript level based on results of global transcriptomic-derived pathway analysis in *SPL13RNAi* plants (**Figure 3.9B, Table S11**) and other flood-tolerant genotypes.

### **3.3. Discussion**

#### **3.3.1 miR156 regulates physiological processes during flooding stress**

Plants survive abiotic stress by employing adaptation or avoidance strategies to maintain essential physiological processes required for growth and development (Voesenek and Bailey-Serres, 2015). The current results showed that *miR156OE* alfalfa plants maintained a functional photosynthesis process as expressed as photosynthesis electron transport,  $V_{\text{cmax}}$ , and maximum rate of carboxylase activity,  $J_{\text{max}}$  during flooding. This was accompanied by a higher dark-adapted chlorophyll fluorescence,  $F_v/F_m$ , and ultimately a stable photosynthetic assimilation rate. Interestingly, *SPL13RNAi* and the flooding tolerant genotype, AAC-Trueman, showed a similar phenotypic response to that of *miR156OE* genotype A8. In contrast, the reduced levels of  $F_v/F_m$  and photosynthesis assimilation rate, but with no effect on  $V_{\text{cmax}}$  and  $J_{\text{max}}$  in AC-Caribou under flooding stress suggests a viable ribulose-1,5-bisphosphate carboxylase/oxygenase (rubisco) enzyme but its activity may be hindered by the scarcity of  $\text{CO}_2$  governed by stomatal conductance under stress. Understanding the maintenance of  $V_{\text{cmax}}$  and  $J_{\text{max}}$  in AC-Caribou under flooding stress would require studies regarding on the rubisco enzymatic activity.

#### **3.3.2 Phaseic acid-dependent regulation of flooding tolerance in alfalfa**

In addition to their role in regulating plant growth and development (Gray, 2004), phytohormones act as signaling molecules to affect plant response to stress (Weng et al.,

2016). Accordingly, the role of phytohormones in alfalfa's response to flooding stress was investigated by determining changes in their profiles under this stress. Phytohormone profiling revealed an increase in the level of ABA and its catabolites under flood stress in tolerant genotypes (AAC-Trueman, moderate-miR156A8 and *SPL13RNAi-6*), whereas WT plants had reduced levels in leaf tissues. Of the different ABA catabolites involved in signalling, phaseic acid (Rodriguez et al., 2016) was recently investigated for its role in plant adaptive plasticity (Weng et al., 2016). The report showed how phaseic acid could have an ABA-like effect, as well as phaseic acid-specific responses during drought stress. In the current study, a significant increase in the amount of phaseic acid was detected in alfalfa genotypes of *SPL13RNAi*, *miR156OE* and AAC-Trueman under flooding stress relative to well-drained counterparts.

Gibberellic acid, GA, is involved in internode elongation resulting in taller plants that benefit under water-submergence (Ayano et al., 2014). The increase in plant height under the influence of GA comes with the cost of energy usage that competes with other physiological processes. Hence, tailoring an appropriate response is crucial to channel resources to the required biological processes. WT plants slightly enhanced the GA abundance with increased plant height while *miR156OE* and *SPL13RNAi* plants reduced their GA levels. This is consistent with the typical alfalfa *miR156OE* phenotype that shows an increase in the number of branches with a decrease in shoot height (Aung et al., 2015b). It seems that *miR156OE* and *SPL13RNAi* plants channel the assimilated carbon sources into the biosynthesis of stress-mitigating metabolites, such as anthocyanin. Increasing plant height might be an important strategy in fully water-submerged plants for the uptake of CO<sub>2</sub> and O<sub>2</sub> necessary for photosynthesis and respiration, respectively, but the current



experiment involved waterlogging only up to the soil surface. It remains to be investigated whether the hormone profile will change in these alfalfa genotypes if plants were completely submerged under water.

### **3.3.3 Genotype-specific enhancement of specialized metabolism and photosynthesis under flooding**

Under flooding stress, plants tends to have a reduced availability of O<sub>2</sub> and CO<sub>2</sub>, which are important for protein biosynthesis and energy production (Branco-Price et al., 2008; Mustroph et al., 2009). On the other hand, gene transcription followed by translation is an energy-consuming process (Lindqvist et al., 2018). In the current study, the flood-tolerant moderate-miR156A8 plants maintained a comparative number of differentially expressed genes between flood-stressed and well-drained plants while others showed mainly reduction under flooding.

Besides the proportion of total genes that were significantly affected by the stress, it is important to identify stress-specific genes and their association/network to understand the regulation mechanism of stress. Based on global transcriptomic profile differences between flood-stressed and well-drained alfalfa genotypes, pathway enrichment analysis was conducted on DEG. The increased expression levels of photosynthesis-related genes in *SPL13RNAi* and flood-tolerant AAC-Trueman genotypes during flooding stress indicates the maintenance of physiological processes. This is in line with the observed maintenance of  $V_{\text{cmax}}$  and  $J_{\text{max}}$  that ultimately resulted in a relatively higher photosynthesis assimilation rate during flooding stress. Under well-drained growth conditions, ROS and radical elements are produced at lower levels and used as signalling molecules (Turkan, 2018). Flood stress induces the production of these small molecules resulting in a negative

feed-back that damages cellular integrity and hinders enzymatic reactions (Zhang et al., 2015). Flood-tolerant plants, on the other hand, reduce ROS levels to maintain normal physiological processes. The use of specialized metabolites to scavenge ROS is well documented in plants (Chen et al., 2019). The observed enrichment of specialized metabolites, specifically those of the phenylpropanoid pathway, suggests that flood-tolerant alfalfa genotypes use a similar strategy to mitigate flooding stress. Moreover, the pathway enrichment analysis showed the enhancement of cell wall metabolism, ROS-scavenging ascorbates and glutathione-associated transcripts. This is in agreement with the transcript profile of *SPL13RNAi* plants, where *FLAVANONE-3-HYDROXYLASE (F3H)*, *FLAVANONE-3'5'-HYDROXYLASE (F3'5H)* and *DIHYDROFLAVONOL-4-REDUCTASE (DFR)* transcript levels were upregulated in accordance with the enhanced level of total monomeric anthocyanin during flooding stress. Analyzing the network of observed global changes in transcriptome to metabolome under flood stress will provide a clearer picture of alfalfa's response to flooding.

### **3.3.4 Identification of novel SPLs in alfalfa**

A previous study identified seven SPLs (SPL2, SPL3, SPL4, SPL6, SPL9, SPL12 and SPL13) that were regulated by miR156 (Aung et al., 2015b; Gao et al., 2016). Here, RNAseq analysis followed by gene ontology analysis suggested the presence of 16 SPLs in alfalfa of which nine were novel sequences. SPLs are transcription factors that positively or negatively regulate the expression of downstream genes having diverse functions in plants (Preston et al., 2016). Identifying new SPLs will shed light on novel molecular factors that control various aspects of alfalfa growth and developmental. The nine newly

identified SPLs (SPL1, SPL1a, SPL2a, SPL7, SPL7a, SPL8, SPL13a, SPL14 and SPL16) can now be subjected to functional characterization to understand their roles in alfalfa.

The seven previously identified SPLs (Gao et al., 2016) and the nine new SPLs reported in the current study are organized into eight clades based on their sequence similarities to those of *M. truncatula*, *Glycine max* and Arabidopsis in the phylogenetic tree. Understanding the clade distribution of the newly identified SPLs along with the other SPLs from different plant species could provide information regarding their putative function considering their similarity in coding sequences. For example, SPLs assigned to clade I, such as AtSPL1, are important for thermo-tolerance at the reproductive stage, redundantly with AtSPL12 (Chao et al., 2017). Accordingly, the newly identified SPL1, SPL1a and SPL14 may have also a role in thermo-tolerance, but this should be validated using gene silencing and overexpressing alfalfa plants under heat stress. Similarly, SPL7a may have similar function to that of SPL2, SPL3, and SPL4, in alfalfa and AtSPL3, AtSPL4 and AtSPL5 in Arabidopsis. In line with this, SPLs from clade II (SPL7a and SPL4) were silenced under flood stress in the current study.

### **3.3.5 miR156-regulated SPLs are involved in alfalfa flooding response**

Identification of SPLs affected by flood stress is important to understand the role of miR156/SPL gene network in alfalfa's response to this stress. In this study, three new SPLs were identified and five of the previously known SPLs were downregulated in *miR156* overexpressing moderate-miR156A8 plants exposed to flood stress. SPL13 is one of the six SPLs (*SPL4*, *SPL7a*, *SPL8*, *SPL9*, *SPL13*, *SPL13a*) that were downregulated in all alfalfa genotypes upon flood stress, and is also silenced by miR156. To further establish the role of SPL13 in the flooding response, alfalfa plants was tested with RNAi-silenced

SPL13 (*SPL13RNAi*) to flooding stress. Similar to *miR156OE*, *SPL13RNAi* plants were able to withstand flooding as manifested by their ability to maintain their physiological activities. It remains to be investigated whether other SPLs that were silenced by flood stress were directly involved in flooding response, and whether the effects of different SPLs were redundant or additive.

### **3.3.6 ABA-dependent regulation of SnRK1 enhances *miR156* expression for flooding tolerance**

In the current study, hormone profiling revealed an increase in ABA metabolites, and transcriptomic analysis showed upregulation of ABA biosynthesis genes. I thus hypothesized that ABA is involved in alfalfa flooding response. Due to the conserved ABA signalling pathway in plants (Weng et al., 2016) the exogenous ABA application effect on SnRK1 was investigated using ABI-insensitive Arabidopsis mutant seedlings (*abil-2*, *abi5-8*). ABIs are involved in ABA signaling in which ABI1 is a calcium binding element while ABI5 is a transcription factor. A reduced transcript abundance of *KIN11* in *abi5-8* than in *abil-2* mutant seedlings under ABA and reduced sugar concentration treatments suggests SnRK1 expression involves ABA signaling. This could be explained if the other calcium binding ABI (ABI2) is still active in the *abil-2* mutant, complementing the defective ABI1. As KIN11 (one of the catalytic domains of SnRK1) is affected by ABA and low sugar availability in Arabidopsis, I investigated whether this response is dependent on the level of *miR156* expression in alfalfa. One-month-old *miR156OE* (A17) alfalfa plants exposed to flood stress were treated with 100  $\mu$ M ABA or organic solvent used for ABA dilution. *SnRK1* was induced in both WT and *miR156OE* genotypes in response to ABA treatment, with the highest level in WT plants. Moreover, under ABA treatment, the

expression levels of the catalytic (*KIN11*), regulatory ( $\beta$  and  $\gamma$ ), *SnRK1* and *SnRK2* were comparable between the genotypes under control condition except for *SnRK2*, which was significantly higher in *miR156OE*. Interestingly, under ABA treatment, the expression of *SnRK1*-associated genes (*SnRK2*, *KIN11*, *SnRK1- $\gamma$* , and *SnRK1- $\beta$ 2* subunits) in *miR156OE* plant was similar to that in WT plants. This suggests the expression of *SnRK1* may not be dependent on the level of *miR156* expression, but rather *SnRK1* may act upstream of *miR156*.

Due to the highly conserved *SnRK* function in plants (Baena-González et al., 2007), and the lack of alfalfa mutants with altered *KIN10* expression, I determined whether the expression of *miR156* is dependent on *SnRK1* using *Arabidopsis* plants with silenced (via RNAi) or overexpressed *KIN10*. When the plants were subjected to 3  $\mu$ M ABA treatment, the expression level of *miR156* was significantly higher in *KIN10* overexpressing plants compared to WT or *KIN10*RNAi plants under control or ABA treatment conditions. The observed ABA-dependent expression of *SnRK1* catalytic subunits (*KIN10* and *KIN11*) with *KIN10* overexpression resulting in higher *miR156* levels suggests that *SnRK1* upregulates *miR156*. Similarly, with the presence of ABA, phosphorylation of *SnRK2* is reported due to lack of PP2C-mediated *SnRK2* dephosphorylation as a result of a complex formation between *PYR/PYL* and *PP2C* (Todaka et al., 2015; Felemban et al., 2019). Moreover, ABA also induces a protein kinase *SnRK1* which is induced by lower energy metabolism along with its  $\alpha$  and  $\beta$  catalytic subunits *KIN10* and *KIN11* through *ABI5*.

To further understand how *SnRK1* increases the expression of *miR156 in vivo*, it is necessary to investigate possible protein-protein interaction between *SnRK1* and *miR156* biogenesis proteins (such as *DCL1*, *SE* and *HYL1*). Under my experimental conditions I

could not detect any protein-protein interaction between SnRK1 to either the DCL1 or SE. Despite the lack of visible interaction with SnRK1, DCL1 have three splice variants while SE has a homologue on chromosome three (Medtr3g006760) with two other splice variants, suggesting other possible interactions. Moreover, the investigated protein-protein interaction was between two proteins at a time while protein interactions may require the presence of more than two proteins. Similarly, it was essential for the presence of three cellulose synthase catalytic subunits (IRREGULAR XYLEM 1, 3, and 5) of CesA family for the proper assembly of cellulose synthesizing complex (Taylor et al., 2003). Consistent with a role for SnRK1 in miR156 biogenesis, it was reported that inactivation of redundant SnRK2 kinases under stress inhibits the biosynthesis of microRNAs involved in stress tolerance (Yan et al., 2017).

### **3.4. Conclusions**

Of the different phytohormones involved in abiotic stress response, ABA's role has been very well documented (Vishwakarma et al., 2017). In the current study, an enhanced level of ABA was found in flooding-tolerant genotypes. ABA-dependent stress tolerance in plants involves regulating genes that control various plant functions, including low energy metabolism-triggered protein kinase SnRK1. Here, an enhanced level of *SnRK1* was found in alfalfa plants under flooding stress, and expression of its catalytic  $\alpha$  subunits KIN10 and KIN11 was ABA-dependent. Sensing a lower energy level associated with reduced photosynthesis dictates metabolite dynamics, considering the carbon skeletons for ROS-scavenging specialized metabolites, such as phenylpropanoids, are derived from sugar. In the current study, a reallocation of resources from energy metabolism into specialized metabolism (anthocyanin) biosynthesis was observed at the transcriptomic and

metabolic levels. Previous reports showed that alfalfa plants with enhanced *miR156* expression level had anthocyanin biosynthesis through the regulation of SPL13/DFR module during drought stress (Chapter two). Similar to the situation with drought stress, there is an enhanced level of *miR156* upon flood stress in alfalfa dictating an enhanced anthocyanin biosynthesis to scavenge ROS. I propose that the switch from normal energy metabolism into conserving energy accompanied with anthocyanin biosynthesis is mediated by the protein kinase SnRK1. Moreover, the reduced but continuous supply of photosynthetic assimilation in flooding-tolerant genotypes provide the carbon skeleton demand to produce specialized metabolites. An enhanced level of SnRK1 governed by ABA and low-energy metabolism enhances *miR156* expression to regulate downstream genes. Subsequently, enhanced levels of *miR156* upon flooding stress silences three newly identified SPLs (*SPL7a*, *SPL8*, *SPL13a*) and three previously identified SPLs (*SPL4*, *SPL9*, *SPL13*) in a sequence-specific manner to regulate downstream genes and physiological functions.

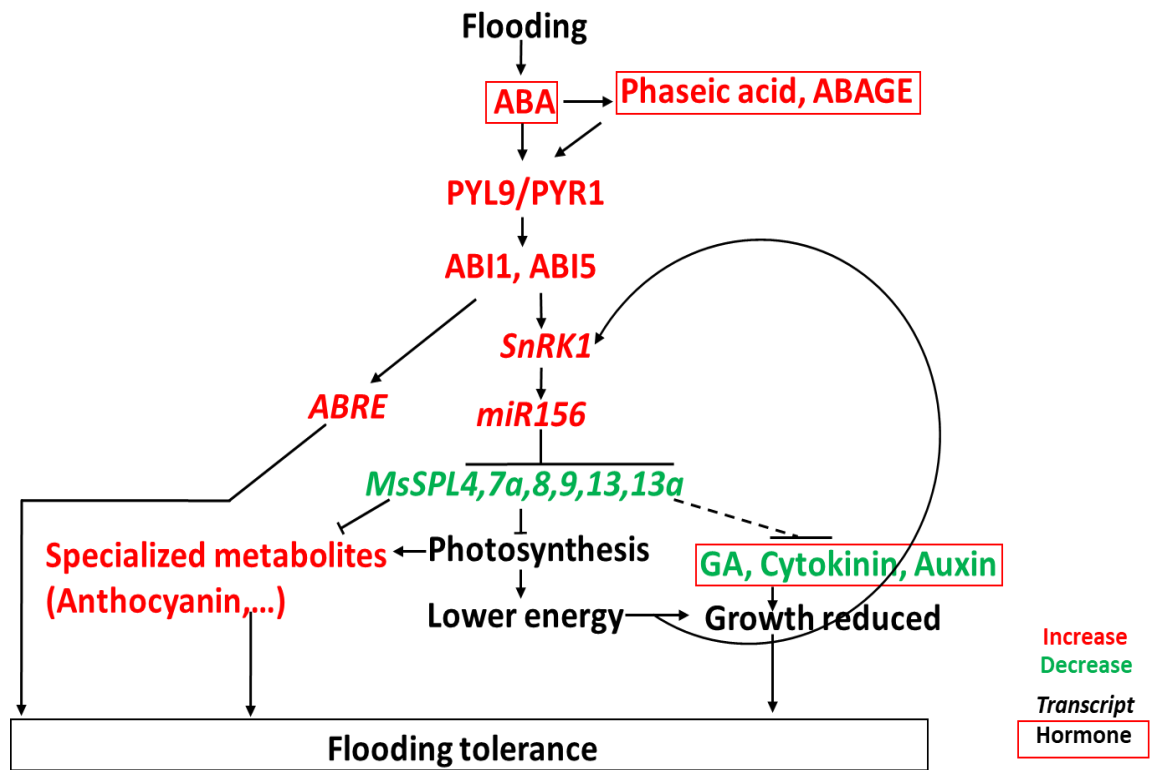
Based on the present results and others in the literature, I propose a model through which the response to flooding stress is regulated in alfalfa (**Figure 3.7**). Upon flooding, ABA is induced triggering PYL/PYR9 signalling molecules for ABA signal transduction. This signalling pathway induces ABI2 and ABI5 through reduced PP2C phosphorylation for increased expression of ABA responsive elements, *ABRE*. Moreover, the induced ABA signalling triggers SnRK1. The increased expression of *SnRK1* triggers *miR156* and channels resources towards the phenylpropanoid pathway. Induced *miR156* expression silences SPL13, to mediate anthocyanin biosynthesis by its regulation of *DFR* (Chapter 2), and other SPLs (*SPL4*, *SPL7a*, *SPL8*, *SPL9*, and *SPL13a*). Increased abundance of ABA

metabolites antagonistically affects gibberellic acid, cytokinin and auxin hormones (Voesenek et al., 2003). To exploit the newly identified SPLs (SPL1, SPL1a, SPL2a, SPL7, SPL7a, SPL8, SPL13a, SPL14, and SPL16) in alfalfa breeding, it will be necessary to investigate their functional roles individually and in combination in response to flooding stress and other physiological responses.



### Figure 3.10 Proposed model for flooding tolerance in alfalfa

In flooding-exposed alfalfa plants, ABA metabolites, mainly phaseic acid, induce ABI and trigger PYL/PYR9 signaling molecules to phosphorylate SnRK1 while reducing PP2C phosphorylation. The increased transcript levels of SnRK1 and its activation domains (KIN10 and KIN11) enhance *miR156* expression. As a result, miR156 orchestrates physiological- and specialized metabolite- associated genes by regulating *SPL4*, *SPL7a*, *SPL8*, *SPL9*, *SPL13*, and *SPL13a* upon flooding. For example, miR156-based *SPL13* transcript level reduction elevated anthocyanin biosynthesis by increasing transcript levels of *DFR* and other phenylpropanoid pathway associated genes during drought stress (Chapter 2). Moreover, *SPL13* and other SPLs modulate physiological adjustments to cope with flooding stress, but further investigation awaits to confirm the role of newly identified SPLs in alfalfa flooding tolerance and other traits. ABA; abscisic acid; ABRE, ABA response elements; PYL9, pyrabactin resistance 1-like9; PYR1, pyrabactin resistance1; PP2C, 2C-type protein phosphatases; ABI2, ABA insensitive1; ABI5, ABA insensitive5; SnRK1, Sucrose non-fermenting-related protein kinase1; miR156, microRNA156; MsSPL4,7a,8,9,13,13a are *SPL4*, *SPL7a*, *SPL8*, *SPL9*, *SPL13*, *SPL13a*; PG hormone, Plant growth hormone.



## **3.5. Methods**

### **3.5.1 Genetic material**

To understand the role of miR156 in regulating flooding tolerance in alfalfa, one field and two greenhouse experiments were performed. The field experiment was undertaken at the Agriculture and Agri-Food Canada (AAFC) Research Centre in Kentville, Nova Scotia, Canada while greenhouse experiments were done at the AAFC Research Center in London, Ontario, Canada. For the field experiment wild-type (WT) and empty vector (EV) alfalfa genotypes, a locally grown alfalfa cultivar AC-Caribou, a positive control genotype AAC-Trueman, *miR156* overexpressing genotypes (low-miR156A8a, moderate-miR156A8, A16, higher-miR156A11, A11a, A17), miR156 regulated *SPL6*RNAi genotypes (SPL6-405, SPL6-425, SPL6-428), and miR156 regulated *SPL13*RNAi genotypes (*SPL13-2*, *SPL13-5*, *SPL13-6*) were used. The transgenic plants were used previously (Aung et al., 2015a; Arshad et al., 2017a). Based on field phenotypic responses, forage yield data, and transcript analysis, the number of genotypes used for greenhouse experimentation was reduced to WT, AC-Caribou, AAC-Trueman, SPL13-5, SPL13-6 and A8.

### **3.5.2 Physiological data measurement**

To understand the role of miR156 and miR156-regulated SPLs in flooding response, physiological parameters were measured as described in chapter 2 section 2.5.5 except the genotypes being used in the current study.

### **3.5.3 Hormone profiling**

Three biological replicates of shoots from WT, AAC-Trueman, moderate-miR156A8 and SPL13-6 plants grown under flooding stress and well-drained for two weeks were

harvested, then flash frozen in liquid nitrogen and kept at  $-80^{\circ}\text{C}$  until use. Leaf samples were lyophilized with a Labconco freeze drier system (Kansas, USA Cat 7934026) at  $-50^{\circ}\text{C}$  for three days and  $\sim 50$  mg of dried samples were used for hormone profiling. Comprehensive phytohormone analysis (ABA and ABA metabolites, cytokinins, auxins, and gibberellins) was performed at the National Research Council of Canada, Saskatoon, SK on a fee for service basis.

A number of compounds namely DPA, ABA-GE, phaseic acid, 7'-OH-ABA, *neoPA*, *trans*-ABA and IAA-Glu were synthesized and prepared by the National Research Council of Canada, Saskatoon, SK, Canada; ABA, IAA-Leu, IAA-Ala, IAA-Asp, IAA, Z, ZR, iPR, and iP were purchased from Sigma–Aldrich; dhZ, dhZR, Z-O-Glu and GAs 1, 3, 4, 7, 8, 9, 19, 20, 24, 29, 44, and 53 were purchased from OIChemim Ltd. (Olomouc, Czech Republic). Deuterated forms of the hormones that were used as internal standards included: *d3*-DPA, *d5*-ABA-GE, *d3*-PA, *d4*-7'-OH-ABA, *d3*-*neoPA*, *d4*-ABA, *d4*-*trans*-ABA, *d3*-IAA-Leu, *d3*-IAA-Ala, *d3*-IAA-Asp, and *d3*-IAA-Glu and were synthesized and prepared at NRCC SK according to Abrams et al. (2003) and Zaharia et al. (2005). The *d5*-IAA was purchased from Cambridge Isotope Laboratories (Andover, MA); *d3*-dhZ, *d3*-dhZR, *d5*-Z-O-Glu, *d6*-iPR, *d6*-iP and *d2*-GAs 1, 3, 4, 7, 8, 9, 19, 20, 24, 29, 34, 44, 51 and 53 were purchased from OIChemim Ltd. (Olomouc, Czech Republic). The deuterated forms of selected hormones used as recovery (external) standards were also prepared and synthesized by NRCC SK. Calibration curves were created for all compounds of interest. Quality control (QCs) samples were run along with the tissue samples.

Analysis was performed at National Research Council of Canada, Saskatoon, SK on a UPLC/ESI-MS/MS utilizing a Waters ACQUITY UPLC system, equipped with a

binary solvent delivery manager and a sample manager coupled to a Waters Micromass Quattro Premier XE quadrupole tandem mass spectrometer via a Z-spray interface. MassLynx™ and QuanLynx™ (Micromass, Manchester, UK) were used for data acquisition and data analysis. The procedure for quantification of ABA and ABA catabolites, cytokinins, auxins, and gibberellins in plant tissue was performed using a modified procedure described in Lulsdorf *et al.* (2013). Briefly, the analyses utilized the Multiple Reaction Monitoring (MRM) function of the MassLynx v4.1 (Waters Inc) control software. The resulting chromatographic traces were quantified off-line by the QuanLynx v4.1 software (Waters Inc.) wherein each trace was integrated and the resulting ratio of signals (non-deuterated/internal standard) was compared with a previously constructed calibration curve to yield the amount of analyte present (ng per sample). Calibration curves were generated from the MRM signals obtained from standard solutions based on the ratio of the chromatographic peak area for each analyte to that of the corresponding internal standard. QC samples, internal standard blanks and solvent blanks were also prepared and analyzed alongside each batch of tissue samples.

### **3.5.4 Total monomeric anthocyanin and polyphenol determination**

Total monomeric anthocyanin (TMA) was determined using a pH differential extraction method (Lee *et al.*, 2005; Cheek *et al.*, 2013) as described in chapter 2 section 2.54 except for the genotypes used in the current study.

### **3.5.5 RNA extraction for qRT-PCR and RNAseq analysis**

The top shoot tip leaves (~50 mg) of WT, AC-Caribou, AAC-Trueman, moderate-miR156A8 and *SPL13*RNAi-6 plants grown under flood stress and well-drained (control) for two weeks was collected for total RNA extraction. Three biological replicates from

individual plants (control and stressed) were collected in Precellys<sup>R</sup> lysing tubes, flash frozen with liquid nitrogen and stored at -80°C until use. Total RNA extraction, cDNA synthesis, and qRT-PCR procedures used in the current study were performed as described in chapter 2 section 2.5.6 and 2.5.7.

Total RNA quality was checked using a Bio-Rad Bioanalyzer for integrity and Nanodrop concentration before RNAseq analysis. NEBNext<sup>®</sup>Ultra<sup>™</sup> kit (New England Biolabs Inc., Canada) was used for mRNA stranded library preparation followed by Illumina NovaSeq6000 sequencing with pair end of 101 nucleotide fragments performed as a fee for service at Genome Quebec, Montreal, QC, Canada.

### **3.5.6 RNAseq and pathway analysis**

RNAseq data was analyzed according to Trapnell et al. (2012) on Biocluster with Linux interface. To identify expression pattern of genes and module identification, R-software environment-based network analysis with weighted gene co-expression network, WGCNA, in the 'BiocManager' package was performed according to Langfelder and Horvath (2008). Differential gene expression-based pathway analysis was done using MapMan free software V3.6 (<https://mapman.gabipd.org/>) with a *M. truncatula* reference sequence, Mt4.0 V2 (<http://www.medicagogenome.org/downloads>) and also manual incorporation of the genes in to phenylpropanoid and ABA biosynthesis pathways.

### **3.5.7 5'RACE-based miR156 cleavage site identification**

To determine whether miR156 downregulates the newly identified *SPL* (*SPL7a*, 8 and 13a) genes via transcript cleavage, 5'RACE was performed according to Gao et al. (2016). In brief, total RNA from leaf tissues of *miR156OE* (higher-miR156A11) genotypes was extracted (RNeasy Plant mini kit, Canada) followed by CIP and Tap treatment to remove

5' phosphate and cap, respectively, according to the manufacturer's protocol (FirstChoice<sup>R</sup> RLM-RACE, Canada). 5'RACE adapter was ligated to the decapped mRNA and reverse transcribed before the subsequent two PCR reactions using the two provided forward primers with designed gene-specific inner (GSI) and outer (GSO) reverse primers (**Table S1**). The PCR products were electrophoresed on a 2% agarose gel, and DNA bands were excised and purified (QIAquick Gel extraction kit, Canada). Purified DNA was cloned in to a pJET1.2 cloning vector (Clone JET PCR cloning kit, Canada) according to the manufacturer's protocol, followed by transformation into chemically competent *E. coli* TOP10 cells (Invitrogen) using a heat shock method. Transformed cells were plated for overnight growth at 37<sup>0</sup>C, and individual colonies were cultured separately and plasmid was purified (GeneJET Plasmid Miniprep kit, Canada), sequenced and scored for the proportion of cleavage sites.

### **3.5.8 Investigating Protein-Protein interaction between SnRK1 and miR156 biogenesis genes**

To investigate the role of SnRK1 in miR156 biogenesis for the interaction between SnRK1 and miR156 biogenesis genes were tested using the yeast-two-hybrid system (Y2H). The whole coding sequences of SnRK1 (Medtr1g034030.1), DICER-LIKE protein (DCL) (Medtr3g102270.2) and the zinc finger protein SERRATE (SE) (Medtr8g043980) were amplified using gene-specific primers with the addition of 'CACC' in the forward primer, for directional cloning (**Table S1**). To construct an entry clone, the amplified coding sequences were cloned into the pENTR<sup>TM</sup> /D-TOPO<sup>®</sup> vector according to the manufacturer's protocol (Invitrogen) and transformed into *E. coli* by heat shock (42<sup>0</sup>C for 90 seconds). For the subsequent Y2H assay, the ProQuest<sup>TM</sup> Two-Hybrid System

(Invitrogen) was used (Singh et al., 2012). In brief, each of the entry clones were LR ligated with pDEST<sup>TM</sup>22 and pDEST<sup>TM</sup>32 separately (two constructs for each entry clone) to create prey (pEXP<sup>TM</sup>22) and bait plasmids (pEXP32). Subsequently, different combinations of the prey and bait plasmids were co-transformed with denatured Salmon sperm DNA and 40% PEG as a carrier into the MaV203 yeast strain by heat shock at 42°C for 7 minutes according to the manufacturer's protocol. Subsequently, the reporter *URA3* gene was used to observe the presence of a specific 2-hybrid interaction between SnRK1 with SE and DCL using SC-Leu-Trp-Ura media plates. The interaction between pEXP<sup>TM</sup>32/Krev1 with pEXP<sup>TM</sup>22/RalGDS-wt was used as a positive control, while pEXP<sup>TM</sup>32/Krev1 against the mutated RalGDS of pEXP<sup>TM</sup>22/RalGDS-m2 was used as a negative control.

### **3.5.9 Investigating SnRK1 regulation by low sugar and ABA in Arabidopsis**

To understand whether the expression of SnRK1 is regulated through the ABA signalling pathway, low-sugar and ABA, two ABA-insensitive Arabidopsis mutants (*abi1-2* and *abi5-8*) were planted in ½ MS medium with different treatment combinations. Three treatment arrangements were set up with media supplemented with T1-control (44 mM sucrose, no ABA), T2 (22 mM sucrose, no ABA), T3 (22 mM sucrose, 1 µM ABA). Tissue culture plates were kept at low-light intensity (10 µmol m<sup>-2</sup>s<sup>-1</sup>) to reduce photosynthesis-mediated sugar supplementation. Three biological replicates of the treatments for each genotype were planted with each biological replicate containing approximately 50 plants. Seedlings were collected to determine for the expression levels of SnRK1-related and selected dark induced genes.



### 3.5.10 Investigating SnRK1 regulation by miR156 in alfalfa

To investigate whether the expression of SnRK1 was upstream of miR156 upon low sugar and ABA treatment in alfalfa, a *miR156* overexpressing genotype (A17) and WT plants were used. Rooted cuttings of both genotypes were arranged into two treatments: T1-control (15 g/L sucrose, no ABA), and T2 (no sucrose, 100  $\mu$ M ABA). All plant roots were submerged in distilled water and kept at low-light intensity (25  $\mu$ mol m<sup>-2</sup>s<sup>-1</sup>), and then plant tissues were collected after 4 hrs of ABA treatment. Subsequently, shoot tip leaves were used to investigate the expression levels of SnRK1-related genes.

### 3.5.11 Investigating *miR156* expression dependence on SnRK1 in Arabidopsis

Arabidopsis seeds used in a previously published work were obtained *in kind* from Dr. Filip Rolland, Department of Biology KU, Leuven, Belgium (Baena-González et al., 2007). Arabidopsis plants with increased (*KIN10-OX1*, *KIN10-OX2*) and silenced (*KIN10RNAi-1*, *KIN10RNAi-2*) expression of the catalytic subunit KIN10, respectively, were used to understand whether *miR156* expression is dependent on activation of SnRK1 during ABA treatment and sugar starvation. The treatment set up was similar to the one used for the investigation of SnRK1 expression by low sugar and ABA (section 3.5.9), except for the genotypes under study. Seedlings were harvested and determined the expression levels of *miR156*.

### 3.5.12 Data analysis

Physiological and hormonal data were first checked for normal distribution using a Shapiro-Wilk test in the R-software environment 3.5.2 followed by Analysis of Variance (ANOVA). Subsequently, *post hoc* Tukey multiple comparison tests were done

accordingly. RNAseq analysis was performed using Biocluster in a Linux interface using scripts illustrated by Trapnell (2012).

### 3.6 References

**Abrams SR, Nelson K, Ambrose SJ** (2003) Deuterated abscisic acid analogs for mass spectrometry and metabolism studies. *Journal of Labelled Compounds and Radiopharmaceuticals* 46: 273-283

**Alexander LV, Zhang X, Peterson TC, Caesar J, Gleason B, Klein Tank AMG, Haylock M, Collins D, Trewin B, Rahimzadeh F, Tagipour A, Rupa Kumar K, Revadekar J, Griffiths G, Vincent L, Stephenson DB, Burn J, Aguilar E, Brunet M, Taylor M, New M, Zhai P, Rusticucci M, Vazquez-Aguirre JL** (2006) Global observed changes in daily climate extremes of temperature and precipitation. *Journal of Geophysical Research: Atmospheres* 111

**Arshad M, Feyissa B, Amyot L, Aung B, Hannoufa A** (2017a) MicroRNA156 improves drought stress tolerance in alfalfa (*Medicago sativa*) by silencing SPL13. *Plant Science* 258: 122-136

**Arshad M, Gruber MY, Wall K, Hannoufa A** (2017b) An insight into microRNA156 role in salinity stress responses of alfalfa. *Frontiers in Plant Science* 8: 356

**Aung B, Gruber MY, Amyot L, Omari K, Bertrand A, Hannoufa A** (2015a) Ectopic expression of LjmiR156 delays flowering, enhances shoot branching, and improves forage quality in alfalfa. *Plant Biotechnology Reports* 9: 379-393

**Aung B, Gruber MY, Amyot L, Omari K, Bertrand A, Hannoufa A** (2015b) MicroRNA156 as a promising tool for alfalfa improvement. *Plant Biotechnology Journal* 13: 779-790

**Aung B, Gruber MY, Hannoufa A** (2015c) The MicroRNA156 system: A tool in plant biotechnology. *Biocatalysis and Agricultural Biotechnology* 4: 432-442

**Ayano M, Kani T, Kojima M, Sakakibara H, Kitaoka T, Kuroha T, Angeles-Shim RB, Kitano H, Nagai K, Ashikari M** (2014) Gibberellin biosynthesis and signal transduction is essential for internode elongation in deepwater rice. *Plant, Cell and Environment* 37: 2313-2324

**Baena-González E, Rolland F, Thevelein JM, Sheen J** (2007) A central integrator of transcription networks in plant stress and energy signalling. *Nature* 448: 938

**Bailey-Serres J, Lee SC, Brinton E** (2012) Waterproofing crops: Effective flooding survival strategies. *Plant Physiology* 160: 1698-1709

**Branco-Price C, Kaiser KA, Jang CJH, Larive CK, Bailey-Serres J** (2008) Selective mRNA translation coordinates energetic and metabolic adjustments to cellular oxygen deprivation and reoxygenation in *Arabidopsis thaliana*. *The Plant Journal* 56: 743-755

**Brown S, Nicholls RJ, Lázár AN, Hornby DD, Hill C, Hazra S, Appeaning Addo K, Haque A, Caesar J, Tompkins EL** (2018) What are the implications of sea-level rise for a 1.5, 2 and 3 °C rise in global mean temperatures in the Ganges-Brahmaputra-Meghna and other vulnerable deltas? *Regional Environmental Change* 18: 1829-1842

**Caudle KL, Maricle BR** (2012) Effects of flooding on photosynthesis, chlorophyll fluorescence, and oxygen stress in plants of varying flooding tolerance. *Transactions of the Kansas Academy of Science* 115:5-18

**Chao LM, Liu YQ, Chen DY, Xue XY, Mao YB, Chen XY** (2017) *Arabidopsis* transcription factors SPL1 and SPL12 confer plant thermotolerance at reproductive stage. *Molecular Plant* 10: 735-748

**Chen Y, Zhang X, Guo Q, Cao L, Qin Q, Li C, Zhao M, Wang W** (2019) Plant morphology, physiological characteristics, accumulation of secondary metabolites and antioxidant activities of *Prunella vulgaris* L. under UV solar exclusion. *Biological Research* 52: 17

**Cheok CY, Chin NL, Yusof YA, Talib RA, Law CL** (2013) Optimization of total monomeric anthocyanin (TMA) and total phenolic content (TPC) extractions from mangosteen (*Garcinia mangostana* Linn.) hull using ultrasonic treatments. *Industrial Crops and Products* 50: 1-7

**Dubois V, Moritz T, García-Martínez JL** (2011) Comparison of the role of gibberellins and ethylene in response to submergence of two lowland rice cultivars, Senia and Bomba. *Journal of Plant Physiology* 168: 233-241

**Felemban A, Braguy J, Zurbriggen MD, Al-Babili S** (2019) Apocarotenoids involved in plant development and stress response. *Frontiers in Plant Science* 10:1168

**Feyissa BA, Arshad M, Gruber MY, Kohalmi SE, Hannoufa A** (2019) The interplay between miR156/SPL13 and DFR/WD40-1 regulate drought tolerance in alfalfa. *BMC Plant Biology* 19: 434

**Fragoso S, Espíndola L, Páez-Valencia J, Gamboa A, Camacho Y, Martínez-Barajas E, Coello P** (2009) SnRK1 isoforms AKIN10 and AKIN11 are differentially regulated in *Arabidopsis* plants under phosphate starvation. *Plant Physiology* 149: 1906-1916

- Fukao T, Barrera-Figueroa BE, Juntawong P, Peña-Castro JM** (2019) Submergence and waterlogging stress in plants: A review highlighting research opportunities and understudied aspects. *Frontiers in Plant Science* 10:340
- Gao R, Austin RS, Amyot L, Hannoufa A** (2016) Comparative transcriptome investigation of global gene expression changes caused by miR156 overexpression in *Medicago sativa*. *BMC Genomics* 17: 658
- Gray WM** (2004) Hormonal regulation of plant growth and development. *PLOS Biology* 2: E311-E311
- Gupta KJ, Zabalza A, Van Dongen JT** (2009) Regulation of respiration when the oxygen availability changes. *Physiologia Plantarum* 137: 383-391
- Hattori Y, Nagai K, Furukawa S, Song X-J, Kawano R, Sakakibara H, Wu J, Matsumoto T, Yoshimura A, Kitano H, Matsuoka M, Mori H, Ashikari M** (2009) The ethylene response factors SNORKEL1 and SNORKEL2 allow rice to adapt to deep water. *Nature* 460: 1026
- Herzog M, Fukao T, Winkel A, Konnerup D, Lamichhane S, Alpuerto JB, Hasler-Sheetal H, Pedersen O** (2018) Physiology, gene expression, and metabolome of two wheat cultivars with contrasting submergence tolerance. *Plant, Cell and Environment* 41: 1632-1644
- Jossier M, Bouly J-P, Meimoun P, Arjmand A, Lessard P, Hawley S, Grahame Hardie D, Thomas M** (2009) SnRK1 (SNF1-related kinase 1) has a central role in sugar and ABA signalling in *Arabidopsis thaliana*. *The Plant Journal* 59: 316-328
- Langfelder P, Horvath S** (2008) WGCNA: An R package for weighted correlation network analysis. *BMC Bioinformatics* 9: 559
- Lee J, Durst R, Wrolstad R** (2005) Determination of total monomeric anthocyanin pigment content of fruit juices, beverages, natural colorants, and wines by the pH differential method: Collaborative study. *Journal of AOAC International* 88: 1269-1278
- Lindqvist LM, Tandoc K, Topisirovic I, Furic L** (2018) Cross-talk between protein synthesis, energy metabolism and autophagy in cancer. *Current Opinion in Genetics and Development* 48: 104-111
- Lu S, Sun YH, Chiang VL** (2008) Stress-responsive microRNAs in *Populus*. *The Plant Journal* 55: 131-151
- Lulsdorf MM, Yuan HY, Slater SMH, Vandenberg A, Han X, Zaharia LI, Abrams SR** (2013) Endogenous hormone profiles during early seed development of *C. arietinum* and *C. anatolicum*. *Plant Growth Regulation* 71: 191-198

**Matthews C, Arshad M, Hannoufa A** (2019) Alfalfa response to heat stress is modulated by microRNA156. *Physiologia Plantarum* 165: 830-842

**Moore B, Zhou L, Rolland F, Hall Q, Cheng W-H, Liu Y-X, Hwang I, Jones T, Sheen J** (2003) Role of the Arabidopsis glucose sensor HXK1 in nutrient, light, and hormonal signaling. *Science* 300: 332-336

**Mustroph A, Zanetti ME, Jang CJH, Holtan HE, Repetti PP, Galbraith DW, Girke T, Bailey-Serres J** (2009) Profiling transcriptomes of discrete cell populations resolves altered cellular priorities during hypoxia in Arabidopsis. *Proceedings of the National Academy of Sciences of the United States of America* 106: 18843-18848

**Preston JC, Jorgensen SA, Orozco R, Hileman LC** (2016) Paralogous SQUAMOSA PROMOTER BINDING PROTEIN-LIKE (SPL) genes differentially regulate leaf initiation and reproductive phase change in petunia. *Planta* 243: 429-440

**Ramon M, Dang TVT, Broeckx T, Hulsmans S, Crepin N, Sheen J, Rolland FA** (2019) Default activation and nuclear translocation of the plant cellular energy sensor SnRK1 regulate metabolic stress responses and development. *The Plant Cell*: 31: 1614-1632

**Rodrigues A, Adamo M, Crozet P, Margalha L, Confraria A, Martinho C, Elias A, Rabissi A, Lumbreras V, González-Guzmán M, Antoni R, Rodriguez PL, Baena-González E** (2013) ABI1 and PP2CA phosphatases are negative regulators of Snf1-related protein kinase1 signaling in Arabidopsis. *The Plant Cell* 25: 3871-3884

**Rodriguez Pedro L** (2016) Abscisic acid catabolism generates phaseic acid, a molecule able to activate a subset of ABA receptors. *Molecular Plant* 9: 1448-1450

**Rogelj J, Popp A, Calvin KV, Luderer G, Emmerling J, Gernaat D, Fujimori S, Strefler J, Hasegawa T, Marangoni G, Krey V, Kriegler E, Riahi K, van Vuuren DP, Doelman J, Drouet L, Edmonds J, Fricko O, Harmsen M, Havlík P, Humpenöder F, Stehfest E, Tavoni M** (2018) Scenarios towards limiting global mean temperature increase below 1.5 °C. *Nature Climate Change* 8: 325-332

**Rubio S, Rodrigues A, Saez A, Dizon MB, Galle A, Kim T-H, Santiago J, Flexas J, Schroeder JI, Rodriguez PL** (2009) Triple loss of function of protein phosphatases type 2C leads to partial constitutive response to endogenous abscisic acid. *Plant Physiology* 150: 1345-1355

**Sato F, Hashimoto T, Hachiya A, Tamura K-i, Choi K-B, Morishige T, Fujimoto H, Yamada Y** (2001) Metabolic engineering of plant alkaloid biosynthesis. *Proceedings of the National Academy of Sciences of the United States of America* 98: 367-372

**Sharma DK, Andersen SB, Ottosen CO, Rosenqvist E** (2015) Wheat cultivars selected for high Fv/Fm under heat stress maintain high photosynthesis, total chlorophyll, stomatal conductance, transpiration and dry matter. *Physiologia Plantarum* 153: 284-298

**Singh R, Lee MO, Lee JE, Choi J, Park JH, Kim EH, Yoo RH, Cho JI, Jeon JS, Rakwal R, Agrawal GK, Moon JS, Jwa NS** (2012) Rice Mitogen-Activated Protein Kinase Interactome Analysis Using the Yeast Two-Hybrid System. *Plant Physiology* 160: 477-487

**Su L, Dai Z, Li S, Xin H** (2015) A novel system for evaluating drought–cold tolerance of grapevines using chlorophyll fluorescence. *BMC Plant Biology* 15: 82

**Taylor NG, Howells RM, Huttly AK, Vickers K, Turner SR** (2003) Interactions among three distinct CesA proteins essential for cellulose synthesis. *Proceedings of the National Academy of Sciences of the United States of America* 100: 1450-1455

**Todaka D, Shinozaki K, Yamaguchi-Shinozaki K** (2015) Recent advances in the dissection of drought-stress regulatory networks and strategies for development of drought-tolerant transgenic rice plants. *Frontiers in Plant Science* 6: 84-84

**Trapnell C, Roberts A, Goff L, Pertea G, Kim D, Kelley DR, Pimentel H, Salzberg SL, Rinn JL, Pachter L** (2012) Differential gene and transcript expression analysis of RNA-seq experiments with TopHat and Cufflinks. *Nature Protocols* 7: 562

**Turkan I** (2018) ROS and RNS: key signalling molecules in plants. *Journal of Experimental Botany* 69: 3313-3315

**Vishwakarma K, Upadhyay N, Kumar N, Yadav G, Singh J, Mishra RK, Kumar V, Verma R, Upadhyay RG, Pandey M, Sharma S** (2017) Abscisic acid signaling and abiotic stress tolerance in plants: A review on current knowledge and future prospects. *Frontiers in Plant Science* 8: 161-161

**Voesenek LACJ, Benschop JJ, Bou J, Cox MCH, Groeneveld HW, Millenaar FF, Vreeburg RAM, Peeters AJM** (2003) Interactions between plant hormones regulate submergence-induced shoot elongation in the flooding-tolerant dicot *Rumex palustris*. *Annals of Botany* 91: 205-211

**Voesenek LACJ, Bailey-Serres J** (2015) Flood adaptive traits and processes: An overview. *New Phytologist* 206: 57-73

**Wang J-W, Schwab R, Czech B, Mica E, Weigel D** (2008) Dual effects of miR156-targeted SPL genes and CYP78A5/KLUH on plastochron length and organ size in *Arabidopsis thaliana*. *The Plant Cell* 20: 1231-1243

- Weng J-K, Ye M, Li B, Noel JP** (2016) Co-evolution of hormone metabolism and signaling networks expands plant adaptive plasticity. *Cell* 166: 881-893
- Wurzinger B, Nukarinen E, Nägele T, Weckwerth W, Teige M** (2018) The SnRK1 kinase as central mediator of energy signaling between different organelles. *Plant Physiology* 176: 1085-1094
- Xu K, Xu X, Fukao T, Canlas P, Maghirang-Rodriguez R, Heuer S, Ismail AM, Bailey-Serres J, Ronald PC, Mackill DJ** (2006) Sub1A is an ethylene-response-factor-like gene that confers submergence tolerance to rice. *Nature* 442: 705-708
- Yan J, Wang P, Wang B, Hsu C-C, Tang K, Zhang H, Hou Y-J, Zhao Y, Wang Q, Zhao C, Zhu X, Tao WA, Li J, Zhu J-K** (2017) The SnRK2 kinases modulate miRNA accumulation in *Arabidopsis*. *PLOS Genetics* 13: e1006753
- Yeung E, van Veen H, Vashisht D, Sobral Paiva AL, Hummel M, Rankenberg T, Steffens B, Steffen-Heins A, Sauter M, de Vries M, Schuurink RC, Bazin J, Bailey-Serres J, Voeselek LACJ, Sasidharan R** (2018) A stress recovery signaling network for enhanced flooding tolerance in *Arabidopsis thaliana*. *Proceedings of the National Academy of Sciences of the United States of America* 115: E6085-E6094
- Yu Y, Jia T, Chen X** (2017) The ‘how’ and ‘where’ of plant microRNAs. *New Phytologist* 216: 1002-1017
- Zaharia LI, Walker-Simmon MK, Rodríguez CN, Abrams SRJJoPGR** (2005) Chemistry of abscisic acid, abscisic acid catabolites and analogs. *Journal of Plant Growth Regulation* 24: 274-284
- Zhang Y, De Stefano R, Robine M, Butelli E, Bulling K, Hill L, Rejzek M, Martin C, Schoonbeek HJ** (2015) Different reactive oxygen species scavenging properties of flavonoids determine their abilities to extend the shelf life of tomato. *Plant Physiology* 169: 1568-1583
- Zhang Z, Wei L, Zou X, Tao Y, Liu Z, Zheng Y** (2008) Submergence-responsive microRNAs are potentially involved in the regulation of morphological and metabolic adaptations in maize root cells. *Annals of Botany* 102: 509-519
- Zou Y, Wang Y, Wang L, Yang L, Wang R, Li X** (2013) miR172b controls the transition to autotrophic development inhibited by ABA in *Arabidopsis*. *PLOS ONE* 8: e64770



## 4. General discussion and future research directions

The frequency and intensity of extreme weather events that are witnessed around the world are well correlated with climate change models that analyzed centuries of fossil records and available weather data (Evans et al., 2018; Hearing et al., 2018; Yeung et al., 2018; Dai and Bloecker, 2019). Subsequently, experiencing '100-year-flooding' events every two to 10 years and prolonged extreme droughts are the new norms in some places around the globe (IPCC, 2019; Marsooli et al., 2019). Furthermore, current climate change models predict frequent weather anomalies that could impact plant production and productivity (Knapp et al., 2008; Sheffield and Wood, 2008; Ward et al., 2013; Dai and Bloecker, 2019; IPCC, 2019). Therefore, to sustain crop production and productivity it is critical to develop cultivars that can tolerate to extreme weather events.

Among plants that are affected by extreme weather events, alfalfa is one of the most important commercial crops grown for various purposes, including human food, animal feed, and bioenergy feedstock (Bora and Sharma, 2011; Bhattarai et al., 2013; Humphries et al., 2018). Despite the importance of alfalfa, its production, productivity, and acreage have been declining over the years (Berhongaray et al., 2019). New plant improvement strategies use molecular marker-assisted breeding tools to enhance stress tolerance and crop yield (Collard and Mackill, 2008). As potential molecular markers, non-protein-coding microRNAs conserved across different plant species are contemplated for improving plant performance. In the current research, I investigated the role of miR156 and its target *SPL13* and other downstream genes in response to drought and flooding stress in alfalfa, which can be further exploited as molecular markers.

Commonalities and differences are observed in plants responding to drought and flooding, even though they are caused by two extremes of water availability. For example, aerenchyma tissue was observed in flooding-exposed *Carex* species facilitating root aeration (Visser et al., 2000). Similarly, root cortical aerenchyma developed in maize under drought, accounting for 50% less root respiration per unit root length (Zhu et al., 2010). The conserved energy in maize was associated with root elongation and other physiological functions to cope with the drought stress. Despite the benefits of root aerenchyma formation in maize, the cavitation should not be large enough to cause an embolism affecting hydraulic conductance (Vasellati et al., 2001). At a molecular level, ROS induction increased with both flooding and drought stresses due to inefficient cellular processes in chloroplast, mitochondrion, and peroxisomes (Asada, 2006). Elevated ROS levels trigger various plant stress tolerance mechanisms, among which tolerant alfalfa cultivars induce ROS-scavenging metabolites (Chapter 2, 3). Contrary to a common aerenchyma formation, differences were also observed in roots exposed to these drought and flood stresses. For example, drought-tolerant plants tended to increase root hair formation (Chapter 2) likely to maximize root surface area while there were lacking in flood stressed plants (Vasellati et al., 2001). Apart from the similarities and differences of responses to these stresses, understanding their regulation mechanism is crucial in developing tolerant cultivars.

#### **4.1 microRNA156 and its role in alfalfa abiotic stress regulation**

The non-protein coding regulatory miR156 affected different aspects of alfalfa, such as delayed flowering (Aung et al., 2015a), increased branching (Aung et al., 2015b), increased heat- (Mathews et al., 2019), drought- (Arshad et al., 2017a; Chapter 2) and flood-stress

tolerance (Chapter 3). These roles of miR156 came to exist through the sequence-specific downregulation of SPL that positively and negatively regulate the expression of downstream genes. Fine-tuning the effect of miR156 by other microRNAs is important, such as miR172 in regulating developmental stage transition (Wang et al., 2015). However, tweaking the microRNAs role was also seen to be dictated by the phytohormone signaling network, indicating the complex regulatory mechanisms. For example, anther and ovule development in Arabidopsis were regulated by miR167 which affects auxin biosynthesis (Wu et al., 2006) while ABA- and gibberellin-responsive miR159 increased seed germination (Reyes and Chua, 2007) and induced flower development (Achard et al., 2004), respectively.

miR156 expression levels are triggered by various intrinsic and extrinsic factors. The intrinsic factors include other regulatory microRNAs, tissue specificity (Chapter 2), and enhanced microRNA biogenesis genes, such as SERRATE (SE), DICER-LIKE1 (DCL1), HYPONASTIC LEAVES1 (HYL1), their translation and post-translational modifications (Fang and Spector, 2007). Under flooding stress (extrinsic factor), for example, enhanced miR156 transcript levels were attained with increased ABA-dependent SnRK1 expression (Chapter 3). These seemed to be acquired through the interaction between ABA-enhanced SnRK1 and miR156-biogenesis genes at the protein levels. Accordingly, forthcoming investigation of protein-protein interaction between SnRK1 and miR156 biogenesis protein with their transcript variants will unravel in-depth the miR156 regulation mechanisms.

## **4.2 miR156-based stress tolerance in alfalfa involves *SQUAMOSA PROMOTER-BINDING PROTEIN-LIKE* transcription factors**

miR156 down-regulates the expression levels of *SQUAMOSA PROMOTER-BINDING PROTEIN-LIKE* transcription factors (SPLs) at the posttranscriptional level to cope with abiotic stress (Gao et al., 2016; Arshad et al., 2017a; Feyissa et al., 2019). Apart from SPL13, miR156 was previously found to down-regulate six other SPLs (SPL2, SPL3, SPL4, SPL6, SPL9, and SPL12) in alfalfa (Gao et al., 2016). In the current study, nine novel SPLs (SPL1, SPL1a, SPL2a, SPL7, SPL7a, SPL8, SPL13a, SPL14, and SPL16) were discovered (Chapter 3) whereby SPL7a, SPL8, and SPL13a were found to be down-regulated and direct targets of miR156 under flooding in a sequence-specific manner. Apart from these, further characterization of the other newly identified SPLs would shed light on their potential role in alfalfa's response to abiotic stress, and potentially other functions. Moreover, I observed the presence of SPL13-interacting proteins using FASP-based proteomics, but validating the peptide sequences was difficult using the *Medicago truncatula* genome as a reference and results were not presented in the thesis. When the alfalfa genome sequence becomes publicly available, these SPL13 interacting proteins may be identified with high confidence. Apart from the proteome analysis, the use of alfalfa genome as a reference in RNAseq analysis will resolve the lack of better genome coverage to map transcripts.

Understanding the molecular function of miR156 and its target SPL genes in alfalfa's response to abiotic stress will provide an important molecular tool that can be used in marker-assisted improvement of not only alfalfa, but potentially also other crops. Results described in my PhD thesis provide an insight into these molecular mechanisms towards

water stress, but further research is clearly required to fully realize the potential of the miR156/SPL network in crop improvement. RNAseq raw data used in the flooding-stress (accession number PRJNA596791) and drought –stress experiments (accession number PRJNA598830) are available online through the national center for biotechnology information sequence archive to be used as a resource in future studies.

### 4.3 References

- Achard P, Herr P, Baulcombe DC, Harberd NP** (2004) Modulation of floral development by a gibberellin-regulated microRNA. *Development* 131:3357-3365
- Arshad M, Feyissa B, Amyot L, Aung B, Hannoufa A** (2017a) MicroRNA156 improves drought stress tolerance in alfalfa (*Medicago sativa*) by silencing SPL13. *Plant Science* 258: 122-136
- Aung B, Gruber MY, Amyot L, Omari K, Bertrand A, Hannoufa A** (2015a) Ectopic expression of LjmiR156 delays flowering, enhances shoot branching, and improves forage quality in alfalfa. *Plant Biotechnology Reports* 9: 379-393
- Aung B, Gruber MY, Amyot L, Omari K, Bertrand A, Hannoufa A** (2015b) MicroRNA156 as a promising tool for alfalfa improvement. *Plant Biotechnology Journal* 13: 779-790
- Asada K** (2006) Production and scavenging of reactive oxygen species in chloroplasts and their functions. *Plant Physiology* 141: 391-396
- Berhongaray G, Basanta M, Jauregui JM** (2019) Water table depth affects persistence and productivity of alfalfa in Central Argentina. *Field Crops Research* 235: 54-58
- Bhattarai K, Brummer C, Monteros MJ** (2013) Alfalfa as a Bioenergy Crop. In MC Saha, HS Bhandari, JH Bouton, eds, *Bioenergy Feedstocks: Breeding and Genetics*, Wiley, New York, 207-231
- Bora KS, Sharma A** (2011) Phytochemical and pharmacological potential of *Medicago sativa*: A review. *Pharmaceutical Biology* 49: 211-220
- Collard BCY, Mackill DJ** (2008) Marker-assisted selection: An approach for precision plant breeding in the twenty-first century. *Philosophical transactions of the Royal Society of London. Series B. Biological Sciences* 363: 557-572
- Dai A, Bloecker CE** (2019) Impacts of internal variability on temperature and precipitation trends in large ensemble simulations by two climate models. *Climate Dynamics* 52: 289-306
- Evans D, Sagoo N, Renema W, Cotton LJ, Müller W, Todd JA, Saraswati PK, Stassen P, Ziegler M, Pearson PN, Valdes PJ, Affek HP** (2018) Eocene greenhouse climate revealed by coupled clumped isotope-Mg/Ca thermometry. *Proceedings of the National Academy of Sciences of the United States of America* 115: 1174
- Fang Y, Spector DL** (2007) Identification of nuclear dicing bodies containing proteins for microRNA biogenesis in living *Arabidopsis* plants. *Current Biology* 17: 818-823

**Feyissa BA, Arshad M, Gruber MY, Kohalmi SE, Hannoufa A** (2019) The interplay between miR156/SPL13 and DFR/WD40–1 regulate drought tolerance in alfalfa. *BMC Plant Biology* 19: 434

**Gao R, Austin RS, Amyot L, Hannoufa A** (2016) Comparative transcriptome investigation of global gene expression changes caused by miR156 overexpression in *Medicago sativa*. *BMC Genomics* 17: 658-658

**Hearing TW, Harvey THP, Williams M, Leng MJ, Lamb AL, Wilby PR, Gabbott SE, Pohl A, Donnadieu Y** (2018) An early cambrian greenhouse climate. *Science Advances* 4: eaar5690

**Humphries A, Ovalle C, del Pozo A, Inostroza L, Barahona V, Ivelic-Saez J, Yu L, Yerzhanova S, Meirman G, Abayev S, Brummer E, Hughes S, Bingham E, Kilian B** (2018) Introgression of alfalfa crop wild relatives for climate change adaptation. In Daniel Basigalup, María del Carmen Spada, Ariel Odorizzi, V Arolfo, eds, *Second World Alfalfa Congress: Global interaction for alfalfa innovation, CORDOBA, ARGENTINA*: 72-76

**IPCC** (2019) An IPCC Special Report on the impacts of global warming of 1.5°C above pre-industrial levels and related global greenhouse gas emission pathways, in the context of strengthening the global response to the threat of climate change, sustainable development, and efforts to eradicate poverty. In Valérie Masson-Delmotte, Panmao Zhai, Hans-Otto Pörtner, Debra Roberts, Jim Skea, Priyadarshi R. Shukla, Anna Pirani, Wilfran Moufouma-Okia, Clotilde Péan, Roz Pidcock, Sarah Connors, J. B. Robin Matthews, Yang Chen, Xiao Zhou, Melissa I. Gomis, Elisabeth Lonnoy, Tom Maycock, Melinda Tignor, T Waterfield, eds, *Summary for Policymakers*.

**Knapp AK, Beier C, Briske DD, Classen AT, Luo Y, Reichstein M, Smith MD, Smith SD, Bell JE, Fay PA, Heisler JL, Leavitt SW, Sherry R, Smith B, Weng E** (2008) Consequences of more extreme precipitation regimes for terrestrial ecosystems. *BioScience* 58: 811-821

**Marsooli R, Lin N, Emanuel K, Feng K** (2019) Climate change exacerbates hurricane flood hazards along US atlantic and gulf coasts in spatially varying patterns. *Nature Communications* 10: 3785

**Matthews C, Arshad M, Hannoufa A** (2019) Alfalfa response to heat stress is modulated by microRNA156. *Physiologia Plantarum* 165: 830-842

**Reyes JL, Chua NH** (2007) ABA induction of miR159 controls transcript levels of two MYB factors during *Arabidopsis* seed germination. *Plant Journal* 49:592-606

- Sheffield J, Wood EF** (2008) Projected changes in drought occurrence under future global warming from multi-model, multi-scenario, IPCC AR4 simulations. *Climate Dynamics* 31: 79-105
- Vasellati V, Oosterheld M, Medan D, Loreti J** (2001) Effects of Flooding and Drought on the Anatomy of *Paspalum dilatatum*. *Annals of Botany* 88: 355-360
- Visser EJW, BÖGemann GM, Van De Steeg HM, Pierik R, Blom CWPM** (2000) Flooding tolerance of *Carex* species in relation to field distribution and aerenchyma formation. *New Phytologist* 148: 93-103
- Wang L, Sun S, Jin J, Fu D, Yang X, Weng X, Xu C, Li X, Xiao J, Zhang Q** (2015b) Coordinated regulation of vegetative and reproductive branching in rice. *Proceedings of the National Academy of Sciences of the United States of America* 112: 15504-15509
- Ward PJ, Jongman B, Weiland FS, Bouwman A, van Beek R, Bierkens MFP, Ligtoet W, Winsemius HC** (2013) Assessing flood risk at the global scale: Model setup, results, and sensitivity. *Environmental Research Letters* 8: 044019
- Wu MF, Tian Q, Reed JW** (2006) Arabidopsis microRNA167 controls patterns of ARF6 and ARF8 expression, and regulates both female and male reproduction. *Development*, 133:4211-4218
- Yeung E, van Veen H, Vashisht D, Sobral Paiva AL, Hummel M, Rankenberg T, Steffens B, Steffen-Heins A, Sauter M, de Vries M, Schuurink RC, Bazin J, Bailey-Serres J, Voesenek LACJ, Sasidharan R** (2018) A stress recovery signaling network for enhanced flooding tolerance in *Arabidopsis thaliana*. *Proceedings of the National Academy of Sciences of the United States of America* 115: E6085-E6094
- Zhu J, Brown KM, Lynch JP** (2010) Root cortical aerenchyma improves the drought tolerance of maize (*Zea mays* L.). *Plant, Cell and Environment* 33: 740-749



## Appendices



**Figure A1 Alignment of sequences amplified by qRT-PCR from *Medicago sativa* with those of their counterparts in *Medicago truncatula*.**

M. tr in the upper panel for each gene stands for *M. truncatula* nucleotide sequence while lower panel labeled with M. st corresponds to *M. sativa* nucleotide sequence followed by gene name: *DIHYDROFLAVONOL 4-REDUCTASE (DFR)*, *MYB112*, *PHOTOSYSTEM I p700 CHLOROPHYLL A APOPROTEIN APS I (PSI)*, *PHOTOSYSTEM II Q(b) (PSII)*, *FLAVONOID GLUCOSYLTRANSFERASE2 (FGT2)*, *PHENYLALANINE AMMONI- LYASE (PAL)*, *DEHYDRATION RESPONSIVE RD-22-LIKE (DRR)*

GGATGGCTCGTTTAGCTATTTTCAGCAAGATCAAGGGTGAGGCTGTGATGTATATTGTAGATGGAAATATTTCA  
 ACGGAAATATGTACTGGCATCTTAATTAGTAATTGAGGCACATATGCACAGCTCAATTGTAACAAGGCAGTTAAA  
 AGCCATACCAACAATCAGGGGCAGACATAGACTCACCTCAAAGTTAGTAGGGCAAGAATTTCTGTGAATAATTA  
 AGTAATACCAATTGAGGTAGTAATAAAGACGTTACAAGAGATCGATCAAATGCTCTAACAGAATACCCGTACAAT  
 AGGGACTTAGGTTGAGCAGTGTTCGCTCTTTTTTGGAAGCAAGTCACAATTGCGTAGAAATTATATATAAAA  
 AAGATCTTTGATTGATACATGAATAAAAAATTTAGATAGATGCACAAATTGTACAAAACATTATTTGATATATGAAA  
 TAAGAGTAAAAATATAGACATATGTATAAATTAAAAAAAAAAAAACTCCGTATTAACATAAATAAGTTAAAGTATA  
 GACACGTGTTCTTAAGAATTAAAAAAAAAATCCATACCCCTTACTAATGTACAAGTAAAAATACAAACACGTGTAT  
 ATATTAAAAAAATTAGATTCATGTATTAATTATTAATATATGAGTAAAAATATAGTACATGTATAAACATAAAAAG  
 AATTTTGTGTTGATTAATATATGAGTTTTTTTTGTGGTGGCCGGGGTTTAAACCCAGACCTTGCATATTTTATGC  
 ATTGTCATACCATTTGAGCTAAGCTCCTGAGGACAAATTAATACTTGAGTAAACTATAAAGTAAACATTATAATA  
 AAAAATGTTTATAAAAAAAAAAACTTGGTTTGGCACTTGCCAATTCTCTCTTTGACAAAAAT

**Figure A2 Promoter sequence of the alfalfa *DIHYDROFLAVONOL-4-REDUCTASE* (*DFR*) gene with putative SBD binding elements.**

Nucleotides are highlighted with green, yellow and gray color represents putative SBD binding motifs with 'GTAC' core sequences, forward primer sequences used for ChIP-qPCR, and coding sequences of *DIHYDROFLAVONOL 4-REDUCTASE* (*DFR*) respectively.

CCCAGTTCGATGTAACCCACTCGTGCACCCAAGTATCTTCAGCATCTTTACTTTCACCAGCGTTTCTGGGTGAGC  
 AAAAAAGGGAAGGCAAAATGCCGCAAAAAGGGAATAAGGGGCGACACGGAAATGTTGAATACTCATACTCTCC  
 TTTTCAATATTATTGAAGCATTATCAGGGTTATTGTCTCATGAGCGGATACATATTTGAATGTATTAGAAAAAT  
 AAACAAATAGGGGTTCCGCGCACATTTCCCGAAAAGTGCCACCTGACGTCTAAGAAACCATTATTATCATGACAT  
 TAACCTATAAAAATAGGCGTATCACGAGGCCGCCCTGCAGCCGAATTATATTATTTTGCCAAATAATTTTAACA  
 AAAGCTCTGAAGTCTTCTTCATTTAAATTCTTAGATGATACTTCATCTGGAAAATTGTCCCAATTAGTAGCATCACGC  
 TGTGAGTAAGTCTAAACCATTTTTTATTGTTGTATTATCTCTAATCTTACTACTCGATGAGTTTTCGGTATTATCTC  
 TATTTTAACTTGGAGCAGGTTCCATTCATTGTTTTTTCATCATAGTGAATAAAATCAACTGCTTAACTTGTGC  
 CTGAACACCATATCCATCCGGCGTAATACGACTCACTATAGGGAGAGCGGCCGCCAGATCTTCCGGATGGCTCGA  
 GTTTTTCAAGATACTATAGGGCACGCGTGGTGCAGGCCCGGCTGGTTCATTTGGAGTAGTGTAGGAAACAC  
 CCAACACATTTTGAATACCATATAAAGAACCTGCCTCCAACCTCTTCAAAGGATTGCCATTAAGTTCCAACAAAGG  
 GTTCCGGAATTTGCGAGCCTTCGTCATCCAAGTTAATTGCTCTTGGATTGGAATTGATTGTCAATTTCTCCCTT  
 TTTGTCAAATTGATTTAAATTCAGATTGGTCTTAAATAACTGCCGACACCGAGAAAATCGCGTGTAGGAACAAC  
 GGACTAC

**Figure A3 Nucleotide sequence of the alfalfa *WD40-1* promoter region**

Nucleotides highlighted with gray color represent coding sequences of *WD40-1* in *M. sativa*.

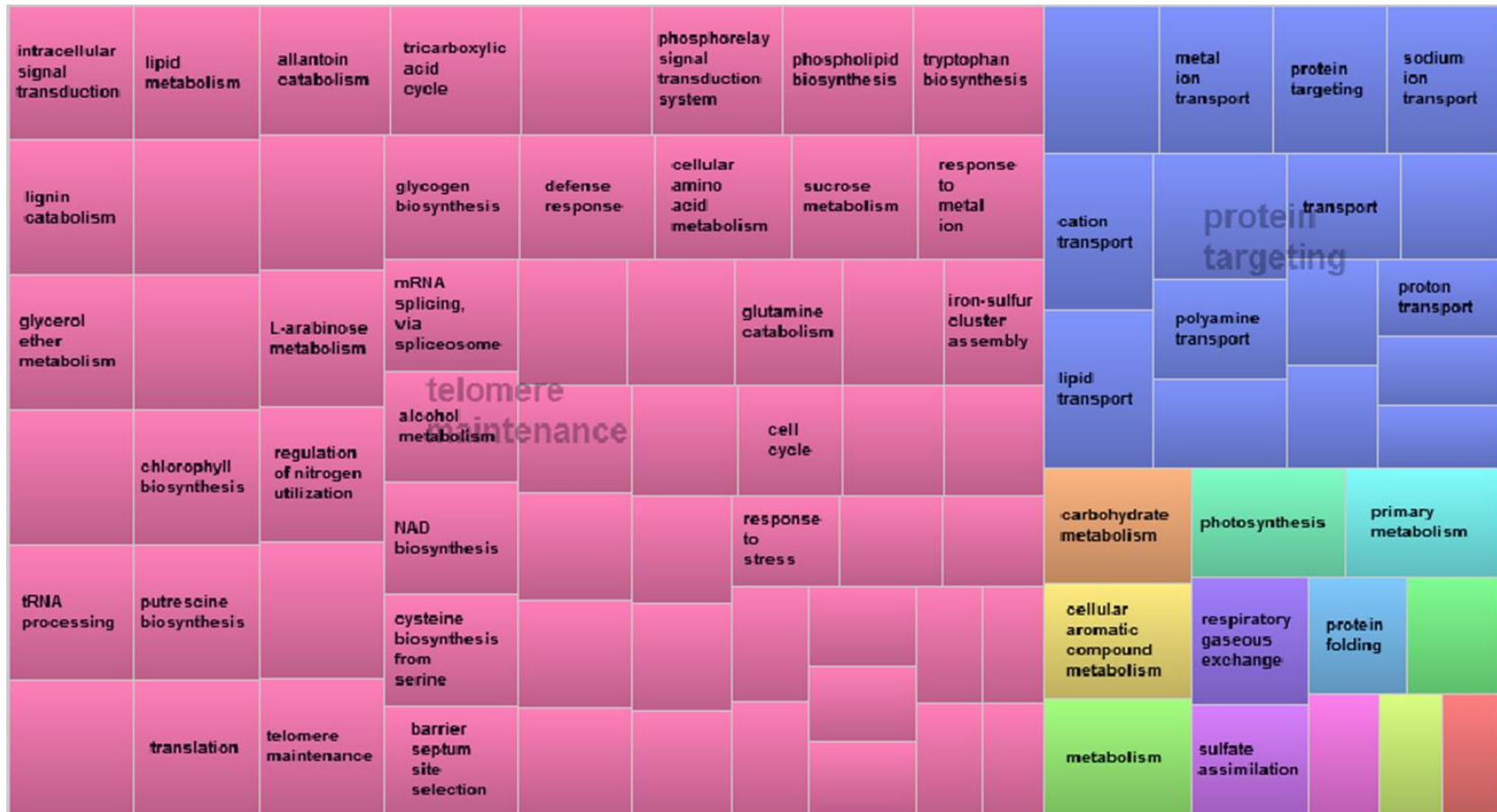
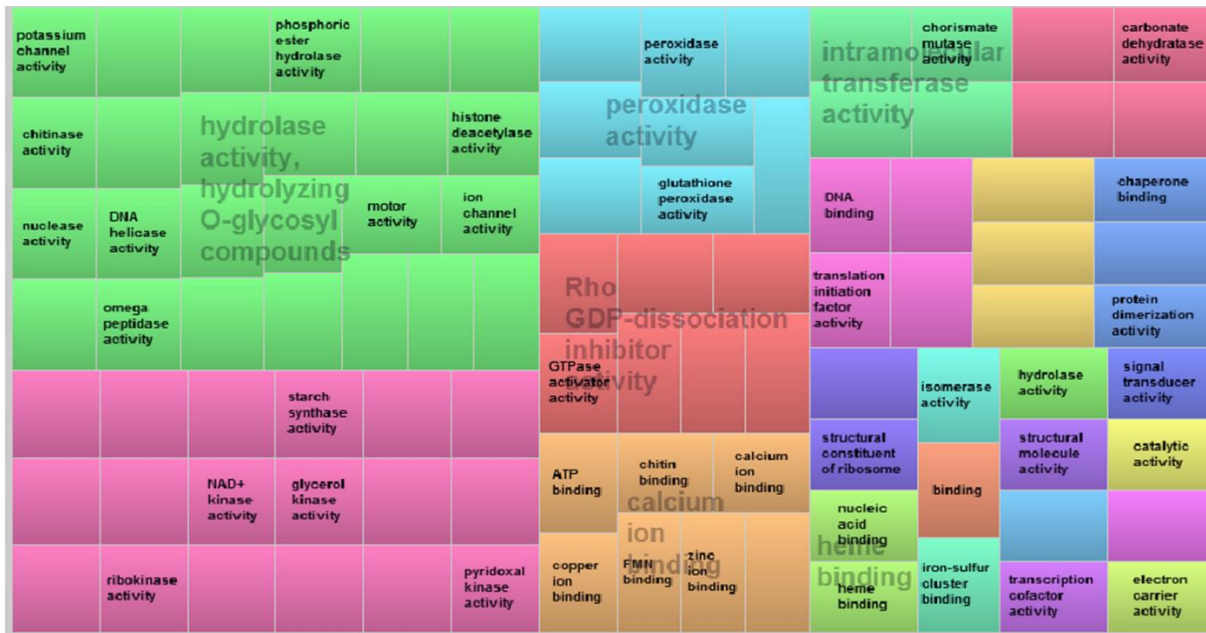


**Figure A4 Differentially affected biological processes tree map between *SPL13*RNAi and EV leaf tissues under drought stress**

Differentially expressed genes that have similar biological processes are represented with same colour, and placed in one box when they are from same pathway.



GO term clouds used for constructing tree maps



**Figure A5 Differentially affected molecular functions tree map and GO term clouds used for constructing tree maps between *SPL13RNAi* and EV leaf tissues under drought stress**

Differentially expressed genes that have similar molecular functions are represented with same colour, and placed in one box when they are from same pathway.

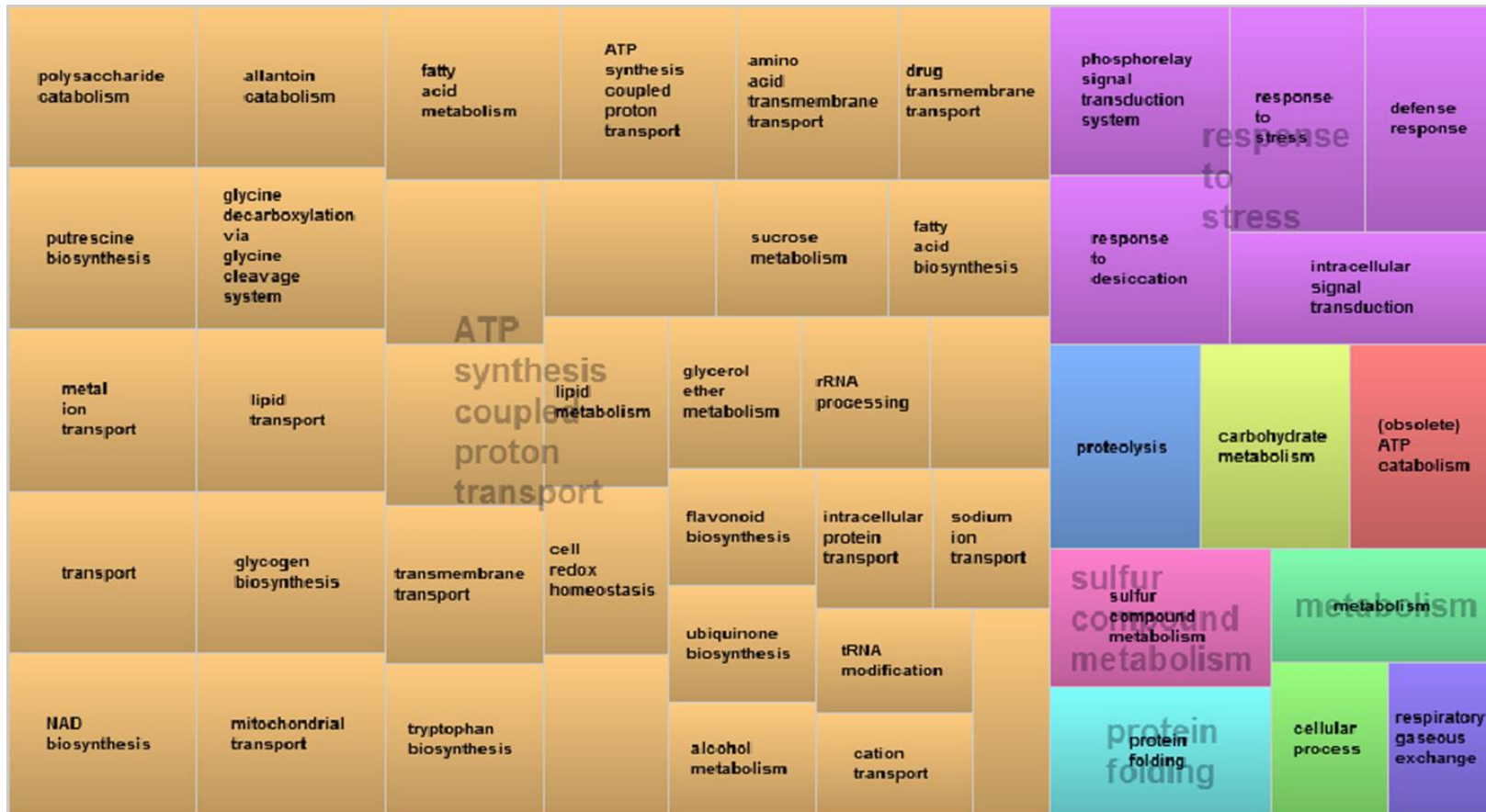


**Figure A6 Differentially affected biological processes tree map between *SPL13*RNAi and EV stem tissues under drought stress**  
Differentially expressed genes that have similar biological processes are represented with same colour, and placed in one box when they are from same pathway.

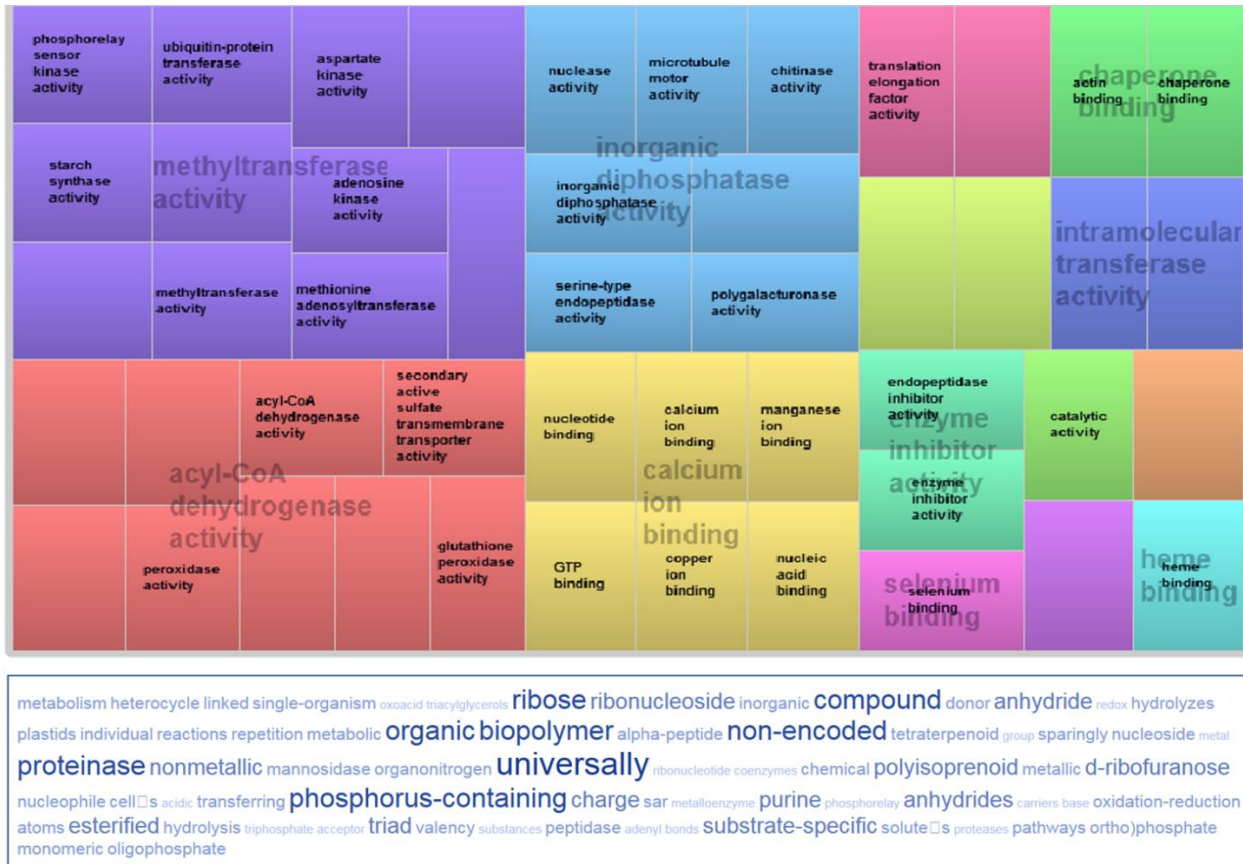


**Figure A7 Differentially affected molecular functions tree map and GO term clouds used for constructing tree maps between *SPL13RNAi* and EV stem tissues under drought stress**

Differentially expressed genes that have similar molecular functions are represented with same colour, and placed in one box when they are from same pathway.



**Figure A8 Differentially affected biological processes tree map between *SPL13*RNAi and EV root tissues under drought stress**

Differentially expressed genes that have similar biological processes are represented with same colour and placed in one box when they are from same pathway.





anabolic heterocycle systematic single-organism oxoacid tri-valent triacylglycerols subcellular gc-rich macromolecular pre-translation transform -cooh compound macroglobulin non-membrane-enclosed donor anhydride hydrolyzes hydrolyzed plastids ch-oh repetition organic biopolymer alpha-peptide definition non-encoded nucleoside-triphosphatase promotor proteinase c-n protamine organonitrogen phosphate-containing nh)-nh2 vacuoles universally coenzymes ch3(cnhx)cooh metallic d-ribofuranose nucleophile acidic transferring phosphorus-containing charge metalloenzyme f-c( phosphorelay anhydrides ntpase amino-acyl protoplast -s- two-component lesser hydrolysis acceptor triad interconnect 5-methyltetrahydropteroyltri-l-glutamate exopeptidase substrate-specific pyridine-containing -(1-4 ortho)phosphate phosphomonoester macromolecules monomeric oligophosphate

**Figure A9 Differentially affected molecular functions tree map and GO term clouds used for constructing tree maps between *SPL13RNAi* and EV root tissues under drought stress**

Differentially expressed genes that have similar molecular functions are represented with same colour and placed in one box when they are from same pathway.

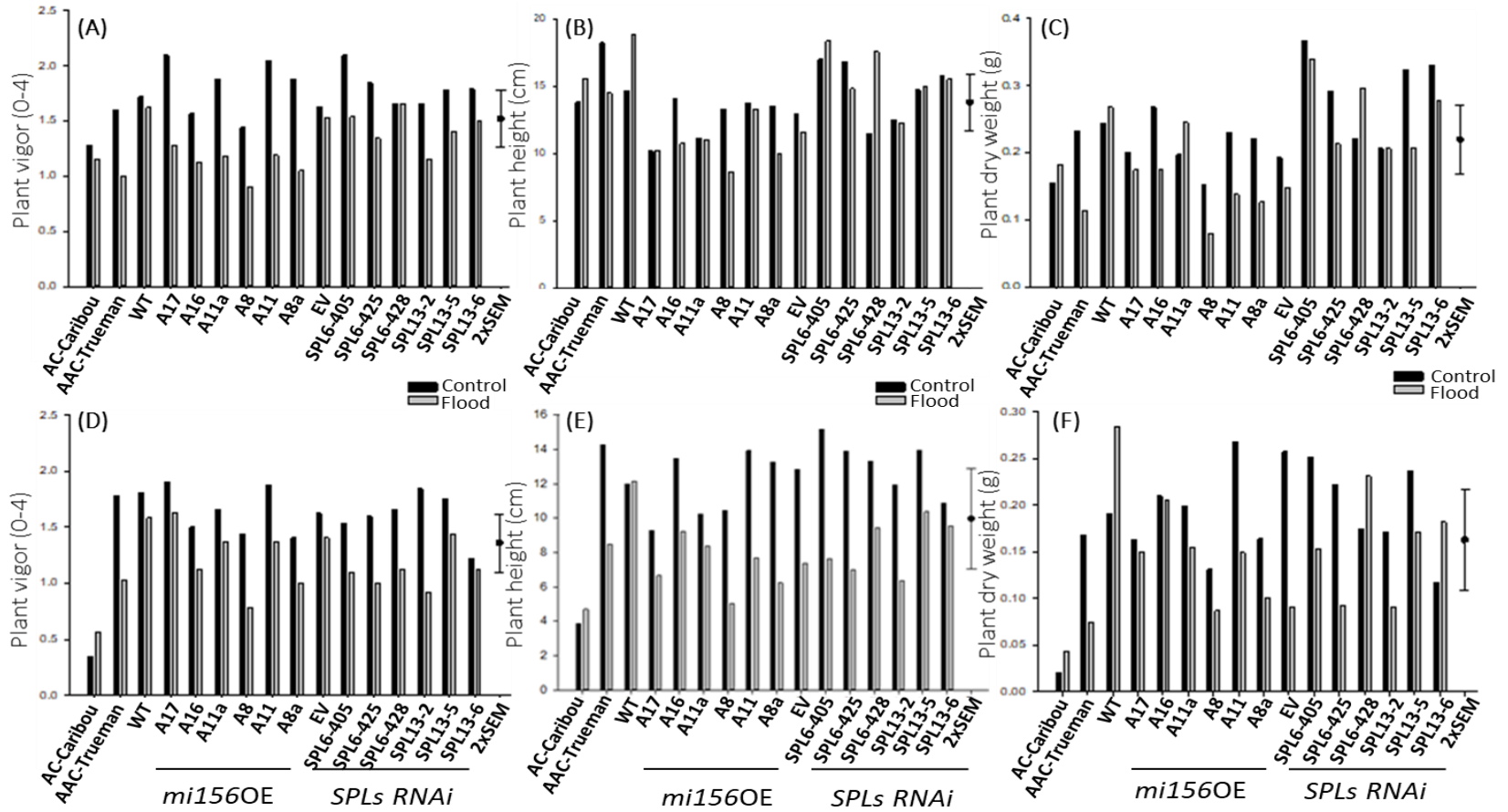


**Figure A10 Performance of different alfalfa genotypes with altered expression of SPLs (SPLRNAi) and miR156 overexpression in response to flooding stress.**

(A) Plant vigor at 6 week post flood, (B) Plant height at 6 week post flood, (C) Dry matter at 6 week post flood, (D) Plant vigor at 12 week post flood, (E) Plant height at 12 week post flood, and (F) Dry matter, 12 week post flood.

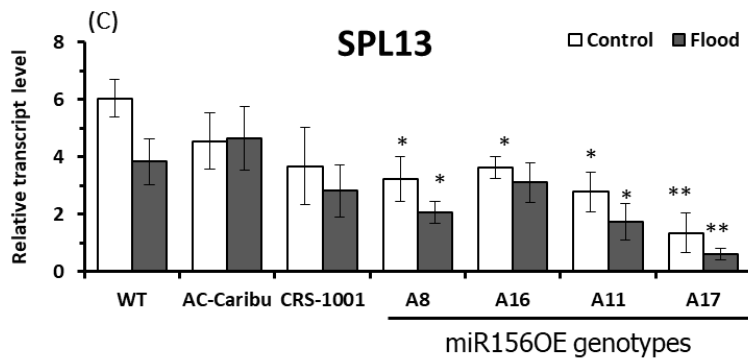
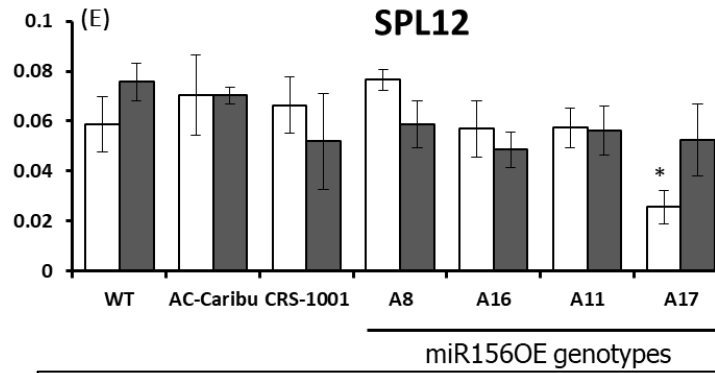
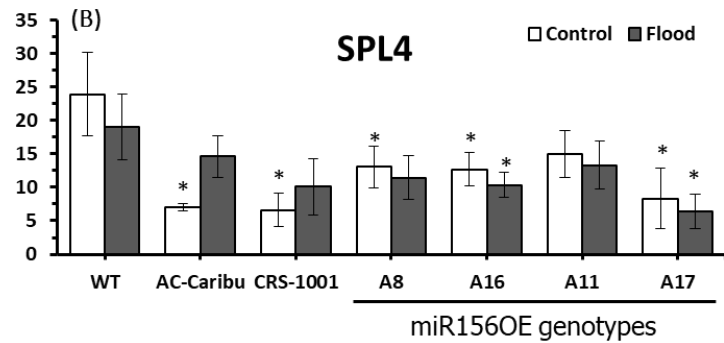
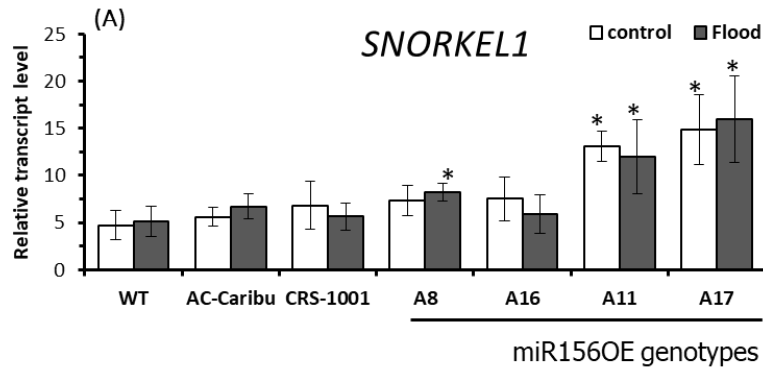


**Figure A11 Investigating the expression of flooding responsive genes, SPLs, and microRNA156 under flooding and well-drained control conditions.**

(A) Transcript analysis of *SNORKEL1*, (B) *SPL4*, (C) *SPL13*, (D) *miR156*, and (E) *SPL12* using qRT-PCR. Expression levels are pairwise compared to wild-type per treatment. n = 4 biological samples with three technical replicates

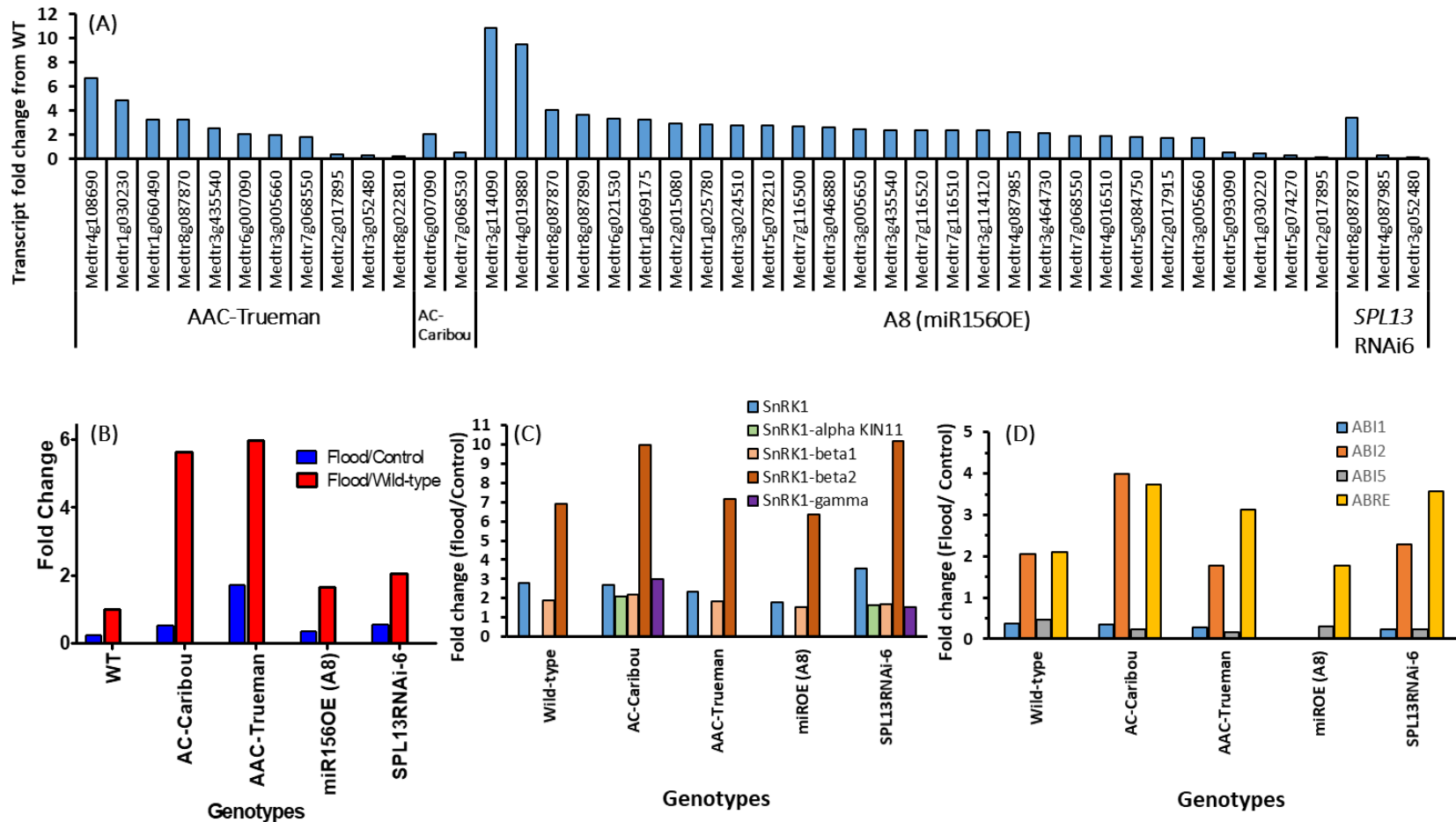


**Figure A12 Transcript levels of flooding-responsive differentially expressed genes under flooding.**

**(A)** Transcript levels of GDSL-like lipase/ acylhydrolase and Pmr5/Cas1p GDSL/SGNH-like acyl-esterase, fold change in **(B)** reticuline oxidase-like protein gene, **(C)** *SnRK1*, and **(D)** ABA insensitive, ABI and responsive elements, ABRE.

<b>MsSPL1</b> Predicted NLSs in query sequence MDADFEGKNQHLYEAVVPEMKGAVGRGSKDWDLNDWRWDGLFTAQQLNS 50 VPTDCRNRFLEIRENVVSNLISGEGSRELEKRRRFGGEGLEMND 100 FGSLNMLGGQVYPIMDGEEKSGKTKIAPVPTSNAVQCQVEDCRADLSN 150 AKDYHRRHKVCDVHSKASKALVGSVMQRFCCQCSRPHVLQ <b>EFDEGKRSCR</b> 200 <b>RRLAGHNKRKRKTH</b> PDTAVVNGGSPNEERGSSYLLMSLLRILSNMHSNGP 250 DHTRNLDGLSHLIGNLTSAGTFNGRNIAASLEGPQELVKAGTSGAAQNV 300	<b>MsSPL1a</b> Predicted NLSs in query sequence MEAFQLYGNGGGSSDL <b>RAMGKNSKEWDLNNKWD</b> SHLFIATSKLTPVPEH 50 RQFLPIPVGGGGGGGSSNSNSSSSCSEQLDLGICQVKEGERKRRVIVVED 100 ELGLGLNKEGGNLSLNLGGGVATWEGNNGKSRVAGGSSSRAPCQVEDC 150 RADLNNAKDYHRRHKVCEIHSKASKALVGNAMQRFCCQCSRPHLLQ <b>EFDE</b> 200 <b>GKRSCRRLRAGHNKRKRKT</b> NQDAVPNGSSPNDDQTSYLLISLLKILSNM 250 QPDRSNQTADQDLLTHLLRSLANQNGEQGRNLSNLLREPENLKEGSL 300	<b>MsSPL2a</b> Predicted NLSs in query sequence MDLNAISPSQWEWDHLPLDTKATENQKLQPPNWTMELDPEINFGLYDT 50 PVGSGSSGSDLIHGSAFNAPKFCVSGEPLLNPRLLKRMYPFEVCPESDS 100 KNLSFSRDLMSLLILEKKCKSNQNLQCPPHCQVEGCGLNLSAKDYHCK 150 RRVCESHAKSPMVVIDGLERRFCQCSRPHDLDFEFDG <b>KKSCRRLSNHN</b> 200 <b>ARRRKYHR</b> QAVQSSQSALSYSRSDGKQMSPTNSKTATNLAWQNMHNSK 250 LPQAKDFLLKPKDNIDTPSTVTMLSHDSNFHFTSKILATKSVNPGVEDF 300
<b>MsSPL7</b> Predicted NLSs in query sequence MESKSPILPMPDPEDLSSVWDLSYLLDFDDIPQLPPLPNPPTPEEN 50 ERIRKRDRLTCSNFLAGVPCACPELDALLEDN <b>GLPGKKRARTARLIFS</b> 100 ELKGYHRRHRVLCRANAATVLDGDKRYCQCGKGFHVLSDFDEGKRSC 150 RRKLERHNRRRRKAVD SAVGVNEVQTVTQNDSDNCDELIDYNSLSR 200 ENIEKRALQDHEEPPVNGSSTPETQNINGDSSVSVFVASAETQANIGKV 250 SDPSKSPSYCDNKSDYSSMCQTGRVSFKLYDWNPAEFPRRLRLQIFQWLA 300	<b>MsSPL7a</b> Predicted NLSs in query sequence MDFGGNMFCLNDRDQSNNTNNGNSNGFTWCSSGTTTGTAWNMNTPFNVE 50 VNSVSAANRTEAGLANALMYPQNEGGGRQYQAYGGVSRGHMPPDPH 100 LTCL <b>KLGKRHYFEDVSGGGVMGEKKGKGGY</b> CGGGKTAAVGGYTAVTRCQ 150 VDGCNVALMNAKEYHRRHKVCEMHSKAPKVVVLGLEQRFCQCSRPHVVS 200 EFDDSKRSCRRLAGHN <b>ERRRKS</b> SHD <b>SVGRNSSQGGCALSLSSRTD</b> SWL 250 SPADLSVRCSAALSELIAENRASIMARQYVSDRDWHLQHHAVEDYKEIQS 300	<b>MsSPL8</b> Predicted NLSs in query sequence MLDYEWGNPNSIMLTGMEDNSGAAATDQHRQIFDHYASQAMLSDNLYNG 50 PGGGPTIDINSGDPTHHHNQFSPHNQHHNHQSFDPRAFHHGSSSTASS 100 YPPQPQPPSMLSLDPLPGHGHSPGFLLPKSEVNRPIDFVGSRLGLN 150 LGGRTYFSEDDFVTRLRYRRSRPEPGSTGSNSPRCQAEGCNADLSQAK 200 HYHRRHKVCEPHSKAATVVAAGLTQRFCQCSRPHLLSEFDNG <b>RSCRKR</b> 250 <b>LADHNRKRKTHPNTQDIHKS</b> HNTLDSSATRSPPESGTQSTSSVTVAVS 300
<b>MsSPL13a</b> Predicted NLSs in query sequence MEWSNLKAPSWDLTEMDQCTLNNIETMDGSIIRRFQDYRTKGFSDVLDKLG 50 HVGNSSTESGLTKSKDVGFTKMTSSSSSTSGSSKRARAINNGTQIVSCL 100 VDGCQADLSNCRDYHRRHKVCELSHKAQVT <b>IGHHKQRFCCQCSRPHALE</b> 150 <b>EFDEGKRSCRRLDGHNRKRKQPEPI</b> TRSSSFLSNYQQTQLLPPSSH 200 VYPSTAMNPTWVGDDVRLHSHNHQMHHLVDKQDLFLGTSSSTSYKE 250 GKQVSPIQNNQPTAAATMNNQLPASSMSRTFSRTNPFSEYKMFCDNNT 300	<b>MsSPL14</b> Predicted NLSs in query sequence MEKVAPLLPLHPPMLSSHQFYDSSNTKRDLLSSYDVVHI PNDWNPK 50 WNWDSIRFMTAKSTTVEPQQVEESLNLNLGSGT <b>LVRPNKRI</b> RSQSPTSAS 100 YPMCQVDNCKEDLSKADYHRRHKVCEAHSKASKALLGNQMRFCQCSR 150 FHPLVEFDEGKRSCRRLRAGHNRRRKRKTQPEVAVGGSPPLNQAANLEI 200 FNLLTAIADGSGKFEERRSQVPDKEQLVQILNRIPLPADLTAKLLDVG 250 NLNAKNDNVQMETSPSYHHRDQDLNAPPAPLTKDFLAVLSTPSTPARN 300	<b>MsSPL16</b> Predicted NLSs in query sequence MDWDWKEFAWDPSGFDEELKNEGDSMDLRLGDQASDSLEKSVHDSGKEDS 50 KAVSSLSPSGSLKRSRLQNGSQSMICSVDCNSDLSDCREYHKRHRVCE 100 KHSKTPVVLVGGKQRFCCQCSRPHSLA <b>FDDVKRSCRRLDGHNRKRK</b> 150 <b>PQPPSLFMAAEKFMNYKGRILHFGSPQTYVNP</b> IMRNIPWATSITEAES 200 GYDHQRLLYRIDKHKQDKGHPHWQELPKSGDVNKAAPGTPISHPIRGAV 250 GSSAGEKGRKLSDDGKPGSFDSCGALYLLSTLQTSSELSLMQSSINSP 300

**Figure A13 Newly found MsSPLs and their nuclear localization signals.**

Amino acid sequence and predicted nuclear localization sequence, NLS of the newly found MsSPLs. Amino acid sequences in red font are predicted NLS using [http://nls-mapper.iab.keio.ac.jp/cgi-bin/NLS\\_Mapper\\_form.cgi](http://nls-mapper.iab.keio.ac.jp/cgi-bin/NLS_Mapper_form.cgi) online tool.

**Table A1 List of primers used and their nucleotide sequences**

No.	Primer	Name of the gene	Forward primer/ Reverse primer	Origin	Use
1	<i>DFR</i>	Dihydroflavonol 4-reductase	GTTTGTGTCACAGGGGCTTC TTCAAGTTTTCTGGGTCGCG	MT	qRT-PCR
2	<i>proDFR-1</i>	Dihydroflavonol 4-reductase promoter region I	CAAGGGTGAGGCTGTGATGT CTGCCCCCTGATTGTTGGTAT	MS	ChIP-qPCR
3	<i>proDFR-2</i>	Dihydroflavonol 4-reductase promoter region II	GGCAGACATAGACTCACC GCAATTGTGACTTGCTTC	MS	ChIP-qPCR
4	<i>proDFR-3</i>	Dihydroflavonol 4-reductase promoter region III	CCATACCCCTTACTAATGTAC CAAATGGTATGGACAATGC	MS	ChIP-qPCR
5	<i>proDFR1-MTR</i>	Dihydroflavonol 4-reductase promoter 1	TTAGGGTGAGGCTGTGATGT TCCATCACCACACTCTCTTG	MT	DFR promoter
6	<i>proDFR2-MTR</i>	Dihydroflavonol 4-reductase promoter 2	TGCATCTAACAGTCCCTTGC TCCATCACCACACTCTCTTG	MT	DFR promoter
7	<i>proDFR3-MTR</i>	Dihydroflavonol 4-reductase promoter 3	AGGGTGAGGCTGTGATGTAT ACCCAGTACCTCCAGTTA	MT	DFR promoter
8	<i>LOB1</i>	Lateral organ boundaries-Like 1	AAGTGTGGGGGAAGTAGTGGAG GCGAAACGCAATGATGAATGTA	MS	ChIP-qPCR
9	<i>MYB112</i>	myb transcription factor 112	TGGGTGATGGAGGTGAAGAA CACCGTTGTTGAGGTTTGG	MT	qRT-PCR
10	<i>WD40-1</i>	WD40-1 transcription factor	GGATGAATCTGTGAACGCCG CTTTGTCCACGGCTCAAACA	MT	qRT-PCR
11	<i>PSI</i>	Photosystem I P700 chlorophyll A	GCTACTAGGACTTGGGTCTCTTTC AGGAAGTGGGATCTCTTTGG	MT	qRT-PCR
12	<i>PSII</i>	Photosystem II Q(B)	CGCAGCTCCTCCAGTAGATATT CCGCCGAAGTAGGAATAATG	MT	qRT-PCR

No.	Primer	Name of the gene	Forward primer/ Reverse primer	Origin	Use
13	<i>FGT2</i>	Flavonoid glucosyltransferase-2	ATAAGAGGTTGGGCACCACA CATTGGTAACCCTGCACTCA	MT	qRT-PCR
14	<i>DRR</i>	Dehydration-responsive RD22-like protein	GGTTGGTGATGTGAATGGAG CTTCCCTGGCTTGATCCTTA	MT	qRT-PCR
15	<i>PAL</i>	Phenylalanine ammonia-lyase	CGTTGGTTAAAATCGGCGGT CTCCGAAAGCTCCACCCTAA	MT	qRT-PCR
16	WD40-SP1	WD40-1 specific primer 1 with AP1	GTAATACGACTCACTATAGGGC CAGTTGCACACTTGTATGTCCCAACTC	MS	Genome walking
17	WD40-SP2	WD40-1 specific primer 2 with AP2	ACTATAGGGCACGCGTGGT GTAGTCCGTTGTTCTACACGCGATTT	MS	Genome walking
18	B1/2- WD40-1	WD40-1 transcription factor	GGGGACAAGTTTGTACAAAAAAGCAG GCTTCTTTCACAACACACTCCTTCA GTAGTCCGTTGTTCTACACGCGATTT	MT	WD40-1OE construction
19	B1/2- WD40-1	WD40-1 transcription factor	GGGGACCACTTTGTACAAGAAAGCTG GGTCTTGCTATTTGCAGCACCAAG	MT	WD40-1OE construction
	B1/2- WD40-1- RNAi	WD40-1 transcription factor	GGGGACAAGTTTGTACAAAAAAGCAG GCTTCGGCTACTGGGAATCAGGACA	MT	WD40-1RNAi construction
	B1/2- WD40-1- RNAi	WD40-1 transcription factor	GGGGACCACTTTGTACAAGAAAGCTG GGTCAGCCTCTGTGTCAGGGCTAA	MT	WD40-1RNAi construction
20	WD1- qPCR-F/R		AGCCAGCAGACTTTGTCCAT AGCCTCTGTGTCAGGGCTAA	MT	qRT-PCR
21	miR156	MicroRNA156	CCTATCTCTGCCTGCTTGACCT AGCACCCTTCCACATAACATA	AT	qRT-PCR
22	KIN10	KIN10 (At3g01090)	AGAATGATGGCACTGTGACG	AT	qRT-PCR

No.	Primer	Name of the gene	Forward primer/ Reverse primer	Origin	Use
21	KIN11	KIN11(At3g29160)	ACAGGTGAAGCAACGCTT CCGTGTTCCAAGTGGCTATC ACATGTGCAGGAATCCAGTG	AT	qRT-PCR
22	DIN1	Senescence-associated protein 1, DIN1 (At4g35770)	CAGAGTCGGATCAGGAATGG ATTTGACCGCTCTCACAAACC	AT	qRT-PCR
23	DIN3	DIN3 (At3g06850)	TCAGCTCGTCATCTGTTTGC ATCAAAGTGGGAGGGTGAAC	AT	qRT-PCR
24	DIN6	Glutamine-dependent asparagine synthetase dark inducible 6 (At3g47340)	AACTTGTCGCCAGATCAAGG GGAACACGTGCCTCTAGTCC	AT	qRT-PCR
25	DIN10	Raffinose synthase family dark inducible 10 (At5g20250)	GATTCCTCGTGCTCGACTCC TTAGCAAGCTGACACCATCAC	AT	qRT-PCR
26	SnRK1	SNF1-related kinase (Medtr1g034030)	GGAGACCCTGCACAGAGAAT CTGAAACTGCTCGCTTGTTG	MT	qRT-PCR
27	SnRK1-KIN11	SNF1 $\alpha$ KIN11 (Medtr6g048250)	TTCTGGTTTGAGCCGTATCC GTTGCCTCATTCCTACTCCTTG	MT	qRT-PCR
28	SnRK1-b1	SNF1-related kinase $\beta$ (Medtr5g098510)	GGCCTTGCTAAGAGTAGGTCAA ACTCAGGAGCATGTGTCCATT	MT	qRT-PCR
29	SnRK1-b2	SNF1-related kinase $\beta$ 2 (Medtr2g095290)	TCGGCTATCCTGCTAATGTC GCGATGAGTGTATCCCAAAG	MT	qRT-PCR
30	SnRK1-g	SNF1 $\gamma$ subunit (Medtr4g103550)	TTTCGATGGGCTCCGTTT AACCCAAGTCTACCACAGGAAC	MT	qRT-PCR
31	SnRK2	SNF2, helicase and zinc finger protein (Medtr2g012830)	AAGACCAAAGGCACACGA AAAGAGGAACAGCCAGCA	MT	qRT-PCR
32	Snorkel	SnorkelERF	TTCCAGAGGAGGGTAGTTAAGA TGGTGCACAGAGTGATTCC	MS	qRT-PCR



No.	Primer	Name of the gene	Forward primer/ Reverse primer	Origin	Use
33	MsSPL1	MsSPL1 (Medtr2g046550)	AGGGTTGGAGATGAACGATG	MT	qRT-PCR
34	MsSPL1a	MsSPL1a (Medtr7g110320)	CACAGGCGCAATCTTTGTCT GTGAGGAGAAATAGCAGGCAGT	MT	qRT-PCR
35	MsSPL2	MsSPL2	CCCACAGCATCAGGTCTAAA GTAGAAGAGGAGGAGGGTGATG	MS	qRT-PCR
36	MsSPL2a	MsSPL2a (Medtr8g080680)	GCAACAGGGTGGAGAAACAC GCTGCAGACGACAACCTTCA	MT	qRT-PCR
37	MsSPL4	MsSPL4	CATCTGTTGCTTCCCATCAC ATGCCAAAGCACCTACCGT	MS	qRT-PCR
38	MsSPL7	MsSPL7 (Medtr2g020620)	CCTCTCATTATGCCAGCCA CCCTGAACTCGATGCTTTGT	MT	qRT-PCR
39	MsSPL7a	MsSPL7a (Medtr7g444860)	GCCGTCGATGATAGCCTTTA CAGGGCACAATGAGAGAAGA	MT	qRT-PCR
40	MsSPL8	MsSPL8 (Medtr8g005960)	GCCATGAATCAGTCCGAGAT TGGCCGCACTTACTTCTCTT	MT	qRT-PCR
41	MsSPL9	MsSPL9	AACCTTCGGCTTGACACCTA GGAAGAGGTGGGTCAGTTCA	MS	qRT-PCR
42	MsSPL13	MsSPL13	ACAGTAACAGTTGGGCACTTAG CACCATGGAGTGGAATTTGAAAGC	MS	qRT-PCR
43	MsSPL13a	MsSPL13a (Medtr8g096780)	CTATCCCATTGATAGGGAAATAGT CTTGGGTTGGAGGAGATGTT	MT	qRT-PCR
44	MsSPL14	MsSPL14 (Medtr1g035010)	GCTGCTGGTTGAAGATGTTG GATCTCCAACATCGGCTTCA	MT	qRT-PCR
45	MsSPL16	MsSPL16 (Medtr7g028740)	GAGCTTCGCACACCTTATGA TTTGACTIONGGTTGTGCTCT	MT	qRT-PCR
			CGTTCCAGACGAAGATTGTG		

No.	Primer	Name of the gene	Forward primer/ Reverse primer	Origin	Use
46	MsSPL7a	MsSPL7aGSP MsSPL7aGIP MsSPL7aGOP	GAGCTCCCATGATTCTGTIG CCTAGCCATTATCGATGCTC CTGCAAATGCCAGTCTCTGTCT	MT	5' RLM-RACE
47	MsSPL8	MsSPL8GSP (Medtr8g005960) MsSPL8GIP MsSPL8GOP	ATGGAGGGTCATCAACTGCT CACGAAGTCAATGGGTCTGT TTCGAAGAACCTGTGGAACC	MT	5' RLM-RACE
48	MsSPL13a	MsSPL13aGSP(Medtr8g096780) MsSPL13aGIP MsSPL13aGOP	TCCATGAGTCGCACGTTTAG CAGGATGATCATGTGTTTGTG CCACTCTGATCATTTGAACCCA	MT	5' RLM-RACE
49	SE	Zinc finger protein SERRATE (SE) (Medtr8g043980)	CACCATGGCAGAAGTTCTCACCCC TATCACGGTGACCTCTTCGTCT	MT	Yeast-two- hybrid
50	DCL1	DCL protein (Medtr3g102270.2)	CACCATGGCCGCACCACTTCTTCT CCAAACAGGGCCTTAGTATCTG	MT	Yeast-two- hybrid
51	SnRK1	SNF1-related kinase (Medtr1g034030.1)	CACCATGGATCCTACTATGAACCA CTCGTCCATTTTCGTCATCGA	MT	Yeast-two- hybrid
52	UBQ10	UBQ10(At4g05320)	GCTCCGACACCATCGACAACG CTGAGGACCAAGTGGAGGGTGGA	AT	qRT-PCR
53	Tubulin	Tubulin	ATCCGTGAAGAGTACCCAGAT AAGAACCATGCACTCATCAGC	AT	qRT-PCR
54	EF1 $\alpha$	Elongation factor alpha	TGCCAGTTGGACGTGTTGAG TCACAACCATAACGGGCTTC	AT	qRT-PCR
55	<i>Acc1</i>	Acetyl CoA Carboxylase1	GATCAGTGAACCTTCGCAAAGTAC CAACGACGTGAACACTACAAC	MS	qRT-PCR
56	<i>Acc2</i>	Acetyl CoA Carboxylase2	GATCAGTGAACCTTCGCAAAGTAC GAGGGATGCTGCTACTTTGATG	MS	qRT-PCR

AT, *Arabidopsis thaliana*; MS, *M. sativa*; MT: *M. truncatula*

**Table A2 Buffers used in ChIP assay and their components**

<b>Buffers</b>	<b>Chemicals</b>	<b>Concentration</b>	<b>Buffers</b>	<b>Chemicals</b>	<b>Concentration</b>	
Extraction buffer 1	Sucrose	0.4 M	Extraction buffer 2	Sucrose	0.25 M	
	Tris-HCl (pH=8)	10 mM		Tris-HCl (pH=8)	10 mM	
	MgCl <sub>2</sub>	10 mM		MgCl <sub>2</sub>	10 mM	
	β-ME	5 mM		Triton X-100	1%	
	PMSF	0.1 mM		β-ME	5 mM	
	Protease inhibitor <sup>1</sup>	2 tablets/ 100 mL		PMSF	0.1 mM	
				Protease inhibitor <sup>1</sup>	1 tablet/10 mL	
Extraction buffer 3	Sucrose	1.7 M	Nuclei lysis buffer	Tris-HCl (pH=8)	50 mM	
	Tris-HCl (pH=8)	10 mM		EDTA	10 mM	
	MgCl <sub>2</sub>	2 mM		SDS	1%	
	Triton X-100	0.15%		Protease inhibitor <sup>1</sup>	1 tablet/10 mL	
	β-ME	5 mM	ChIP dilution buffer	Triton X-100	1.10%	
	PMSF	0.1 mM		EDTA	1.2 mM	
	Protease inhibitor <sup>1</sup>	1 tablet/10 mL		Tris-HCl (pH=8)	16.7 mM	
	Sucrose	1.7 M	NaCl	167 mM		
	Elution buffer	SDS	1%	High salt wash buffer	SDS	0.10%
		NaHCO <sub>3</sub>	0.1M		Triton X-100	1%
Low salt wash buffer	SDS	0.10%	EDTA		2 mM	
	Triton X-100	1%	Tris-HCl pH=8)		20 mM	
	EDTA	2 mM	NaCl	500 mM		
	Tris-HCl (pH=8)	20 mM	LiCl wash buffer	LiCl	0.25 M	
	NaCl	150 mM		IGEPAL-CA630	1%	
		Deoxycholic acid		1%		
TE buffer	EDTA	1 mM	EDTA	1 mM		
	Tris-HCl (pH=8)	10 mM	Tris-HCl (pH=8)	10 mM		

<sup>1</sup> Obtained from Sigma-Aldrich, Canada

**Table A3 Increased differentially expressed genes and their functions common in all tissues of *SPL13RNAi* plants**

<b>No.</b>	<b>Gene</b>	<b>Function</b>	<b>No.</b>	<b>Gene</b>	<b>Function</b>
1	Medtr2g008110	Vacuolar iron transporter-like protein	18	Medtr2g072940	PPR containing protein, putative
2	Medtr6g007897	Gibberellin-regulated family protein	19	Medtr5g095960	Nicotinamide mononucleotide adenylyltransferase, putative
3	Medtr5g098420	Fasciclin-like arabinogalactan protein	20	Medtr5g097480	GRAS family transcription factor
4	Medtr7g020820	Proline dehydrogenase	21	Medtr5g088990	Plastocyanin-like domain protein
5	Medtr4g079700	Pmr5/Cas1p GDSL/SGNH-like acyl-esterase family protein	22	Medtr2g079120	VQ motif protein
6	Medtr5g090100	LRR receptor-like kinase	23	Medtr2g022610	Hypothetical protein
7	Medtr7g070050	Abscisic acid receptor	24	Medtr5g017650	Plant cadmium resistance protein
8	Medtr8g064180	Xyloglucan endotransglucosylase/hydrolase family protein	25	Medtr5g074400	WRKY transcription factor
9	Medtr5g081860	MYB transcription factor MYB51	26	Medtr5g089370	Synaptobrevin-like protein
10	Medtr5g089110	F-box plant-like protein	27	Medtr5g075710	RNA-binding KH domain protein
11	Medtr5g077430	LRR receptor-like kinase	28	Medtr5g077280	Transmembrane protein, putative
12	Medtr5g088550	Hypothetical protein	29	Medtr5g076250	Lecithin retinol acyltransferase
13	Medtr5g073180	Hypothetical protein	30	Medtr5g082620	Phosphatidylinositol-specific phospholipase C
14	Medtr3g071740	Polyketide cyclase/dehydrase and lipid transporter	31	Medtr5g089190	Las1 family protein, putative
15	Medtr5g081850	Fcf2 pre-rRNA processing protein	32	Medtr2g075410	Brassinazole-resistant 1 protein
16	Medtr5g092560	DEAD-box ATP-dependent RNA helicase-like protein	33	Medtr5g093580	Co-factor for nitrate reductase and xanthine dehydrogenase
17	Medtr7g106450	CCAAT-binding transcription factor	34	Medtr5g071070	ARM repeat CCCH-type zinc finger protein

No.	Gene	Function	No.	Gene	Function
35	Medtr5g072930	Cytochrome P450 family 71 protein	53	Medtr2g078760	Protein phosphatase 2C-like protein
36	Medtr5g079610	Plastid movement impaired protein	54	Medtr5g093880	Hydroxyproline-rich glycoprotein family protein
37	Medtr5g096700	BTB/POZ domain plant protein	55	Medtr1g109660	Fiber protein Fb34
38	Medtr1g090290	Ethylene response factor	56	Medtr1g052470	Transcription factor bHLH122-like protein
39	Medtr5g083910	LRR receptor-like kinase	57	Medtr5g082660	NLI interacting factor-like phosphatase
40	Medtr1g013130	Zinc finger-like protein	58	Medtr8g107000	MAP kinase kinase kinase-like protein
41	Medtr5g030500	Abscisic acid receptor PYR1-like protein	59	Medtr5g090130	N-acetyl-D-glucosamine kinase-like protein
42	Medtr1g040430	Ethylene response factor	60	Medtr5g075580	Ubiquitin-conjugating enzyme E2
43	Medtr1g111550	MFS transporter	61	Medtr2g437530	DREPP plasma membrane protein
44	Medtr2g035405	Allantoate amidohydrolase	62	Medtr5g020570	Ubiquitin-protein ligase
45	Medtr5g098510	SNF1-related kinase regulatory subunit beta-2	63	Medtr5g081880	Hypothetical protein
46	Medtr2g023070	Senescence regulator	64	Medtr5g018050	Sucrose nonfermenting 1(SNF1)-related kinase
47	Medtr5g089750	Lateral root primordium (LRP)-like protein	65	Medtr5g083740	PLAC8 family protein
48	Medtr2g038200	Heat shock-like protein, putative	66	Medtr3g083370	1-Aminocyclopropane-1-carboxylate oxidase
49	Medtr1g105495	Xyloglucan endotransglucosylase/hydrolase family protein	67	Medtr5g093560	SWAP (suppressor-of-white-APricot)/surp domain protein, putative
50	Medtr5g087790	Ethylene insensitive transcription factor	68	Medtr2g105010	CBL-interacting kinase
51	Medtr4g073690	Nodulin-like/MFS transporter	69	Medtr3g073960	DUF581 family protein
52	Medtr5g087410	Indole-3-acetaldehyde oxidase			

---

<b>No.</b>	<b>Gene</b>	<b>Function</b>
70	Medtr5g087360	LRR receptor-like kinase
71	Medtr1g084990	Hypothetical protein
72	Medtr7g090470	Triacylglycerol lipase SDP1
73	Medtr5g075640	Root phototropism-like protein
74	Medtr1g098310	DUF3511 domain protein

---

**Table A4 Top 50 out of 154 decreased differentially expressed genes and their functions common to all *SPL13*RNAi tissues**

<b>No.</b>	<b>Gene</b>	<b>Function</b>	<b>No.</b>	<b>Gene</b>	<b>Function</b>
1	Medtr2g095440	ABC transporter family protein	17	Medtr3g464580	Asparagine synthetase [glutamine-hydrolyzing] protein
2	Medtr3g108800	Plasma membrane H <sup>+</sup> -ATPase	18	Medtr2g013060	Allantoinase
3	Medtr3g087490	PLAT-plant-stress protein	19	Medtr8g088110	Cold acclimation protein WCOR413
4	Medtr4g120130	Glyoxysomal fatty acid beta-oxidation MFP-A protein	20	Medtr8g107370	Phosphoethanolamine N-methyltransferase
5	Medtr6g007170	D-glycerate dehydrogenase/hydroxypyruvate reductase	21	Medtr2g042330	NAD-dependent aldehyde dehydrogenase family protein
6	Medtr3g064140	Class I glutamine amidotransferase superfamily pr.	22	Medtr4g037690	Transmembrane amino acid transporter family protein
7	Medtr4g009960	Eukaryotic translation initiation factor 3 subunit	23	Medtr1g092860	RNA-binding (RRM/RBD/RNP motif) family protein, putative
8	Medtr4g134290	6-Phosphofructokinase	24	Medtr2g018780	Early-responsive to dehydration stress protein (ERD4)
9	Medtr3g087950	Gamma-glutamyltranspeptidase	25	Medtr4g011620	Drug resistance transporter-like ABC domain protein
10	Medtr8g070540	CTP synthase-like protein	26	Medtr3g101780	ABA response element-binding factor
11	Medtr1g115500	Glutathione S-transferase	27	Medtr4g006320	Translation initiation factor IF-2
12	Medtr8g463180	Plastocyanin-like domain protein	28	Medtr5g038380	Peptide/nitrate transporter plant
13	Medtr8g089180	UDP-D-glucose/UDP-D-galactose 4-epimerase	29	Medtr5g035090	Pmr5/Cas1p GDSL/SGNH-like acyl-esterase family protein
14	Medtr0110s0020	Glycoside hydrolase family 1 protein	30	Medtr7g091880	Galactinol-raffinose galactosyltransferase
15	Medtr3g082150	Glucose-1-phosphate adenylyltransferase family protein	31	Medtr7g027175	Omega-hydroxypalmitate O-feruloyl transferase
16	Medtr2g046150	DUF538 family protein	32	Medtr5g025750	Transmembrane protein, putative

<b>No.</b>	<b>Gene</b>	<b>Function</b>	<b>No.</b>	<b>Gene</b>	<b>Function</b>
33	Medtr7g105070	Desacetoxyvindoline 4-hydroxylase, putative	49	Medtr1g083950	Universal stress family protein
34	Medtr7g104080	Starch branching enzyme I	50	Medtr6g011530	2-Aminoethanethiol dioxygenase-like protein
35	Medtr4g415290	Glycerol-3-phosphate acyltransferase			
36	Medtr7g108930	Sucrose synthase			
37	Medtr3g068125	Transferring glycosyl group transferase			
38	Medtr4g104680	Quinolate synthetase A protein			
39	Medtr4g134090	Peroxisomal acetoacetyl-coenzyme A thiolase			
40	Medtr3g010190	Sec14p-like phosphatidylinositol transfer family protein			
41	Medtr4g007030	Vacuolar ATP synthase subunit D, putative			
42	Medtr5g012870	Auxin canalization protein			
43	Medtr5g020060	Plant/MUD21-2 protein			
44	Medtr6g048440	Beta-carotene hydroxylase			
45	Medtr8g041390	Nodulin MtN21/EamA-like transporter family protein			
46	Medtr2g023500	Lactoylglutathione lyase-like protein			
47	Medtr6g004520	Aldose 1-epimerase family protein			
48	Medtr7g096890	Cofilin/actin-depolymerizing factor-like protein			



**Table A5 Top 50 out of 2824 increased differentially expressed genes and their functions which are specific to *SPL13RNAi* leaf tissues**

No.	Gene	Function	No.	Gene	Function
1	Medtr6g486230	Transmembrane protein, putative	19	Medtr8g479390	Multi-copper oxidase-like protein
2	Medtr1g069085	Hypothetical protein	20	Medtr7g063560	Hypothetical protein
3	Medtr8g469010	Ribonucleoside-diphosphate reductase small chain	21	Medtr4g122270	DNA replication licensing factor MCM2, putative
4	Medtr5g094310	Kinesin motor domain protein	22	Medtr4g096700	DNA replication licensing factor MCM4
5	Medtr6g032885	ARM repeat protein	23	Medtr7g104720	Glutaredoxin (GRX) family protein
6	Medtr7g013610	Core histone H2A/H2B/H3/H4	24	Medtr7g113830	Transcription factor
7	Medtr1g093900	Piriformospora indica-insensitive-like protein	25	Medtr8g006420	Hypothetical protein
8	Medtr3g466760	Expansin A10	26	Medtr2g070870	Plant gibberellin 2-oxidase
9	Medtr3g089570	Pollen Ole e I family allergen	27	Medtr7g033570	Cytochrome P450 family protein
10	Medtr4g072190	SAUR-like auxin-responsive family protein	28	Medtr8g075950	Chalcone-flavanone isomerase family protein
11	Medtr8g087890	GDSL-like lipase/acylhydrolase	29	Medtr5g066320	Chromosome-associated kinesin KIF4A-like protein
12	Medtr3g072840	Camphor resistance CrcB-like protein	30	Medtr3g014290	Aspartic proteinase nepenthesin-like protein
13	Medtr7g093910	Core histone H2A/H2B/H3/H4	31	Medtr8g086520	Nucleobase-ascorbate transporter-like protein
14	Medtr5g014300	NAC transcription factor-like protein	32	Medtr6g028030	Annexin D8
15	Medtr8g090000	Minichromosome maintenance (MCM2/3/5) family protein	33	Medtr3g102660	GASA/GAST/Snakin
16	Medtr4g019880	GDSL-like lipase/acylhydrolase	35	Medtr5g029770	Core histone H2A/H2B/H3/H4
17	Medtr2g100070	Glucose-methanol-choline (GMC) oxidoreductase family protein	36	Medtr7g114870	IQ calmodulin-binding motif protein

No.	Gene	Function
18	Medtr6g021530	GDSL-like lipase/acylhydrolase
37	Medtr1g094250	Hypothetical protein
37	Medtr7g062310	Laccase/diphenol oxidase family protein
38	Medtr1g079490	Germin family protein
39	Medtr4g128690	Flavonoid glucosyltransferase
40	Medtr5g078200	Glucan endo-1,3-beta-glucosidase-like protein
41	Medtr8g039540	Aspartic proteinase nepenthesin-like protein
42	Medtr7g103440	LRR receptor-like kinase
43	Medtr1g023570	Glyoxal oxidase amino-terminal protein
44	Medtr7g072630	Ovate transcriptional repressor
45	Medtr4g051880	Late embryogenesis abundant protein
46	Medtr0268s0080	Ribonucleoside-diphosphate reductase small chain
47	Medtr4g082050	EF hand calcium-binding family protein
48	Medtr5g011250	Leucoanthocyanidin dioxygenase-like protein
49	Medtr3g104570	IQ calmodulin-binding motif protein
50	Medtr6g081040	Kinase interacting (KIP1-like) family protein

**Table A6 Top 50 out of 572 increased differentially expressed genes and their functions which are specific to *SPL13*RNAi stem tissues**

No.	Gene	Function	No.	Gene	Function
1	Medtr8g035880	Zinc-binding dehydrogenase family oxidoreductase	17	Medtr5g093530	Exocyst subunit exo70 family protein
2	Medtr5g081070	Hypothetical protein	18	Medtr3g012420	Nodulin MtN21/EamA-like transporter family protein
3	Medtr3g084960	Transmembrane amino acid transporter family protein	19	Medtr2g099010	Salt tolerance-like protein
4	Medtr7g100100	Cys2-His2 zinc finger transcription factor	20	Medtr8g077420	MYB family transcription factor
5	Medtr4g128590	Xyloglucan endotransglucosylase/hydrolase family protein	21	Medtr3g102980	C2H2-type zinc finger protein
6	Medtr4g100420	Ethylene response factor	22	Medtr1g108640	DUF4228 domain protein
7	Medtr7g071050	UDP-glucosyltransferase family protein	23	Medtr8g090350	Ethylene response factor
8	Medtr2g020850	Transmembrane protein, putative	24	Medtr2g102060	Small GTPase family RAB protein
9	Medtr3g070880	ARM repeat CCCH-type zinc finger protein	25	Medtr8g098485	BTB/POZ domain plant protein
10	Medtr2g081580	Calcium-binding EF-hand protein	26	Medtr4g131720	Hypothetical protein
11	Medtr8g068520	Transmembrane protein	27	Medtr8g089920	Avr9/Cf-9 rapidly elicited protein, putative
12	Medtr3g070230	Nematode resistance HSPRO2-like protein	28	Medtr7g093030	Myb-like transcription factor family protein
13	Medtr1g013410	Transmembrane protein	29	Medtr7g106340	E3 ubiquitin-protein ligase PUB23-like protein
14	Medtr8g069835	Hypothetical protein	30	Medtr8g106530	Transmembrane protein, putative
15	Medtr7g112500	Transmembrane protein, putative			

16 Medtr5g087440 Hypothetical protein

---

<b>No.</b>	<b>Gene</b>	<b>Function</b>
31	Medtr1g105860	Cysteine-rich RLK (receptor-like kinase) protein
32	Medtr1g098690	Hsp20/alpha crystallin family protein
33	Medtr3g088520	Beta-like galactosidase
34	Medtr3g104560	Cytochrome P450 family protein
35	Medtr1g100777	Heat shock transcription factor B2A
36	Medtr5g069640	Acyl-CoA thioesterase, putative
37	Medtr2g006850	Hypothetical protein
38	Medtr5g066730	BTB/POZ domain plant protein
39	Medtr2g014830	NB-LRR type disease resistance protein
40	Medtr1g077790	Plastocyanin-like domain protein
41	Medtr5g090740	AAA domain protein
42	Medtr7g084760	Xyloglucan endotransglucosylase/hydrolase family protein
43	Medtr4g061300	Hypothetical protein
44	Medtr2g086770	Transmembrane protein, putative
45	Medtr2g097620	Zinc finger, C3HC4 type (RING finger) protein, putative
46	Medtr2g436900	C2 domain protein
47	Medtr4g116273	Hypothetical protein
48	Medtr2g017970	Fasciclin domain protein
49	Medtr1g021730	Inositol polyphosphate 5-phosphatase I
50	Medtr8g022310	Chaperone DnaJ domain protein

---

**Table A7 Top 50 out of 385 increased differentially expressed genes and their functions which are specific to *SPL13RNAi* root tissues**

No.	Gene	Function	No.	Gene	Function
1	Medtr3g103260	Hypothetical protein	17	Medtr1g041285	EF hand calcium-binding family protein
2	Medtr5g066020	AT hook motif DNA-binding family protein	18	Medtr8g014930	LRR receptor-like kinase
3	Medtr3g063120	(3S)-linalool/(E)-nerolidol/(E,E)-geranyl linalool synthase	19	Medtr1g030630	Heavy metal transport/detoxification superfamily protein
4	Medtr8g054490	Hypothetical protein	20	Medtr5g075680	Mn-specific cation diffusion facilitator transporter MTP81
5	Medtr3g011890	Salt stress response/antifungal domain protein	21	Medtr5g021270	MADS-box transcription factor
6	Medtr2g022430	Xyloglucanase-specific endoglucanase inhibitor protein	22	Medtr2g039620	Basic helix loop helix (BHLH) DNA-binding family protein
7	Medtr3g111610	GNS1/SUR4 membrane family protein	23	Medtr8g104520	Receptor-like kinase
8	Medtr2g022330	Extracellular dermal glycoprotein	24	Medtr7g081780	LRR receptor-like kinase family protein
9	Medtr4g128580	Xyloglucan endotransglucosylase/hydrolase family protein	25	Medtr6g462640	Cytochrome P450 family 71 protein
10	Medtr7g058830	Serine/Threonine kinase, plant-type protein	26	Medtr5g005520	Cysteine-rich receptor-kinase-like protein
11	Medtr1g096310	Caffeic acid O-methyltransferase	27	Medtr8g018510	Seed linoleate 9S-lipoxygenase
12	Medtr5g005530	Cysteine-rich receptor-like kinase	28	Medtr5g083030	Ubiquitin-protein ligase, PUB17
13	Medtr2g435310	Pathogenesis-related protein bet V I family protein	29	Medtr3g102450	Receptor-like kinase
14	Medtr6g016640	Proline dehydrogenase	30	Medtr8g066850	Transmembrane protein, putative
15	Medtr8g095030	LRR receptor-like kinase			

16 Medtr0062s0020 Glycoside hydrolase family 18 protein      31 Medtr4g094698 VQ motif protein

<b>No.</b>	<b>Gene</b>	<b>Function</b>
32	Medtr2g087900	Cellulose synthase H1-like protein
33	Medtr1g090520	LRR receptor-like kinase family protein
34	Medtr5g035980	Transducin/WD40 repeat protein
35	Medtr4g013230	Phosphate-responsive 1 family protein
36	Medtr5g093090	GDSL-like lipase/acylhydrolase
37	Medtr2g036310	UPF0481 plant-like protein
38	Medtr2g020710	Sugar porter (SP) family MFS transporter
39	Medtr5g092150	Cytochrome P450 family protein
40	Medtr5g073480	Exocyst subunit exo70 family protein
41	Medtr1g114640	GRAM domain protein/ABA-responsive-like protein
42	Medtr5g089820	DUF4228 domain protein
43	Medtr5g044710	Ureide permease-like protein
44	Medtr1g090667	FAD/NAD(P)-binding oxidoreductase family protein
45	Medtr0056s0160	Flavonol synthase/flavanone 3-hydroxylase
46	Medtr1g014240	Lectin receptor kinase
47	Medtr8g036235	Transcription factor bHLH122-like protein
48	Medtr2g029910	Peroxidase family protein
49	Medtr4g087810	Phospholipase A1
50	Medtr4g084480	Glycoside hydrolase family 17 protein

**Table A8 GO-term analysis represented molecular function, biological process and cellular components in leaf tissues**

<b>Biological process (top 45)</b>	<b>Molecular function</b>	<b>Cellular component</b>
Telomere maintenance	Phosphorelay response regulator activity	Extracellular region
Translation	Transcription factor activity, sequence-specific DNA binding	Microtubule associated complex
Alcohol metabolic process	Transcription cofactor activity	Ribosome
Glutamine catabolic process	Structural constituent of ribosome	Nuclear pore
Porphyrin-containing compound biosynthetic process	Catalytic activity	Phosphopyruvate hydratase complex
Mo-molybdopterin cofactor biosynthetic process	Uroporphyrinogen decarboxylase activity	Photosystem I
Response to metal ion	Signal transducer activity	Nucleus
Glycerol ether metabolic process	Rho GDP-dissociation inhibitor activity	Chromatin
Cellular amino acid metabolic process	Structural molecule activity	Golgi transport complex
Pseudouridine synthesis	binding	Mitochondrial matrix
Nucleobase-containing compound metabolic process	Calcium ion binding	Intracellular
tRNA processing	Electron carrier activity	Core TFIIH complex
Allantoin catabolic process	Hydrolase activity, hydrolyzing O-Glycosyl compounds	Cytoplasm
Regulation of nitrogen utilization	Peroxidase activity	Transcription factor TFIIA complex
L-arabinose metabolic process	Carbon-nitrogen ligase activity, with Glutamine as amido-N-donor	Signal peptidase complex
mRNA splicing, via spliceosome	Intramolecular transferase activity	Protein phosphatase type 2A complex
Mature ribosome assembly	Transferase activity, transferring alkyl or aryl (other than methyl) groups	Endoplasmic reticulum
Polysaccharide catabolic process	Isomerase activity	Origin recognition complex

<b>Biological process (top 45)</b>	<b>Molecular function</b>	<b>Cellular component</b>
Protein dephosphorylation	Transcription regulatory region Sequence-specific DNA binding	Protein kinase CK2 complex
Cell wall macromolecule catabolic process	Hydrolase activity	Ubiquitin ligase complex
Positive regulation of transcription elongation from RNA polymerase II promoter	Protein dimerization activity	Cytoskeleton
Defense response	Iron-sulfur cluster binding	Membrane
Protein methylation	Heme binding	Integral component of plasma membrane
Response to stress		Integral component of membrane
Regulation of cyclin-dependent protein Serine/threonine kinase activity		Plasma membrane
Intracellular signal transduction		
Tetrahydrobiopterin biosynthetic process		
Drug transmembrane transport		
Sucrose metabolic process		
Glycine decarboxylation via glycine cleavage system		
Signal peptide processing		
Histidine biosynthetic process		
Barrier septum site selection		
Tricarboxylic acid cycle		
Cell cycle		
Proteolysis		
Putrescine biosynthetic process		
Phosphatidylinositol dephosphorylation		
Lipid metabolic process		
Oxidation-reduction process		



---

**Biological process (top 45)**

---

Iron-sulfur cluster assembly

NAD biosynthetic process

Lignin catabolic process

DNA-templated transcription, initiation

(obsolete) ATP catabolic process

---

**Table A9 GO-term analysis represented molecular function, biological process and cellular components in stem tissues**

<b>Biological process (top 45)</b>	<b>Molecular function (top 45)</b>	<b>Cellular component</b>
(obsolete) ATP catabolic process	Acyl-CoA dehydrogenase activity	Extracellular region
Response to stress	Ubiquinol-cytochrome-c reductase activity	Chloroplast
Defense response	Hydroxymethylglutaryl-CoA reductase (NADPH) activity	Anaphase-promoting complex
Intracellular signal transduction	Secondary active sulfate transmembrane transporter activity	Nuclear pore
Response to desiccation	Glutathione peroxidase activity	Phosphopyruvate hydratase complex
Phosphorelay signal transduction system	Peroxidase activity	Transcription factor TFIIA complex
Metabolic process	Zinc ion transmembrane transporter activity	Microtubule associated complex
Cellular process	NADH dehydrogenase (ubiquinone) activity	Protein phosphatase type 2A complex
ATP synthesis coupled proton transport	Peptide-methionine (S)-S-oxide reductase activity	Photosystem II
Carotenoid biosynthetic process	Enzyme inhibitor activity	Nucleosome
Transmembrane transport	Endopeptidase inhibitor activity	Chromatin
Alcohol metabolic process	Heme binding	Endoplasmic reticulum
Mitochondrial transport	Adenosylmethionine decarboxylase activity	Ubiquitin ligase complex
rRNA processing	Inorganic diphosphatase activity	Membrane
Glycogen biosynthetic process	Adenosylhomocysteinase activity	Integral component of plasma membrane
Tetrahydrobiopterin biosynthetic process	Serine-type endopeptidase activity	Integral component of membrane
Glycerol ether metabolic process	Polygalacturonase activity	Cytoplasm
Drug transmembrane transport	Chitinase activity	Plasma membrane
Flavonoid biosynthetic process	Microtubule motor activity	Intracellular
Sucrose metabolic process	Nuclease activity	
Glycine decarboxylation via glycine	Intramolecular transferase activity	
Cleavage system		
tRNA modification	Peptidyl-prolyl cis-trans isomerase activity	

<b>Biological process (top 45)</b>	<b>Molecular function (top 45)</b>	<b>Cellular component</b>
Cell redox homeostasis	Carbon-nitrogen ligase activity, with Glutamine as amido-N-donor	
Ubiquinone biosynthetic process	Asparagine synthase (glutamine- hydrolyzing) activity	
Sodium ion transport	Methyltransferase activity	
Putrescine biosynthetic process	Methionine adenosyltransferase activity	
Ubiquitin-dependent protein catabolic process	Adenosine kinase activity	
Lipid transport	5-methyltetrahydropteroyltriglutamate- homocysteine S-methyltransferase activity	
Phosphatidylinositol dephosphorylation transport	Aspartate kinase activity Phosphorylase activity	
Fatty acid metabolic process	Transferase activity, transferring Phosphorus-containing groups	
Phosphatidylinositol phosphorylation cation transport	Ubiquitin-protein transferase activity 3-deoxy-7-phosphoheptulonate synthase activity	
Lipid metabolic process	Starch synthase activity	
Amino acid transmembrane transport	Phosphorelay sensor kinase activity	
Oxidation-reduction process	Selenium binding	
Fatty acid biosynthetic process	Chaperone binding	
Allantoin catabolic process	Actin binding	
NAD biosynthetic process	Oxidoreductase activity	
Tryptophan biosynthetic process	Calcium ion binding	
Metal ion transport	Copper ion binding	
Intracellular protein transport	Manganese ion binding	
Polysaccharide catabolic process	Nucleic acid binding	

---

<b>Biological process (top 45)</b>	<b>Molecular function (top 45)</b>	<b>Cellular component</b>
Protein folding	GTP binding	
Respiratory gaseous exchange	Nucleotide binding	
Sulfur compound metabolic process	Transcription regulatory region sequence-specific DNA binding	

---

**Table A10 GO-term analysis represented molecular function, biological process and cellular components in root tissues**

<b>Biological process</b>	<b>Molecular function</b>	<b>Cellular component</b>
(obsolete) ATP catabolic process	Phosphorelay response regulator activity	Phosphopyruvate hydratase complex
Response to stress	Transcription factor activity, sequence-specific DNA binding	Photosystem I
Defense response	Catalytic activity	Protein phosphatase type 2A complex
Intracellular signal transduction	GTPase activity	Nucleosome
Phosphorelay signal transduction system	Secondary active sulfate transmembrane Transporter activity	Endoplasmic reticulum
Metabolic process	Serine-type carboxypeptidase activity	Ubiquitin ligase complex
Metal ion transport	Hydrolase activity, hydrolyzing O-glycosyl compounds	Cytoskeleton
Transmembrane transport	Polygalacturonase activity	Cytoplasm
Proton transport	Microtubule motor activity	Intracellular
Mitochondrial transport	ATPase activity, coupled to transmembrane Movement of substances	Extracellular region
Drug transmembrane transport	Rho GDP-dissociation inhibitor activity	Membrane
Lipid transport	Transporter activity	Integral component of membrane
Transport	Calcium ion binding	
Cation transport	Copper ion binding	
Amino acid transmembrane transport	Zinc ion binding	
Phosphatidylinositol dephosphorylation	FMN binding	
Glycogen biosynthetic process	Nucleic acid binding	
Glycerol ether metabolic process	GTP binding	
Sucrose metabolic process	Ammonium transmembrane transporter activity	
Cellular amino acid metabolic process	Cytochrome-c oxidase activity	

<b>Biological process</b>	<b>Molecular function</b>	<b>Cellular component</b>
Fatty acid metabolic process	Gamma-glutamyltransferase activity	
Lipid metabolic process	Adenosine kinase activity	
Oxidation-reduction process	6-phosphofructokinase activity	
Fatty acid biosynthetic process	5-methyltetrahydropteroyltriglutamate-Homocysteine S-methyltransferase activity	
NAD biosynthetic process	Protein kinase activity	
Polysaccharide catabolic process	Phosphorelay sensor kinase activity	
Primary metabolic process	Methyltransferase activity	
Mature ribosome assembly	Peroxidase activity	
Protein folding	Acid-amino acid ligase activity	
Allantoin catabolic process	Asparagine synthase (glutamine-hydrolyzing) activity	
Regulation of cyclin-dependent protein Serine/threonine kinase activity	CTP synthase activity	
Glycine decarboxylation via glycine cleavage system	Intramolecular transferase activity	
tRNA modification	Oxidoreductase activity	
Proteolysis	Actin binding	
Sulfur compound metabolic process	Protein dimerization activity	
Sulfate assimilation	Hydrolase activity	
Carbohydrate metabolic process		
Photosynthesis		
Embryo development		

**Table A11 List of significantly affected ABA-related genes fold-changes from well-drained control plants**

<b>Gene name</b>	<b>Gene ID</b>	<b>Wild-type</b>	<b>AC- Caribou</b>	<b>AAC- Trueman</b>	<b>miROE (A8)</b>	<b>SPL13RNAi-6</b>
PYL9	Medtr3g090980	NS	1.47	1.94	1.31	1.61
	Medtr8g027805	NS	1.48	NS	NS	1.36
	Medtr1g028380	4.96	16.94	4.41	8.92	10.64
PYR1	Medtr5g030500	NS	0.55	NS	NS	0.63
ABA-receptor	Medtr7g070050	NS	0.29	NS	NS	0.67
	Medtr1g016480	1.73	2.35	2.17	1.45	2.77
	Medtr5g083270	NS	0.28	2.80	2.30	NS
	Medtr4g014460	NS	0.39	2.07	NS	NS
ABA induced bHLH	Medtr8g027495	NS	0.45	NS	0.63	0.68
	Medtr7g117670	0.58	0.50	NS	0.61	0.66
	Medtr7g096350	NS	NS	NS	1.35	NS
ABA/WDS Induced protein	Medtr1g098680	0.51	0.46	0.46	0.56	0.66
XDH1	Medtr2g098030	1.71	1.75	2.18	1.59	1.95
Zeta-Carotene isomerase	Medtr3g084950	NS	NS	NS	NS	0.62
	Medtr8g097190	NS	NS	2.36	NS	NS
Beta-Carotene Isomerase	Medtr7g095920	NS	NS	NS	NS	0.38
ABA-responsive protein	Medtr2g035190	4.48	8.03	NS	NS	NS
ABA-responsive (TB2/DP1, HVA22) family protein	Medtr1g024930	0.29	0.20	0.32	0.64	0.21
ABA response element-binding factor	Medtr4g085910	2.12	3.73	3.13	1.78	3.57
ABA-responsive-like protein	Medtr8g100065	NS	NS	1.79	NS	1.77
	Medtr1g114640	NS	NS	NS	2.66	NS
	Medtr7g083570	NS	NS	2.13	1.69	NS

	<b>Gene ID</b>	<b>Wild-type</b>	<b>AC- Caribou</b>	<b>AAC- Trueman</b>	<b>miROE (A8)</b>	<b><i>SPL13RNAi-6</i></b>
	Medtr6g077990	NS	4.41	NS	NS	NS
	Medtr8g100065	NS	1.57	NS	NS	NS
ABA induced plasma membrane protein	Medtr4g117600	0.45	NS	NS	NS	0.38
PSY	Medtr5g076620	NS	NS	NS	NS	0.65
	Medtr3g450510	0.41	0.23	NS	0.71	0.29
	Medtr5g090780	0.46	0.275	NS	0.58	0.19
PDS	Medtr3g084830	NS	1.48	1.53	NS	1.38
LCY-e	Medtr2g040060	0.27	0.33	0.57	0.56	0.28
LCY-b	Medtr7g090150	NS	0.69	NS	NS	NS
	Medtr8g465870	NS	NS	1.69	NS	NS
CHY	Medtr1g100070	0.37	0.24	0.61	0.67	0.25
	Medtr6g048440	NS	1.49	NS	NS	NS
CCD1	Medtr3g109610	NS	4.07	25.13	NS	20.98
	Medtr8g037315	NS	NS	1.92	1.37	NS
CCD4	Medtr5g025270	0.25	0.28	0.17	0.41	0.43
	Medtr5g025230	0.29	0.34	0.18	0.43	0.41
ZEP	Medtr4g022850	4.03	7.71	2.67	2.21	6.09
	Medtr5g017350	3.03	3.23	2.44	2.08	5.61
VDE	Medtr8g092050	NS	0.62	NS	NS	0.63
	Medtr7g116630	0.57	0.56	NS	0.71	0.53
NSY	Medtr7g007280	0.46	0.34	0.35	0.65	0.35
	Medtr6g025680	NS	NS	NS	NS	3.13
	Medtr6g018550	4.05	NS	NS	NS	NS
NCED3	Medtr2g070460	1.85	6.70	4.75	1.63	6.49
	Medtr5g025610	0.52	NS	NS	0.62	1.89
	Medtr1g019410	3.38	11.56	5.12	2.25	6.13



	<b>Gene ID</b>	<b>Wild-type</b>	<b>AC- Caribou</b>	<b>AAC- Trueman</b>	<b>miROE (A8)</b>	<b><i>SPL13RNAi-6</i></b>
Cytochrome P450 family ABA- 8 hydroxylase	Medtr4g086040	NS	0.55	0.58	0.59	0.52
	Medtr8g072260	0.28	0.21	NS	1.81	0.62
	Medtr1g037580	NS	NS	0.49	1.84	NS
Sucrose nonfermenting 1(SNF1)-related kinase	Medtr1g034030	2.78	2.71	2.34	1.78	3.53
	Medtr8g079560	NS	1.92	1.74	NS	1.71
	Medtr4g099240	NS	1.79	1.62	1.45	NS
	Medtr5g018050	NS	NS	NS	1.42	NS
SNF1-related kinase regulatory subunit $\beta$ -2	Medtr5g098510	6.88	9.98	7.16	6.33	10.14
	Medtr2g095290	1.92	2.20	1.85	1.54	1.70
	Medtr2g026695	0.60	0.54	0.51	NS	0.58
SNF1-related kinase catalytic subunit $\alpha$ KIN11	Medtr6g048250	NS	2.10	NS	NS	1.65
	Medtr6g012990	NS	1.85	NS	NS	1.36
SNF1-related kinase regulatory subunit $\gamma$ 1	Medtr4g103550	NS	3.00	NS	NS	1.56
Snf1-related kinase interactor 1, putative	Medtr4g007700	NS	2.44	1.97	NS	2.36
SNF2 family amino- terminal protein	Medtr4g118720	NS	1.59	NS	NS	1.59
	Medtr7g050445	0.28	0.19	NS	NS	0.15
SNF2, helicase and zinc finger protein	Medtr2g012830	1.54	2.14	1.69	1.34	1.64

NS: Not significant

**Table A12 Differentially expressed genes associated with phenylpropanoid pathway fold changes in *SPL13RNAi* plants**

No.	Gene ID	Gene annotation	Fold change
1	Medtr7g016700	chalcone and stilbene synthase family protein	11.20
2	Medtr3g083910	chalcone and stilbene synthase family protein	79.20
3	Medtr5g007713	chalcone and stilbene synthase family protein	17.04
4	Medtr1g097935	chalcone and stilbene synthase family protein	4.41
5	Medtr3g083920	chalcone and stilbene synthase family protein	3.88
6	Medtr1g097910	chalcone and stilbene synthase family protein	3.14
7	Medtr1g098140	chalcone and stilbene synthase family protein	2.70
8	Medtr7g084300	chalcone and stilbene synthase family protein	1.76
9	Medtr3g093980	chalcone-flavanone isomerase family protein	1.70
10	Medtr2g072510	chalcone-flavanone isomerase family protein	0.65
11	Medtr7g094980	chalcone-flavanone isomerase family protein	0.52
12	Medtr1g115840	chalcone-flavanone isomerase family protein	0.36
13	Medtr8g075950	chalcone-flavanone isomerase family protein	0.09
14	Medtr5g022010	chalcone-flavanone isomerase family protein, putative	0.21
15	Medtr5g011250	leucoanthocyanidin dioxygenase-like protein	38.30
16	Medtr4g015790	leucoanthocyanidin dioxygenase-like protein	0.68
17	Medtr3g070860	leucoanthocyanidin dioxygenase-like protein	0.32
18	Medtr7g068650	leucoanthocyanidin dioxygenase-like protein	0.16
19	Medtr8g075830	naringenin 3-dioxygenase (flavanone-3-hydroxylase)	35.47
20	Medtr3g058610	naringenin 3-dioxygenase (flavanone-3-hydroxylase)	0.66
21	Medtr3g091350	flavonol synthase/flavanone 3-hydroxylase	21.59
22	Medtr5g055680	flavonol synthase/flavanone 3-hydroxylase	19.07
23	Medtr5g055690	flavonol synthase/flavanone 3-hydroxylase	4.69
24	Medtr5g059130	flavonol synthase/flavanone 3-hydroxylase	2.24
25	Medtr5g048850	flavonol synthase/flavanone 3-hydroxylase	1.48
26	Medtr5g065010	flavonol synthase/flavanone 3-hydroxylase	0.55
27	Medtr3g450680	2-hydroxyisoflavanone dehydratase	107.47
28	Medtr7g051020	2-hydroxyisoflavanone dehydratase	3.01
29	Medtr1g104930	2-hydroxyisoflavanone dehydratase	2.08
30	Medtr4g070340	allergenic isoflavone reductase-like protein Bet protein	11.48
31	Medtr5g020760	isoflavone reductase-like protein	7.29
32	Medtr1g022440	dihydroflavonol 4-reductase-like protein	6.07
33	Medtr2g013250	dihydroflavonol 4-reductase-like protein	0.58
34	Medtr4g109470	flavonoid hydroxylase	54.22
35	Medtr3g024520	flavonoid hydroxylase	15.85
36	Medtr3g084520	flavonoid glucosyltransferase	5.26
37	Medtr3g084530	flavonoid glucosyltransferase	2.57
38	Medtr4g128690	flavonoid glucosyltransferase	3.86
39	Medtr4g485630	flavonoid glucosyltransferase	0.13

No.	Gene ID	Gene annotation	Fold change
40	Medtr4g031800	flavonoid glucosyltransferase	0.08
41	Medtr3g083620	flavonoid O-methyltransferase-like protein	0.19
42	Medtr2g089650	anthocyanin 5-aromatic acyltransferase	3.48
43	Medtr7g014160	anthocyanin 5-aromatic acyltransferase	2.28
44	Medtr4g015180	anthocyanin 5-aromatic acyltransferase	2.19
45	Medtr7g014205	anthocyanin 5-aromatic acyltransferase	0.66
46	Medtr7g015860	anthocyanin 5-aromatic acyltransferase	0.36
47	Medtr2g089670	anthocyanin 5-aromatic acyltransferase	0.11
48	Medtr2g018590	1-O-acylglucose:anthocyanin acyltransferase	0.72
49	Medtr5g098720	phenylalanine ammonia-lyase-like protein	2.07
50	Medtr7g101395	phenylalanine ammonia-lyase-like protein	0.60
51	Medtr7g101425	phenylalanine ammonia-lyase-like protein	0.59
52	Medtr2g064495	shikimate/quinic acid hydroxycinnamoyltransferase	0.16
53	Medtr4g009040	cinnamoyl-CoA reductase	1.78
54	Medtr5g072620	cinnamoyl-CoA reductase-like protein	2.01
55	Medtr3g031650	cinnamoyl-CoA reductase-like protein	1.70
56	Medtr4g077100	cinnamoyl-CoA reductase-like protein	0.50
57	Medtr4g006940	cinnamoyl-CoA reductase-like protein	0.42
58	Medtr1g107425	cinnamyl alcohol dehydrogenase-like protein	2.00
59	Medtr3g005170	cinnamyl alcohol dehydrogenase-like protein	1.57
60	Medtr5g031180	cinnamyl alcohol dehydrogenase-like protein	1.48
61	Medtr4g115300	cinnamyl alcohol dehydrogenase-like protein	0.41
62	Medtr1g025950	cinnamyl alcohol dehydrogenase-like protein	0.37
63	Medtr5g031430	cinnamyl alcohol dehydrogenase-like protein	0.36
64	Medtr5g031190	cinnamyl alcohol dehydrogenase-like protein	0.25
65	Medtr1g073180	4-coumarate:CoA ligase-like protein	2.63
66	Medtr4g057730	4-coumarate:CoA ligase-like protein	6.82
67	Medtr5g007640	4-coumarate:CoA ligase-like protein	1.56
68	Medtr4g128337	4-coumarate:CoA ligase-like protein	1.36
69	Medtr4g005750	4-coumarate:CoA ligase-like protein	0.61
70	Medtr2g105570	4-coumarate:CoA ligase-like protein	0.60
71	Medtr1g063110	4-coumarate:CoA ligase-like protein	0.12
72	Medtr2g024310	malonyl-CoA decarboxylase	1.67
73	Medtr6g015830	malonyl-CoA:isoflavone 7-O-glucoside malonyltransferase	15.18
74	Medtr6g015315	malonyl-CoA:isoflavone 7-O-glucoside malonyltransferase	3.92
75	Medtr6g015320	malonyl-CoA:isoflavone 7-O-glucoside malonyltransferase	2.45
76	Medtr3g031380	malonyl CoA-acyl carrier transacylase	0.43
77	Medtr4g088160	cytochrome P450 family flavone synthase	2.94
78	Medtr8g059425	UDP-glucosyltransferase family protein	6.69

No.	Gene ID	Gene annotation	Fold change
79	Medtr2g040530	UDP-glucosyltransferase family protein	4.75
80	Medtr3g479470	UDP-glucosyltransferase family protein	4.73
81	Medtr7g102560	UDP-glucosyltransferase family protein	4.17
82	Medtr2g083430	UDP-glucosyltransferase family protein	4.02
83	Medtr7g071050	UDP-glucosyltransferase family protein	3.88
84	Medtr4g064987	UDP-glucosyltransferase family protein	3.19
85	Medtr7g013200	UDP-glucosyltransferase family protein	3.15
86	Medtr3g009490	UDP-glucosyltransferase family protein	2.98
87	Medtr7g046490	UDP-glucosyltransferase family protein	2.38
88	Medtr6g014270	UDP-glucosyltransferase family protein	2.37
89	Medtr2g059240	UDP-glucosyltransferase family protein	2.22
90	Medtr0184s0030	UDP-glucosyltransferase family protein	2.11
91	Medtr5g070040	UDP-glucosyltransferase family protein	2.09
92	Medtr8g006730	UDP-glucosyltransferase family protein	2.00
93	Medtr8g466240	UDP-glucosyltransferase family protein	1.98
94	Medtr8g006710	UDP-glucosyltransferase family protein	1.95
95	Medtr7g117170	UDP-glucosyltransferase family protein	1.87
96	Medtr8g071070	UDP-glucosyltransferase family protein	1.70
97	Medtr7g013180	UDP-glucosyltransferase family protein	1.53
98	Medtr4g123553	UDP-glucosyltransferase family protein	1.43
99	Medtr5g067170	UDP-glucosyltransferase family protein	0.66
100	Medtr5g072860	UDP-glucosyltransferase family protein	0.65
101	Medtr2g046620	UDP-glucosyltransferase family protein	0.64
102	Medtr5g029800	UDP-glucosyltransferase family protein	0.59
103	Medtr8g009055	UDP-glucosyltransferase family protein	0.58
104	Medtr8g027870	UDP-glucosyltransferase family protein	0.56
105	Medtr0078s0010	UDP-glucosyltransferase family protein	0.54
106	Medtr3g008010	UDP-glucosyltransferase family protein	0.53
107	Medtr7g047030	UDP-glucosyltransferase family protein	0.53
108	Medtr7g102490	UDP-glucosyltransferase family protein	0.48
109	Medtr6g042310	UDP-glucosyltransferase family protein	0.47
110	Medtr2g083490	UDP-glucosyltransferase family protein	0.47
111	Medtr4g024020	UDP-glucosyltransferase family protein	0.44
112	Medtr0536s0010	UDP-glucosyltransferase family protein	0.44
113	Medtr6g014250	UDP-glucosyltransferase family protein	0.44
114	Medtr4g077960	UDP-glucosyltransferase family protein	0.41
115	Medtr1g107325	UDP-glucosyltransferase family protein	0.40
116	Medtr6g035295	UDP-glucosyltransferase family protein	0.39
117	Medtr6g005600	UDP-glucosyltransferase family protein	0.38
118	Medtr8g008970	UDP-glucosyltransferase family protein	0.37
119	Medtr8g068330	UDP-glucosyltransferase family protein	0.35
120	Medtr2g008210	UDP-glucosyltransferase family protein	0.33

No.	Gene ID	Gene annotation	Fold change
121	Medtr2g083380	UDP-glucosyltransferase family protein	0.32
122	Medtr6g038300	UDP-glucosyltransferase family protein	0.32
123	Medtr8g006260	UDP-glucosyltransferase family protein	0.29
124	Medtr7g012120	UDP-glucosyltransferase family protein	0.28
125	Medtr3g069690	UDP-glucosyltransferase family protein	0.21
126	Medtr8g068340	UDP-glucosyltransferase family protein	0.20
127	Medtr5g035560	UDP-glucosyltransferase family protein	0.20
128	Medtr5g016660	UDP-glucosyltransferase family protein	0.19
129	Medtr2g034990	UDP-glucosyltransferase family protein	0.18
130	Medtr4g117890	UDP-glucosyltransferase family protein	0.18
131	Medtr0891s0010	UDP-glucosyltransferase family protein	0.17
132	Medtr7g055710	UDP-glucosyltransferase family protein	0.17
133	Medtr6g078320	UDP-glucosyltransferase family protein	0.14
134	Medtr2g008226	UDP-glucosyltransferase family protein	0.13
135	Medtr4g059370	UDP-glucosyltransferase family protein	0.13
136	Medtr8g044140	UDP-glucosyltransferase family protein	0.13
137	Medtr2g008220	UDP-glucosyltransferase family protein	0.06
138	Medtr5g075440	UDP-glucosyltransferase family protein	0.01
139	Medtr6g033675	UDP-glucosyl transferase 88A1	3.77
140	Medtr6g033725	UDP-glucosyl transferase 88A1	2.69
141	Medtr4g485640	UDP-glucosyltransferase 73B2	1.84
142	Medtr1g088480	UDP-glucuronic acid decarboxylase-like protein	1.66
143	Medtr3g095910	UDP-glucuronate:xylan alpha-glucuronosyltransferase	0.63
144	Medtr1g019530	UDP-glucuronate:xylan alpha-glucuronosyltransferase	0.60
145	Medtr5g090580	UDP-glucose flavonoid 3-O-glucosyltransferase	1.63
146	Medtr5g098930	UDP-glucose flavonoid 3-O-glucosyltransferase	0.56
147	Medtr7g076310	UDP-galactose transporter 1	1.57
148	Medtr1g098640	UDP-glucose:sterol glucosyltransferase	1.42
149	Medtr8g446850	UDP-glcnac-adolichol phosphate glcnac-1-P-transferase	0.66
150	Medtr5g043970	UDP-glucose 6-dehydrogenase family protein	0.49
151	Medtr7g012950	UDP-glucose 6-dehydrogenase family protein	0.48
152	Medtr2g096660	UDP-glucuronic acid decarboxylase	0.54
153	Medtr5g079670	myb transcription factor	70.77
154	Medtr1g086510	myb transcription factor	57.44
155	Medtr2g033170	myb transcription factor	20.99
156	Medtr1g110460	myb transcription factor	19.02
157	Medtr4g123040	myb transcription factor	11.36
158	Medtr2g096380	myb transcription factor	6.62
159	Medtr3g083540	myb transcription factor	5.89
160	Medtr4g057635	myb transcription factor	5.36
161	Medtr5g016510	myb transcription factor	4.15

No.	Gene ID	Gene annotation	Fold change
162	Medtr5g009460	myb transcription factor	3.92
163	Medtr4g094982	myb transcription factor	4.40
164	Medtr4g100720	myb transcription factor	2.58
165	Medtr2g011660	myb transcription factor	2.75
166	Medtr4g063100	myb transcription factor	2.71
167	Medtr7g087130	myb transcription factor	2.28
168	Medtr8g028655	myb transcription factor	2.00
169	Medtr0123s0070	myb transcription factor	1.91
170	Medtr8g095390	myb transcription factor	1.71
171	Medtr3g064500	myb transcription factor	1.53
172	Medtr8g020330	myb transcription factor	1.44
173	Medtr1g067000	myb transcription factor	0.75
174	Medtr6g477860	myb transcription factor	0.64
175	Medtr4g102380	myb transcription factor	0.60
176	Medtr4g019370	myb transcription factor	0.59
177	Medtr3g028740	myb transcription factor	0.54
178	Medtr4g073420	myb transcription factor	0.54
179	Medtr1g063940	myb transcription factor	0.50
180	Medtr8g098860	myb transcription factor	0.48
181	Medtr4g065017	myb transcription factor	0.47
182	Medtr8g468380	myb transcription factor	0.43
183	Medtr2g097910	myb transcription factor	0.41
184	Medtr7g061550	myb transcription factor	0.36
185	Medtr5g078140	myb transcription factor	0.36
186	Medtr7g096930	myb transcription factor	0.36
187	Medtr1g085040	myb transcription factor	0.30
188	Medtr7g117730	myb transcription factor	0.23
189	Medtr7g109320	myb transcription factor	0.21
190	Medtr5g082910	myb transcription factor	0.21
191	Medtr4g082040	myb transcription factor	0.11
192	Medtr4g121460	myb transcription factor	0.05
193	Medtr2g034790	myb transcription factor	0.05
194	Medtr2g023100	myb transcription factor	0.03
195	Medtr1g086180	MYB family transcription factor	0.60
196	Medtr1g022290	MYB family transcription factor	0.59
197	Medtr8g077420	MYB family transcription factor	0.17
198	Medtr3g111920	MYB family transcription factor	0.11
199	Medtr3g111880	MYB family transcription factor	0.08
200	Medtr7g089210	MYB family transcription factor	0.06
201	Medtr8g077390	MYB family transcription factor	0.03
202	Medtr1g026870	transcription repressor MYB5	0.33
203	Medtr3g110028	transcription repressor MYB5	0.15

<b>No.</b>	<b>Gene ID</b>	<b>Gene annotation</b>	<b>Fold change</b>
204	Medtr5g081860	MYB transcription factor MYB51	1.51
205	Medtr7g067080	MYB transcription factor MYB51	1.45
206	Medtr3g462790	MYB transcription factor MYB51	1.43
207	Medtr7g110830	myb transcription factor MYB64	0.29
208	Medtr5g037080	MYB-like transcription factor family protein	4.54
209	Medtr4g081710	myb-like transcription factor family protein	3.81
210	Medtr2g086450	myb-like transcription factor family protein	2.70
211	Medtr1g111830	MYB-like transcription factor family protein	2.31
212	Medtr7g115530	myb-like transcription factor family protein	2.29
213	Medtr6g444980	myb-like transcription factor family protein	2.16
214	Medtr8g086410	MYB-like transcription factor family protein	2.12
215	Medtr6g032990	myb-like transcription factor family protein	2.09
216	Medtr1g053835	myb-like transcription factor family protein	2.04
217	Medtr7g069660	MYB-like transcription factor family protein	2.02
218	Medtr4g113140	myb-like transcription factor family protein	1.99
219	Medtr7g088070	myb-like transcription factor family protein	1.74
220	Medtr2g027860	myb-like transcription factor family protein	1.38
221	Medtr7g098250	myb-like transcription factor family protein	1.36
222	Medtr4g086835	myb-like transcription factor family protein	0.63
223	Medtr4g111975	MYB-like transcription factor family protein	0.62
224	Medtr1g090670	myb-like transcription factor family protein	0.57
225	Medtr1g093080	myb-like transcription factor family protein	0.49
226	Medtr8g077990	Myb transcription factor-like protein	0.71
227	Medtr7g105890	Myb/SANT-like DNA-binding domain protein	10.91
228	Medtr4g128540	Myb/SANT-like DNA-binding domain protein	7.00
229	Medtr0693s0050	Myb/SANT-like DNA-binding domain protein	6.52
230	Medtr1g016370	Myb/SANT-like DNA-binding domain protein	5.55
231	Medtr7g020870	myb/SANT-like DNA-binding domain protein	3.39
232	Medtr2g026725	Myb/SANT-like DNA-binding domain protein	0.60
233	Medtr6g035370	myb/SANT-like DNA-binding domain protein	0.36
234	Medtr1g061640	Myb/SANT-like DNA-binding domain protein	0.28
235	Medtr7g114860	Myb/SANT-like DNA-binding domain protein	0.18
236	Medtr8g085310	Myb/SANT-like DNA-binding domain protein	0.15
237	Medtr1g094045	Myb/SANT-like DNA-binding domain protein	0.10
238	Medtr5g078860	R2R3-myb transcription factor	17.10
239	Medtr5g078910	R2R3-myb transcription factor	16.71
240	Medtr6g012180	R2R3-myb transcription factor	0.61
241	Medtr3g039990	R2R3-myb transcription factor	0.46
242	Medtr0140s0030	R2R3-myb transcription factor	0.45
243	Medtr3g100180	myb-like DNA-binding domain protein	1.74
244	Medtr2g084230	myb-like DNA-binding domain, shaqkyf class protein	4.10
245	Medtr3g450310	myb-like DNA-binding domain, shaqkyf class protein	3.04

No.	Gene ID	Gene annotation	Fold change
246	Medtr6g071625	myb-like DNA-binding domain, shaqkyf class protein	1.68
247	Medtr1g112370	myb-like DNA-binding domain, shaqkyf class protein	0.53
248	Medtr2g016220	myb-like DNA-binding domain, shaqkyf class protein	0.32
249	Medtr5g017980	myb-like DNA-binding domain, shaqkyf class protein	0.29
250	Medtr0223s0040	myb-like DNA-binding domain, shaqkyf class protein	0.20
251	Medtr1g100653	myb transcription factor MIXTA-like protein	2.36
252	Medtr7g011170	myb transcription factor mixta-like protein	0.41
253	Medtr6g012690	myb transcription factor mixta-like protein	0.32
254	Medtr8g031360	myb transcription factor MIXTA-like protein	0.23
255	Medtr1g043080	myb-related transcription factor LBM1	12.26
256	Medtr1g021590	transducin/WD40 repeat protein	62.78
257	Medtr3g074070	transducin/WD40 repeat protein	2.50
258	Medtr8g073335	transducin/WD40 repeat protein	2.14
259	Medtr3g491920	transducin/WD40 repeat protein	1.85
260	Medtr3g010010	transducin/WD40 repeat protein	1.60
261	Medtr7g114370	transducin/WD40 repeat protein	1.44
262	Medtr7g022190	transducin/WD40 repeat protein	1.42
263	Medtr7g074450	transducin/WD40 repeat protein	1.37
264	Medtr2g028050	transducin/WD40 repeat protein	1.36
265	Medtr5g090420	transducin/WD40 repeat protein	1.36
266	Medtr6g093060	transducin/WD40 repeat protein	0.69
267	Medtr7g016970	transducin/WD40 repeat protein	0.67
268	Medtr4g130280	transducin/WD40 repeat protein	0.66
269	Medtr4g105700	transducin/WD40 repeat protein	0.62
270	Medtr1g059090	transducin/WD40 repeat protein	0.60
271	Medtr1g081830	transducin/WD40 repeat protein	0.60
272	Medtr1g007740	transducin/WD40 repeat protein	0.48
273	Medtr5g077160	transducin/WD40 repeat protein	0.28
274	Medtr4g066000	transducin/WD40 domain protein	0.17
275	Medtr6g004040	katanin p80 WD40 repeat subunit B1-like protein	0.68
276	Medtr1g087120	WD40/YVTN repeat containing domain-containing protein	1.33
277	Medtr1g072320	bHLH transcription factor	20.17
278	Medtr5g048860	BHLH transcription factor	1.77
279	Medtr4g108360	BHLH transcription factor	1.72
280	Medtr4g131160	BHLH transcription factor	1.47
281	Medtr3g498695	BHLH transcriptional factor	0.31
282	Medtr3g116770	BHLH transcription factor	0.14
283	Medtr1g084160	transcription factor bHLH147	3.81
284	Medtr3g498825	transcription factor bHLH137	0.73
285	Medtr5g030770	transcription factor bHLH93	0.39
286	Medtr7g072470	transcription factor bHLH93-like protein	2.09



<b>No.</b>	<b>Gene ID</b>	<b>Gene annotation</b>	<b>Fold change</b>
287	Medtr4g079760	transcription factor bHLH107-like protein	0.18
288	Medtr6g488100	BHLH transcription factor-like protein	2.08
289	Medtr8g103065	BHLH transcription factor-like protein	1.99
290	Medtr2g101520	BHLH transcription factor-like protein	1.93
291	Medtr7g063470	bHLH transcription factor-like protein	1.82
292	Medtr7g096650	bHLH transcription factor-like protein	1.44
293	Medtr4g051565	bHLH transcription factor-like protein	1.36
294	Medtr4g087300	BHLH transcription factor-like protein	0.67
295	Medtr3g112170	BHLH transcription factor-like protein	0.35
296	Medtr1g052470	transcription factor bHLH122-like protein	1.69
297	Medtr4g065870	transcription factor bHLH122-like protein	1.61
298	Medtr1g070870	basic helix loop helix protein BHLH4	1.75
299	Medtr8g099880	basic helix loop helix protein BHLH8	5.73
300	Medtr7g083900	basic helix loop helix protein BHLH23	0.53
301	Medtr1g043430	BHLH domain class transcription factor	1.42
302	Medtr5g030420	basic helix loop helix (BHLH) family transcription factor	1.46
303	Medtr8g067280	basic helix loop helix (bHLH) family transcription factor	0.65
304	Medtr8g024790	basic helix loop helix (bHLH) family transcription factor	0.53
305	Medtr4g094762	basic helix loop helix (BHLH) DNA-binding family protein	5.10
306	Medtr5g014520	basic helix loop helix (bHLH) DNA-binding family protein	0.49
307	Medtr0246s0020	basic helix loop helix (bHLH) DNA-binding family protein	0.46
308	Medtr5g014600	basic helix loop helix (bHLH) DNA-binding family protein	0.44
309	Medtr1g093750	basic helix loop helix (BHLH) DNA-binding family protein	0.34
310	Medtr3g099620	basic helix loop helix (BHLH) DNA-binding family protein	0.31
311	Medtr2g022280	basic helix loop helix (BHLH) DNA-binding family protein	0.16
312	Medtr4g012430	BZIP protein	1.81
313	Medtr2g102050	BZIP protein	1.41
314	Medtr3g109450	BZIP protein	0.12
315	Medtr2g086340	bZIP transcription factor	11.48
316	Medtr3g109310	BZIP transcription factor	9.97
317	Medtr1g008990	BZIP transcription factor	3.94
318	Medtr1g098590	BZIP transcription factor	2.08
319	Medtr3g078830	BZIP transcription factor	2.05

No.	Gene ID	Gene annotation	Fold change
320	Medtr6g034945	bZIP transcription factor	1.99
321	Medtr5g038550	BZIP transcription factor	1.74
322	Medtr1g023690	BZIP transcription factor	1.66
323	Medtr2g099050	bZIP transcription factor	1.52
324	Medtr3g436010	BZIP transcription factor	1.46
325	Medtr8g091250	BZIP transcription factor	0.65
326	Medtr4g072090	BZIP transcription factor	0.63
327	Medtr3g094020	bZIP transcription factor	0.50
328	Medtr5g075390	bZIP transcription factor	0.34
329	Medtr5g087740	BZIP transcription factor	0.32
330	Medtr3g467120	bZIP transcription factor	0.31
331	Medtr8g075130	BZIP transcription factor	0.30
332	Medtr6g016375	BZIP transcription factor	0.18
333	Medtr8g091650	BZIP family transcription factor	1.70
334	Medtr8g040120	BZIP family transcription factor	1.57
335	Medtr7g092750	BZIP family transcription factor	3.62
336	Medtr5g060950	BZIP family transcription factor	3.36
337	Medtr0126s0080	BZIP family transcription factor	5.61
338	Medtr2g086420	BZIP family transcription factor	4.81
339	Medtr4g079500	bZIP family transcription factor	0.08
340	Medtr2g090900	bZIP family transcription factor	0.07
341	Medtr4g070860	BZIP transcription factor bZIP124	5.60
342	Medtr3g117120	BZIP transcription factor bZIP124	3.76
343	Medtr7g081705	BZIP transcription factor bZIP80	0.68
344	Medtr7g115120	transcription factor bZIP88	0.17
345	Medtr8g028150	bZIP transcription factor family protein	3.09
346	Medtr7g116890	bZIP transcription factor family protein	2.02
347	Medtr8g077950	bZIP transcription factor family protein	0.74
348	Medtr6g080440	glutathione S-transferase	10.11
349	Medtr1g115195	glutathione S-transferase	13.77
350	Medtr1g067170	glutathione S-transferase	1.99
351	Medtr5g090910	glutathione S-transferase	1.86
352	Medtr7g100320	glutathione S-transferase	1.85
353	Medtr3g450790	glutathione S-transferase	1.42
354	Medtr1g115500	glutathione S-transferase	0.28
355	Medtr2g072120	glutathione S-transferase tau	0.55
356	Medtr4g134380	glutathione S-transferase tau 5	3.41
357	Medtr4g134370	glutathione S-transferase tau 5	2.22
358	Medtr1g090150	glutathione S-transferase, amino-terminal domain protein	12.28
359	Medtr3g064700	glutathione S-transferase, amino-terminal domain protein	57.00

<b>No.</b>	<b>Gene ID</b>	<b>Gene annotation</b>	<b>Fold change</b>
360	Medtr1g090060	glutathione S-transferase, amino-terminal domain protein	23.95
361	Medtr7g065265	glutathione S-transferase, amino-terminal domain protein	8.86
362	Medtr7g065230	glutathione S-transferase, amino-terminal domain protein	6.47
363	Medtr2g070070	glutathione S-transferase, amino-terminal domain protein	5.80
364	Medtr3g099757	glutathione S-transferase, amino-terminal domain protein	4.48
365	Medtr2g070120	glutathione S-transferase, amino-terminal domain protein	3.73
366	Medtr3g467420	glutathione S-transferase, amino-terminal domain protein	2.62
367	Medtr8g061950	glutathione S-transferase, amino-terminal domain protein	2.44
368	Medtr3g088635	glutathione S-transferase, amino-terminal domain protein	1.91
369	Medtr4g019780	glutathione S-transferase, amino-terminal domain protein	1.61
370	Medtr1g059970	glutathione S-transferase, amino-terminal domain protein	1.59
371	Medtr3g066060	glutathione S-transferase, amino-terminal domain protein	0.53
372	Medtr3g005720	glutathione S-transferase, amino-terminal domain protein	0.52
373	Medtr2g070060	glutathione S-transferase, amino-terminal domain protein	0.47
374	Medtr8g098430	glutathione S-transferase, amino-terminal domain protein	0.43
375	Medtr1g026140	glutathione S-transferase, amino-terminal domain protein	0.37
376	Medtr2g070210	glutathione S-transferase, amino-terminal domain protein	0.34
377	Medtr5g037380	glutathione S-transferase, amino-terminal domain protein	0.24

**Table A13 Differentially expressed genes associated with glycolysis and TCA fold changes in *SPL13*RNAi plants**

No.	Gene ID	Gene annotation	Fold change
1	Medtr7g079080	1-Aminocyclopropane-1-carboxylate synthase	13.94
2	Medtr8g028600	1-Aminocyclopropane-1-carboxylate synthase	2.06
3	Medtr8g098930	1-Aminocyclopropane-1-carboxylate synthase	0.68
4	Medtr4g097540	1-Aminocyclopropane-1-carboxylate synthase	0.11
5	Medtr5g085330	1-Aminocyclopropane-1-carboxylate oxidase	6.45
6	Medtr3g083370	1-Aminocyclopropane-1-carboxylate oxidase	3.54
7	Medtr2g025120	1-Aminocyclopropane-1-carboxylate oxidase	2.97
8	Medtr3g088565	1-Aminocyclopropane-1-carboxylate oxidase	2.64
9	Medtr1g043760	1-Aminocyclopropane-1-carboxylate oxidase	0.16
10	Medtr8g024120	1-Aminocyclopropane-1-carboxylate oxidase	0.07
11	Medtr1g070120	Aminocyclopropanecarboxylate oxidase	0.06
12	Medtr8g028435	1-Aminocyclopropane-1-carboxylate oxidase-like protein	129.71
13	Medtr1g032220	1-Aminocyclopropane-1-carboxylate oxidase-like protein	30.29
14	Medtr1g032250	1-Aminocyclopropane-1-carboxylate oxidase-like protein	20.03
15	Medtr1g032140	1-Aminocyclopropane-1-carboxylate oxidase-like protein	7.65
16	Medtr4g099390	1-Aminocyclopropane-1-carboxylate oxidase-like protein	1.99
17	Medtr4g117880	1-Aminocyclopropane-1-carboxylate oxidase-like protein	0.33
18	Medtr5g065880	Glucose-6-phosphate isomerase	0.72
19	Medtr6g009330	Glucose-6-phosphate isomerase	0.63
20	Medtr7g116910	Glucose-6-phosphate 1-epimerase-like protein	3.59
21	Medtr4g092780	Glucose-6-phosphate 1-epimerase-like protein	0.15
22	Medtr1034s0010	Glucose-6-phosphate 1-dehydrogenase	0.66
23	Medtr0590s0010	Glucose-6-phosphate 1-dehydrogenase	0.60
24	Medtr7g111760	Glucose-6-phosphate 1-dehydrogenase	0.52
25	Medtr0275s0010	Glucose-6-phosphate 1-dehydrogenase	0.54
26	Medtr4g070430	Glucose-1-phosphate adenyltransferase family pr.	48.87
27	Medtr3g116860	Glucose-1-phosphate adenyltransferase family pr.	6.51
28	Medtr5g097010	Glucose-1-phosphate adenyltransferase family pr.	1.76
29	Medtr3g082150	Glucose-1-phosphate adenyltransferase family pr.	0.75
30	Medtr4g131760	Glucose-1-phosphate adenyltransferase family pr.	0.24
31	Medtr7g111020	Glucose-1-phosphate adenyltransferase family pr.	0.23
32	Medtr2g022700	Glucose-6-phosphate/phosphate translocator-like pr.	60.42

No.	Gene ID	Gene annotation	Fold change
33	Medtr7g066120	Fructose-1,6-bisphosphatase	0.40
34	Medtr4g093620	Fructose-1,6-bisphosphatase	0.51
35	Medtr6g035305	Fructose-1,6-bisphosphatase, cytosolic-like protein	0.29
36	Medtr2g008030	Fructose-1,6-bisphosphatase, cytosolic-like protein	0.17
37	Medtr1g061050	Fructose-bisphosphate aldolase	1.69
38	Medtr5g069050	Fructose-bisphosphate aldolase	0.67
39	Medtr5g096670	Fructose-bisphosphate aldolase	0.08
40	Medtr4g057670	Fructose-bisphosphate aldolase class I	0.58
41	Medtr4g071860	Fructose-bisphosphate aldolase class I	0.45
42	Medtr6g069660	Fructose-bisphosphate aldolase class-II protein	1.38
43	Medtr3g464770	Fructose-6-phosphate-2-kinase/fructose-2, 6-bisphosphatase	0.46
44	Medtr8g066450	Fructose-6-phosphate-2-kinase/fructose-2, 6-bisphosphatase	0.53
45	Medtr5g071900	Fructose-6-phosphate-2-kinase/fructose-2, 6-bisphosphatase	0.43
46	Medtr4g132700	Pyrophosphate-fructose-6-phosphate 1-phosphotransferase	1.95
47	Medtr1g035230	Pyrophosphate-fructose-6-phosphate 1-phosphotransferase	0.51
48	Medtr2g025020	Pyrophosphate-fructose-6-phosphate 1-phosphotransferase	0.43
49	Medtr7g080270	Glucosamine-fructose-6-phosphate aminotransferase	0.69
50	Medtr4g124470	Lysine-ketoglutarate reductase/saccharopine dehydrogenase	13.14
51	Medtr2g012570	Lysine ketoglutarate reductase trans-splicing-like protein	2.84
52	Medtr4g058800	Lysine ketoglutarate reductase trans-splicing-like protein	3.62
53	Medtr2g005330	Lysine ketoglutarate reductase trans-splicing-like protein	1.99
54	Medtr8g089820	Lysine ketoglutarate reductase trans-splicing protein	2.23
55	Medtr3g086610	Lysine ketoglutarate reductase trans-splicing protein	1.77
56	Medtr2g015310	Glutamate receptor 27	10.77
57	Medtr3g105595	Glutamate receptor 32	1.67
58	Medtr2g088450	Glutamate receptor 32	1.59
59	Medtr5g024350	Glutamate receptor 32	1.54
60	Medtr1g028510	Tetrahydrofolylpolyglutamate synthase	0.48
61	Medtr1g027020	NADH glutamate synthase	0.71
62	Medtr7g089970	Ferredoxin-dependent glutamate synthase	0.60

No.	Gene ID	Gene annotation	Fold change
63	Medtr3g064740	Glutamate decarboxylase	3.28
64	Medtr6g029460	NADP-specific glutamate dehydrogenase	0.18
65	Medtr7g085630	NADP-specific glutamate dehydrogenase	0.28
66	Medtr1g062710	Nodulin/glutamate-ammonia ligase-like protein	3.72
67	Medtr5g033230	Glutamate-glyoxylate aminotransferase	0.45
68	Medtr3g118070	Glutamate-1-semialdehyde 2,1-aminomutase	0.29
69	Medtr2g023430	Gaba-receptor-associated protein ubiquitin domain protein	2.94
70	Medtr2g088230	Gaba-receptor-associated protein ubiquitin domain protein	1.56
71	Medtr4g101090	Gaba-receptor-associated protein ubiquitin domain protein	1.49
72	Medtr4g048510	Gaba-receptor-associated protein ubiquitin domain protein	1.38
73	Medtr1g109620	Trehalose-6-phosphate synthase domain protein	5.24
74	Medtr1g032730	Trehalose-6-phosphate synthase domain protein	4.47
75	Medtr0034s0170	Trehalose-6-phosphate synthase	2.46
76	Medtr2g073260	Trehalose-6-phosphate synthase	1.55
77	Medtr4g080160	Trehalose-6-phosphate synthase domain protein	0.75
78	Medtr4g129270	Trehalose-6-phosphate synthase domain protein	0.50
79	Medtr8g105740	Trehalose-6-phosphate synthase domain protein	0.38
80	Medtr4g036090	Trehalose-phosphate phosphatase	0.40
81	Medtr4g101600	Trehalose-phosphate phosphatase	1.96
82	Medtr8g014530	Hexokinase	0.57
83	Medtr6g088795	Hexokinase	0.53
84	Medtr2g100710	6-Phosphofructokinase	3.85
85	Medtr5g032570	6-Phosphofructokinase	2.50
86	Medtr4g134290	6-Phosphofructokinase	2.40
87	Medtr8g102190	6-Phosphofructokinase	2.23
88	Medtr6g090130	6-Phosphofructokinase	2.04
89	Medtr8g006290	Phosphoglycerate mutase family protein	4.47
90	Medtr4g092840	Phosphoglycerate mutase family protein	0.71
91	Medtr2g013570	Phosphoglycerate mutase	0.51
92	Medtr3g111310	Phosphoglycerate mutase family protein	0.51
93	Medtr6g018680	Phosphoglycerate kinase	0.45
94	Medtr2g095260	2-Phosphoglycerate kinase	0.45
95	Medtr1g056720	2-Phosphoglycerate kinase	2.14
96	Medtr2g066110	Phosphoglycerate kinase-like protein	0.21
97	Medtr6g011290	Phosphoglycerate mutase-like protein	0.44

No.	Gene ID	Gene annotation	Fold change
98	Medtr7g009060	Phosphoglycerate mutase-like protein	0.58
99	Medtr7g080530	Phosphoglycolate phosphatase-like protein	0.44
100	Medtr1g107480	D-3-phosphoglycerate dehydrogenase family pr.	0.54
101	Medtr5g014310	Aluminum activated malate transporter family pr.	2.95
102	Medtr4g051575	Aluminum activated malate transporter family pr.	2.70
103	Medtr4g098570	Aluminum activated malate transporter family protein	2.44
104	Medtr2g009220	2-Oxoglutarate/malate translocator	0.37
105	Medtr4g065007	2-Oxoglutarate/malate translocator	0.21
106	Medtr1g116500	2-Isopropylmalate synthase	0.54
107	Medtr2g104610	3-Isopropylmalate dehydrogenase	0.38
108	Medtr4g092690	Glyoxysomal malate dehydrogenase	0.24
109	Medtr8g463760	Malate dehydrogenase	0.60
110	Medtr1g076130	Cytoplasmic-like malate dehydrogenase	0.57
111	Medtr1g043040	Cytoplasmic-like malate dehydrogenase	0.57
112	Medtr8g005980	Cytoplasmic-like malate dehydrogenase	0.40
113	Medtr2g034090	ATP:citrate lyase	0.49
114	Medtr2g062920	ATP-citrate synthase alpha chain protein	0.30
115	Medtr3g048920	Citrate synthase 3, peroxisomal protein	1.62
116	Medtr5g077070	NADP-dependent isocitrate dehydrogenase	1.34
117	Medtr4g103680	Argininosuccinate synthase	0.34
118	Medtr7g092860	Adenylosuccinate lyase	0.46
119	Medtr5g081750	Adenylosuccinate lyase	0.49
120	Medtr8g028120	Glyoxylate/succinic semialdehyde reductase	0.60
121	Medtr2g099910	Glyoxylate/succinic semialdehyde reductase	0.27
122	Medtr5g020050	Succinate dehydrogenase [ubiquinone] flavoprotein subunit	2.13
123	Medtr1g492610	Succinate dehydrogenase [ubiquinone] iron-sulfur subunit	1.45
124	Medtr0018s0260	Succinate dehydrogenase [ubiquinone] iron-sulfur subunit	1.35
125	Medtr6g077820	Succinyl-CoA ligase [ADP-forming] subunit alpha-2	0.53
126	Medtr2g103280	Biotin carboxyl carrier acetyl-CoA carboxylase	1.75
127	Medtr6g015020	Biotin carboxyl carrier acetyl-CoA carboxylase	0.52
128	Medtr7g013100	Biotin carboxyl carrier acetyl-CoA carboxylase	0.51
129	Medtr7g080290	Biotin carboxyl carrier acetyl-CoA carboxylase	0.49
130	Medtr8g101330	Acetyl-CoA carboxylase biotin carboxylase subunit	0.49
131	Medtr4g050863	Acetyl-coA carboxylase carboxyltransferase beta subunit	0.19

No.	Gene ID	Gene annotation	Fold change
132	Medtr5g022940	Aytoplasmic-like aconitate hydratase	1.84
133	Medtr4g048190	Cytoplasmic-like aconitate hydratase	1.35
134	Medtr8g104540	Cytoplasmic phosphoglucomutase	0.66
135	Medtr5g091060	4-Hydroxyphenylpyruvate dioxygenase	1.95
136	Medtr5g090980	4-Hydroxyphenylpyruvate dioxygenase	1.57
137	Medtr5g045000	Glucosamine-6-phosphate isomerase/6-phosphogluconolactonase	1.99
138	Medtr1g028320	Glucosamine-6-phosphate isomerase/6-phosphogluconolactonase	0.35
139	Medtr1g028330	Glucosamine-6-phosphate isomerase/6-phosphogluconolactonase	0.26
140	Medtr7g017900	Decarboxylating-like 6-phosphogluconate dehydrogenase	0.73
141	Medtr8g099185	Decarboxylating-like 6-phosphogluconate dehydrogenase	0.71
142	Medtr8g088900	6-Phosphogluconate dehydrogenase-like protein	0.65
143	Medtr1g087900	Fumarate hydratase	0.43
144	Medtr3g115920	Glyceraldehyde-3-phosphate dehydrogenase B	0.31
145	Medtr7g084800	Glyceraldehyde-3-phosphate dehydrogenase	0.23
146	Medtr1g014320	NADP-dependent glyceraldehyde-3-phosphate dehydrogenase	4.48
147	Medtr4g108800	Ribulose-phosphate 3-epimerase	0.43
148	Medtr4g021210	Ribulose bisphosphate carboxylase/oxygenase activase	0.47
149	Medtr2g105480	Ribulose bisphosphate carboxylase/oxygenase activase	0.32
150	Medtr7g007200	Ribulose bisphosphate carboxylase small chain	0.06
151	Medtr7g007120	Ribulose bisphosphate carboxylase small chain	0.05
152	Medtr7g007230	Ribulose bisphosphate carboxylase small chain	0.02
153	Medtr4g051270	Ribulose bisphosphate carboxylase large chain domain protein	0.30
154	Medtr6g055010	Ribulose bisphosphate carboxylase large chain domain protein	0.25
155	Medtr2g092930	Phosphoenolpyruvate carboxylase	3.58
156	Medtr1g094010	Phosphoenolpyruvate carboxylase	1.44
157	Medtr2g076670	Phosphoenolpyruvate carboxylase	1.42
158	Medtr1g094000	Phosphoenolpyruvate carboxylase	1.37
159	Medtr8g463920	Phosphoenolpyruvate carboxylase	0.58
160	Medtr4g079860	Phosphoenolpyruvate carboxylase	0.38
161	Medtr5g430730	Phosphoenolpyruvate carboxykinase [ATP] protein	1.95
162	Medtr2g015560	Pyruvate decarboxylase	1.54



<b>No.</b>	<b>Gene ID</b>	<b>Gene annotation</b>	<b>Fold change</b>
163	Medtr7g069540	Pyruvate decarboxylase	0.32
164	Medtr2g009330	Pyruvate decarboxylase	0.07
165	Medtr5g046610	Pyruvate decarboxylase	0.41
166	Medtr6g004020	Pyruvate kinase family protein	0.71
167	Medtr1g076540	Pyruvate kinase family protein	0.48
168	Medtr6g034195	Pyruvate kinase family protein	0.40
169	Medtr1g105965	Pyruvate kinase family protein	0.28
170	Medtr4g083340	Pyruvate kinase family protein	0.12
171	Medtr4g118350	Pyruvate orthophosphate dikinase	3.28
172	Medtr6g060570	Phosphopyruvate hydratase	2.65
173	Medtr7g103620	Phosphopyruvate hydratase	0.72
174	Medtr7g024460	Pyruvate dehydrogenase (acetyl-transferring) kinase	0.55
175	Medtr3g076630	Pyruvate dehydrogenase E1 beta subunit	0.53
176	Medtr5g036600	Pyruvate dehydrogenase complex E1 alpha subunit	1.48
177	Medtr1g112510	D-glycerate dehydrogenase/hydroxypyruvate reductase	0.29
178	Medtr4g013135	D-glycerate dehydrogenase/hydroxypyruvate reductase	0.21
179	Medtr6g007170	D-glycerate dehydrogenase/hydroxypyruvate reductase	1.97

## Curriculum vitae

**Name:** Biruk Ayenew Feyissa

**Degrees:** **The University of Western Ontario**

London, Ontario, Canada (PhD)

**Ben-Gurion University of the Negev**

Bersheba, Israel (MSc)

**Jimma University**

Jimma, Ethiopia (MSc)

**Alemaya University**

Dire Dawa, Ethiopia (BSc)

**Awards:** -Best Student Oral Presenter, Plant Canada 2019 conference

University of Guelph, Canada, July 2019

-Genome Canada travel bursary, Bioinformatics workshop

Montreal, Quebec, Canada, July 2018

-Gordon Research Seminar Travel Award, GRS conference

Waterville Valley, NH, USA, June 2018

-George H. Duff travel bursary,

Plants from sea to sky, University of British Columbia, Canada, 2017

Plant biology, Montreal, Quebec, Canada July 2018

-COST FA1106 Quality Fruit, Metabolomics training

Wageningen University, Netherlands, December 2013

-MASHAV, Molecular biology post-graduate training

Hebrew University of Jerusalem,

Robert H. Smith Faculty of Agriculture, Food & Environment, Rehovot, Israel

February- April 2012

**Selected Publications:**

**FEYISSA BA**, Amyot L, Papadopoulos Y, Kohalmi SE, Hannoufa A, **2019** ABA-dependent SnRK1 expression mediate miR156/SPL module for flooding response in alfalfa, (Under review)

- FEYISSA BA**, Arshad M, Gruber M, Kohalmi SE, and Hannoufa A, **2019** The Interplay Between miR156-SPL13 and DFR-WD40-1 regulate drought tolerance in alfalfa, *BMC Plant Biology* 19:434.
- Hannoufa A, Matthews C, **FEYISSA BA**, Gruber M and Arshad M, **2018** Progress Toward Deep Sequencing-Based Discovery of Stress-Related MicroRNA in Plants and Available Bioinformatics Tools, *Progress in Botany*, Springer, Berlin, Heidelberg.
- Wei S, Gruber M, **FEYISSA BA**, Amyot L, Hannoufa A and Li X, **2018** COP9 signalosome subunit 5A affects phenylpropanoid metabolism, trichome formation and transcription of key genes of a regulatory tri-protein complex in Arabidopsis, *BMC Plant Biology* 18:134.
- Gao R, **FEYISSA BA**, Croft M and Hannoufa A **2018** Gene editing by CRISPR/CAS9 in the obligatory out-crossing *Medicago sativa*, *Planta* 247(4):1043-1050.
- Arshad M, **FEYISSA BA**, Amyot L, Aung B and Hannoufa A **2017** MicroRNA156 improves drought stress tolerance in alfalfa (*Medicago sativa*) by silencing SPL13, *Plant Science*, 258:122-136.
- Degu A, **AYENEW B**, Cramer G and Aaron Fait **2016** Polyphenolic responses of grapevine berries to light, temperature, oxidative stress, abscisic acid and jasmonic acid show specific developmental-dependent degrees of metabolic resilience to perturbation, *Food Chem*, 212:828-36.
- AYENEW B**, Degu A, Manela N, Perl A, Oren-Shamir M and Fait A **2015** Metabolite profiling and transcript analysis reveal specificities in the response of a berry derived cell culture to abiotic stresses, *Frontier in Plant Science*, 6:728.
- Manela N, Oliva M, Ovadia R, Sikron-Persi N, **AYENEW B**, Fait A, Galili G, Perl A, Weiss D and Oren-Shamir M, **2015** Phenylalanine and tyrosine levels are rate-limiting factors in production of health promoting metabolites in *Vitis vinifera* cv. Gamay Red cell suspension, *Frontier in Plant Science*, 6:538.